DOE/NASA/0335-3
NASA CR-187146
GARRETT NO. 31-8071(03)

ADVANCED TURBINE TECHNOLOGY APPLICATIONS PROJECT (ATTAP)

1990 ANNUAL REPORT

Engineering Staff of
Garrett Auxiliary Power Division
A Unit of Allied-Signal Aerospace Company

March 1991

Prepared for
NATIONAL AERONAUTICS AND SPACE ADMINISTRATION
Lewis Research Center
Cleveland, Ohio 44135
Under Contract DEN3-335

for
U.S. DEPARTMENT OF ENERGY
Office of Transportation Technologies
Heat Engine Propulsion Division
Washington, D.C. 20585

DOE/NASA/0335-3
NASA CR-187146
GARRETT NO. 31-8071(03)

ADVANCED TURBINE TECHNOLOGY APPLICATIONS PROJECT (ATTAP)

1990 ANNUAL REPORT

Engineering Staff of
Garrett Auxiliary Power Division
A Unit of Allied-Signal Aerospace Company

March 1991

Prepared for
NATIONAL AERONAUTICS AND SPACE ADMINISTRATION
Lewis Research Center
Cleveland, Ohio 44135
Under Contract DEN3-335

for
U.S. DEPARTMENT OF ENERGY
Office of Transportation Technologies
Heat Engine Propulsion Division
Washington, D.C. 20585

Disclaimer

Printed in the United States of America

Available from

National Technical Information Service
U.S. Department of Commerce
5285 Port Royal Road
Springfield, Virginia 22161

NTIS Price Codes

Printed copy: A09
Microfiche copy: A01

TABLE OF CONTENTS

TABLE OF CONTENTS (Contd)

LIST OF FIGURES

LIST OF FIGURES (Contd)

LIST OF FIGURES (Contd)

LIST OF FIGURES (Contd)

LIST OF FIGURES (Contd)

LIST OF FIGURES (Contd)

LIST OF TABLES

LIST OF TABLES (Contd)

LIST OF TABLES (Contd)

ACRONYMS AND ABBREVIATIONS

AFM	Abrasive Flow MAchining
AGT	Advanced Gas Turbine
ANOVA	Analysis of Variance
ASEA	Swedish Subcontractor to GCC (HIP Encapsulation Process)
ASME	American Society of Mechanical Engineers
ASTM	American Society for Testing Materials
atm	Atmosphere
ATTAP	Advanced Turbine Technology Applications Project
B_4C	Boron Carbide
C	Celsius
CAD	Computer Aided Design
CBO	Carborundum Company
CFDC	Combined Federal Driving Cycle
CIP	Cold Isostatic Pressing
cm	Centimeter
CVD	Chemical Vapor Deposition
DOE	Department of Energy
ECU	Electronic Control Unit
EPIC	Elastic-Plastic Impact Computations (Computer Code)
F	Fahrenheit
FEM	Finite Element Model
FOD	Foreign Object Damage
FPI	Fluorescent Penetrant Inspection
FRSL	Flat-Rated Sea Level
FSH	Flow Separator Housing
g	Gram
GAPD	Garrett Auxiliary Power Division
GCC	Garrett Ceramic Components
HIP	Hot-Isostatic Pressing
HP	High Pressure
hr	Hour
ID	Inside Diameter
IM	Injection Molding
in	Inch
IQI	Image Quality Indicator
K	Kelvin
kg	Kilogram
K_{IC}	Critical Stress Intensity Factor
ksi	Thousands of Pounds Per Square Inch
LAS	Lithium Aluminum Silicate
lbs	Pounds
LP	Low Pressure
MFXR	Microfocus X-Ray Radiography
mg	Milligram
mm	Millimeter
MOR	Modulus of Rupture
MPa	Mega Pascals
mpg	Miles per Gallon

ACRONYMS AND ABBREVIATIONS (Contd)

N/A	Not Applicable
NASA	National Aeronautics and Space Administration
NDE	Nondestructive Evaluation
NTC	Norton/TRW Ceramics
OD	Outside Diameter
ORNL	Oak Ridge National Laboratory
PEEP	Pressure-Assisted Endothermic Extraction Process
PMMA	Polymethylmethacrylate
PSC	Pressure Slip Casting
psi	Pounds Per Square Inch
RBSN	Reaction-Bonded Silicon Nitride
RIT	Regenerator Inlet Temperature
RPD	Reference Powertrain Design
R.T.	Room Temperature
rpm	Revolutions Per Minute
SAE	Society of Automotive Engineers
SASC	Sintered Alpha Silicon Carbide
sec	Seconds
SFC	Specific Fuel Consumption
shp	Shaft Horsepower
SEM	Scanning Electron Microscope
Si_3N_4	Silcon Nitride
SiC	Silicon Carbide
Si-SiC	Siliconized Silicon Carbide
SL	Sea Level
SPC	Statistical Process Control
SOP	Standard Operating Procedure
SOW	Statement of Work
SSN	Sintered Silicon Nitride
TIPS	Turbine Inlet Particle Separator
TIT	Turbine Inlet Temperature
UDRI	University of Dayton Research Institute
W	Watt
WDX	Wavelength Dispersive X-Ray
WEEP	Water Endothermic Extraction Process
YSZ	Yttria-Stabilized Zirconia
Y_2O_3	Yittrium Oxide
μin	Microinch
σ_1	First Principal Stress (SIG1)
2-D	Two Dimensional
3-D	Three Dimensional

This Page Intentionally Left Blank

1.0 SUMMARY

This report summarizes work performed by Garrett Auxiliary Power Division (GAPD), a unit of Allied-Signal Aerospace Company, during calendar year 1990, toward development and demonstration of structural ceramic technology for automotive gas turbine engines. This work was performed for the Department of Energy (DOE) under National Aeronautics and Space Administration (NASA) Contract DEN3-335, Advanced Turbine Technology Applications Project (ATTAP). GAPD is utilizing the AGT101 regenerated gas turbine engine developed under the previous DOE/NASA Advanced Gas Turbine (AGT) program as the ATTAP engine test bed for ceramic engine technology demonstration. ATTAP is focussing on improving AGT101 test bed reliability, development of ceramic design methodologies for impact damage resistance, improvement of fabrication and materials processing technology by domestic U.S. ceramics fabricators, improved combustion system and regenerator technology, and demonstration of technology advancements in a series of durability tests. This is the third in a series of technical summary reports published annually over the course of the five-year contract.

1.1 Test Bed Engine Design, Analysis, and Materials Assessment

Work progressed on improvements to the AGT101 engine test bed for enhanced operational characteristics. Chief among these was the completion of the redesign of the turbine stage to incorporate an impact-resistant rotor. Other activities to improve the test bed engine included:

- Continued development of regenerator seals, concentrating on a coating system to provide the strain tolerance and chemical stability necessary for good durability at engine operating conditions

- Identification of an optimum mechanical turbine inlet particle separator (TIPS) configuration with the capability to successfully separate particles from the hot gas stream prior to ingestion into the rotating turbine components

- Design of a revised means of positioning and supporting the lithium aluminum silicate (LAS) flow separator housing (FSH) to assure its survivability under all engine pressure conditions

- o Modification of the ceramic bolt assemblies which locate and fix the ceramic turbine shroud module in position within the engine structures

- o Redesign of the combustor cap to achieve improved control of the temperature of critical spring elements, better heat retention characteristics, and easier assembly

- o Incorporation of a new material, NiResist, for fabrication of the exhaust housing replacing the previous ductile cast iron housing

- o Redesign of the transition duct, flow separator, and turbine shroud seal to improve reliability.

Incorporation of these improvements into the AGT101 engine will make it a more reliable test bed for verification of the ATTAP ceramic technologies.

Three silicon carbide (SiC) materials were assessed during this reporting period. Norton/TRW (NTC) NT-235, based on Norton Company NC-430, was assessed and found acceptable for certain ATTAP applications. NTC's improved silicon carbide, designated NT-230, was also assessed, with favorable results compared to NT-235. NT-230 was selected as a candidate material for the fabrication of ATTAP transition ducts on a trial basis.

Dow Corning beta SiC was also assessed, and found suitable for use in ATTAP, possibly as a stator material. Dow Corning has thus far demonstrated shape capability only on small components, some of these using existing molds for silicone rubber parts. Further evaluation is on hold, pending Dow Corning's ability to further develop shape forming capability.

Analyses of the Reference Powertrain Design (RPD) and a cost analysis for fabrication of an engine similar to the AGT101 on a volume basis are scheduled for the final program year. No activity was devoted to this area during this reporting period.

1.2 Ceramic Component Design

Progress was made during 1990 in developing impact design methods and designing an impact-resistant ceramic turbine rotor. Methods for predicting local impact damage were demonstrated during this reporting period. These methods combine a micro-damage model

with an impact finite element model (FEM) to predict crack formation near the point of impact. Simulation of both plate and particle impact damage, observed in testing, demonstrated that these methods can successfully predict local impact damage in ceramics.

The impact design methods were successfuly employed in reducing the turbine blade stresses that would be produced by impacts from combustor carbon. The initial turbine redesign has a calculated impact stress approximately 59 percent of the value for the baseline AGT101 radial turbine. Additional analyses have identified an improved blade design that could be expected to further reduce the impact stress to only 23 percent of the stress calculated for the AGT101 radial turbine. Both impact-resistant blade designs are being fabricated into single-blade ceramic subelements that will be impact tested, to calibrate the analyses and demonstrate reduced impact stress and improved impact resistance.

The turbine section of the ATTAP test bed engine was also redesigned, to accommodate the improved, impact-resistant turbine rotor. The majority of this redesign effort was completed during 1990. Results from analyses of the redesigned ceramic components revealed:

- Rotor three-dimensional (3-D) FEM analyses showed stresses in the impact-resistant rotor at flat-rated and maximum power occur at different locations than in the AGT101 radial turbine, but the maximum stress levels are comparable.

- Stator 3-D thermal and stress analyses showed low stress levels during lightoff transients

- Analyses of other redesigned structures (shroud, baffle, and transition duct) showed no excessive stress

- Redesigned ceramic seal assembly with improved loading and piloting features was shown to have acceptable stress levels

These results indicate no substantial increase in risk with the new ceramic impact-resistant rotor and structures over the AGT101 radial turbine designs.

1.3 Materials Characterization and Ceramic Component Fabrication

The three ceramic subcontractors (Norton/TRW, Carborundum Co., and Garrett Ceramic Components) continued development of fabrication techniques suited to the production of ATTAP components. By the end of 1990, the ability to fabricate component shapes with properties comparable to the material baseline properties was being demonstrated. Subcontractor efforts were emphasizing the delivery of engine quality components (Milestone 3) with decreased emphasis on further process development.

GN-10 silicon nitride bladed rotors from Garrett Ceramic Components (GCC), fabricated with a tool from the prior AGT101 design, were characterized for material properties, including surface strength. GN-10 rotor flexural strengths exceeded the 1989 baseline levels. As-processed surface strength was 55 percent of the machined strength.

Norton/TRW NT154 unbladed rotor hubs, and bars coprocessed with stators were also characterized. NT154 rotor hub data met or exceeded baseline properties. NT154 stator properties were below previous strength levels.

Detailed accounts of subcontractor progress are given in the Appendices to this report. As the new impact-tolerant rotor and stator designs were being developed, close coordination with the subcontractors resulted in several benefits. Among these was selection of an even number of rotor blades to offer easier fabrication; modification of the rotor blade geometry to assure that tooling could be readily separated from the formed (yet fragile) component; and definition of a datum structure (reference points) to simplify machining and inspection. Also, constraints were placed upon the stator sidewall thickness in response to Norton/TRW formability concerns.

For both the rotor and stator designs, models for casting trials of the preliminary geometries were formed using stereolithography. Working from computer aided design (CAD) data files, this "desktop manufacturing" process builds a model of the part geometry by solidifying a liquid polymer resin with a guided laser beam, slice by slice, until the part is fully replicated in plastic. Although the surface finish is limited by the thickness of the slices, this method was nonetheless very useful in allowing the rotor and stator subcontractors to perform initial casting trials with the new geometries well before finalized drawings of the parts were available. The savings in development time for the new-geometry parts is estimated at 3-6 months.

1.4 Component Rig Testing

During this reporting period, progress was made in preparation for heated spin pit tests. The objective of the hot spin pit testing is to verify the accuracy of life prediction analysis methods. The analytical predictions will be verified for non-bladed ceramic disks. Spin pit capability was demonstrated using titanium disks running at up to 100,000 rpm under ambient temperature and pressure conditions. The titanium proof disks were of the same geometry as the ceramic disks being made for the verification test. In a separate test to verify furnace capabilities, eight silicon carbide heater rods successfully heated the insulated chamber to 2500F in one hour.

Combustor rig testing concentrated on eliminating carbon formation, thus avoiding foreign object damage (FOD) to the turbine. A stepped pilot combustor and a constant-diameter pilot combustor were tested in combination with both old and new nozzle configurations. Improvements were demonstrated during light-off conditions using the new nozzle design.

Regenerator rig testing concentrated on hot seal durability. Hot seals were tested that incorporated the baseline coating configuration with a new mechanical seal design to relieve thermal stress. The seal durability results looked very promising after 72 hours of testing. Also, experiments accomplished in conjunction with the durability testing provided information helpful in reducing regenerator drive torque.

Structural proof tests were continued, to qualify ceramic hardware for use in engine tests. Three baffles, one transition duct, six inner diffusers, and seven outer diffusers were screened. All hardware tested survived the 25 percent overstress screening tests.

Testing of the turbine inlet particle separator (TIPS) designs was completed. Using a Taguchi test matrix, an optimum configuration was determined that provided separation efficiency of 98.7 percent with a pressure loss of only 3 percent. Program activity on this component has been concluded.

A turbine test rig is being fabricated to validate the theoretical aerodynamic design of the AGT101 impact-resistant rotor. Obtaining actual aerodynamic trends will allow accurate predictions of turbine performance in the engine. The test rig design was completed and fabrication was initiated.

2.0 INTRODUCTION

This report is the third in a series of Annual Technical Summary Reports for ATTAP, authorized under the DOE-sponsored NASA Contract DEN3-335. Included as Appendices are subcontractor reports provided by Norton/TRW Ceramics Co., the Carborundum Co., and Garrett Ceramic Components. The project is administered by Mr. Thomas Strom, Project Manager, NASA-Lewis Research Center, Cleveland, Ohio. This report presents work plans and progress for calendar year 1990.

Project efforts conducted under this contract are part of the DOE Gas Turbine Highway Vehicle System Program. This program is oriented to provide the United States automotive industry the high-risk, long-range technology necessary to produce gas turbine engines for automobiles with reduced fuel consumption and reduced environmental impact.

The Garrett AGT101 ATTAP test bed engine (Figure 1) is designed such that, when installed in a 3000-pound inertia weight automobile, it will provide:

- Low emissions
- Fuel economy of 42 mpg on diesel fuel
- Multifuel capability
- Competitive costs with current spark-ignition engines
- Noise and safety characteristics that meet U.S. federal standards

The AGT101 is nominally a 100-shp engine, capable of speeds to 100,000 rpm and operation at turbine inlet temperatures (TIT) to 1371C (2500F) with a specific fuel consumption (SFC) level of 0.3 pounds/hp-hr over much of the operating range.

ATTAP is oriented toward developing the high-risk technology of ceramic structural component design and fabrication, such that industry can carry this technology forward to production in the 1990s. The AGT101 engine, continued in use from the prior DOE-sponsored AGT Project, is being used as the Garrett ATTAP test bed engine for verification of the durability of ceramic components, and their suitability for service at Reference Powertrain Design (RPD) conditions.

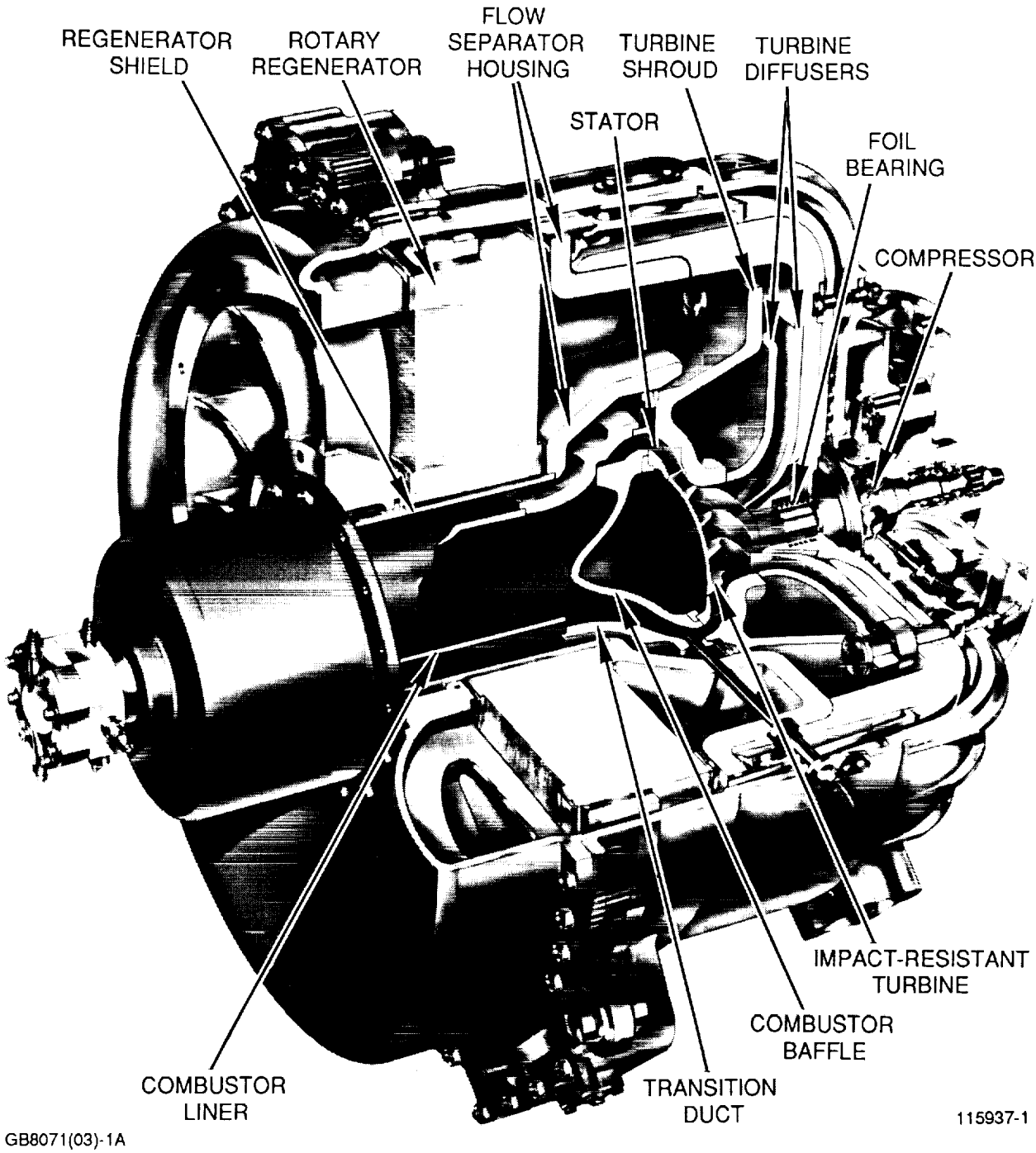

Figure 1. Garrett AGT101 ATTAP Test Bed Engine

The ATTAP milestone schedule is depicted in Figure 2. The program will continue technology work into calendar year 1992, culminating in the demonstration of ceramic engine operation for 300 hours under conditions simulating the combined federal driving cycle (CFDC) for automotive engines. In addition, an RPD Cost Analysis will be performed in the final program year to provide the U.S. automotive industry with data on the cost of producing engines with structural ceramic materials.

This report reviews the efforts conducted in the third full year of ATTAP in development of ceramic technology, and improvements made to the test bed engine and test rigs. Appendices include progress reports prepared by the major ATTAP subcontractors to GAPD: Norton/TRW Ceramics, Carborundum Company, and Garrett Ceramic Components.

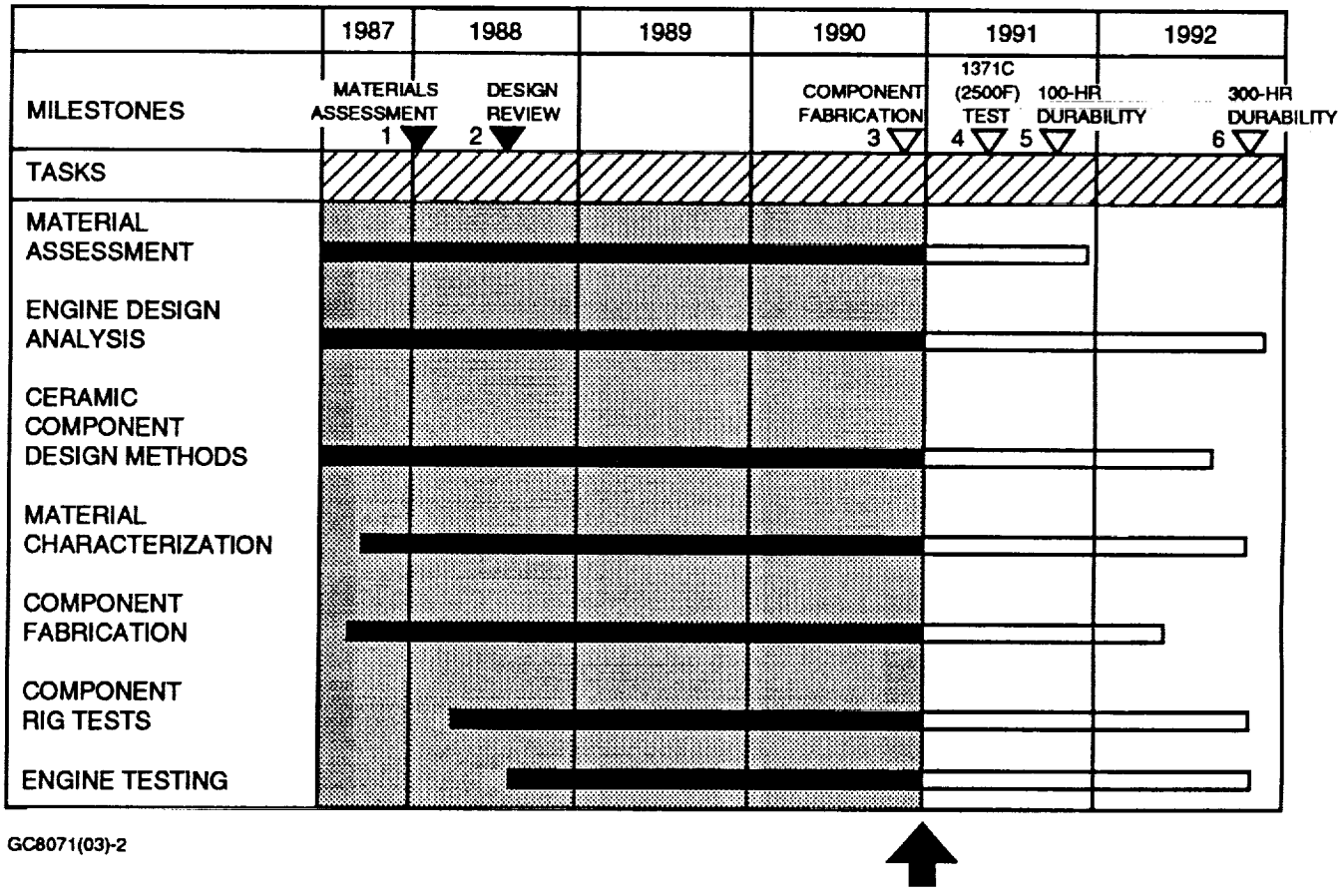

Figure 2. ATTAP Milestone Schedule.

3.0 TEST BED ENGINE DESIGN, ANALYSIS AND MATERIALS ASSESSMENT

3.1 Materials Assessment

Three new materials were assessed during 1990, including two siliconized silicon carbide (Si-SiC) materials from Norton/TRW and a beta silicon carbide (ß-SiC) from Dow Corning.

Norton/TRW Siliconized Silcon Carbides

Two Norton/TRW Si-SiC materials, designated NT-235 and NT-230, were assessed in parallel. NT-235 is the Norton/TRW version of Norton Company NC-430. NT-230 is an improved Si-SiC material using a finer SiC starting power than NT-235. Si-SiC is of interest for ATTAP since its process is amenable to large complex shapes (with no shrinkage from casting through densification), and since the raw materials and process are cost competitive compared to sintered silicon nitrides and carbides.

The flexural strength of NT-235 and NT-230 are shown in Figure 3. NT-235 maintains average strength above 30 ksi up to 2500F. The strength results for NT-230 were encouraging. NT-230 exhibited approximately two times the flexural strength of NT-235, averaging above 60 ksi from room temperature to 2500F.

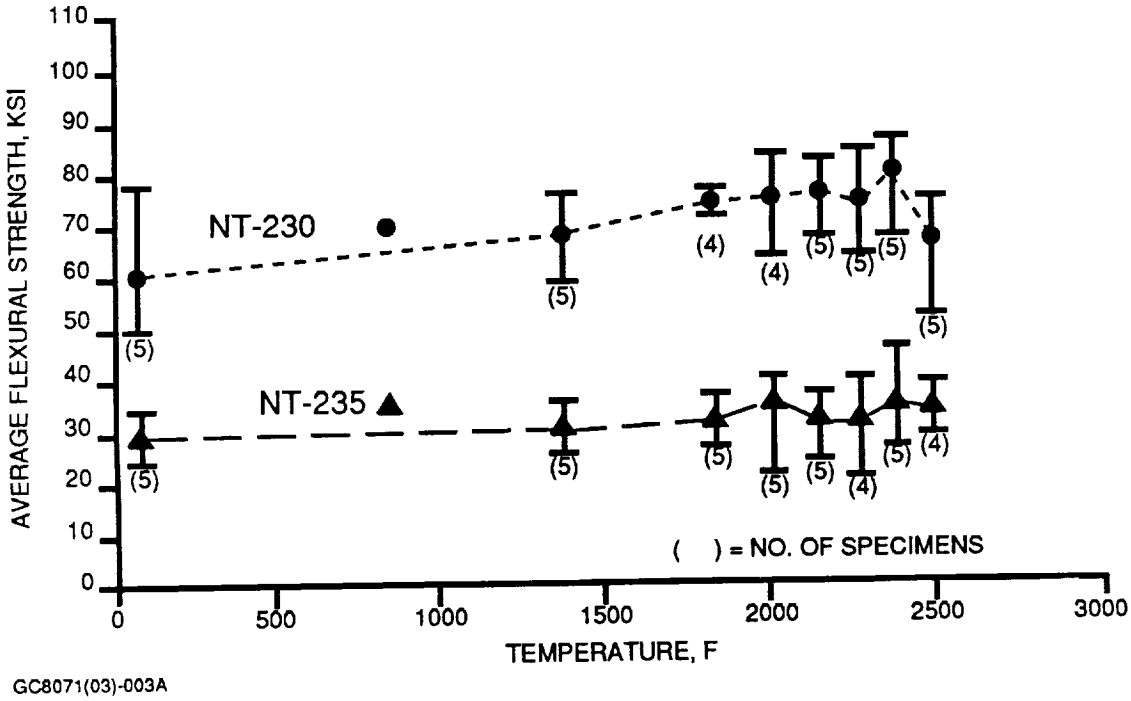

Figure 3. Test Results Show Norton/TRW NT-230 Has Twice the Strength of NT-235 Si-SiC.

The flexural stress rupture characteristics for NT-235 and NT-230 are compared in Table 1. The test results illustrate the superior stress rupture characteristics of the NT-230 material compared to NT-235. Based on the encouraging test results and processing advantages of NT-230, it has been selected as a second material source for ATTAP transition ducts. Additional characterization testing of NT-230 is planned in 1991.

Dow Corning Beta Silicon Carbide

Dow Corning ß-SiC is of interest for ATTAP due to its potential for forming net-shape components. The Dow Corning ß-SiC forming process uses pre-ceramic polymer binders for injection molding rather than a conventional plastic fugitive binder. The pre-ceramic polymer is converted to SiC prior to sintering, which yields excellent as-fired tolerances and surface finish.

TABLE 1. FLEXURAL STRESS RUPTURE TEST RESULTS FOR NORTON/TRW NT-235 AND NT-230 SILICONIZED SILICON CARBIDES

Material	Stress, ksi	Stress Rupture Life, Hours			
		2200F	2300F	2400F	2500F
NT-235	20.3			>160 >160	>160 >160
	25.4	>160 >160	>160 >160		
	27.6			>160 >160	>160 >160
	32.6	85 1	0.7 0.2		
Flexural Strength, ksi		36.1	35.0	37.7	36.7
NT-230	29.0				>160 >160
	36.3			>160 >160	>160 >160
	43.5		>160 >160	>160 >160	
	50.8	>160 >160	>160 >160		
	58.0	>160 >160			
Flexural Strength, ksi		77.2	75.0	80.1	67.6

Tests performed by Norton/TRW using 4 x 3 x 50 mm specimens and 40 by 20 mm four-point flexure spans.
>Indicates test was terminated without specimen failure.

8071(03)-1A

The flexural strength of Dow Corning ß-SiC is shown in Figure 4. The elevated temperature strength averaged between 50 and 60 ksi up to 2500F, which is in agreement with Dow Corning data. The specimens tested at room temperature all exhibited chamfer failures and low strengths (~40 ksi). Handling damage or a machining problem is suspected, and the room temperature testing will be repeated in 1991.

Toughness testing using long bar chevron notch specimens was performed on Dow Corning ß-SiC at room temperature and 2200F. The chevron notch test specimen and test parameters are shown in Figure 5. The measured toughness values were 2.45 and 3.59 $ksi*in^{1/2}$, respectively.

Flexural stress rupture testing of Dow Corning ß-SiC is in progress.

3.2 Reference Powertrain Design (RPD)

No modifications were made to the RPD during 1990.

3.3 Reference Powertrain Design Cost Analysis

The RPD Cost Analysis is scheduled for the final year of ATTAP.

3.4 Test Bed Improvements

Improvements to the AGT101 engine are being developed to provide a more reliable test bed for evaluation of ATTAP ceramic components. These improvements include an impact-resistant turbine rotor, regenerator seals employing a more chemically stable and thermal strain tolerant coating, and a combustor with improved atomization and less tendency to coke formation. Also, redesign of structural components to accommodate the impact-resistant rotor has resulted in additional envelope for the critical sealing elements between the flow separator, turbine shroud, and transition duct. Advantage has therefore been taken to improve the design of these seals. Evaluation of a modified system to locate and support the flow separator housing has also been performed. The impact-resistant rotor design activities are discussed in Section 4.2.10; the remaining activities are discussed in detail in the following paragraphs.

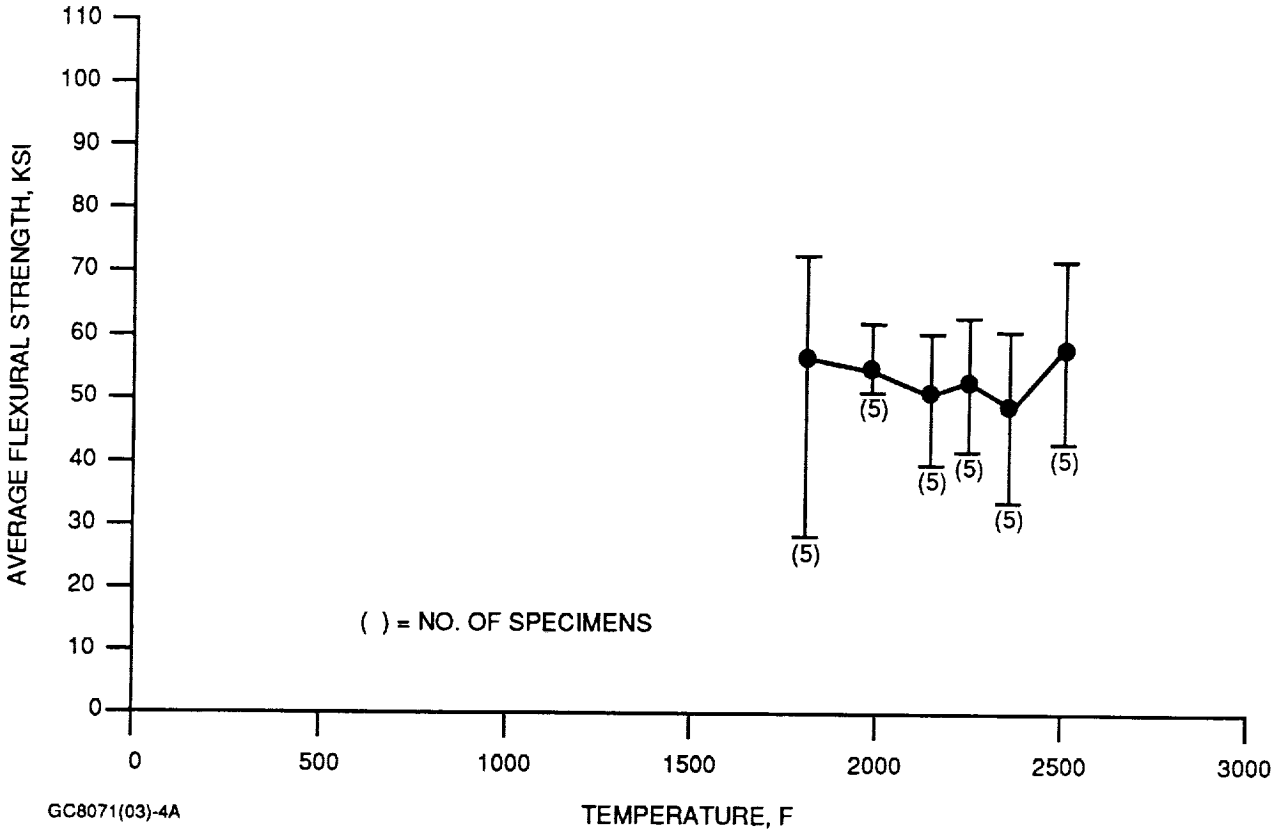

Figure 4. Elevated Temperature Test Results for Dow Corning Beta Silicon Carbide.

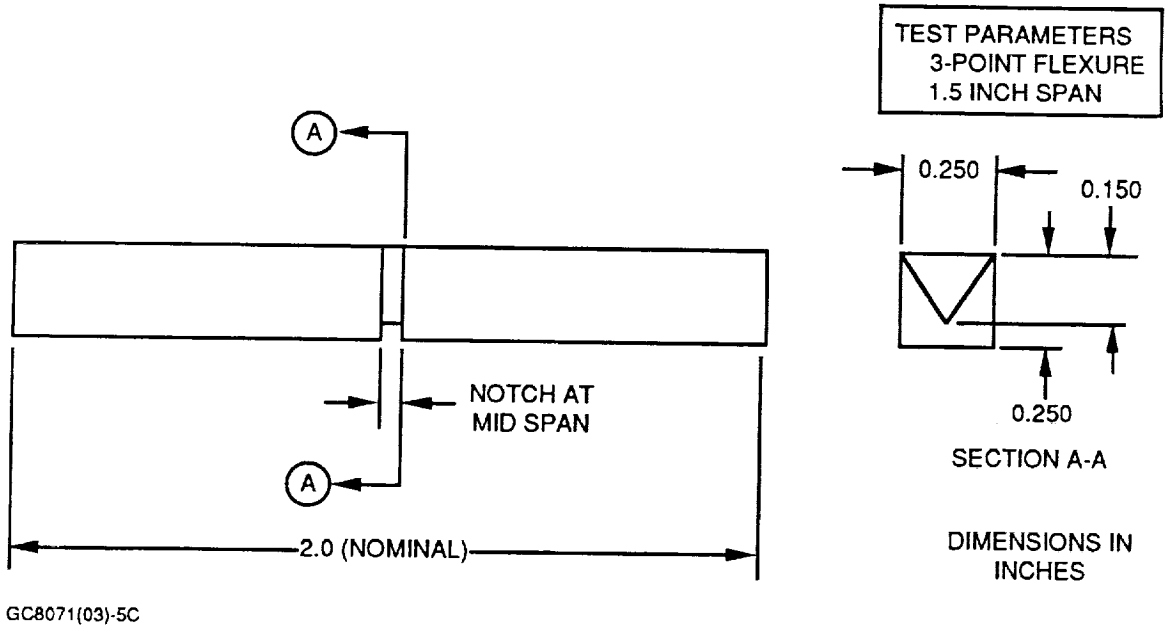

Figure 5. Chevron Notch Bend Specimen Design Was Used to Measure Fracture Toughness of Dow Corning Beta Silicon Carbide.

3.4.1 Regenerator Metallic Seal Development

Summary

Regenerator metallic seal development activities are aimed at improving the durability of the ATTAP seal system. During 1990, an alternate seal coating system (designated as Series 1) was identified which has superior chemical stability compared to the baseline system. Series 1 and baseline seal coatings were compared after one-hour static air heat treatments between 871C (1600F) and 1093C (2000F) [maximum regenerator seal temperature is 982C (1800F)]. For the baseline coating, interfacial reaction was observed beginning at the lowest heat treatment temperature, 871C (1600F). The Series 1 seal coating system was stable up to 1038C (1900F). After the 1093C (2000F) exposure, only minimal reaction of the Series 1 coating was noted.

Details of Seal Coating Development

At the end of 1989, an improved ceramic coated metallic regenerator seal shoe was identified. This configuration consisted of a new substrate, Haynes 230 (replacing the existing Inconel 601), NiCrAlY bond coat, I-00 intermediate coat, and I-112 top coat. Although this was the most stable configuration developed in 1989, chemical reactions between the bond coat and the I-00 interlayer were evident at 982C (1900F) and substrate attack was seen beginning at 1038C (1900F).

The goal for 1990 was to develop a chemically stable and strain-tolerant coating which would improve regenerator seal durability. Based on chemical thermodynamic analysis, alternate coating configurations were identified that do not use I-00 as a coating interlayer. Evaluation of three configurations was completed, including two new configurations and the 1989 system for comparison. All three systems include Haynes 230 substrate, NiCrAlY bond coating, and I-112 top coat. The three different intermediate coatings were: I-00 (Baseline), Y_2O_3 stabilized ZrO_2 (YSZ), and Al_2O_3 (Figure 6). The two new intermediate coatings showed no reaction in the chemical thermodynamic analysis.

The coated test coupons were heat treated at temperatures between 871C and 1093C (between 1600F and 2000F) at 55.6C (100F) intervals, for one hour in air to evaluate interfacial stability [982C (1800F) is the maximum ATTAP regenerator seal temperature].

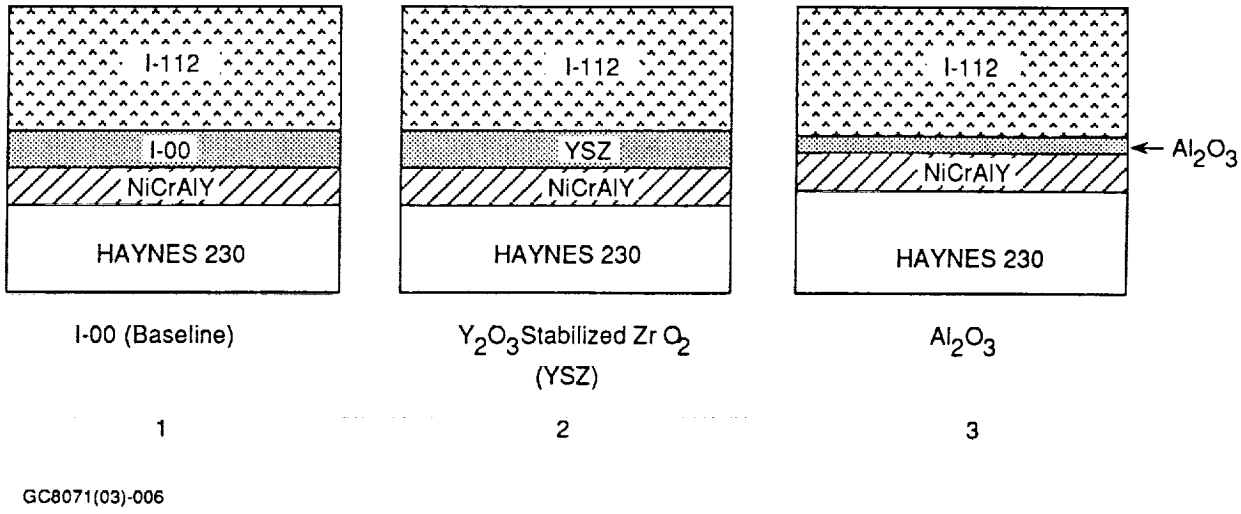

Figure 6. Three Regenerator Seal Coating Systems Were Evaluated During 1990.

Metallographic analysis of the heat-treated coupons indicated only the YSZ intermediate coating interfaces were stable at 982C (1800F), the seal design temperature. The YSZ interlayer was stable to 1038C (1900F); the I-00 coating reacted at 871C (1600F); and the Al_2O_3 interlayer reacted at 982C (1800F).

Scanning electron microscopy (SEM) and wavelength dispersive x-ray (WDX) analyses provided further evidence that the YSZ coating was the most stable intermediate coating tested. Coating systems containing the I-00 and YSZ intermediate coatings are compared in Figures 7 and 8, respectively. Figure 7 shows evidence of reaction between the I-00 intermediate coating and the NiCrAlY bond coat, following a one-hour heat treatment at 982C (1900F). Calcium and fluorine diffused into the bond coat from the I-00 layer. Oxidation and chrome depletion of the bond coat was also observed. Figure 8 shows no interdiffusion of elements across the YSZ coating interfaces after heat treatment at 982C (1800F).

In addition to chemical compatability, the thermal strain tolerance of the coating system was also addressed. Thermal strain tolerance testing was performed in a computer-controlled burner facility. The test goal was 1000 cycles from 204C (400F) to 982C (1800F) in 4 minutes. The samples are held at 982C (1800F) for 5 minutes, and then air quenched to 204C (400F). This test exposes the coating to a more severe environment than the seal would encounter in normal operation.

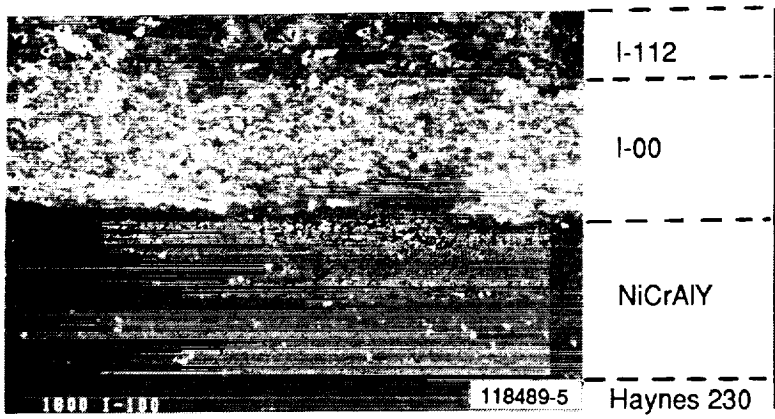

(a) SECTION THROUGH SPECIMEN WITH I-00 COATING

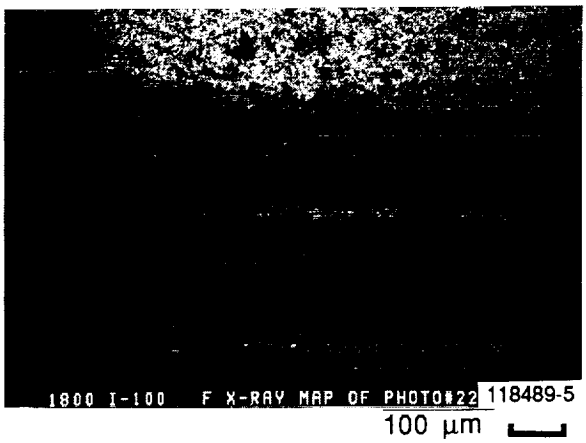

(b) FLUORINE WDX ELEMENT MAP

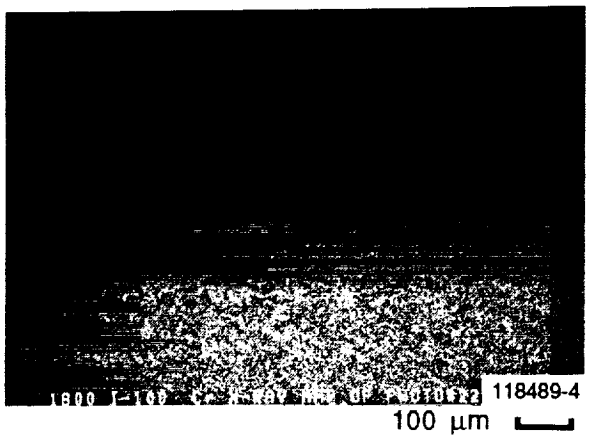

(c) CHROMIUM WDX ELEMENT MAP

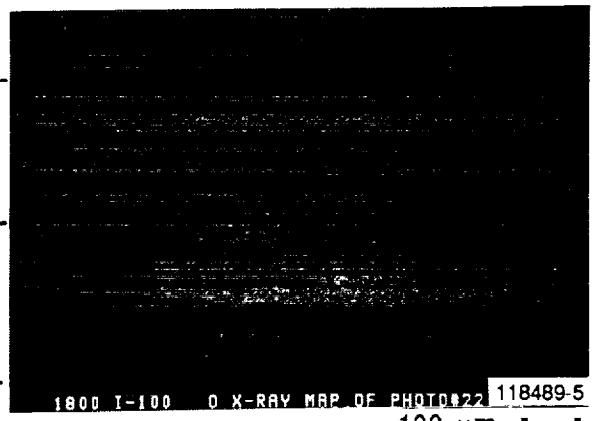

(d) OXYGEN WDX ELEMENT MAP

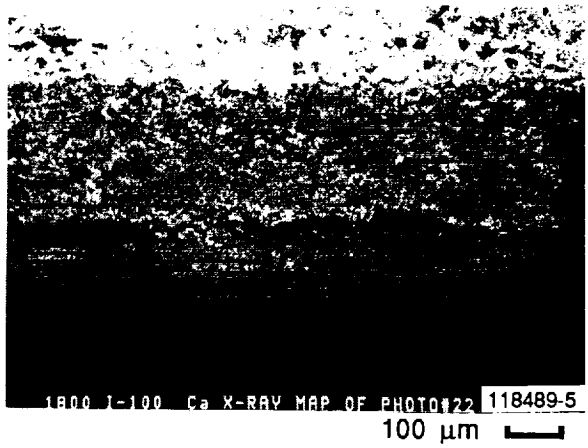

(e) CALCIUM WDX ELEMENT MAP

GB6990(19)-2A

Figure 7. **SEM Micrographs and WDX Element Maps Show Reaction Between I-00 and NiCrAlY Coatings After Heat Treatment at 982C (1800F) for One Hour.**

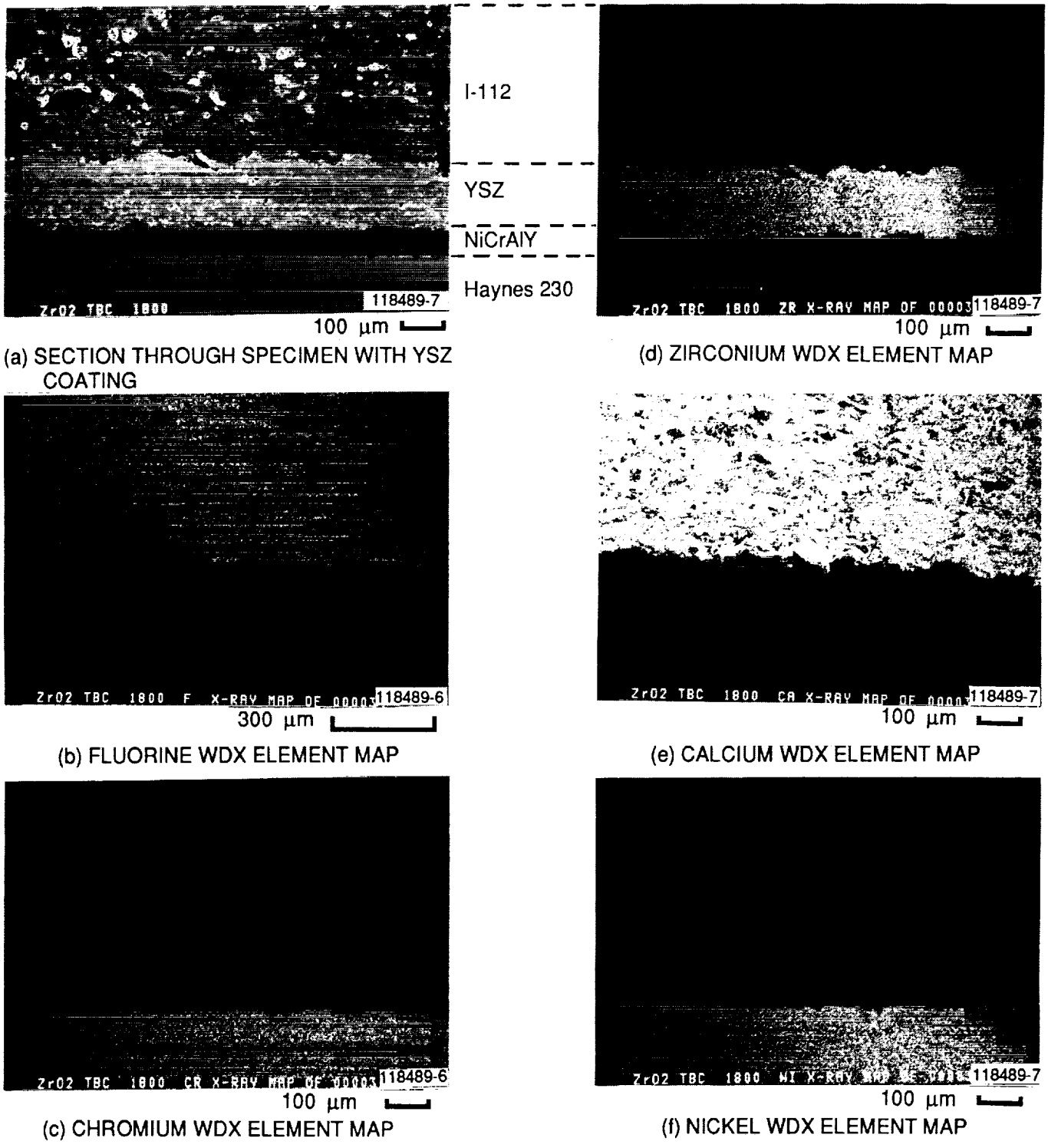

Figure 8. SEM Micrographs and WDX Element Maps Show No Interdiffusion Across YSZ Coating Interfaces After Heat Treatment at 982C (1800F) for One Hour.

Testing revealed failures in both systems with the I-00 and YSZ interlayers at a variety of different intervals during testing. Although both systems failed, they failed at different areas in the coating. The I-00 system failed at the NiCrAl/I-00 interface and the YSZ system failed at the YSZ/I-112 interface. The failure of the YSZ system was very clean, which suggests no chemical reactions occurred. The failure resulted from a weak mechanical bond at the interface. Activity has been defined for 1991 to address this mechanical weakness of the YSZ system. A system with a graded transition from the YSZ layer to the I-112 layer will be tested, as well as top coat segmentation to reduce surface strain (Figure 9).

3.4.2 Combustor Design

The main goal of the combustor improvement program is to provide clean burning over all AGT101 engine operating conditions, using DF-2 diesel fuel. In 1990, two parallel redesign efforts were initiated, to solve the coking problem in the AGT101 combustor section.

The first combustion system component redesign enlarged the pilot combustor. Figure 10(a) shows the stepped pilot combustor (baseline) design and Figure 10(b) shows the new enlarged, constant-diameter (with respect to the liner) pilot combustor. This new, enlarged combustor design moves the walls away from the primary burning zone and provides additional area for more efficient burning. Three-dimensional (3-D) analysis of the constant-diameter pilot combustor was accomplished using the AGT101 steady-state engine operating conditions, to optimize the hole geometry with respect to airflow, pressure drop, and velocity profiles.

The second component redesigned was the fuel nozzle. The redesign was initiated to improve fuel atomization, to simplify the nozzle design, and to provide easier cleaning and inspection. A pure-airblast concept was developed, because of inherent reliability shown in previous development testing. The redesigned nozzle was evaluated for spray angle, fuel droplet size (atomization criteria), pressure drop, and effects of differing air-assist pressures (Figure 11). Because of the experimental nature of these tests, further discussion will be addressed in Section 6.2.

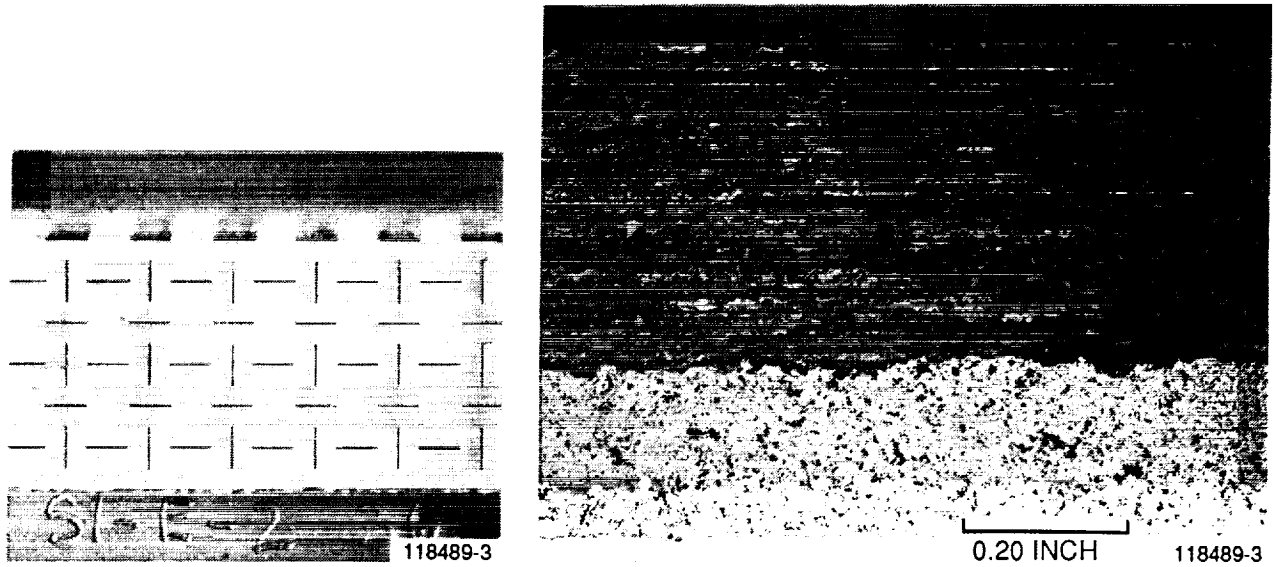

(a) SPECIMEN SIZE 1.50 X 1.25 INCHES

(b) PHOTOMICROGRAPH OF SECTION THROUGH SEGMENTATION

GB8071(03)-9

Figure 9. Top Coat Segmentation Will Be Evaluated for Strain Reduction.

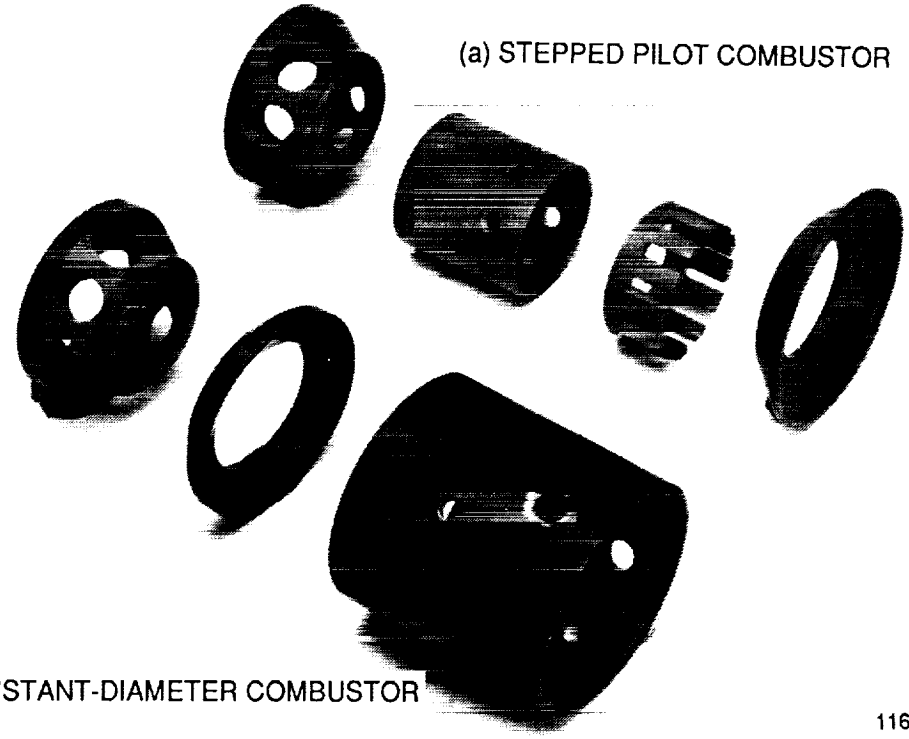

GB8071(03)-10

116457-2

Figure 10. AGT101 Ceramic Stepped Pilot Combustor (a) Was Redesigned in 1990 to Provide Increased, Constant Diameter (b) for Reduced Coking.

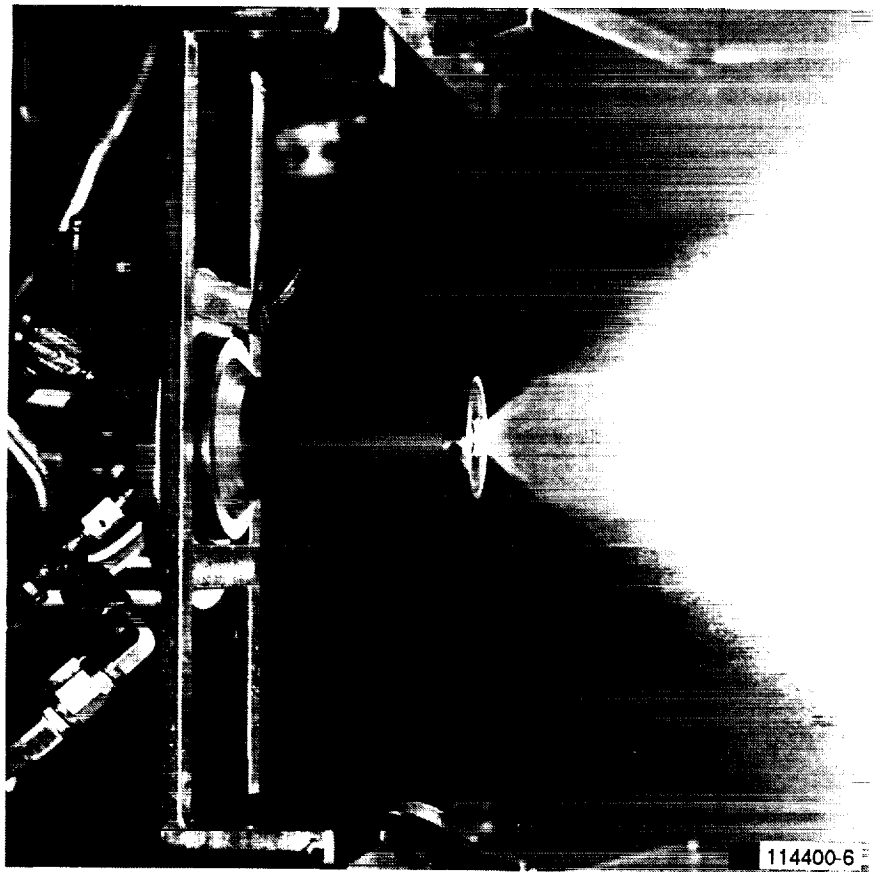

GB8071(03)-11

Figure 11. Second-Generation Simplex Airblast Fuel Nozzle Design Was Evaluated in 1990.

3.4.3 Seals

One of the critical sealing locations of the ATTAP test bed engine is at the flow separator housing (FSH) transition duct and turbine shroud junction. If the seal is not adequate in this area, there is a direct loss to the system due to air flowing from the compressor to the downstream side of the turbine. During the AGT101 program, seal improvements included changing the original single seal design to a dual seal configuration. Since then, a triple seal has been designed for use in the ATTAP test bed engine.

During 1990, the triple seal configuration was modified, as shown in Figure 12, as a result of other design changes to the ceramic flowpath hardware to incorporate the impact-resistant turbine stage.

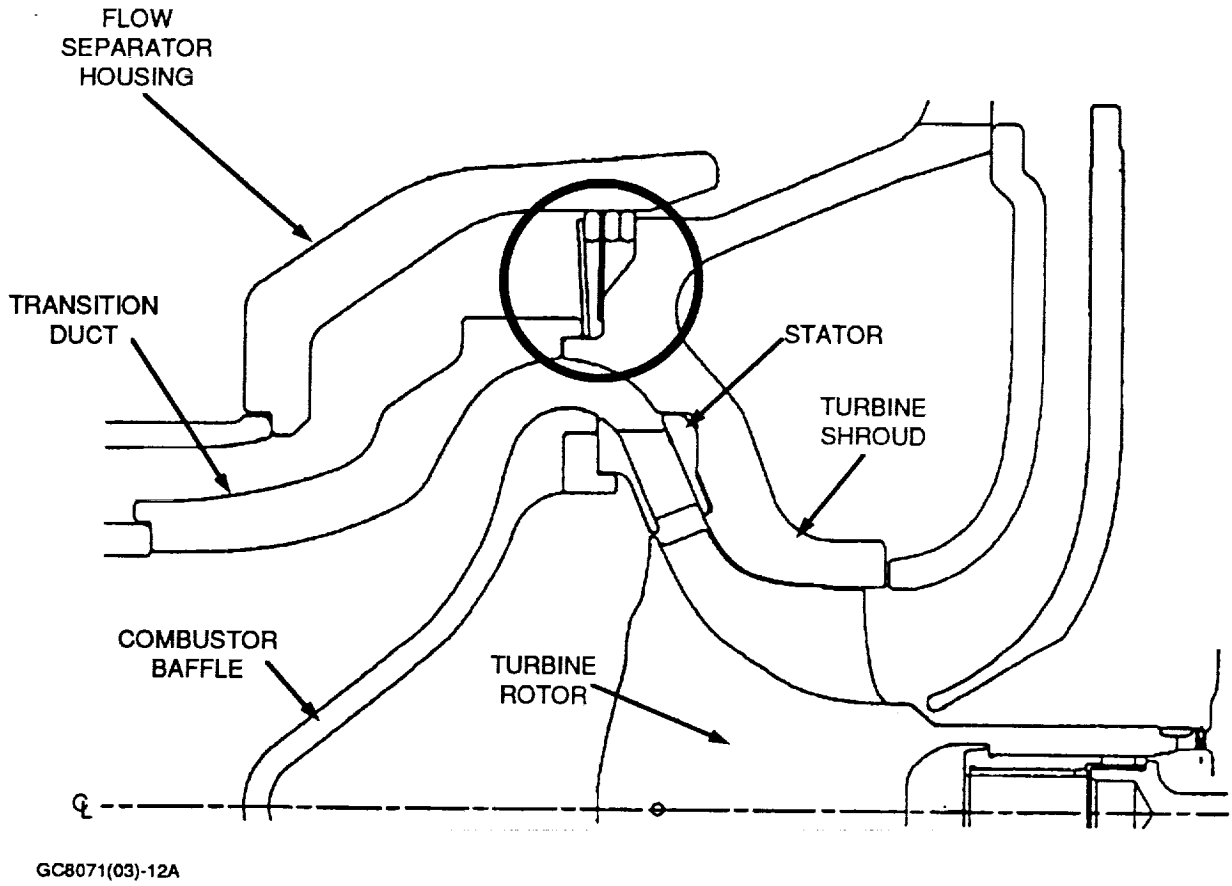

Figure 12. Triple Seal Configuration Was Modified to Accommodate the Impact-Resistant Turbine Inlet Flowpath.

3.4.4 Turbine Inlet Particle Separator (TIPS) Design

The overall goal of the TIPS test program was to identify a means of separating particles from the gas stream in order to eliminate foreign object damage (FOD) from particle impacts on the ceramic turbine rotor. To accomplish this task, a two-step approach was utilized: first, verify the TIPS concept, and second, assess the feasibility of the ceramic TIPS concept.

To verify the TIPS design, several alternatives were fabricated and evaluated. The center-flow TIPS design exhibited the best separation efficiency, 97.5 percent, with a pressure loss of approximately 3 percent. Experimental parametric evaluation, using Taguchi methods and high-speed photography, was accomplished to fine-tune the TIPS conceptual design.

Following verification of the TIPS concept and determination of an effective geometry, incorporation into the engine was considered. The feasibility assessment of the ceramic TIPS concept utilized aerothermodynamic data from the AGT101 ceramic engine, two-dimensional (2-D) temperature analysis of the TIPS components, and material feasibility and fabricability information. The aerothermodynamic data (Figure 13) showed engine gas temperatures in the combustion region could reach 1893C (3440F). The 2-D thermal analysis took into consideration this engine gas temperature data, coupled with the radiation, convection, and conduction components of heat transfer. The TIPS center-flow cone design was then analytically placed in the combustor at three different axial locations and the temperature of the cone at each location was calculated (Figure 14).

The results of this study showed that the TIPS cone temperatures would exceed the available ceramic material capabilities. This lead to a decision not to implement the ceramic TIPS center-flow concept into the AGT101 ceramic test bed engine for ATTAP. Subsequently, program activity on this component has been discontinued.

3.4.5 Flow Separator Housing (FSH) Support

The FSH support system shown in Figure 15 underwent design changes during this past year. The earlier design was complex; the size, tight tolerances, and irregular-shape holes contributed to manufacturing difficulties. The new design deletes the irregular-shaped holes and simplifies the hardware, which should reduce the machining time and cost. Size and tolerance ranges remain the same. A proof test rig was developed to test the redesigned support system. The rig, shown in Figure 16, simulated the pressure loads and ring support translation found in the engine.

The proof test was successful. During this test, the FSH support was subjected to a 1700 lb load with a translation of 0.130 inch. (The predicted load and translation in an engine are approximately 1550 lbs and 0.065 inch). The lithium aluminum silicate (LAS) block was undamaged and there was no deflection of the metal hardware. Further development and testing of the system are planned for the upcoming reporting period.

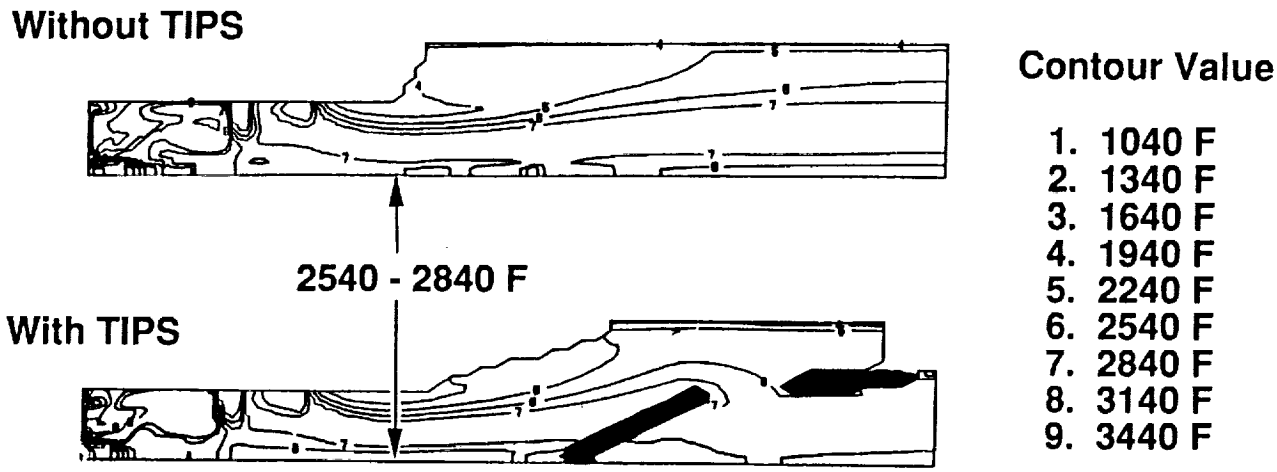

Figure 13. **Aerothermodynamic Data Shows Gas Temperatures in the Combustor Can Reach 1893C (3440F).**

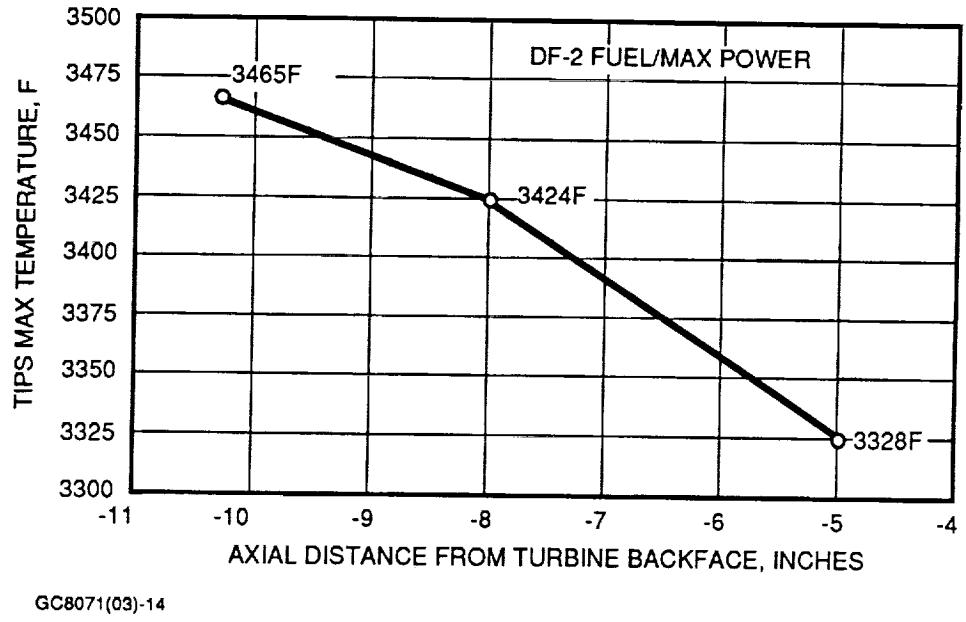

Figure 14. **Calculations Show TIPS Temperatures Would Exceed Present Ceramic Material Capabilities.**

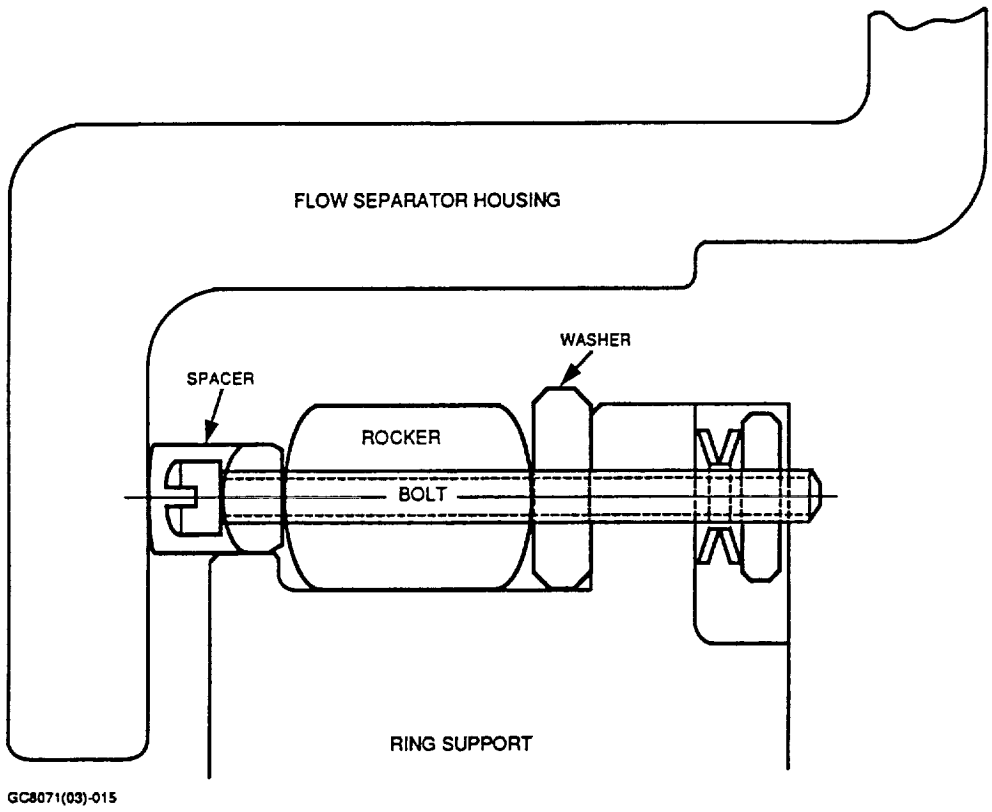

Figure 15. Redesign of the FSH Support Was Accomplished.

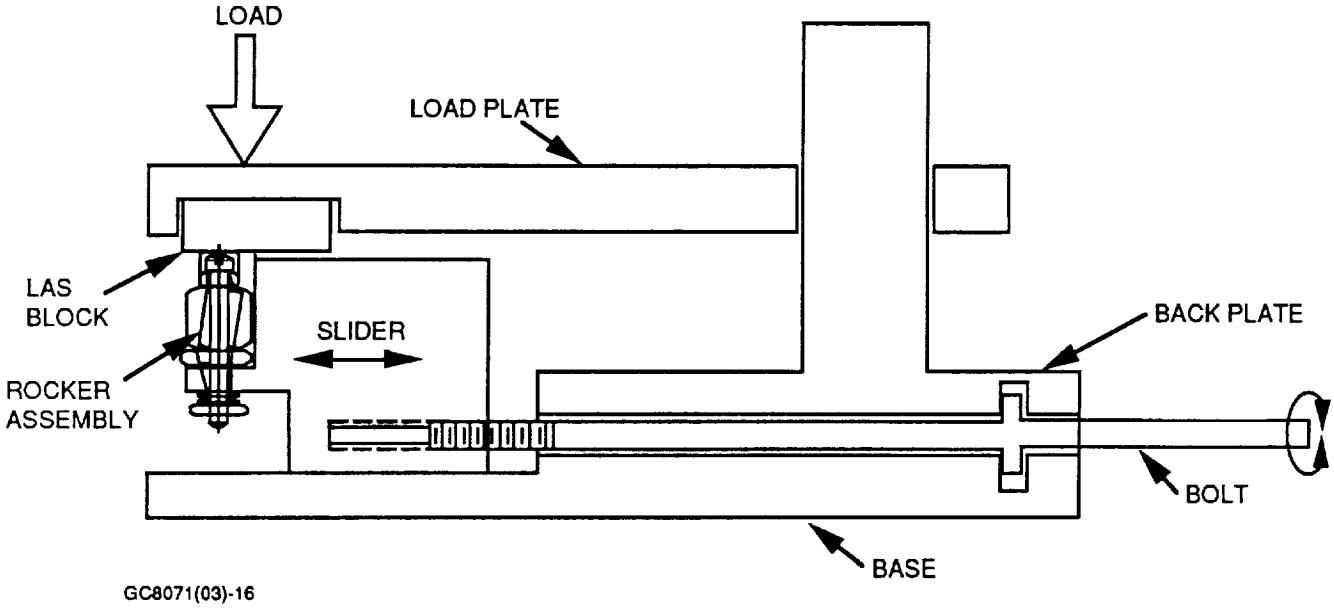

Figure 16. FSH Support Test Rig Simulated Pressure Loads and Ring Support Translation.

3.4.6 Ceramic Bolt Assembly

From the results of an analysis performed during this reporting period, it was determined that deflections in the metallic portions of the ceramic bolt assembly used to attach the ceramic turbine shroud to the metallic housing could cause failure. Therefore, the bolt assembly (Figure 17) was redesigned to ensure integrity during engine operation.

Three ceramic bolt assemblies were tested at room temperature to better understand the predicted deflections. A finite element model (FEM) analysis was performed to predict temperatures, stresses, and deflections of the bolt assembly at various operating conditions. The analysis predicted yielding of the locking nut at the bolt assembly proof load of 30 in-lb torque. Also, the locking nut could not withstand the stresses induced at the operating temperature of 760C (1400F).

A redesign provided a solution with minimal cost and effort. Dimensional changes increased the sleeve thickness by 0.005 inch, and decreased the locking nut and ceramic bolt outer diameters by 0.010 inch. Also, the material of the locking nut and sleeve was changed from Hastelloy X to Astroloy C.

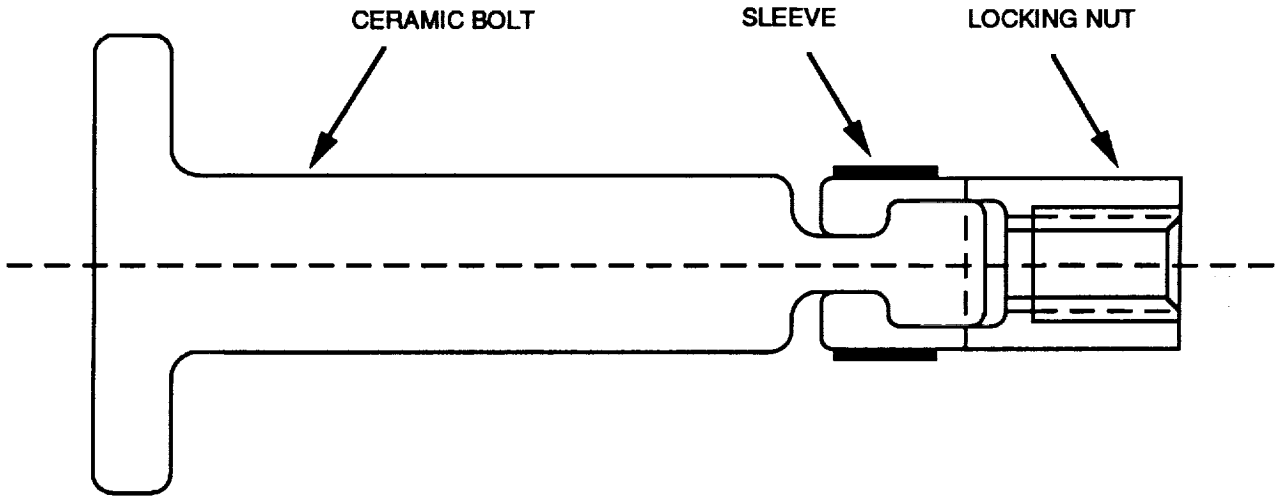

GC8071(03)-17

Figure 17. The Locking Nut and Sleeve of the ATTAP Ceramic Bolt Assembly Were Modified for Increased Reliability.

4.0 CERAMIC COMPONENT DESIGN

4.1 Design Methods for Impact Damage Resistance

Work concentrated on the experimental observation and analytical modeling of two types of impact damage:

- o Local damage near the point of impact
- o Structural failure away from the point of impact due to bending stresses

Experimental work has guided the development of impact models for both modes of failure. Structural impact predictions use fast fracture methods, and local damage methods use micro-mechanical models integrated with FEM stress methods to predict damage evolution during the impact process.

The impact methods development work is being performed in collaboration with the University of Dayton Research Institute (UDRI) in Dayton, Ohio.

4.1.1 Experimental Observations of Structural Impact Damage

Structural impact response data were generated to support development of the structural impact model. Structural impact test specimens (Figure 18) were fabricated from SN-84 type silicon nitride (Si_3N_4) and are being impact tested at UDRI. The geometry of the test specimens was varied to evaluate the effects of blade thickness, length, stiffness, and surface strength on impact resistance. A schematic of the impact target test setup is shown in Figure 19. The matrix of tests planned is shown in Table 2.

A majority of the impact tests will be accomplished with 0.1-inch diameter graphite projectiles at room temperature; but other projectile materials, projectile sizes, and impact locations will also be used. Details of the impact conditions and specimen variables are listed in Table 2 (highlighted portion). High-speed photography is being used to document the impact event(s), and strain gages will be attached to selected test specimens to evaluate the response of the specimen during impact.

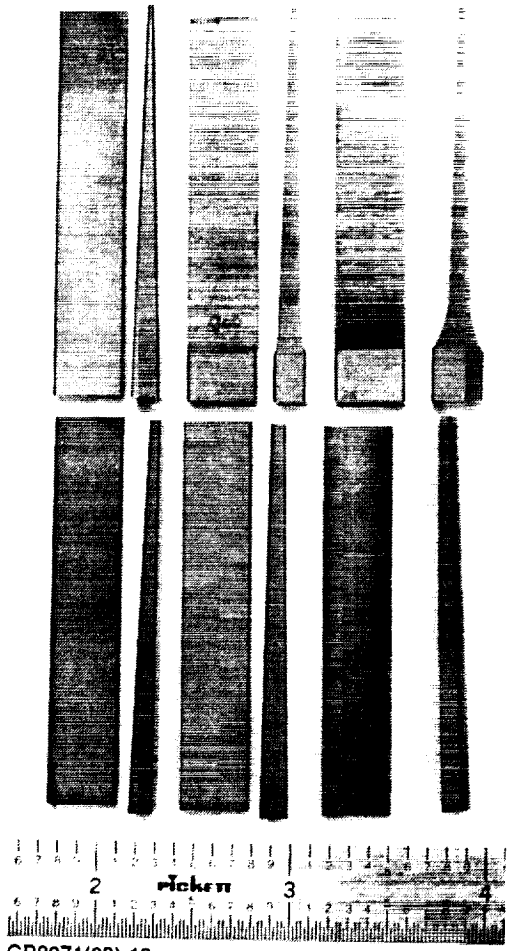

Figure 18. Impact Test Specimens Were Fabricated to Evaluate Effects of Blade Geometry on Impact Resistance.

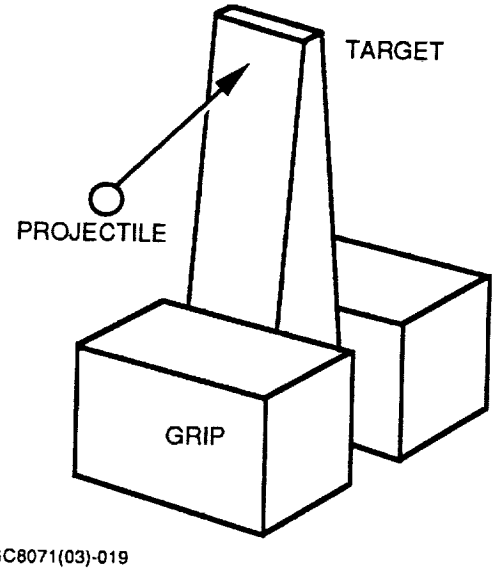

Figure 19. Schematic of Target Used for Examination of Structural Impact Damage.

TABLE 2. STRUCTURAL IMPACT TEST VARIABLES

TEST NUMBER	SPECIMEN TYPE	NUMBER OF SPECIMENS	SPECIMEN VARIABLES												IMPACT EXPERIMENT VARIABLES											
			THICKNESS AT TIP (IN)			TAPER ANGLE		FILLET RADIUS			MACHINING DIRECTION		CURVED SHAPE		OVER HANG		IMPACT LOCATION		BALL MATERIAL		BALL SIZE		IMPACT ANGLE		TEMP (F)	
			0.03	0.05	0.075	1.0°	1.6°	0.0"	0.25"	0.5"	A	B	Y	N	1.6"	0.9"	A	B	A	B	0.1"	0.2"	90°	45°	75	2300
1	1	10		•		•		•			•			•	•		•		•		•		•		•	
2	1	8		•		•		•			•			•		•	•		•		•		•		•	
3	1	10		•		•		•			•			•	•		•			•	•		•		•	
4	1	8		•		•		•			•			•	•		•		•			•	•		•	
5	1	8		•		•		•			•			•	•		•		•		•		•			•
6	1	8		•		•		•			•			•	•		•		•		•			•	•	
7	1	8		•		•		•			•			•	•			•	•		•		•		•	
8	2	10			•	•		•			•			•	•		•		•		•		•		•	
9	2	10			•	•		•			•			•		•	•		•		•		•		•	
10	6	10	•				•	•			•			•	•		•		•		•		•		•	
11	4	5		•		•			•		•			•			•		•		•		•		•	
12	3	5		•		•				•	•			•			•		•		•		•		•	
13	4	5		•		•			•		•			•				•	•		•		•		•	
14	3	5		•		•				•	•			•				•	•		•		•		•	
15	5	10		•		•		•			•		•		•		•		•		•		•		•	
16	7	10		•		•		•				•		•	•		•		•		•		•		•	
17	8	10			•	•		•				•		•	•		•		•		•		•		•	

GC8071(03)-99B

4.1.2 Experimental Observations of Local Impact Damage

During this reporting period, experimental work and characterization of local impact damage was conducted in support of the Phase II Impact Model Development effort. Sintered SN-84 Si_3N_4 flexure bars were impact tested at UDRI. Si_3N_4 projectiles are currently used to generate experimental data, but the model will be applicable to other projectile materials and will be used to design rotors for resistance against engine carbon particle impacts. The characterization will include optical microscopy, non-destructive evaluation (NDE), and measurement of retained flexure strength. This information is needed for calibration of the local damage model used in the Elastic-Plastic Impact Computations (EPIC) computer code.

During this reporting period, critical impact velocity data was generated for the baseline test condition. Testing was also completed for SN-84 flexure bars with as-densified surfaces. Impact damage data for as-densified surfaces is essential because this represents some of the important engine component surfaces, e.g., rotor blades. Two high-toughness Si_3N_4 materials

(Allied-Signal AS440 and AS721) were impacted at room temperature to evaluate the effect of toughness on localized damage. Results from these tests, discussed below, will support model development for local damage by characterizing the effects of surface condition and material toughness.

Thirty SN-84 Si_3N_4 1/4x1/8x2 inch flexure bars with machined surfaces were impacted with 1/32-inch diameter Si_3N_4 projectiles at room temperature to generate baseline critical impact velocity data. Specimen surface impact damage was assessed by visual inspection at 200X magnification using a reflected light microscope with polarized light and by fluorescent penetrant inspection (FPI). The impacted bars were later tested in 4-point bending and fractography was performed, which showed that all failures originated from impact damage. The inspection and strength degradations results are shown in Figure 20; the critical impact damage velocity was estimated to be 690 ft/sec. The large variation in retained strength indicated was due to the fact that the impact damage flaws do not have the same severity in all directions. Bars not showing significant strength degradation did not have flaws oriented in the worst-stressed (transverse) direction during the strength testing.

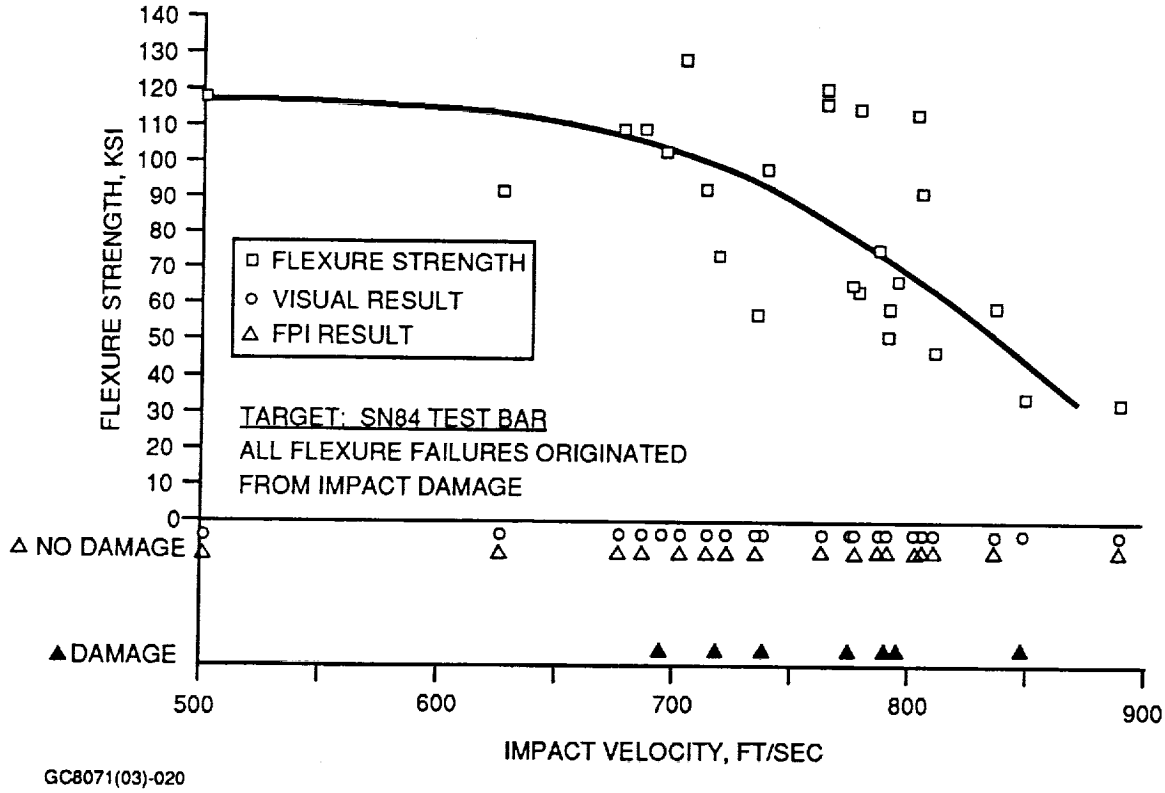

Figure 20. Critical Impact Velocity Was Determined for 1/32-Inch Diameter Si_3N_4 Projectiles.

The critical velocities for differing diameter spherical Si_3N_4 projectiles tested so far are plotted in Figure 21. The data shows good correlation for the projectile size range tested. The critical projectile diameter at a rotor tip speed of 2300 ft/sec is estimated to be about 0.0078 inch (1/128 inch).

Impact testing was also completed for identical SN-84 bars with as-densified surfaces at room temperature using 1/32-inch diameter Si_3N_4 projectiles. The comparison of impact damage resistance between machined and as-densified surfaces is essential to make the results meaningful for engine components. Specimen surface impact damage was assessed by visual inspection and the results are presented in Figure 22. The critical velocity was 490 ft/sec. This is approximately 200 ft/sec less than the results obtained from the baseline targets, which had machined surfaces. This lower velocity is not unexpected, since SN-84 test bars with as-densified surfaces show typical strength degradation of about 30 percent compared with machined bars. It is expected that the critical velocity for local damage from carbon particles in engine components will be higher than the velocity for Si_3N_4 projectiles. This will be confirmed in subsequent carbon projectile impact studies.

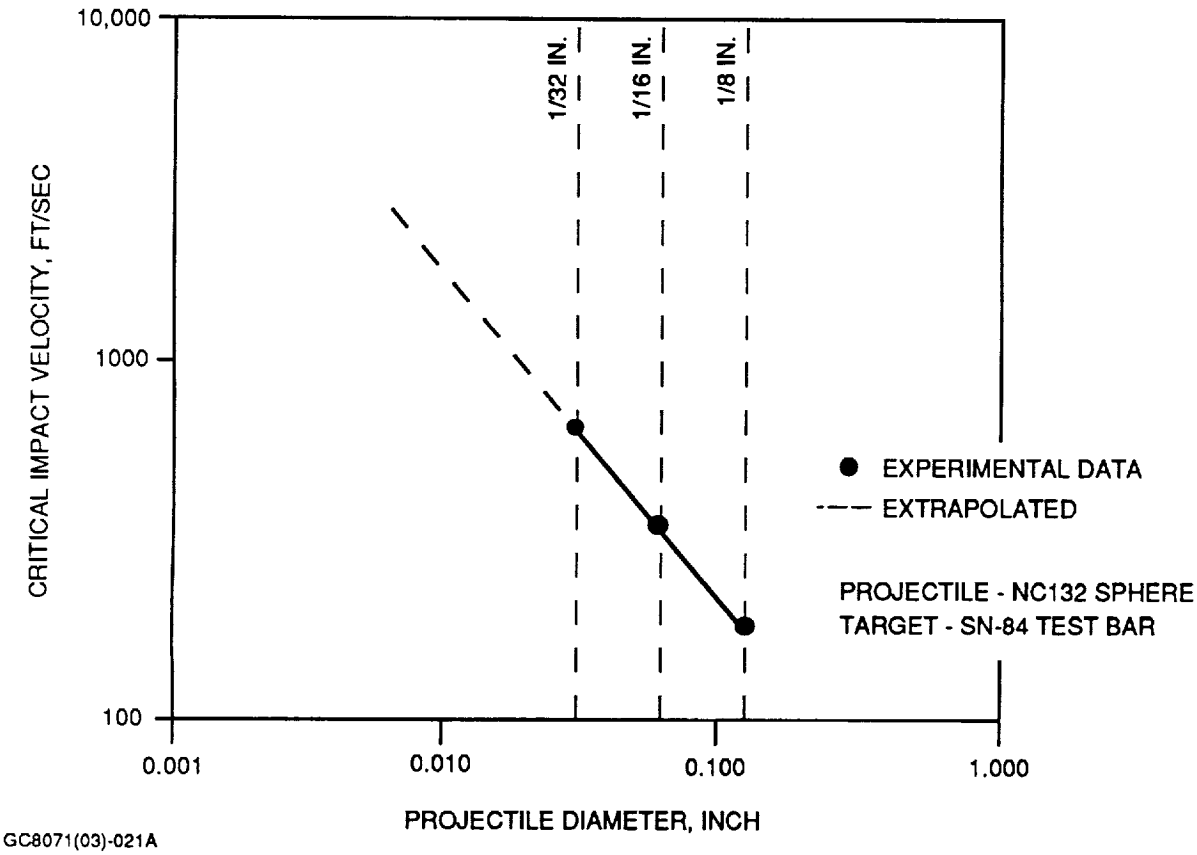

Figure 21. Critical Si_3N_4 Projectile Size for Localized Damage.

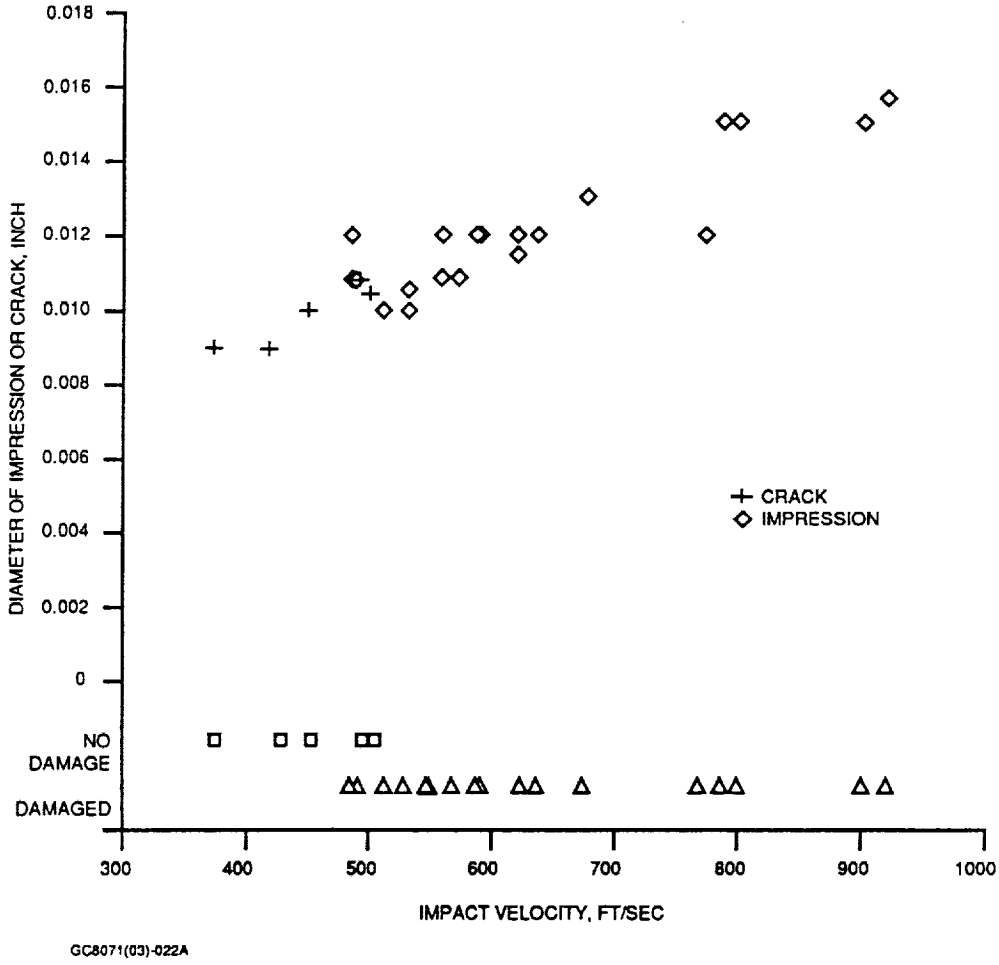

Figure 22. Impact Test Results for SN-84 Si_3N_4 Bars With As-Densified Surfaces Show Lower Critical Velocity Than for Machined Surfaces. Diameter of Impact Cracks Increased With Impact Velocity.

The diameters of the impressions or cracks on the impact surfaces were also measured and are presented in Figure 22. The diameter of the cracks increased with increasing impact velocity. The impact bars are to be flexure tested in four-point bending at room temperature, to evaluate strength degradation due to impact damage.

Flexure bars 1/4x1/8x2 inch in size made from two high-toughness Si_3N_4 materials (AS440 and AS721) were impacted at room temperature to evaluate the effect of fracture toughness (K_{IC}) on impact damage resistance. The high-toughness materials selected were in-situ acicular grain-toughened silicon nitrides supplied by Allied-Signal Research and Technology. Preliminary results (single data points obtained with 1/32-inch diameter Si_3N_4 projectiles) indicate the critical impact velocity for these materials was lower than for the baseline SN-84 Si_3N_4 target material (627 ft/sec for AS440 and 604 ft/sec for AS721, vs 690 ft/sec for SN-84). This result is not unexpected, if localized impact resistance is more affected by surface strength of the target material rather than fracture toughness. Additional testing is planned to verify the decrement in impact tolerance for the lower strength, high toughness materials.

Microscopic impact damage characterization was conducted to identify damage characteristics, including impression depth, macro-damage, and micro-damage to assist impact methods model development. Specimens were impacted at selected velocities and temperatures (see Table 3) to generate specific types of damage for evaluation. Damage features on the fractured surfaces (as shown schematically in Figure 23) and polished specimen surfaces were examined.

TABLE 3. IMPACT TEST MATRIX FOR MICROSCOPIC DAMAGE CHARACTERIZATION

Projectile Diameter, Inch	Target Temperature, F	Range of Impact Velocities, ft/sec	Number of Specimens	Expected Impact Damage
1/16	Room	320-350	3	Impression
1/16	Room	450-475	3	Ring Cracks
1/16	Room	580-620	3	Radial Cracks
1/16	2300	130-220	3	Impression
1/16	2300	280-310	3	Radial Cracks
1/16	2300	450-500	3	Ring Cracks
1/8	Room	220-260	4*	Ring Cracks

*One specimen will have three impacts

8071(03)-3A

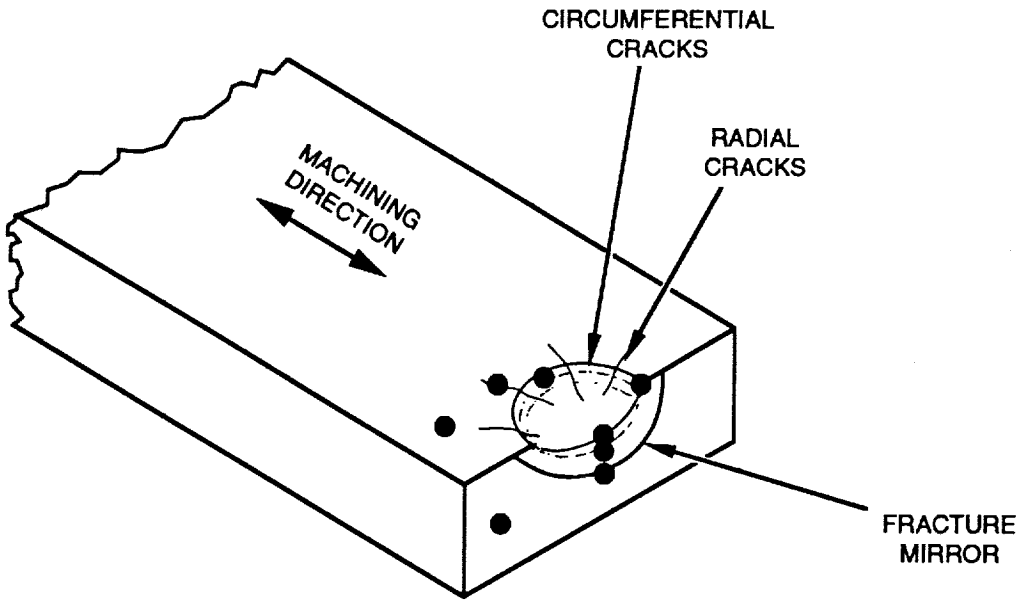

● LOCATIONS EXAMINED UNDER HIGH MAGNIFICATION

GC8071(03)-23

Figure 23. Damage Features on Impacted Bars Were Examined.

A special microscopy investigation of local impact damage was accomplished as a joint effort between GAPD and UDRI. UDRI developed a new technique to prepare impacted specimens for scanning electron microscope (SEM) examination that yields more details of the sub-surface damage than previously seen. The new technique incorporates specimen thinning, notching, and precracking to create a low-energy fracture plane across the impact location, which eliminates crack branching and other confusing features that are observed on a typical fracture surface if the specimen is broken using the standard flexure test technique. Figure 24 shows SEM photos of a fracture surface intersecting an impact site. The target was SN-84 Si_3N_4, and the projectile was a 1/16-inch diameter Si_3N_4 ball impacting at 441 ft/sec at room temperature. A Hertzian crack approximately 40 microns deep (indicated by arrow H) and two circumferential cracks approximately 10 microns deep (arrow C) can be observed. The circumferential cracks also turned into a Hertzian-type crack [indicated by the arrow in Figure 24(b).

Since impact events occur at high impact velocity, materials parameters generated for high strain rates are needed to calibrate the impact model. Preliminary results generated by UDRI for SN-84 Si_3N_4 (shown in Figure 25) indicate approximately 4.5 times difference between dynamic (high strain rate) and static strength. Strain rates up to 10^4 in/in/sec were

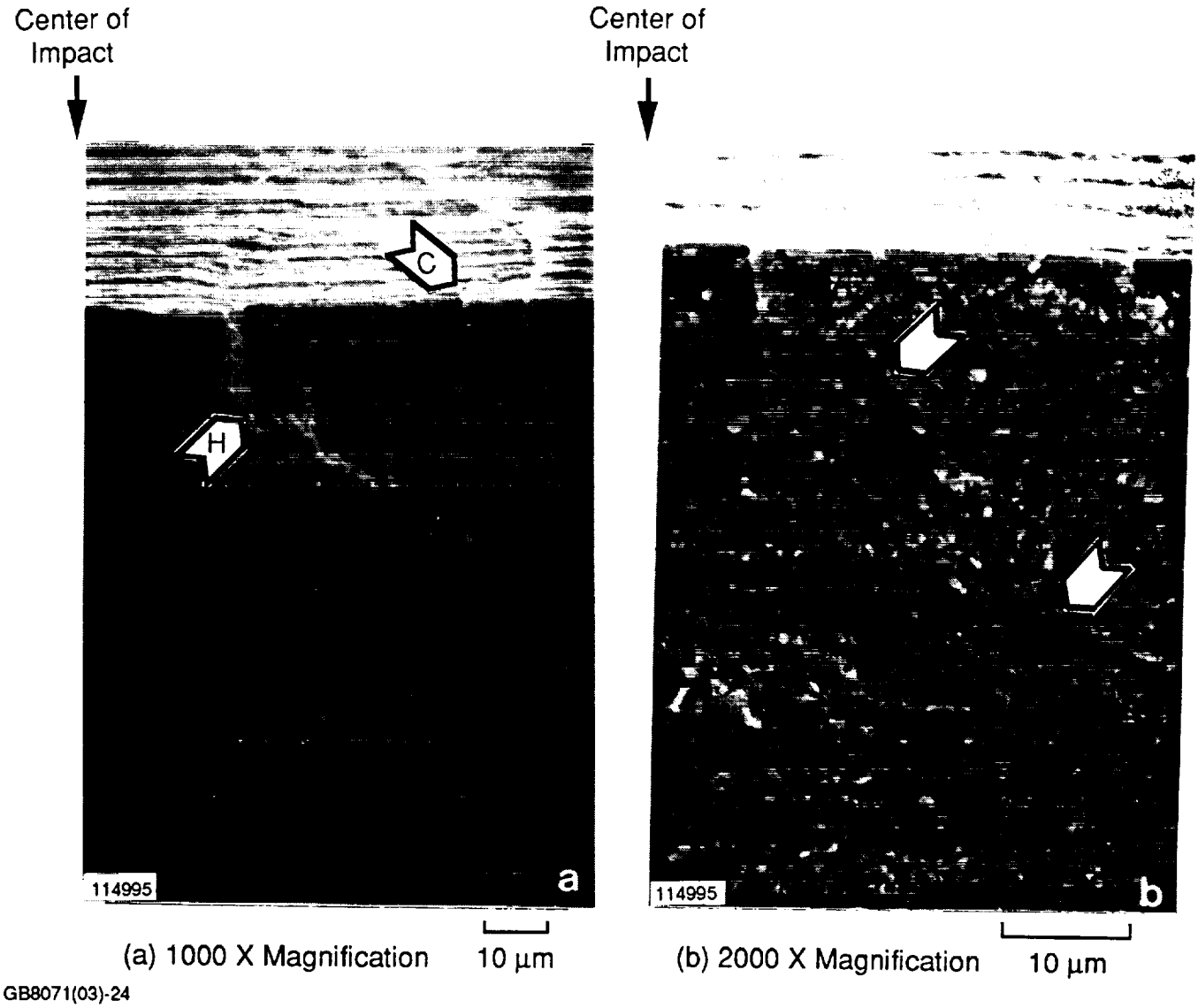

Figure 24. Fracture Surface Across Impact Site Shows Hertzian (H) and Circumferential (C) Cracks.

generated, using the split Hopkinson's bar arrangement which uses a torsional bar spring to deliver the high strain rate loading. Low strain rate tests were accomplished using a standard Instron Universal Testing Machine. Tensile strength data were generated from diameteral compression disk specimens and compression strength data were generated from cylindrical specimens, as shown in Figure 25. High-speed photography was used to verify whether acceptable specimen fracture occurred in the diametral compression tests. Figure 26 shows photographs illustrating a typical fracture sequence.

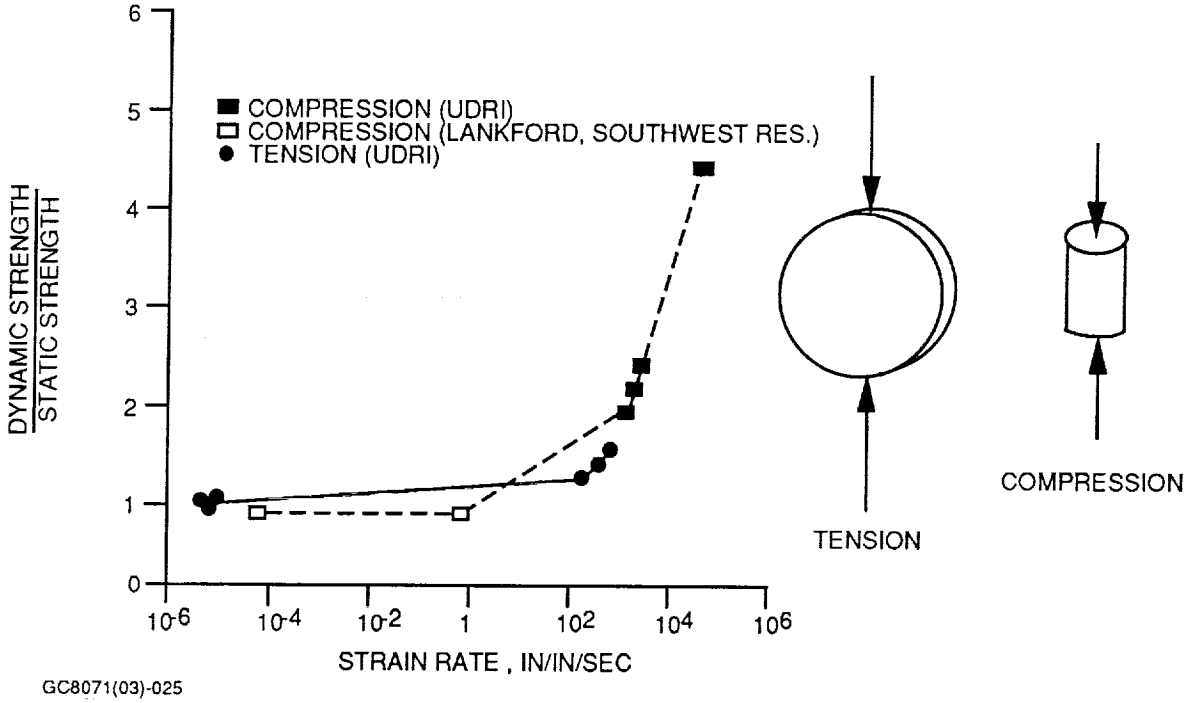

Figure 25. The Effects of High Strain Rate on Si_3N_4 Strength Have Been Established.

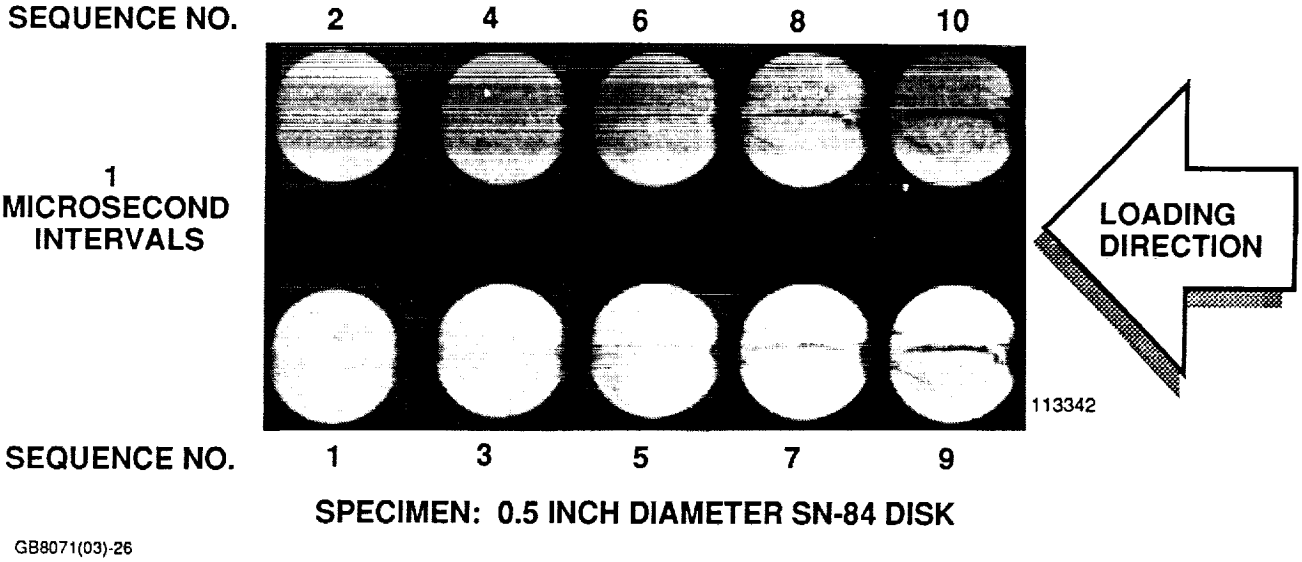

Figure 26. High-Speed Photography Is Being Used to Validate Diametral Disk Compression Tests.

ORIGINAL PAGE
BLACK AND WHITE PHOTOGRAPH

4.1.3 Structural Impact Failure Modeling

Structural impact design methods are being developed and used to design impact-resistant ceramic turbine wheels to survive carbon impact. Structural impact failure refers to fast fracture of a ceramic component by impact-induced stresses, which are usually dictated by the dynamic response of the structure. GAPD's approach to develop methods for predicting structural impact failure is depicted in Figure 27. EPIC-3, a finite element impact code using Lagrangian representation, has been adapted for impact stress analysis. The behavior of the interface between target and projectile is modeled by the so-called slideline logic, which includes conservation of mass, momentum, and energy between the nodes of the target and the nodes of the projectile which come into contact.

Impact tests have demonstrated the capability of EPIC-3 to predict impact failures. When EPIC-3 was used to analyze three different ceramic blades impacted by graphite spheres, the calculated maximum principal stress on the blades was found in the same area where the blades fractured in the impact tests. The magnitude of the stresses was close to the surface tensile strength of the blade material. This implied that fast fracture of ceramic blades will occur if the maximum impact stress exceeds the material strength.

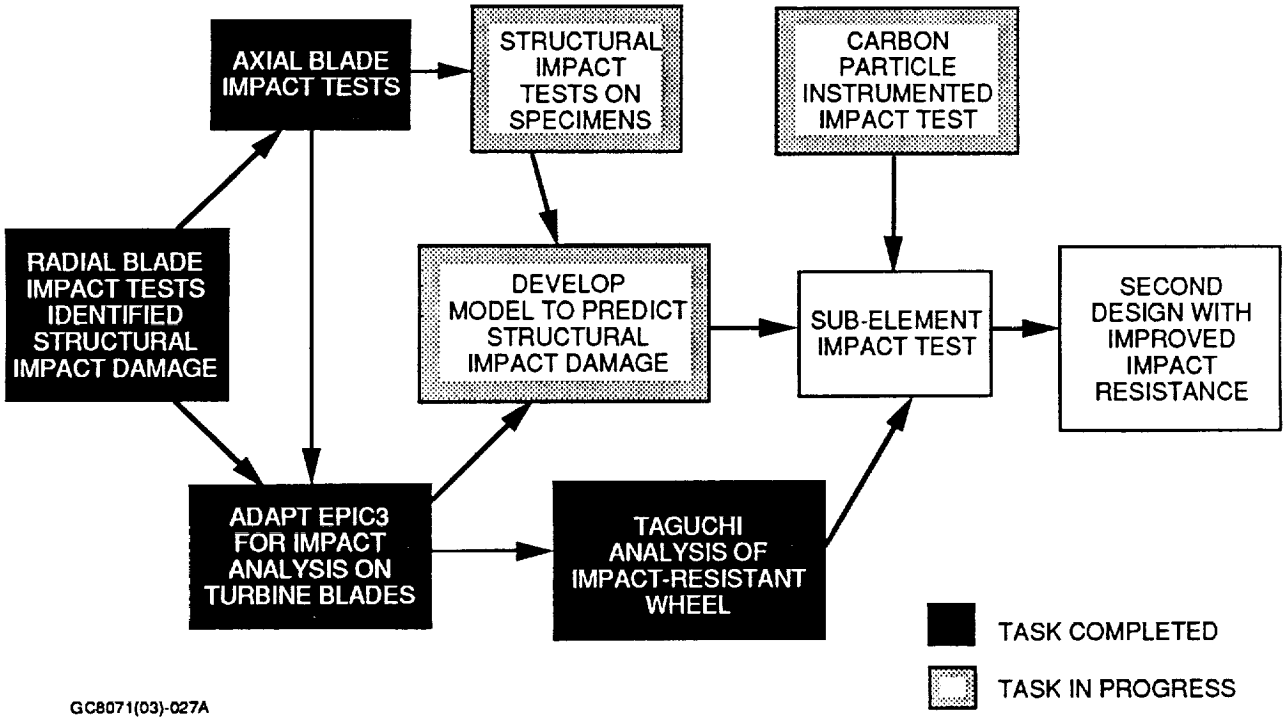

Figure 27. ATTAP Ceramic Design Methodology is Addressing Structural Impact Damage.

After EPIC-3 was demonstrated to be an effective tool for impact stress analysis, it was used in conjunction with the Taguchi statistical method in the design of an improved impact-resistant ceramic turbine blade. In the first phase of this study, seven design parameters were identified as potentially sensitive to blade impact resistance. These parameters (Figure 28) are: blade thickness, blade taper-ratio from hub to tip, blade width at inlet, beta angle at inlet, fillet radius, hub stiffness, and tip speed. Each parameter was given two values and an L_{12} orthogonal array was created with 12 different blade designs.

Impact stresses were calculated for each of the 12 blade designs, using EPIC-3. These analyses simulated a graphite sphere of 0.1-inch diameter impacting the suction side of the blade at the radial corner of the inducer. The highest possible impact velocity was used in the simulations. This impact velocity occurs when a particle enters the turbine with negligible tangential velocity and is hit by a blade rotating at full speed.

The maximum principal stress determined for each blade in the L_{12} array is listed in Table 4. The large difference between the highest stress, 778 ksi for Blade 2, and the lowest, 203 ksi for Blade 7, indicates the sensitivity of impact stress to the design parameters evaluated. The results from the Taguchi study are summarized in Table 5. The strongest factors were identified as blade thickness, beta angle, fillet radius, and tip speed. Taper-ratio, hub stiffness, and blade height had little effect.

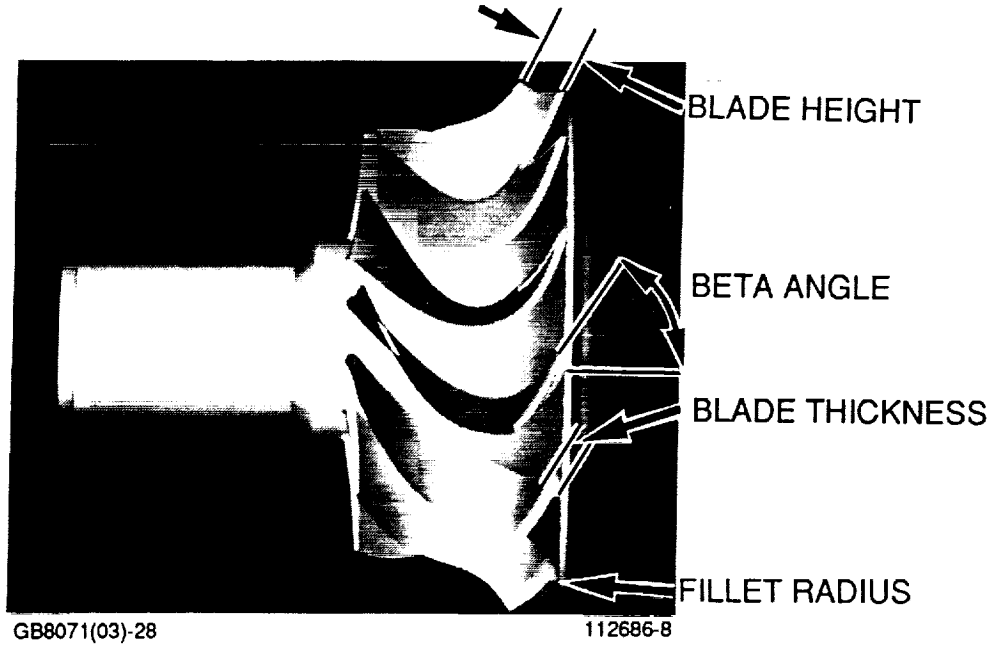

Figure 28. Design Parameters Influencing Impact Resistance Were Evaluated.

TABLE 4. ORTHOGONAL ARRAY OF 12 BLADES AND IMPACT STRESS ANALYSIS RESULTS

Blade No.	Thickness	Taper Ratio	Height	Beta Angle	Fillet Radius	Impact Velocity	Hub Stiffness	σ1 (Max)*
1	Thin	Small	Short	Small	Small	Low	High	0.94
2	Thin	Small	Short	Small	Small	High	Low	1.13
3	Thin	Small	Tall	Large	Large	Low	High	0.43
4	Thin	Large	Short	Large	Large	Low	Low	0.47
5	Thin	Large	Tall	Small	Large	High	High	0.84
6	Thin	Large	Tall	Large	Small	High	Low	0.86
7	Thick	Small	Tall	Large	Small	Low	Low	0.29
8	Thick	Small	Tall	Small	Large	High	Low	0.42
9	Thick	Small	Short	Large	Large	High	High	0.32
10	Thick	Large	Tall	Small	Small	Low	High	0.54
11	Thick	Large	Short	Large	Small	High	High	0.47
12	Thick	Large	Short	Small	Large	Low	Low	0.54

*Normalized relative to AGT101 radial blade.

8071(03)-4B

TABLE 5. SUMMARY OF TAGUCHI IMPACT STUDY RESULTS

	(A) Thickness	(B) Taper Ratio	(C) Height	(D) Beta Angle	(E) Fillet Radius	(F) Impact Velocity	(G) Hub Stiffness
Level 1	3700 (536.7)	2800 (406.2)	3060 (443.8)	3498 (507.3)	3356 (486.7)	2551 (370.0)	2950 (427.8)
Level 2	2049 (297.2)	2949 (427.7)	2689 (390.0)	2251 (326.5)	2394 (347.2)	3197 (463.7)	2799 (406.0)
Influence	1651 (239.5)	-148 (-21.5)	371 (53.8)	1247 (180.8)	962 (139.5)	-645 (-93.5)	150 (21.8)
Stress values for each combination in MPa (ksi)							

8071(03)-5

Since interactions are confounded in L_{12} orthogonal arrays, a further study using an L_8 orthogonal array was conducted. The three strongest parameters (blade thickness, beta angle, and fillet radius) and their interactions were examined, and the results are summarized in Table 6. The results show that the interactions among the three parameters were negligible.

Due to aerodynamic constraints, the fillet radius cannot be increased; but there is still a certain range for the blade thickness and the beta angle to vary. Therefore, a matrix of nine blades was selected to determine the impact stress as a function of blade thickness and beta angle. The results are shown in Figure 29. The lowest calculated impact stress is 23 percent of the impact stress in the baseline AGT101 radial blade design. A blade geometry definition will be selected based on this plot, along with aerodynamic and thermal stress analysis considerations. This blade and the initial impact-resistant blade will be fabricated into single ceramic blade subelement test specimens for impact testing. These tests will demonstrate the impact resistance of both blades and the usefulness of these methods for improving impact resistance.

TABLE 6. INTERACTIONS AMONG DESIGN PARAMETERS WERE FOUND TO BE INSIGNIFICANT FROM THE L8 MATRIX ANALYTICAL RESULTS

No.	Factors	Level 1	Level 2	Percent Influence
1	Thickness	Thin	Thick	71.42
2	Beta Angle	Small	Large	13.86
3	1 x 2 Interaction	--	--	1.45
4	Fillet Radius	Small	Large	10.69
5	1 x 4 Interaction	--	--	2.38
6	2 x 4 Interaction	--	--	0.07
7	1 x 2 x 4 Interaction	--	--	0.13

8071(03)-6A

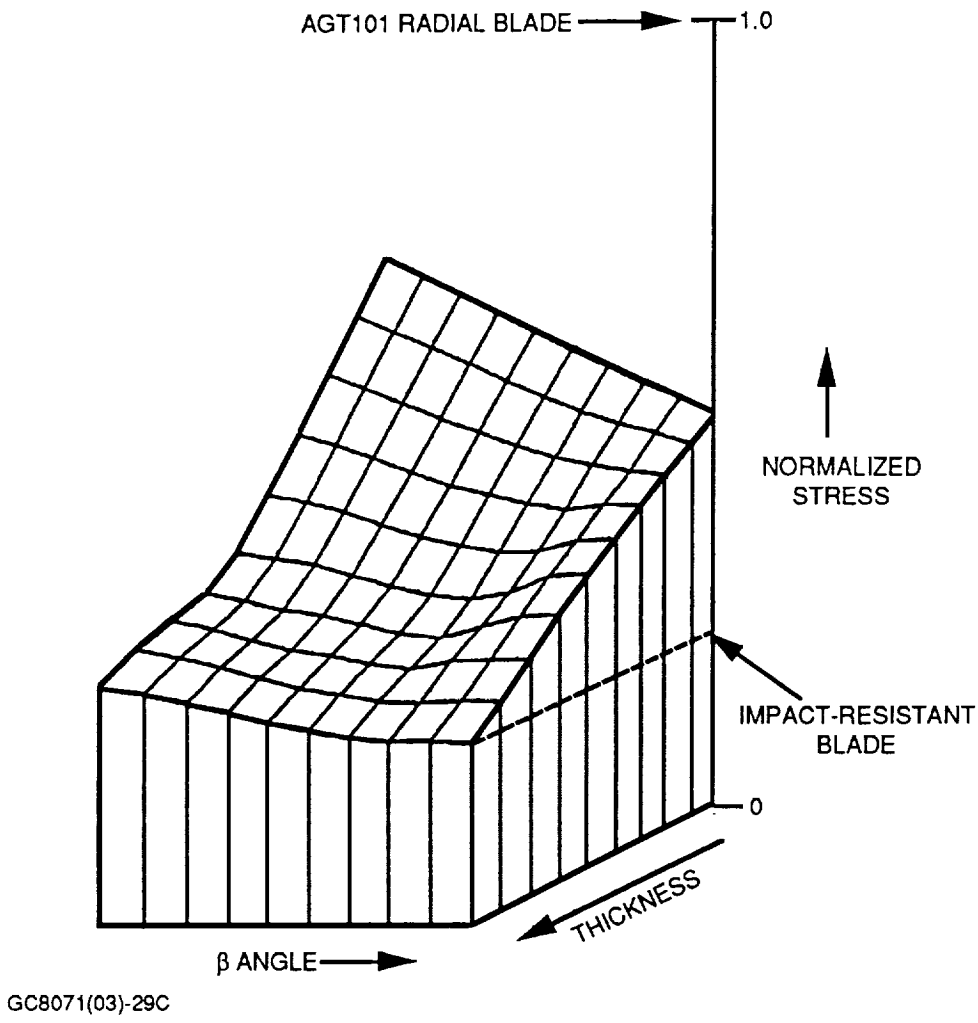

Figure 29. Maximum Impact Stresses Varied As a Function of Blade Thickness and Beta Angle.

The impact stresses reported here are higher than the stresses these blades will actually see in engine operation. In these impact analyses, the projectile deformation remained elastic regardless of the magnitude of the stresses. However, it was observed that graphite balls pulverize at impact velocities of 200 to 400 ft/sec, which are below the impact velocities used in the analyses (approximately 1870 ft/sec). As a consequence, all of the calculated impact stress values are higher than actual impact stresses for two reasons:

- o First, a portion of the energy in the system is consumed in generating a large amount of new surface during pulverization of the projectile (occuring during an actual impact);

- o Second, the impact load imparted by the small, pulverized particles is expected to be less than a single particle of the same mass, as simulated in the current analyses.

A graphite spherical projectile impact test on instrumented ceramic rods is underway to generate the information needed to model the effect of pulverization and incorporate the model into our impact simulations.

4.1.4 Local Impact Damage Modeling

The microphysical model being developed in the ATTAP ceramic impact design study is aimed at predicting critical impact velocities causing local impact damage under differing impact conditions. The baseline assumptions made in this local impact model are:

(1) Ceramics behave inelastically by yielding and developing micro-cracking when local impact stresses exceed threshold values.

(2) Micro-cracks nucleate when the maximum principal stress exceeds the material tensile strength, or when the compressive hydrostatic stress exceeds the Hugoniot strength of the material.

(3) Growth of micro-cracks is governed by Griffith criterion.

(4) Damage to the material may be measured by the volume fraction of cracks and pores introduced by impact.

(5) Impact damage degrades the elastic modulus of the material, and thus alters stress wave propagation.

Impact damage occurring at the micro-structural level will in turn change the load-carrying capability of the material. Because both the stress wave and the material damage evolve concurrently during an impact event, the material behavior model and the damage model are incorporated into every step of the time integration in the EPIC-3 stress wave computer code. When the calculated damage parameter reaches a critical value in an element, this element can no longer support tensile load, corresponding to the formation of a macrocrack at that location. This model has shown success in modeling simple impact problems. Two of the experimental observations being studied are discussed below.

Figure 30 illustrates a plate impact test setup. The longitudinal stress wave is measured and recorded by a pressure gage mounted at the interface of the Si_3N_4 plate and the polymethylmethacrylate (PMMA) plastic foam backing material. The newly-developed micro-physical model is then used to simulate the same impact event. Excellent agreement was observed between the measured and the calculated stresses, as shown in Figure 31.

The low-velocity plate impact (165 ft/sec) did not cause damage during the compression cycle of the stress wave. Therefore, there was no stress relaxation associated with modulus degradation during the compressive period of loading. This is indicated by the approximately constant compressive stress during the first wave in Figure 31(a). For the higher-velocity impact (785 ft/sec), the compressive stress wave caused material damage, and the accumulating material damage caused a decrease in the material load-carrying capability. This is demonstrated by the decrease of the stress wave magnitude shown by the slanted line during the first compressive wave in Figure 31(b).

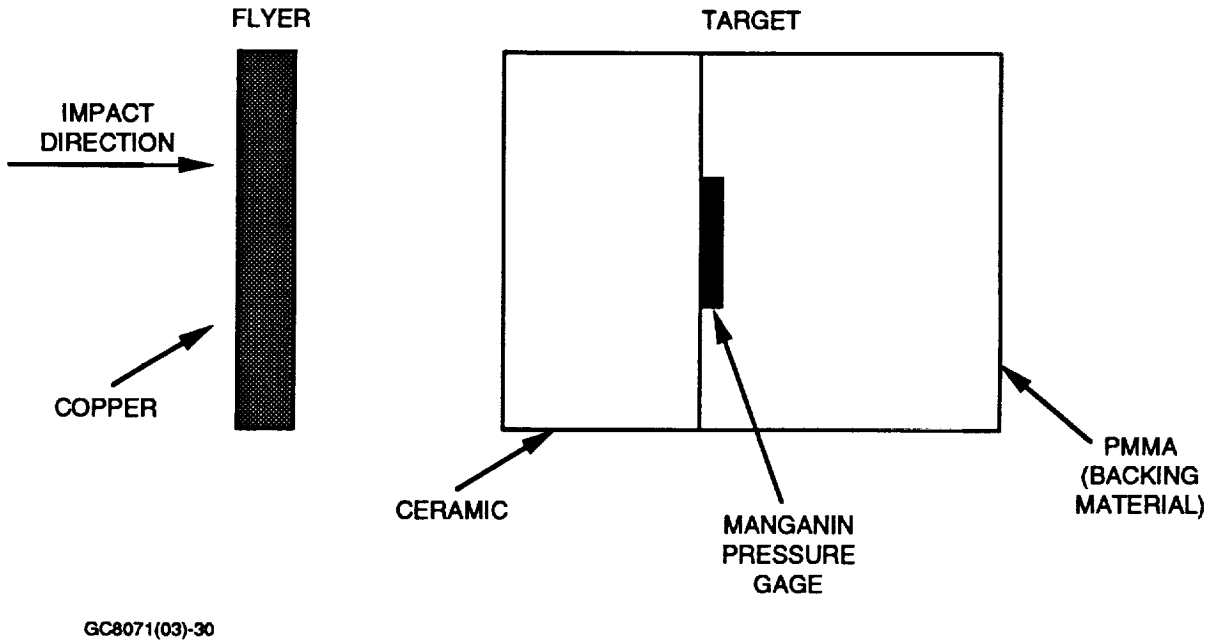

Figure 30. Numerical Simulation of a Plate Impact Was Conducted to Verify the Impact Model.

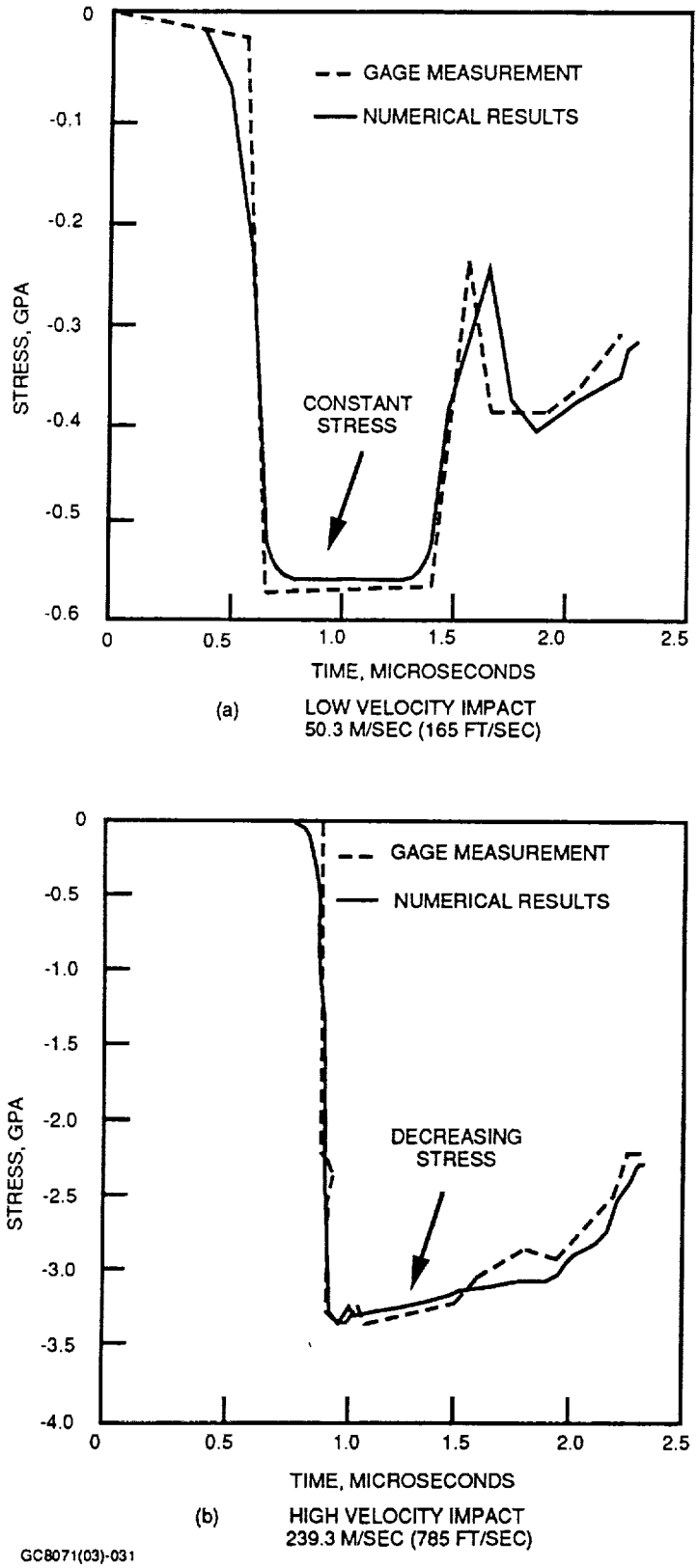

Figure 31. Numerical Simulation Results Agreed Well With Plate Impact Test Results.

The local impact damage model was also used to simulate a particle impact. Figure 32 shows a finite element model (FEM) of a sphere impacting a flat plate. This was a simulation of the baseline local impact damage test reported in Section 4.1.2. When the critical impact velocity determined from the experiment was used in the analysis, the most severe damage predicted by the model was concentrated in one element; the element position corresponded with the location of circumferential cracks observed in the test specimens. This example demonstrated that the model can successfully predict the critical impact velocity for local impact damage.

Currently, GAPD's main effort is directed toward fine-tuning the model and deriving a systematic method to determine the material constant used in the model. This local impact damage model is now being extended from two dimensional (2-D) into 3-D simulations. The model will then be used to predict the critical impact veolcity and the pattern of local cracks for components with complicated geometry such as the ceramic stators. These analyses will then be verified with ceramic stator impact tests.

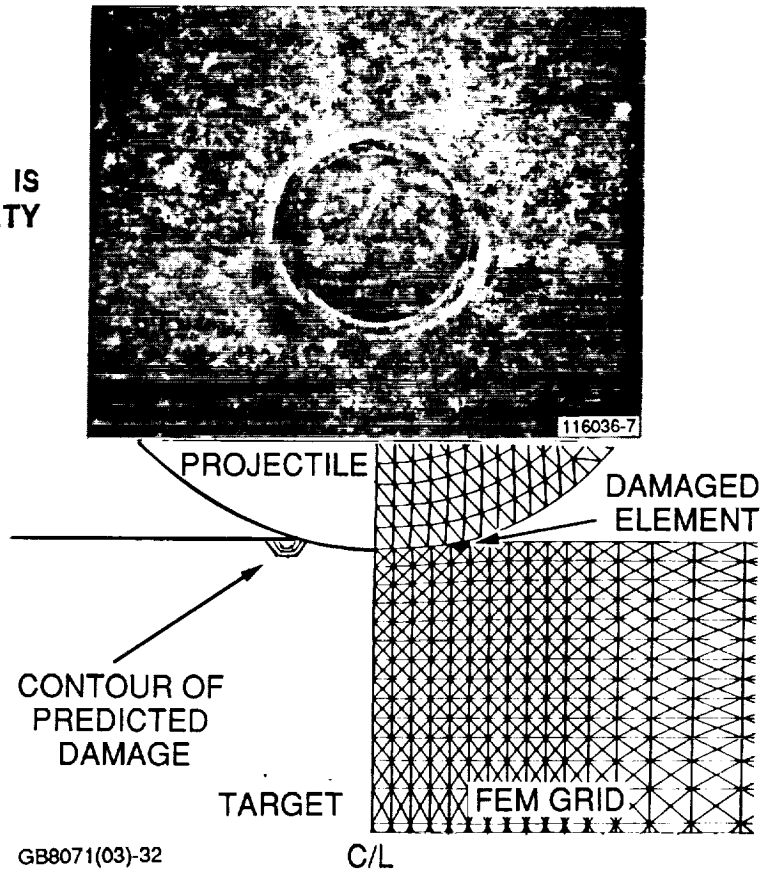

Figure 32. Microphysical Model Can Predict the Location of Local Ring Cracks Under the Critical Input Velocity.

4.2 Ceramic Components Analyses

Impact-Resistant Turbine Structures Analysis

The new impact-resistant turbine required a redesign of the configuration of several ceramic structural components. Components that were significantly redesigned (Figure 33) include 1) the turbine shroud, 2) the stator, 3) the transition duct, 4) the combustor baffle, and 5) the spring seals at the shroud/flow separator housing (FSH) interface. Minor modifications were also incorporated into 6) the inner and 7) the outer diffusers. Analyses performed on these components include pressure loading and transient thermal cycles. The cycles analyzed consisted of start and acceleration to idle speed, hold at idle for a given time (10 or 110 seconds), and then acceleration to the flat-rated speed, sea level (FRSL) condition, as shown in Figure 34.

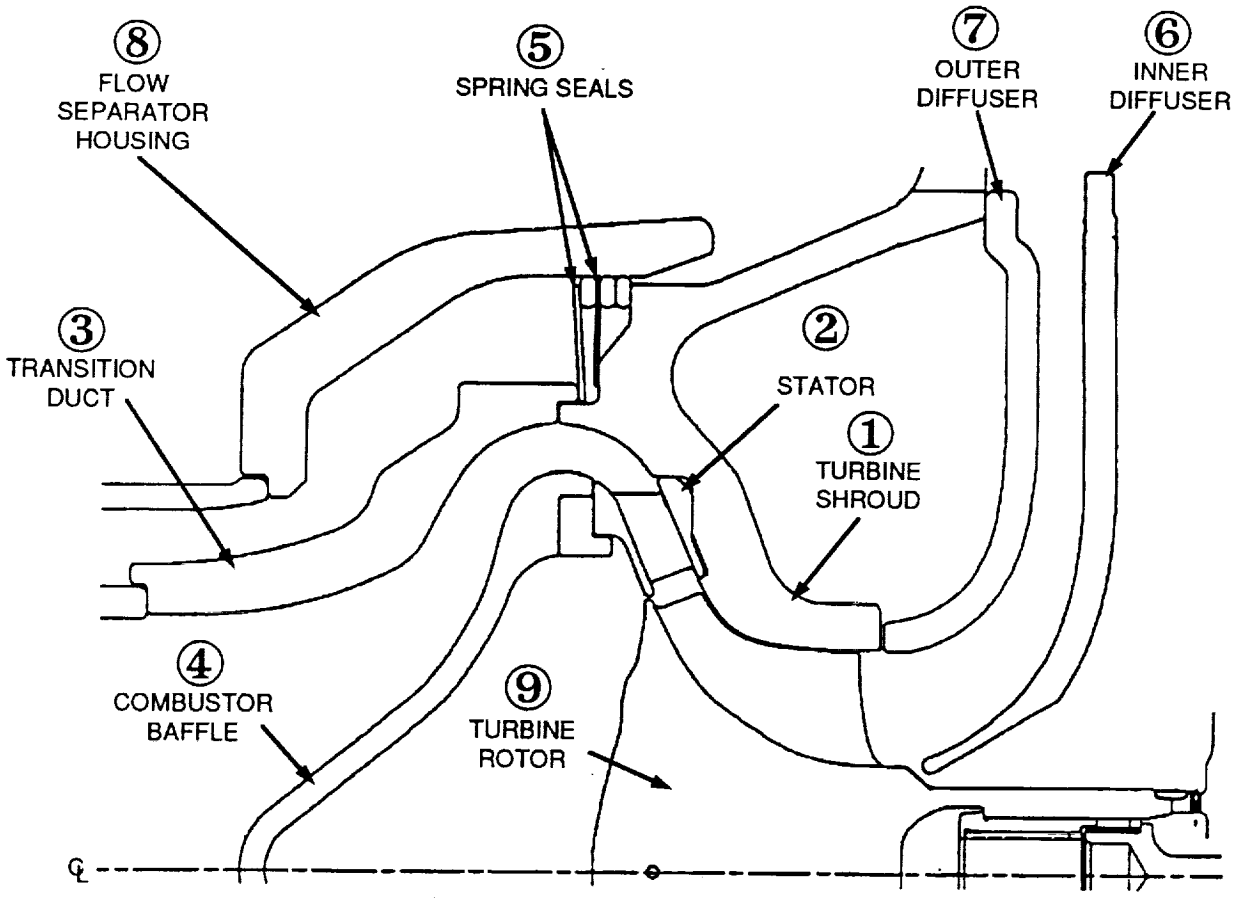

Figure 33. Final ATTAP Impact-Resistant Structural Component Designs.

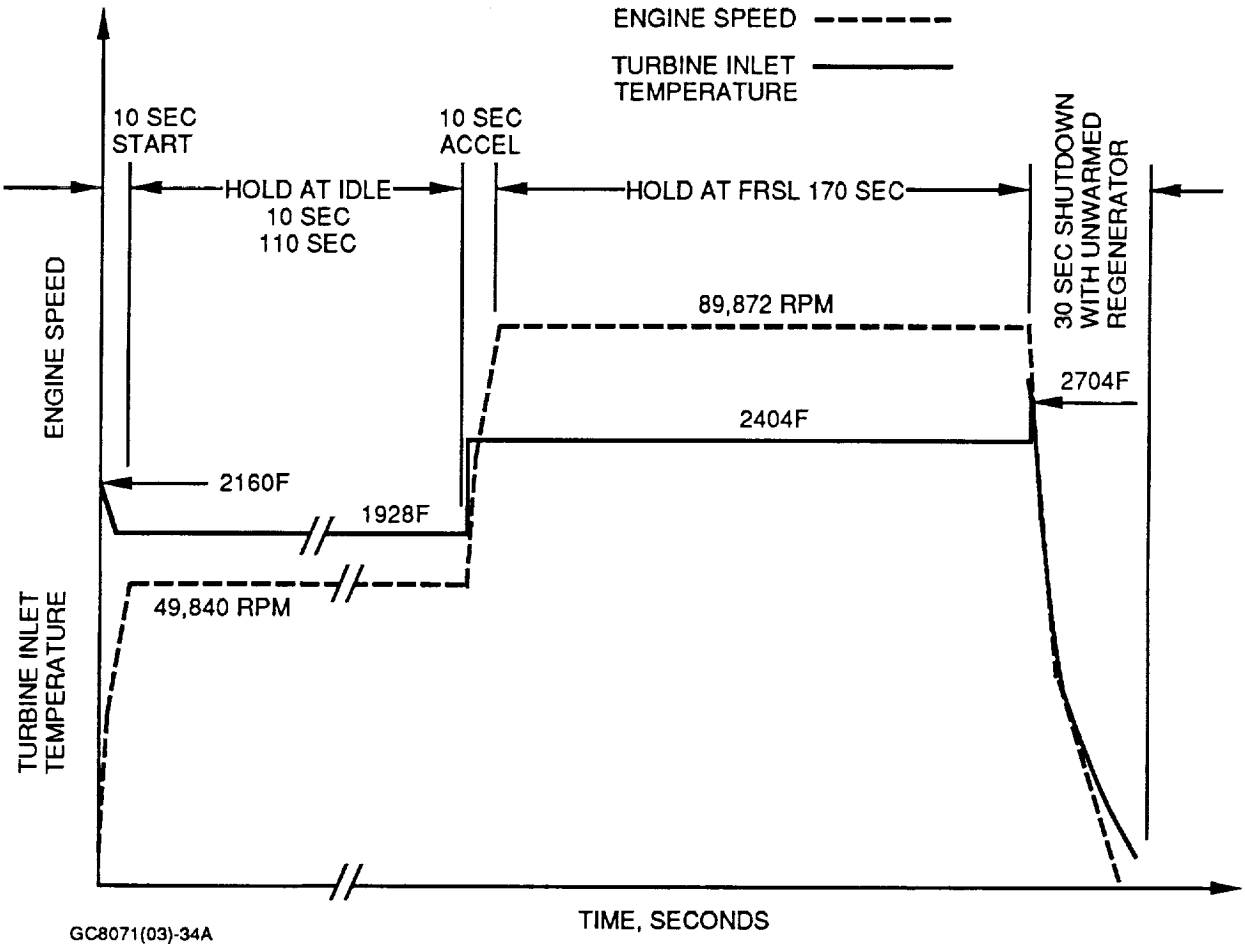

Figure 34. Transient Cycles With 10 and 110 Seconds Hold Time at Idle Are Being Used to Analyze the Impact-Resistant Components.

4.2.1 Turbine Shroud

The turbine shroud redesign efforts concentrated on development of a configuration that would accept the impact-resistant turbine and evaluation of the several silicon nitride materials that could be used for the component. The stator/shroud interface must provide a radial point to position the stator as required for aerodynamic performance and to avoid contact with the rotor throughout the operating range. Particular attention was paid to the design of the spring seal area of the turbine shroud, and to the piloting of the outer diffuser.

The baseline material used for the turbine shroud is Kyocera SN-252 silicon nitride. The final design was analyzed using 10- and 110-second hold cycles, with a steady-state analysis at the FRSL condition. The FRSL analysis yielded a maximum principal stress of 17.6 ksi at the piston seal area, as shown in Figure 35. Figure 36 shows the deformed shape of the shroud and the FRSL steady-state temperature distribution. The maximum stresses for the analyzed transient cycles are 39.0 ksi for the 10-second hold and 35.9 ksi for the 110-second hold; these are below the maximum stress goal of 40 ksi for the shroud. Figure 37 shows the transient stress level at the maximum stress location for the 10- and 110-second hold cycles.

The effect of cycle idle-hold-time on the shroud thermal stresses was investigated. The maximum stress is linearly dependent on the hold time, as shown in Figure 38. The effect of different silicon nitride materials was also studied. There is little difference in maximum stress for SN-260, SN-252 or NT154, as shown in Figure 39. This indicates that thermal conductivity has little influence on shroud stresses (SN-260 and SN-252 have much higher thermal conductivity than NT154).

The turbine shroud flowpath contour design was based on the thermal and mechanical loading and deflections of the turbine shroud and the impact-resistant turbine wheel. A summary of the turbine shroud deflections is given in Figure 40. The structural deflections, with the turbine wheel deflections, provide for 0.010 inch running clearance at the turbine inducer and 0.015 inch running clearance at the turbine exducer for the FRSL steady-state condition.

4.2.2 Outer Diffuser

The original outer diffuser of the AGT101 engine required minor modifications to accommodate the new flowpath. The changes consisted of increasing the inducer diameter to ensure that the diametral shift of the diffuser due to tolerance stackup does not introduce a negative step in the flowpath. Analysis of the outer diffuser shows that the thermal stresses resulting from the 10-second and 110-second hold cycles are more severe than experienced in the AGT101 engine start cycles. The steady-state FRSL stress is only 0.5 ksi, resulting from the nearly isothermal condition of the diffuser. The 10- and 110-second hold cycle stresses are 38.1 and 36.6 ksi, respectively. Since the geometry and operating environment are not significantly changed from the AGT101 radial turbine configuration, the redesigned diffuser should not be of high failure risk.

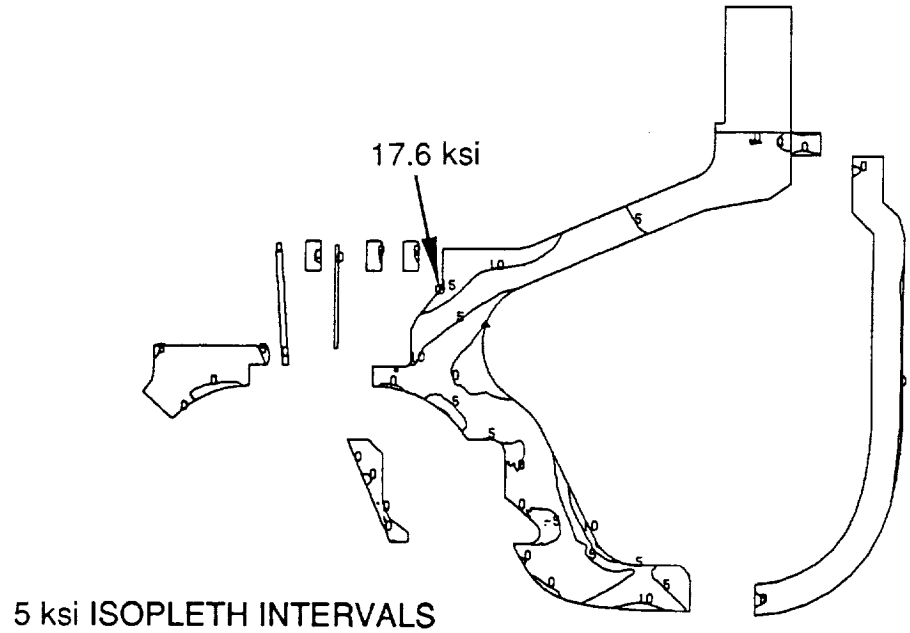

(a) MAXIMUM PRINCIPAL STRESS

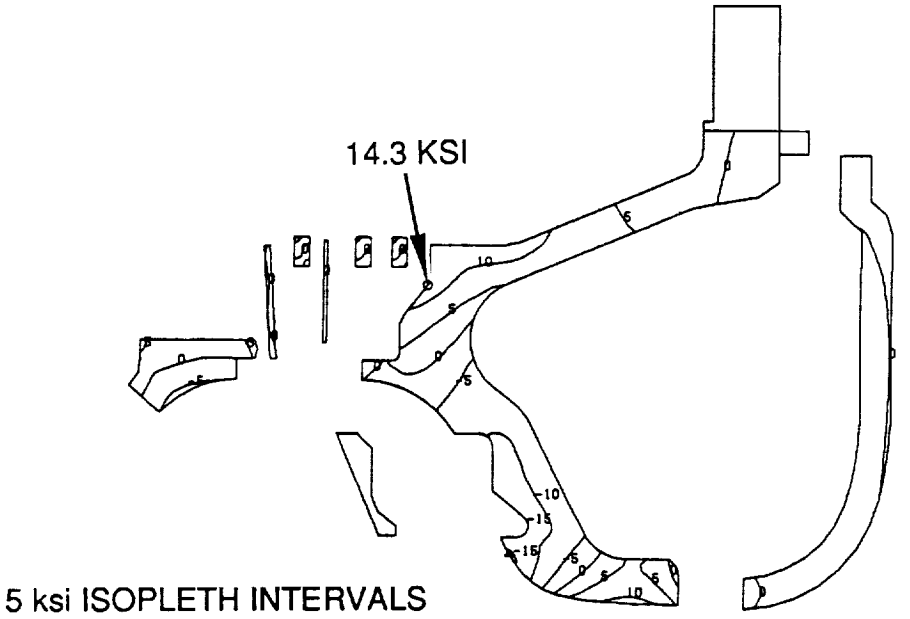

GB8071(03)-35

(b) HOOP STRESS

Figure 35. ATTAP Redesigned Turbine Shroud Stress Levels for Steady-State, Flat-Rated Conditions.

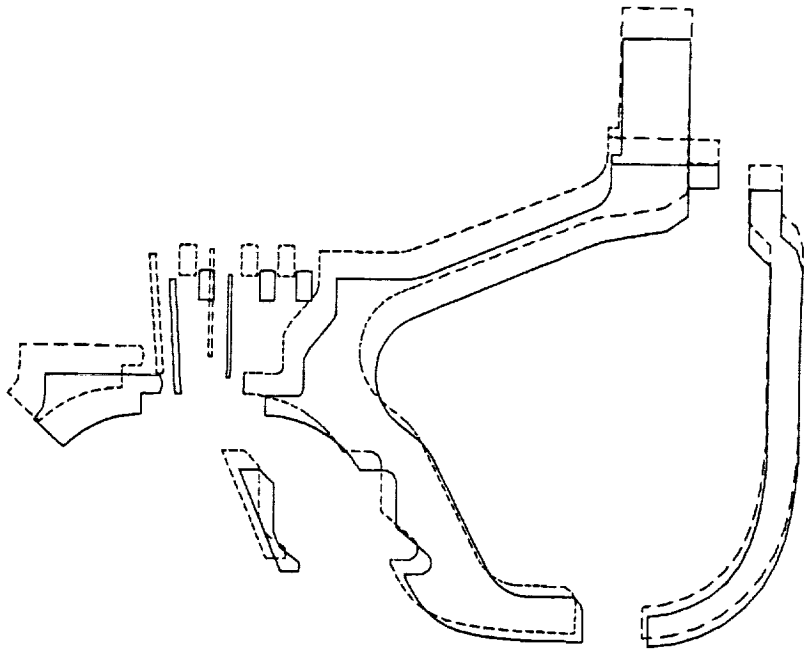

(a) DISPLACEMENTS

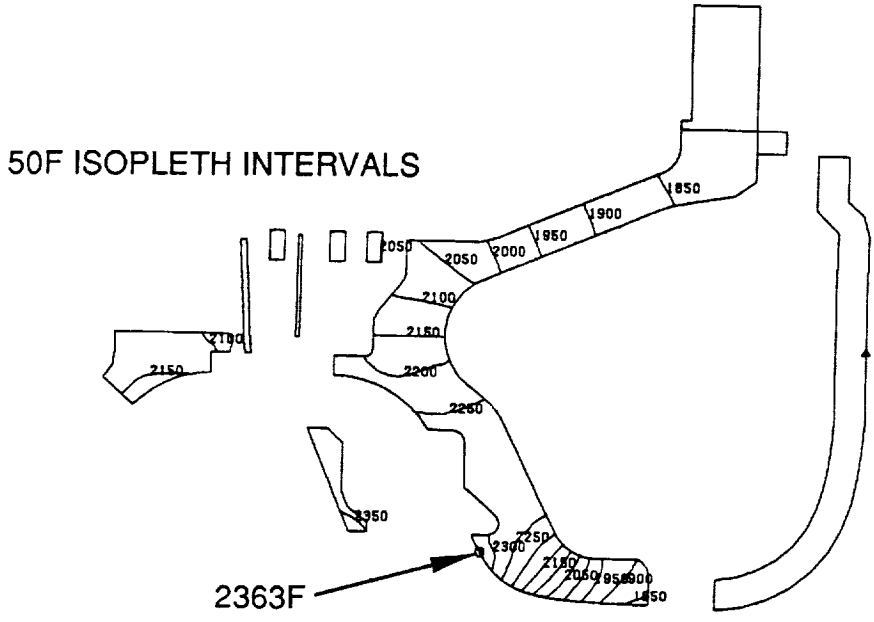

GB8071(03)-36

(b) TEMPERATURES

Figure 36. ATTAP Redesigned Turbine Shroud Deformation and Temperature Levels for Steady-State, Flat-Rated Conditions.

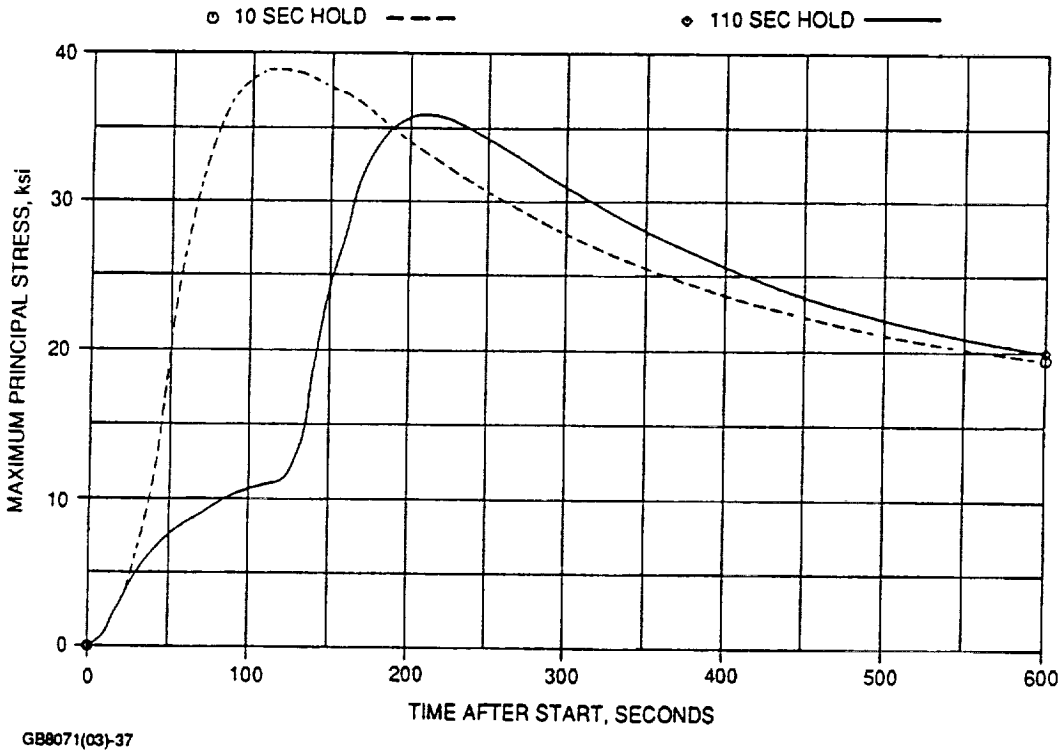

Figure 37. **ATTAP Redesigned Turbine Shroud Transient Thermal Stresses (at Peak Stress Location).**

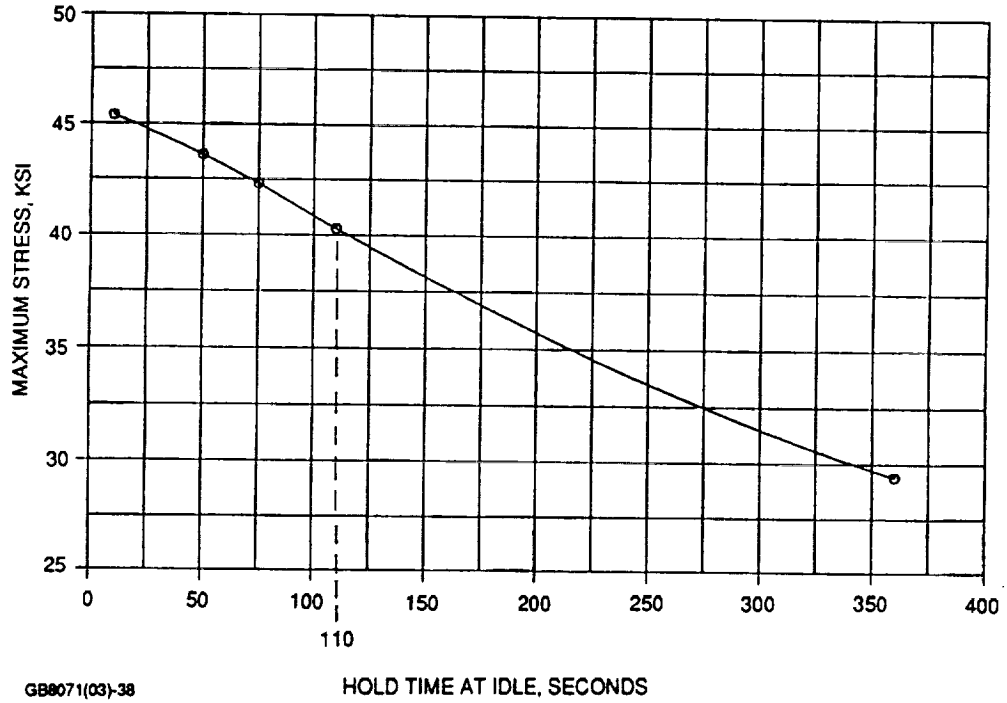

Figure 38. **Impact-Resistant Turbine Shroud Peak Transient Stress Is Dependent Upon Hold Time at Idle.**

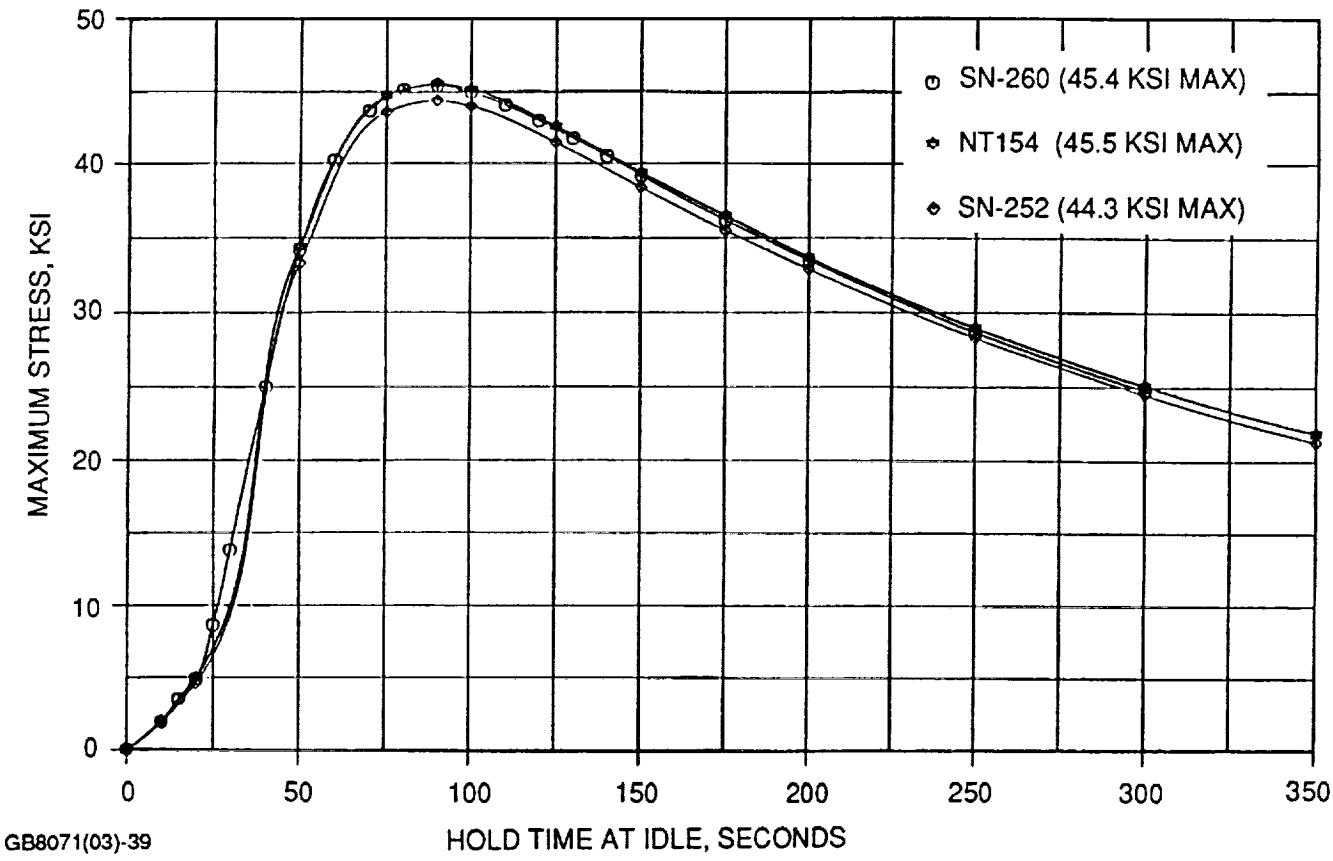

Figure 39. Little Difference in Maximum Turbine Shroud Stress Is Seen for Materials With Different Thermal Conductivity.

4.2.3 Inner Diffuser

A slight change was incorporated into the inner diffuser, consisting of increasing the gap between the diffuser ID and the turbine wheel at the turbine exducer region. This change was needed to avoid possible contact between the inner diffuser and the turbine wheel at maximum material (size) conditions.

4.2.4 Stators

Stator temperature and stresses were evaluated with 3-D finite element model (FEM) analyses. Transient temperatures were calculated and used to determine stress levels, and the effects of mechanical loads on the stator stress were studied.

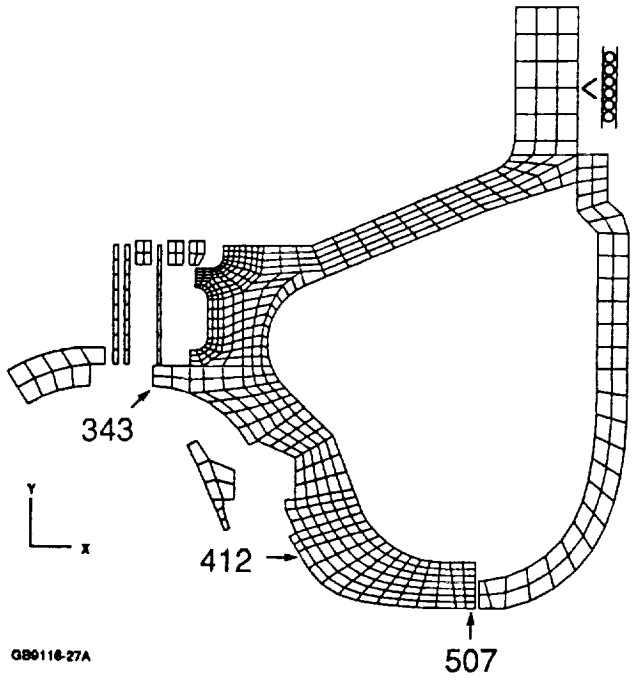

GB8071(03)-40

NODE NUMBER	343		412		507	
OPERATING MODE	DEFLECTION, MILS					
	Δx	Δy	Δx	Δy	Δx	Δy
PRESSURE LOAD	0.0	0.2	0.0	0.2	0.0	0.2
STEADY-STATE IDLE	-12.1	12.3	-7.8	7.6	-2.8	6.4
STEADY-STATE FLAT RATED	-16.2	15.6	**-10.7**	**9.6**	-5.2	6.5
TRANSIENT TO IDLE	-2.2	3.3	2.0	3.1	6.0	4.8
TRANSIENT TO FLAT RATED						
10 SEC HOLD	-2.2	3.5	5.4	4.5	12.4	8.1
50 SEC HOLD	-2.5	4.0	4.9	4.6	11.9	8.0
75 SEC HOLD	-2.9	4.4	4.5	4.8	11.5	8.0
110 SEC HOLD	-3.1	4.6	4.0	4.8	10.0	7.8
360 SEC HOLD	-3.5	7.1	3.9	6.4	10.3	7.5

8071(03)-40

Figure 40. Summary of ATTAP Impact-Resistant Turbine Shroud Deflection Values.

Thermal transient stress (σ_1) values for the 10- and 110-second hold time cycles are shown in Figure 41. At 34 seconds after start, σ_1, reaches 27.5 ksi for the 10-second hold cyle, and reaches 16 ksi at 140 seconds after start for the 110-second hold cycle. Steady-state thermal stresses in the stator are low. For silicon carbide (SiC) material, peak stator stresses would be approximately 24 percent higher than for silicon nitride, mostly due to the higher modulus of elasticity of SiC.

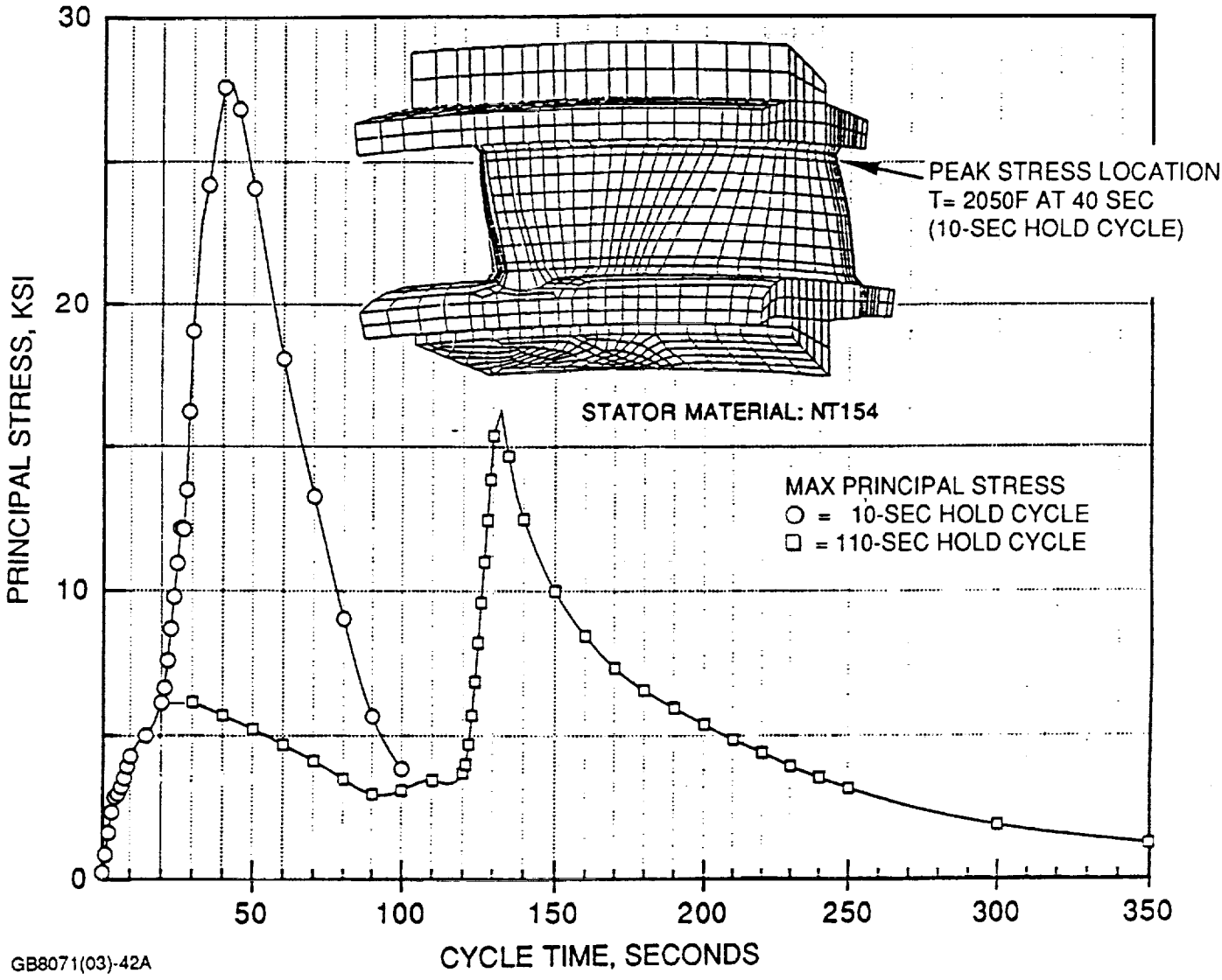

Figure 41. ATTAP Redesigned Stator Peak Thermal Transient Stress.

Two mechanical load cases can affect stator stresses. First, forces generated by the pressure differential across the baffle are transmitted axially through the stator. In the worst case, two stators slightly wider than the rest could be oriented opposite one other, such that each bears approximately half the total load transmitted from the baffle. Second, localized pinching of the stator platform occurs, due to transient temperature gradients through the stator platforms causing them to bow outward or "butterfly," as shown schematically in Figure 42. These two mechanical load cases, treated as static or constant with cycle time, were superimposed on the results of the thermal transient analysis, by adding the component stresses, then recalculating σ_1. Results from all three load cases are listed in Table 7. Stress results from the transient temperature distributions only are designated as Load Case I.

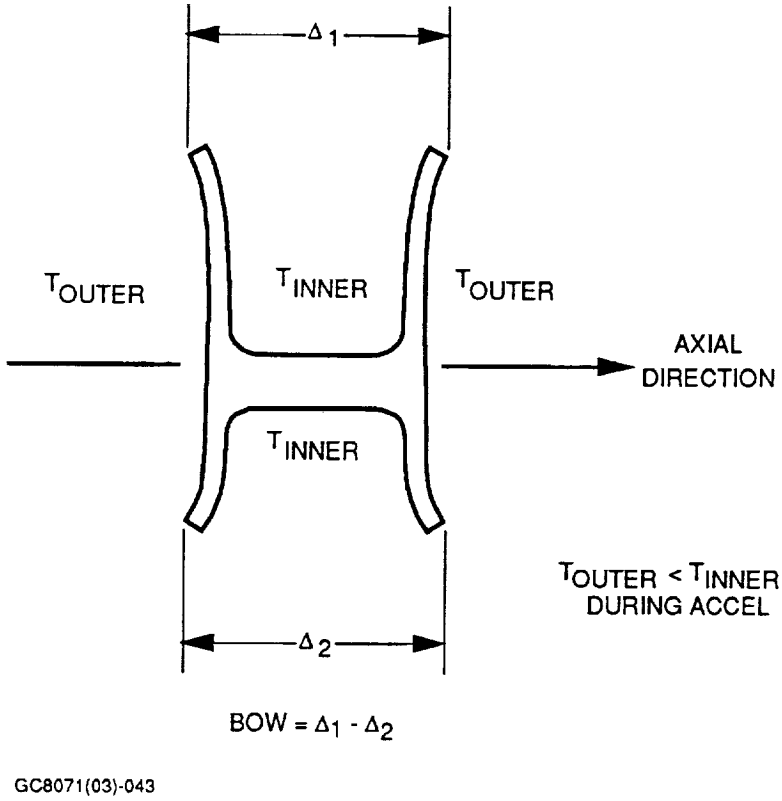

Figure 42. Simplified Schematic of Stator Bow Due to Temperature Gradients.

TABLE 7. EFFECT OF POTENTIAL LOADS ON ATTAP STATOR PEAK PRINCIPAL STRESS

Load Case	10 Second Hold Cycle	110 Second Hold Cycle
I - Thermal Transient	27.50 ksi	16.50 ksi
II - Baffle Pressure Load	1.33 ksi	1.33 ksi
III - Platform Bow, Pinch	2.60 ksi	2.60 ksi
I+II*	25.60 ksi	13.70 ksi
I+III*	30.00 ksi	17.80 ksi
II+III*	2.87 ksi	2.87 ksi
I+II+III*	28.10 ksi	16.30 ksi

* Component stresses SIGx, SIGy, SIGz, TAUxy, TAUyz, TAUxz from combined load cases were added, then SIG1, SIG2, SIG3 were recalculated.

All values calculated for peak stress location, stator trailing edge.

8071(03)-7A

Table 7 shows that mechanical loading of the stator has a negligible effect on the trailing edge, where peak stress reaches its highest level during the 10-second hold cycle. These stator stress levels are within the capabilities of NT154 silicon nitride.

4.2.5 Combustor Baffle

The combustor baffle for the impact-resistant configuration displays two distinct peak stress regions: at the axial face and in the strut fillet. Figure 43 shows peak stresses for the axial face of 16.6 ksi for the 10-second hold cycle and 8.3 ksi for the 110-second hold cycle. Peak stress in the strut fillet, predicted with the 3-D baffle FEM shown in Figure 44, indicates that the peak stress in the strut fillet will reach 19 ksi at 34 seconds after start for the 10-second hold cycle. This final baffle design has lower stress levels than the AGT101 radial configuration and should provide higher reliability.

4.2.6 Transition Duct

The transition duct geometry has required little iteration during the impact-resistant design process. Figure 45 shows peak stresses of 16.6 ksi for the 10-second hold cycle and 15.9 ksi for the 110-second hold cycle at the duct inlet end OD, using sintered alpha silicon carbide (SASC) material. At the discharge end of the transition duct (Figure 46), the peak stress will reach 13.7 ksi for the 10-second hold cycle and 13.1 ksi for the 110-second hold cycle, using SASC material properties.

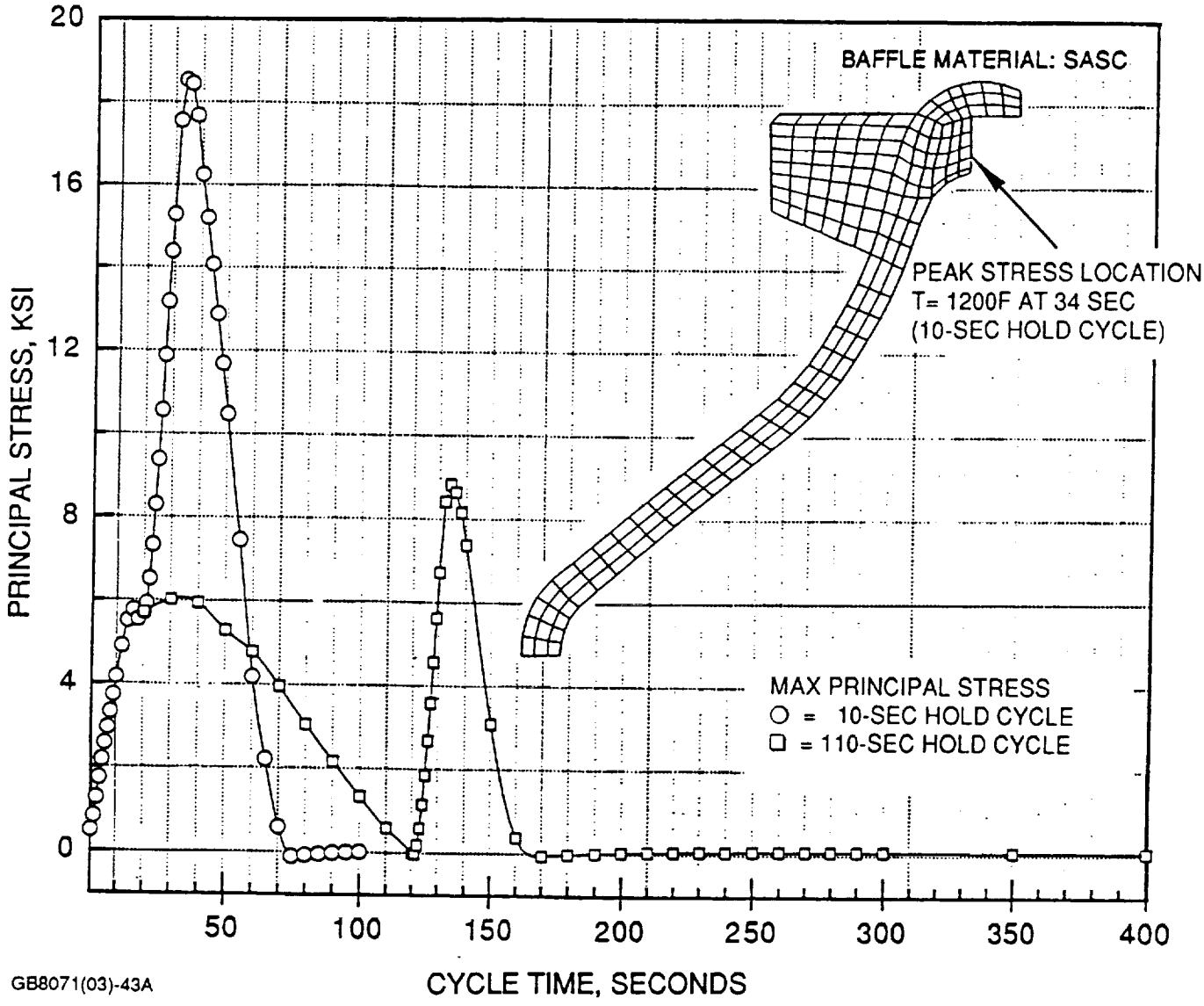

Figure 43. ATTAP Redesigned Combustor Baffle Peak Stresses at Axial Face.

4.2.7 Ceramic Seal Assembly

The transition duct for the impact-resistant configuration has a significantly larger radial gap to the flow separator housing (FSH), necessitating design modifications to the ceramic seal assembly. The new arrangement of this seal assembly is shown in Figure 47.

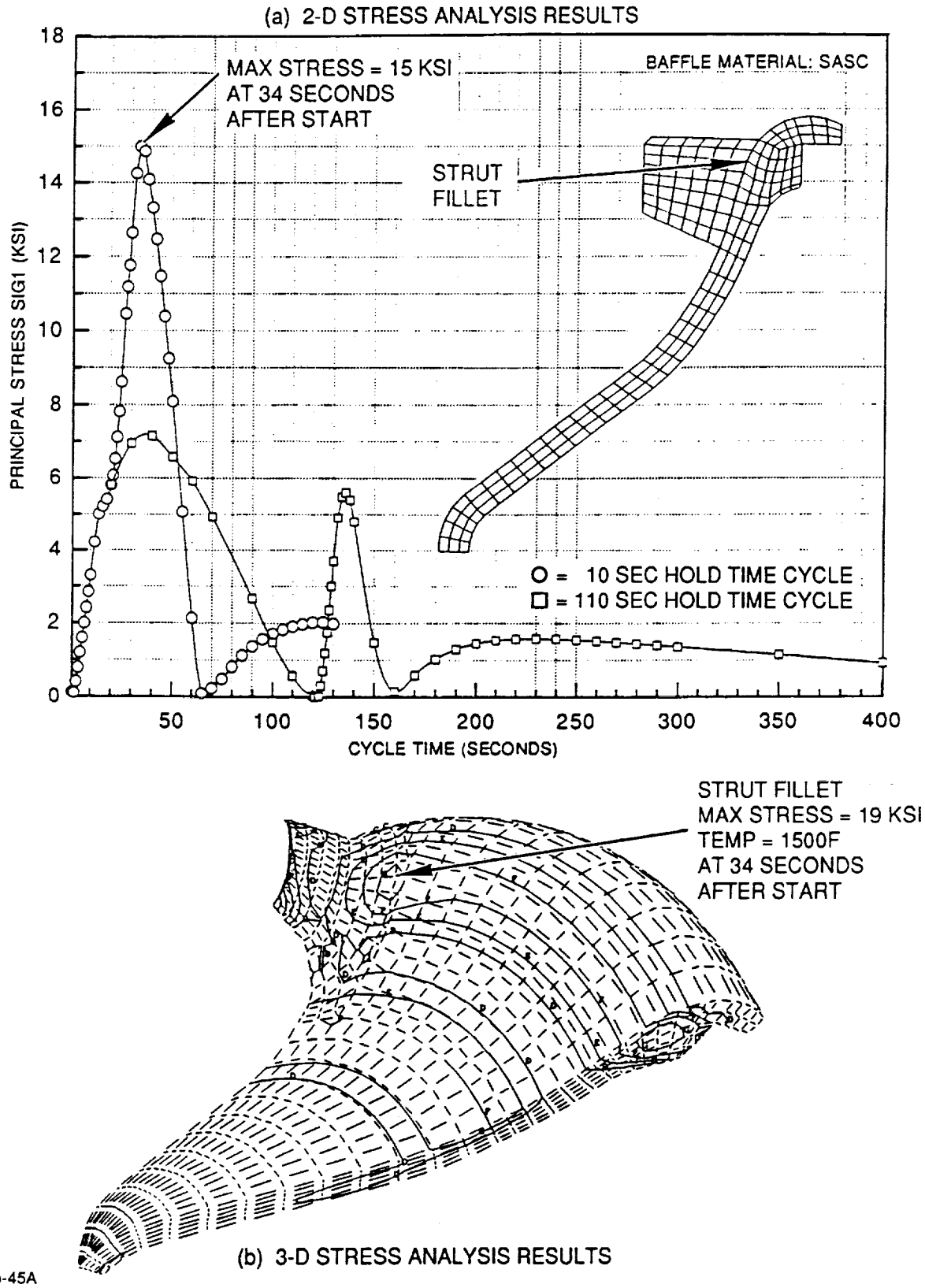

Figure 44. ATTAP Redesigned Combustor Baffle Peak Stresses at Strut Fillet.

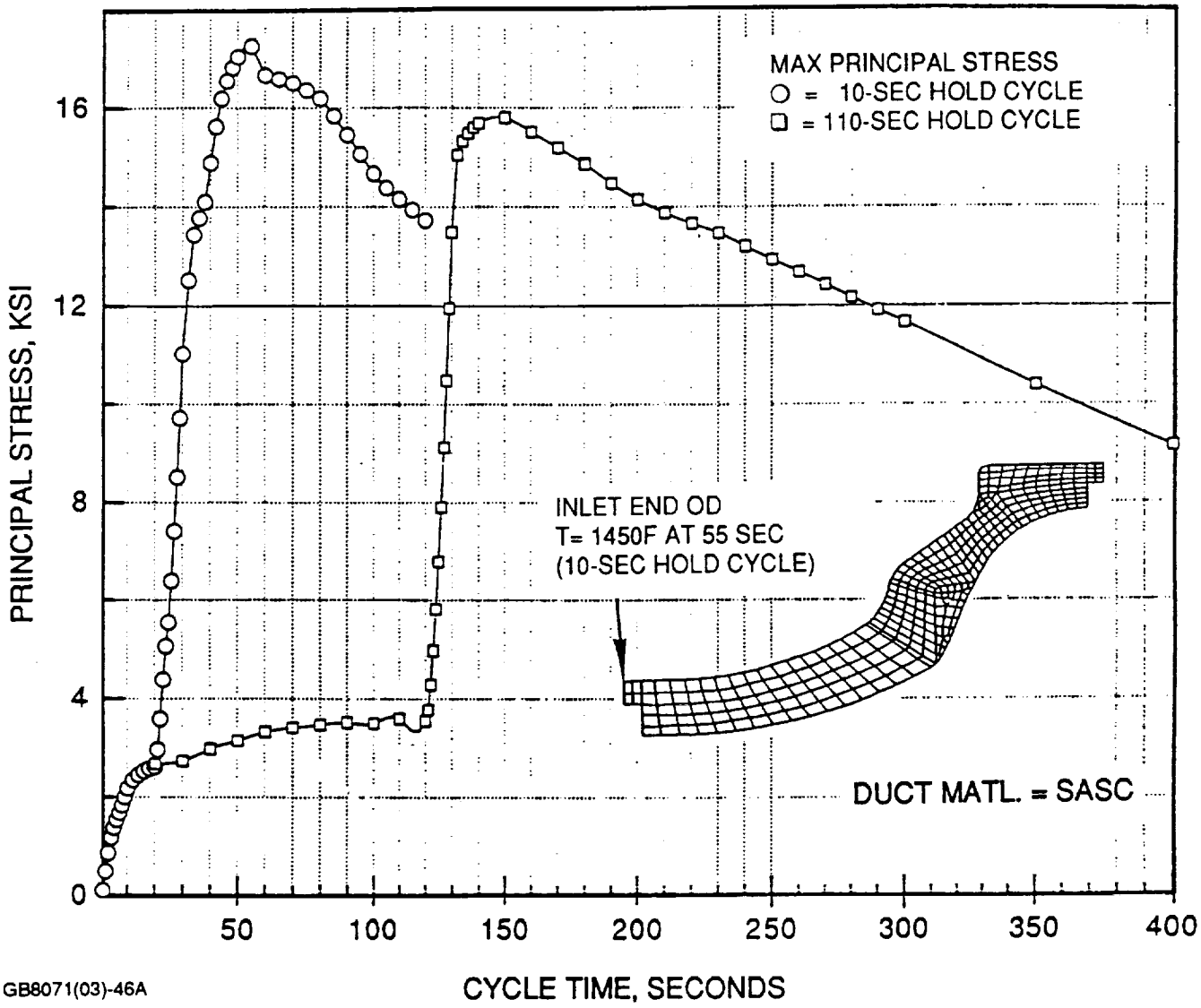

Figure 45. ATTAP Transition Duct Peak Stresses at Inlet End OD.

The ceramic seal arrangement resists flow along two paths. Spring seal A resists leakage from the turbine inlet to turbine exhaust flow, and spring seal B resists leakage from the regenerator exit to turbine inlet flow. Both seals are loaded by axial interference between the transition duct and piston ring type seals (these have not been redesigned) touching the FSH.

The maximum stress in Seal A is 13 ksi (at the OD), due to a possible maximum pressure differential of 55 psi (at the center) across that spring. Peak stresses in Seal A due to thermal loads and interference are low, as shown in Figure 47. Seal B displays a maximum stress due

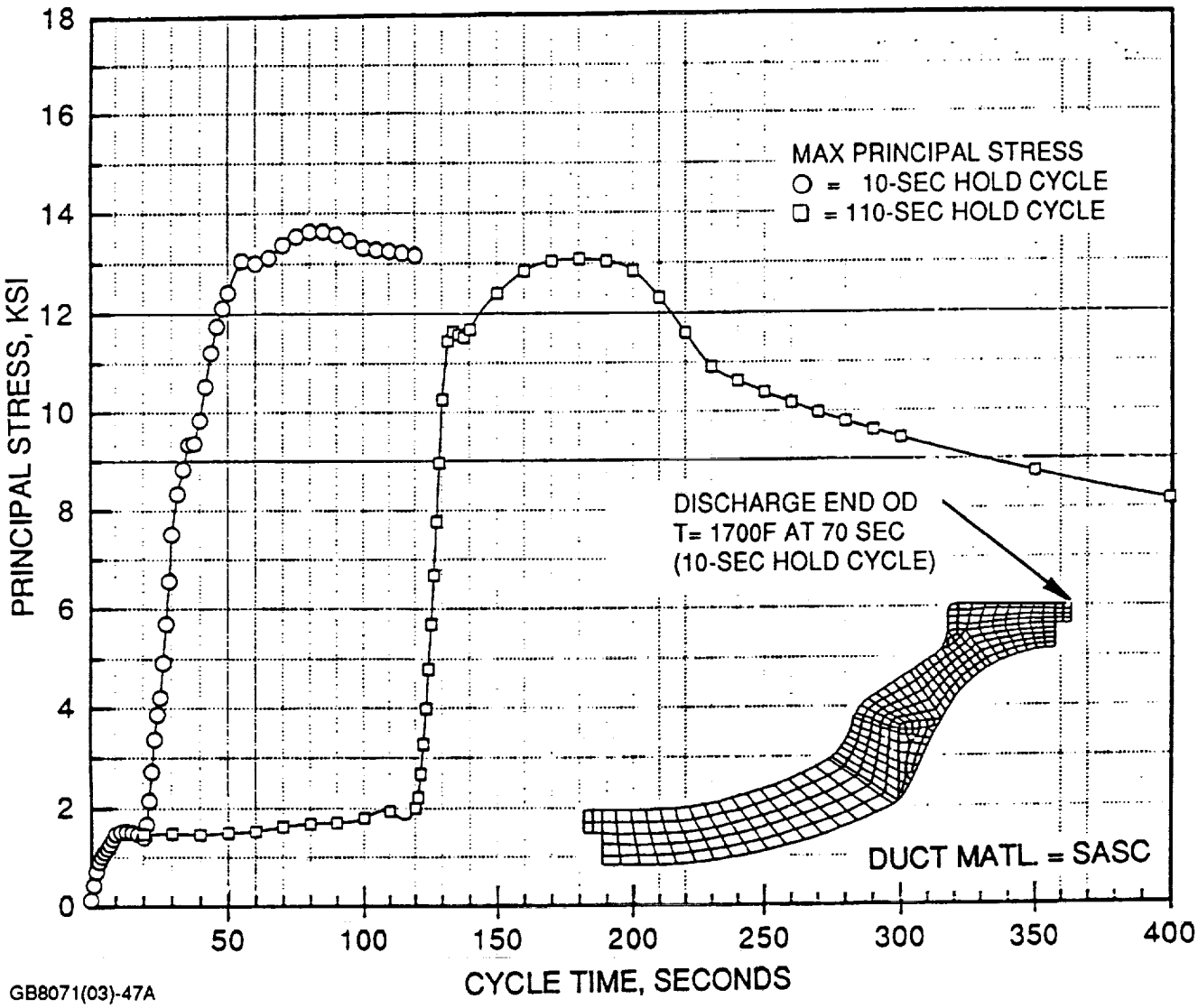

Figure 46. ATTAP Transition Duct Peak Stresses at Discharge End OD.

to thermal loads at the OD of less than 5 ksi. Peak stress due to pressure loads and axial interference occurs at the ID of Seal B, as shown in Figure 48. Since the axial interference of Seal B is between 30 and 55 mils throughout the estimated operating conditions, the peak stress is less than 36 ksi (shown by the intersection of the 55-mil line and the σ maximum curve). Seal B will resist approximately 4 psi differential pressure, twice that needed to seal between regenerator exhaust and turbine inlet flow.

Since peak stresses from pressure loads, axial interference, and thermal loads occur at different locations in both seals, high peak stresses from combined loads are not of concern.

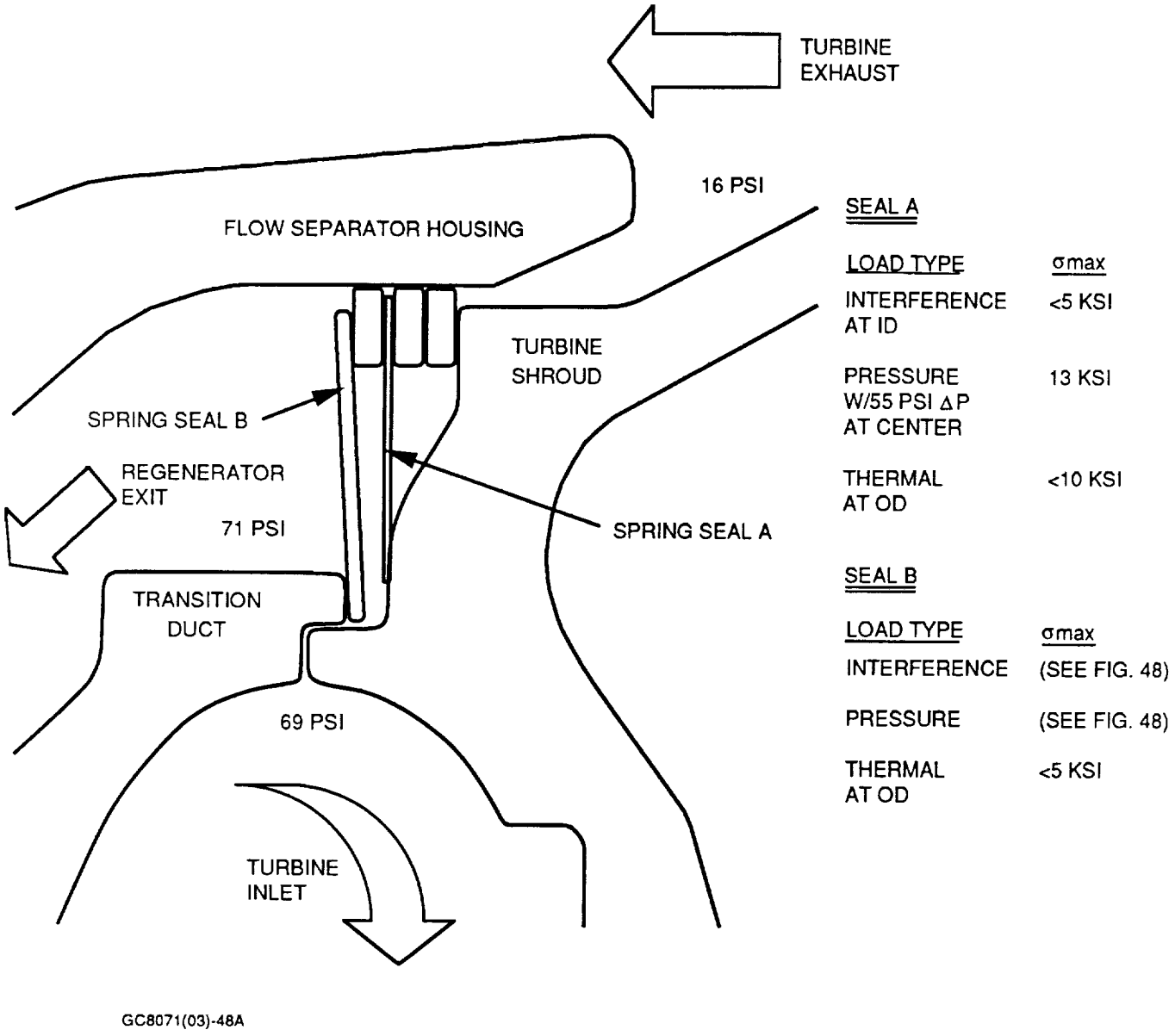

Figure 47. ATTAP Interhousing Seal Arrangement and Stress Summary.

4.2.8 Flow Separator Housing

During 1990, the flow separator housing (FSH) analysis was completed, based on pressure loads alone. Results from these analyses were used in conjunction with trends from past thermal analyses to identify preferred geometries. It was found that a lithium aluminum

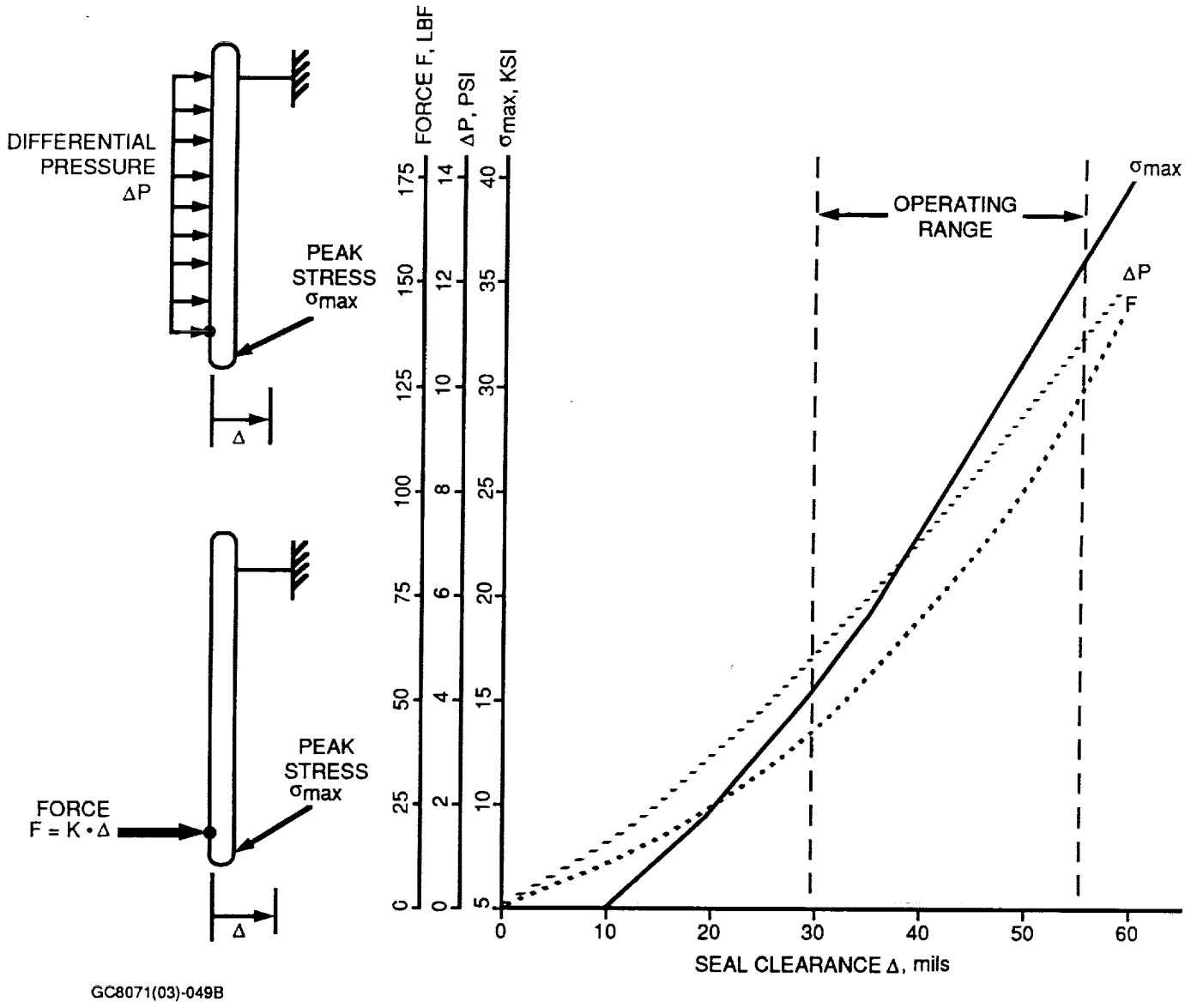

Figure 48. ATTAP Seal B Peak Stress, Sealing Capability, and Interference Forces Over Operating Range.

silicate (LAS) FSH with gussets on low pressure (LP) and high pressure (HP) sides, with a thicker flange, and with a 4-point support would be the best combination among those studied (see Figures 49 through 51). Use of the thick flange would be limited to applications in which the metallic hot regenerator seal is eliminated and the regenerator core rubs directly against the FSH. Verification of this best combination will be conducted by performing the analysis with thermal loads superimposed on the pressure loads. Data from an upcoming engine test will be used to determine the thermal boundary conditions to conduct the thermal analysis.

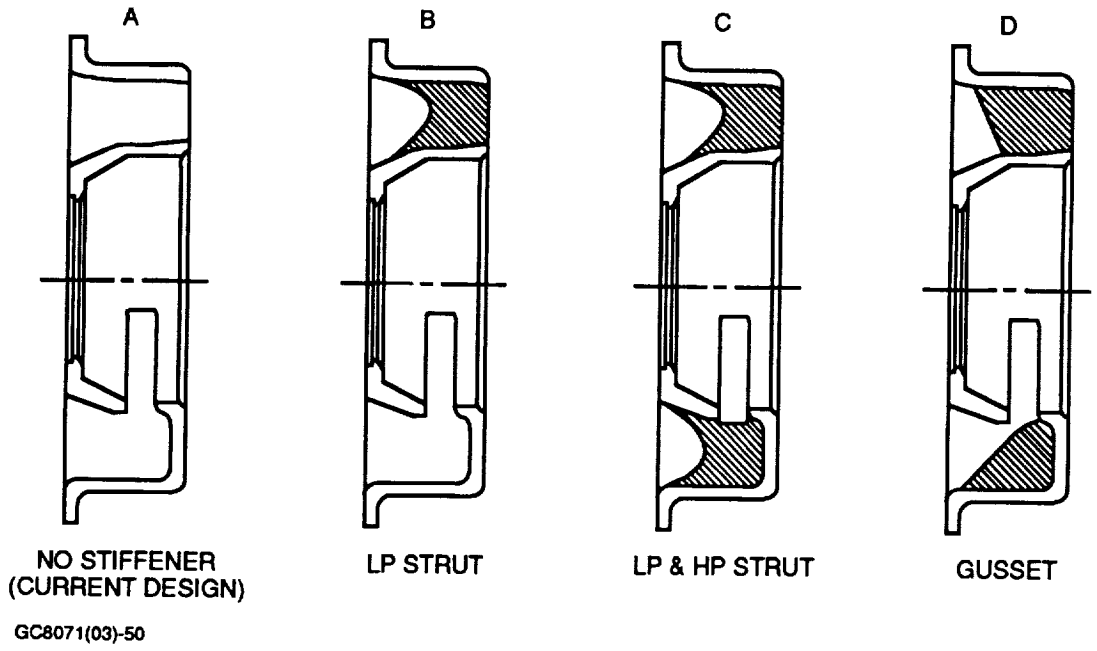

Figure 49. Four Flow Separator Housing (FSH) Configurations Were Studied.

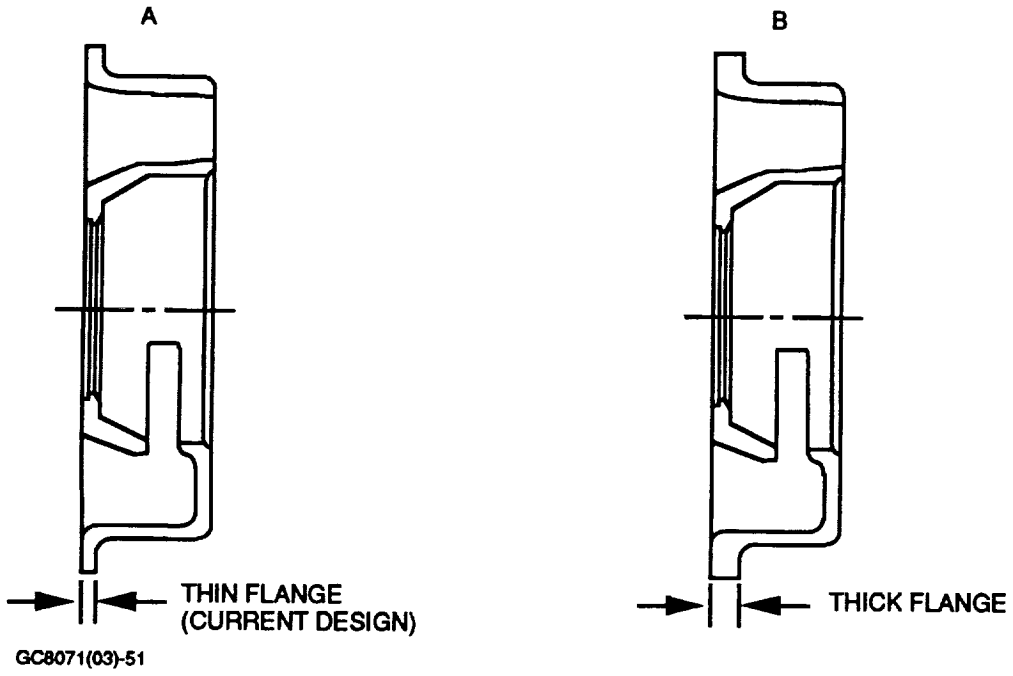

Figure 50. FSH Flange Thickness Variations Were Studied.

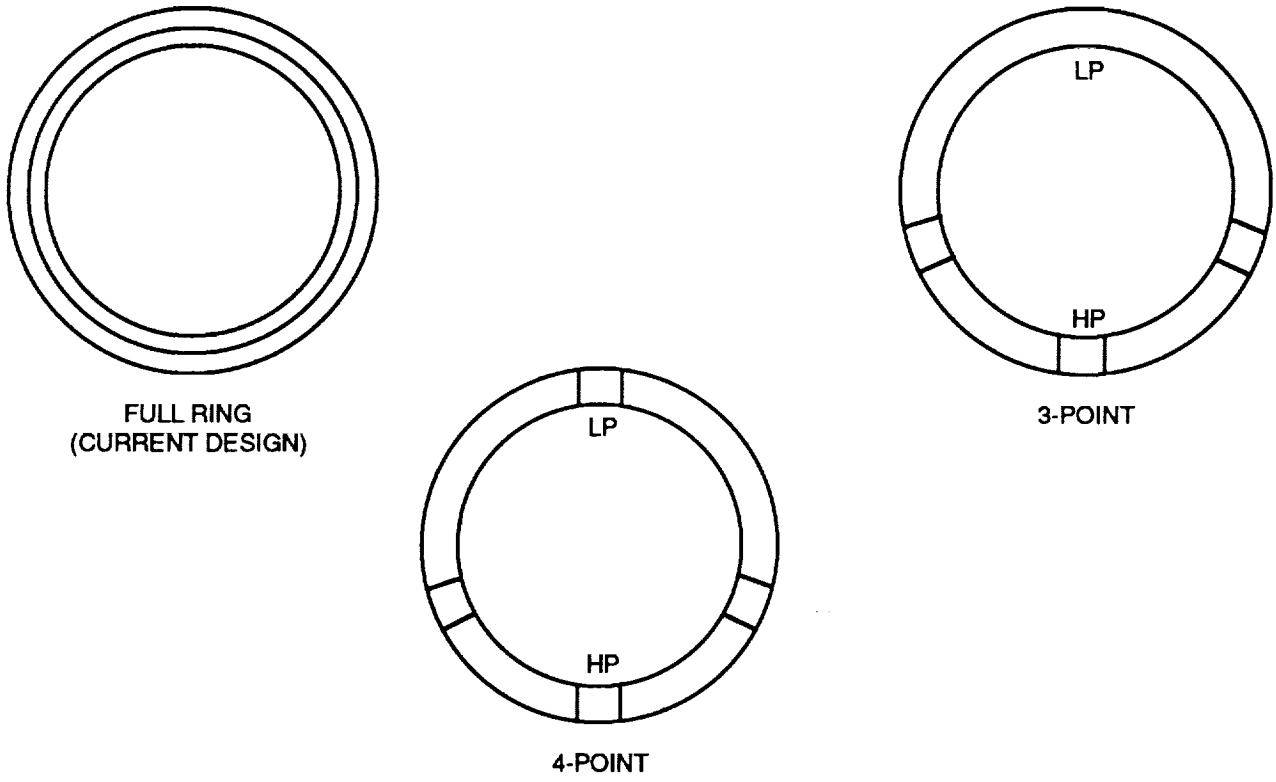

Figure 51. Three FSH Flange Support Configurations Were Studied.

4.2.9 Turbine Attachment System

The turbine attachment system was redesigned and rig tested during this reporting period. The attachment system currently employs a collet retainer piloted with a sleeve retainer (with two axial slots for compliance), as shown in Figure 52(a), (top). Both are made of stainless steel. This design produces local high stress (77 ksi, mostly radial) in the ceramic rotor in the vicinity of the point of contact, due to the tieshaft load of 5000 lbf at the assembly (cold engine) condition. During operation, the tieshaft load is relaxed to 1000 lbf, which is further countered by a centrifugal effect, resulting in low stresses in the rotor (29 ksi).

The redesign, Figure 52(b), (bottom) involved replacing the cylindrical sleeve with a solid ceramic 'plug', and changing the collet material to nickel-based IN718 alloy. The redesign reduced the stress by 30 percent. The radial stress on the rotor is a function of the radially

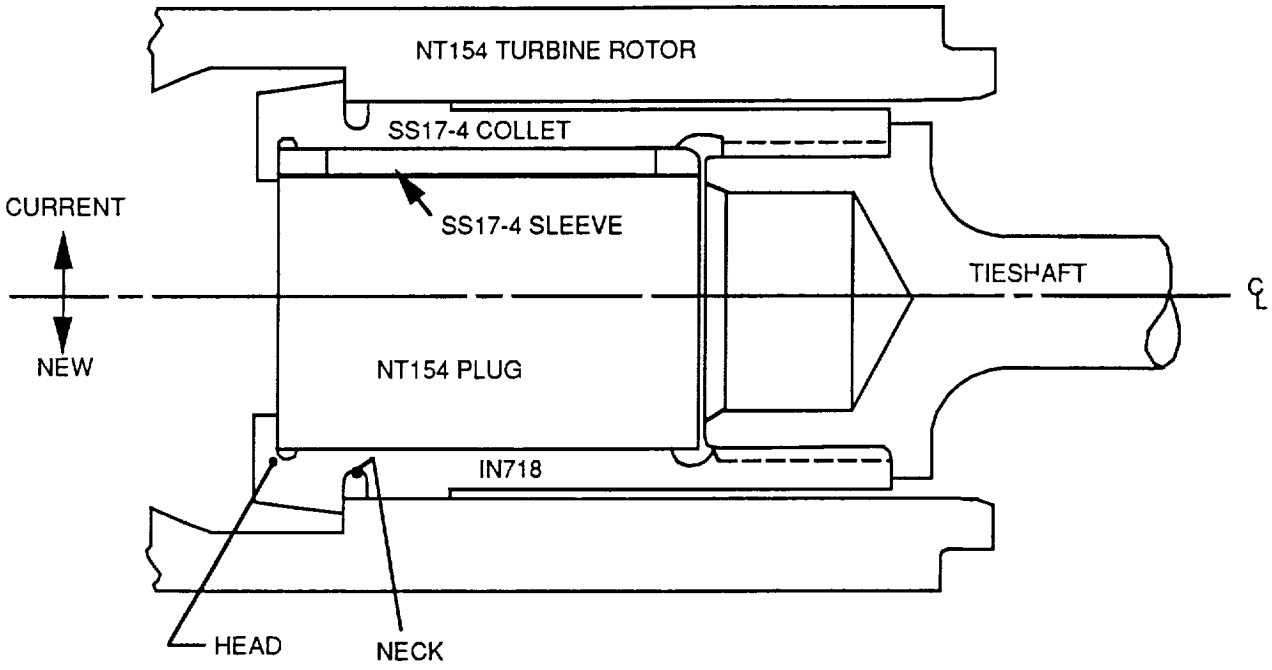

Figure 52. ATTAP Turbine Attachment Systems Compared. (a) Current Attachment Design (Top Half); (b) Redesigned Attachment (Bottom Half).

inward bending of the collet tangs. The 'plug' design restricts this bending, thereby lowering the stresses. Both the current and new designs were tested in a rig. As shown in Figure 53, the results indicate there is an order of magnitude reduction in the radial motion of the collet tangs with the new design. This agrees well with the analysis, imparting confidence to the prediction of a 30 percent lowering of the rotor stresses.

4.2.10 Impact-Resistant Turbine Design

A new ceramic turbine rotor design with improved resistance to impact failures was selected. The new turbine design has significantly lower impact stress values than the baseline AGT101 radial turbine, with little or no degradation in aerodynamic performance and mechanical reliability.

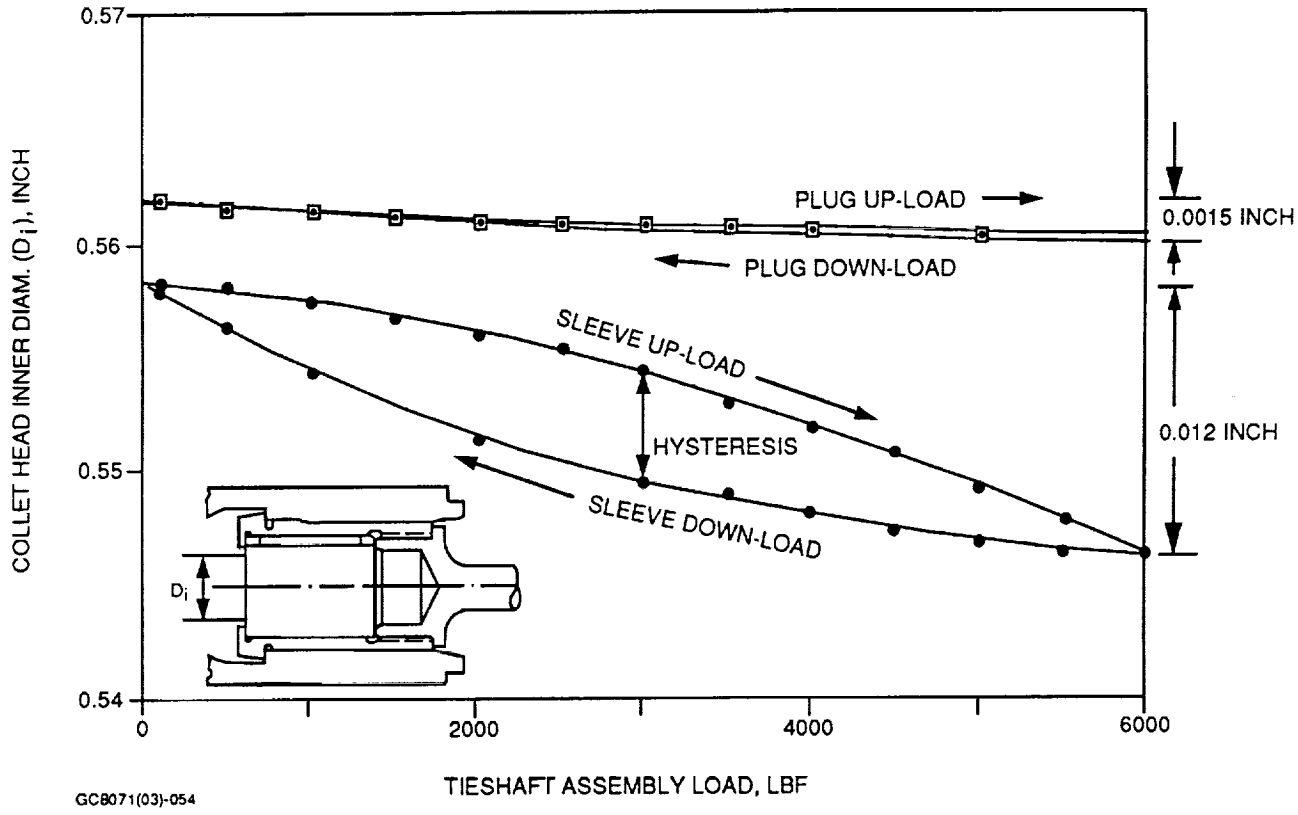

Figure 53. ATTAP Turbine Attachment Rig Test Results Show New 'Plug' Design Lowers Stress.

Aerodynamic Design

To provide the AGT101 test bed engine with a ceramic turbine having improved particle impact resistance, major changes in the turbine geometry were incorporated. Two turbine designs were undertaken in 1990, to provide flexibility in applying impact-resistant features; a clearer understanding of the effects on both aerodynamic performance and mechanical integrity would then be available. Subsequent to detailed analysis and experimental development, a single impact-resistant turbine design will be generated, having minimal or no performance degradation compared to the baseline AGT101 radial turbine.

The baseline AGT101 radial turbine rotor tip speed was 2300 ft/sec at the design conditions for engine maximum power. Resistance to particle impacts could be improved by reducing rotor tip speed; therefore, both of the new designs would have reduced rotor inlet diameters. Also, the original turbine flowpath was to be maintained as closely as possible, to

minimize redesign of neighboring structures. Using these guidelines, the two new impact-resistant designs were initiated.

Following a pitchline vector diagram analysis of the turbine, two flowpath designs were generated. The first rotor design has a tip speed of 1850 ft/sec, and the second has a tip speed of 1700 ft/sec. The preliminary designs were the result of a trade-off study conducted on the turbine performance parameters, with geometry constraints to optimize efficiency. The two impact-resistant turbine designs have predicted efficiencies that agree well with the original AGT101 radial turbine design.

Increased rotor inducer blade thickness is an important design feature added for improved particle impact resistance. Manufacturability of the ceramic component was also taken into account, which will affect the behavior of the flowfield within the rotor passages. The blade definitions, as well as the rotor flowpaths, resulted from optimizing the flow through the rotors, using an axisymmetric pseudo-inviscid analysis.

Following the rotor detail designs, stators were designed using a 2-D analysis of several sections of the vane from hub to shroud. Again, mechanical and manufacturing concerns helped determine the design of the vanes.

With the turbine component designs completed, detailed manufacturing drawings of the parts were initiated, including hardware for both the engine and the test rigs. The 1850 ft/sec tip speed rotor configuration was chosen for engine development, due to initial analysis that indicated favorable impact resistance. Fabrication of this configuration by the ATTAP ceramic subcontractors was initiated. Computer aided design (CAD) models of the components were created to aid the design process. Figure 54 shows the CAD rotor model.

The exhaust diffuser design from the original AGT101 turbine has been maintained. Turbine rig tests have demonstrated its favorable performance. The inlet to the new turbine was simplified, compared to the AGT101 design. This was easily accomplished by reducing the required curvature.

At the same time the parts drawings were started, a 3-D aerodynamic analysis of the components began. Information obtained from this analysis can be applied to subsequent turbine design iterations.

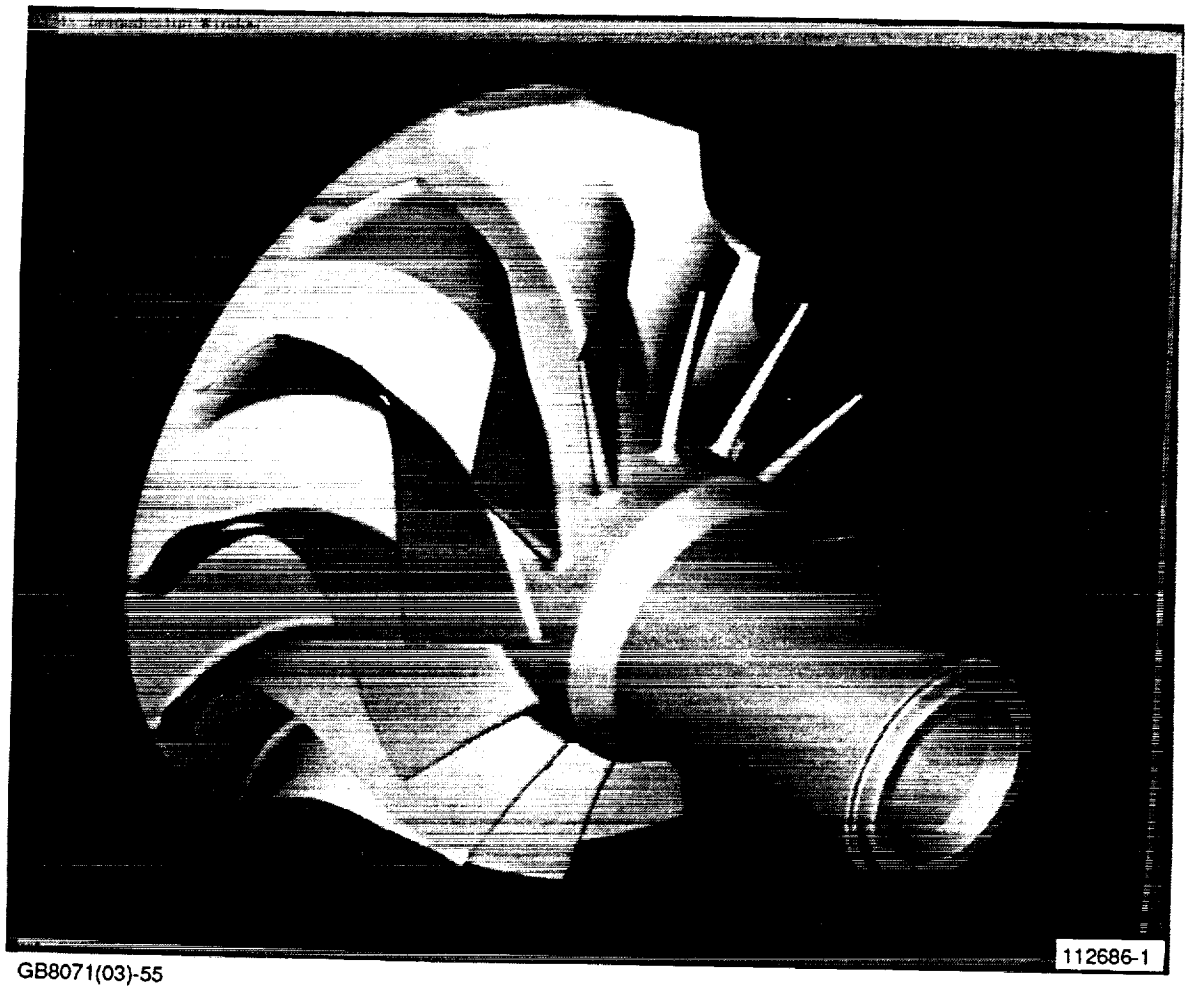

GB8071(03)-55

Figure 54. Computer Model of 1850 ft/sec Tip Speed Turbine Rotor Aided the Design Process.

A 3-D viscous analysis was performed on the 1850 ft/sec rotor and stator designs. The viscous analysis velocity vectors through the rotor are presented in Figure 55. The blade passage has a favorable velocity field. The results of the 3-D analyses of the vane also predicted no adverse secondary flow behavior. By comparing the 3-D results with the 2-D 1850 ft/sec tip speed turbine design, the characteristics of the 1700 ft/sec tip speed turbine were interpolated, which avoided conducting a time-consuming and expensive 3-D analysis of the 1700 ft/sec configuration.

The result of the analyses will be correlated with the results of the planned turbine component rig testing.

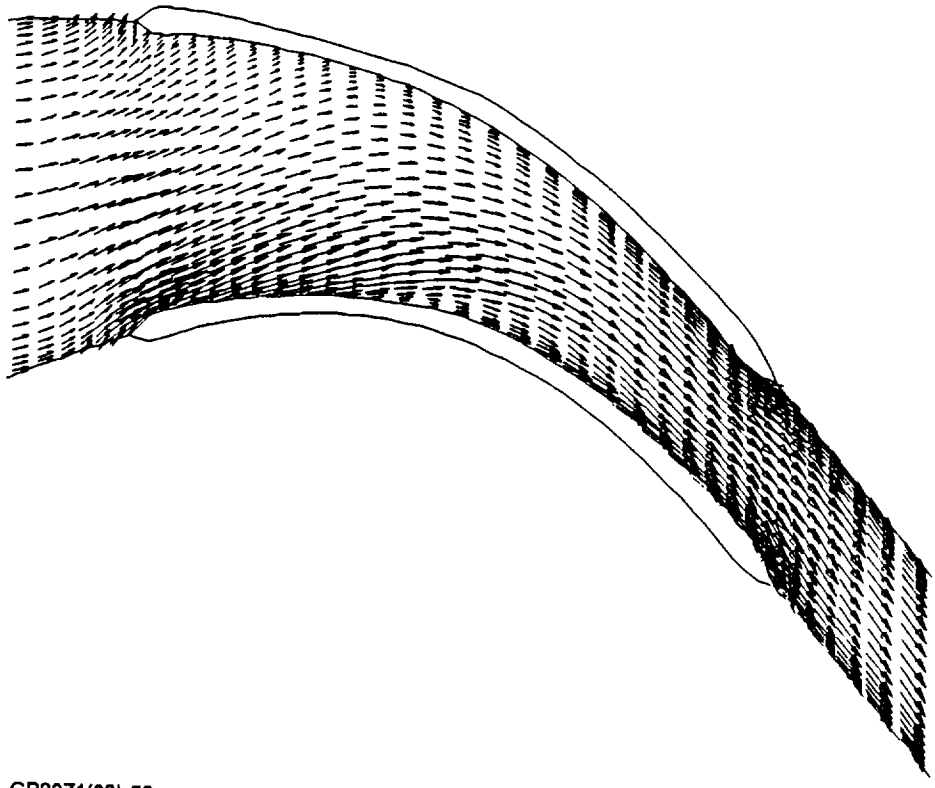

GB8071(03)-56

Figure 55. 3-D Viscous Analysis Results Indicate Favorable Flow Behavior Through the 1850 ft/sec Rotor Passage.

Mechanical Design

Mechanical and aerodynamic analyses were performed concurrently to develop turbine design(s) with improved impact resistance without compromising aerodynamic performance or mechanical integrity. Reduction in impact stress was used as the measure of improved impact resistance of the new designs. Impact stresses were calculated using the EPIC impact finite element computer code. These analyses simulated a 0.1 inch diameter carbon particle impacting the inducer corner of each blade. The maximum operating blade-tip speed was used for the impact velocity. The impact analyses predicted impact stress for the 1850ft/sec blade that is only 59 percent of the value for the current radial blade design for identical impact conditions.

A more detailed impact study was also performed. These analyses, described in Section 4.1.3, identified an improved impact-resistant blade design with predicted impact stress only 23 percent of the current value for the AGT101 ceramic radial turbine wheel. Single-blade

ceramic subelements will be fabricated for both impact-resistant turbine designs, and the subelements will be impact tested to demonstrate improved survivability at increased impact failure velocities resulting from the reduced impact stress levels.

A 3-D rotor thermal stress analysis, under steady-state conditions, was completed on the impact-resistant turbine rotor. A finite element model (FEM) of the 1850 ft/sec tip speed design is shown in Figure 56. Note that the impact-resistant turbine stage does not include a backshroud. A summary of the thermal stress analysis results are presented in Figure 57 for steady-state maximum power, flat rated sea level (FRSL), and idle conditions. Steady-state stresses are dominated by rotational effects, due to weak radial temperature gradients.

For this blade shape, all the peak steady-state stresses occur on the suction side. The highest steady-state stress is 46.4 ksi at maximum power (100,000 rpm, 2500F TIT); the highest stresses for FRSL (90,000 rpm, 2404F TIT) and idle (50,000 rpm, 1928F TIT) are 41 and 15 ksi, respectively.

Results for the AGT101 radial turbine at steady-state maximum power conditions are also shown in Figure 57 for comparison. Some improvements are evident for the impact-resistant turbine. Significant reduction of the saddle stress is predicted (7 vs 37 ksi), which

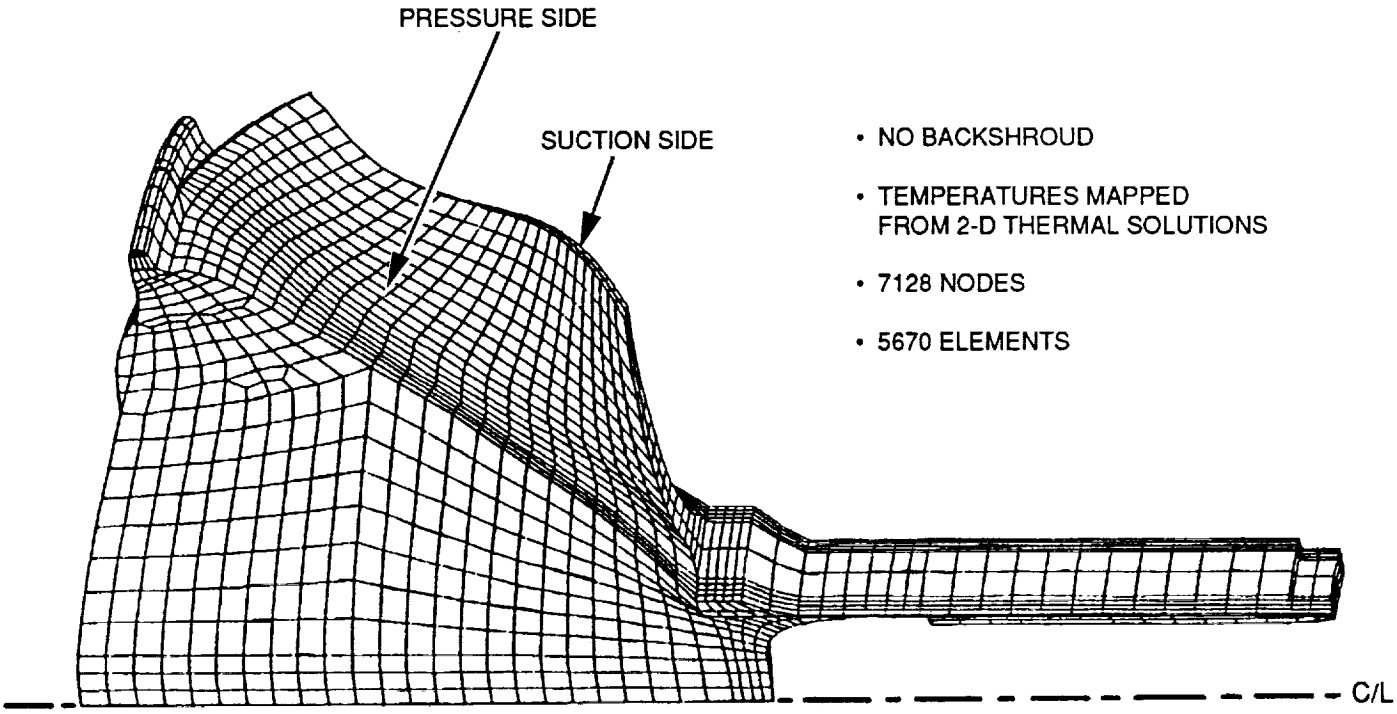

GC8071(03)-57

Figure 56. 3-D Rotor FEM is Being Used for Stress Analysis and Risk Assessment.

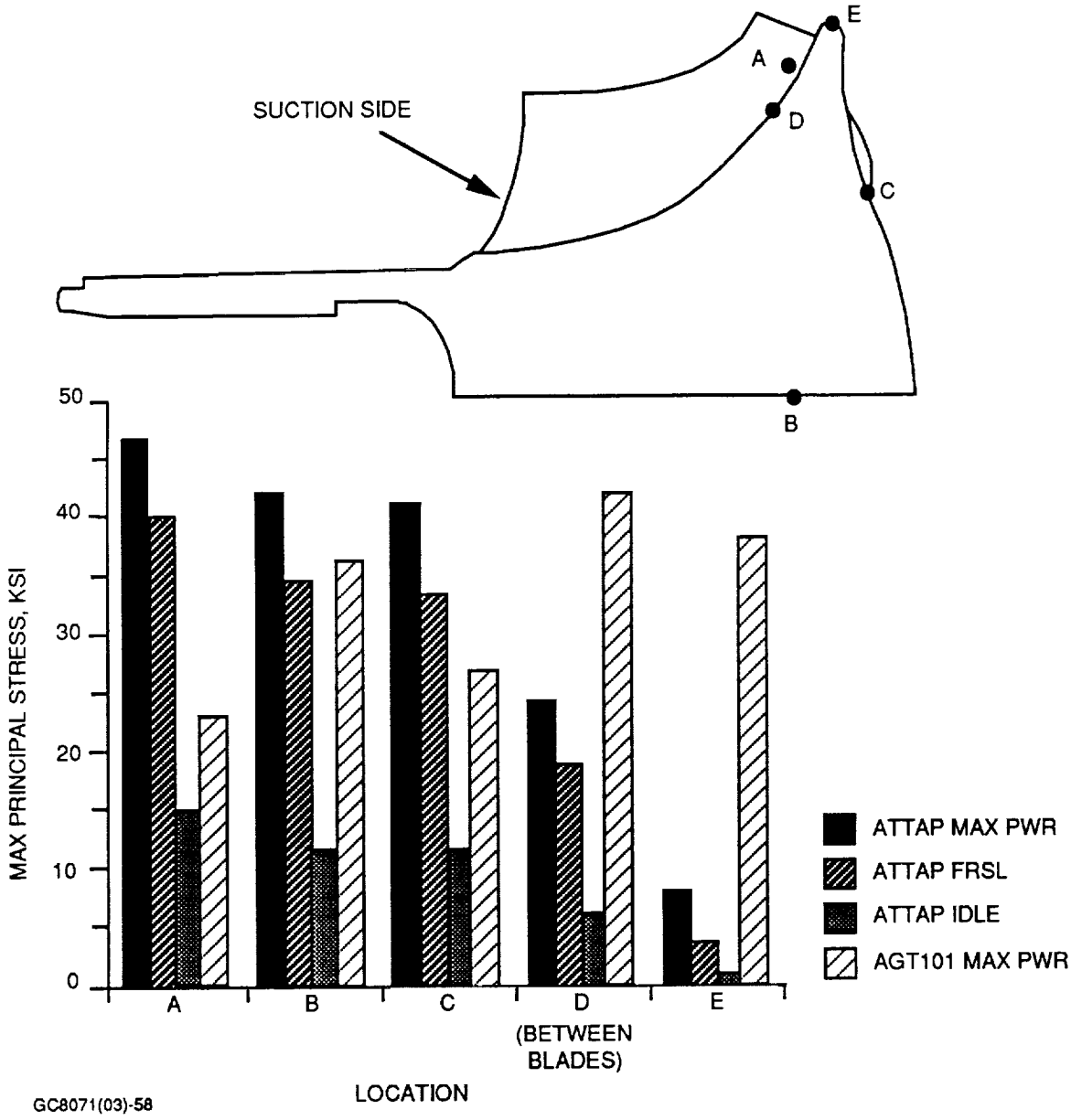

Figure 57. Comparison of ATTAP and AGT101 Turbine Rotor Steady-State Stresses.

gives an advantage in the event of a shutdown with an unwarmed regenerator core. Also, reduction of the high stress from the surface area between blades (point D) is expected to significantly aid slow crack growth probability of survival. The overall stress levels, however, are similar for the radial and impact-resistant rotors.

A transient thermal stress analysis is currently in progress. Following completion of the thermal analysis, a risk analysis will be performed, to determine the probability of the impact-resistant turbine rotor surviving fast fracture and slow crack growth.

5.0 MATERIALS CHARACTERIZATION AND CERAMIC COMPONENT FABRICATION

5.1 Materials Characterization

5.1.1 Property Measurements

During 1990, GAPD converted to metric test specimens measuring 4 by 3 by 50 mm (ASTM C1161, Specimen Size B) for flexural strength and flexural stress rupture tests. Some testing for 1990 was performed before the transition to the metric specimens. For those tests, specimens measuring 0.250 by 0.125 by 2.0 inch were used. The specimen size and test configuration used are referenced with each data set.

All further flexual strength and stress rupture tests to be performed in 1991 and for the duration of ATTAP will use metric specimens (ASTM C1161, Size B).

5.1.1.1 GCC GN-10 Rotor Characterization

Four slip cast GN-10 silicon nitride bladed AGT101 radial rotors (2/90 vintage) were machined into test specimens for component property characterization. The rotors were cast by Garrett Ceramic Components (GCC) using Slip Revision 15. Fast fracture flexural strength, chevron notch fracture toughness, and flexural stress rupture testing was performed.

The strength test results are shown in Table 8. The strength data are plotted as a function of temperature in Figure 58 and are compared to 1989 vintage GN-10 (baseline) characterized under ATTAP. The rotor flexural strengths were better than the 1989 GN-10 baseline.

Fractography was performed on all fast fracture specimens to characterize the fracture-initiating flaws. Fractures typically originated at the tensile surface, either at machining grooves or at the edge chamfer. Approximately 5 percent of the specimens failed at dark inclusions. In previous vintages of GN-10, dark inclusions were elemental silicon. For comparison, approximately 20 percent of the 1989 vintage GN-10 test specimens failed at silicon inclusions.

TABLE 8. GCC GN-10 ROTOR FLEXURAL STRENGTH TEST RESULTS

Material: GN-10 (Slip Rev. 15) Rotors Date Received: 02/90
Test Specimens: 0.250 x 0.125 x 2.0 inch
Test: 4-Point Flexure Test Span: 1.5 x 0.75 inch

Test Temp., F	Average MOR, ksi	Specimen Quantity	Weibull Modulus	Percent Surface Fractures	Percent Internal Fractures	Predominant Fracture Originals
R.T.	126.1	49	9.7	95	5	Surface - Machined surface, chamfers, dark inclusions
1400	112.5	10	–	100	0	
1800	113.7	10	–	90	10	
2000	110.3	10	–	78	22	
2200	100.7	30	13.9	90	10	
2300	97.7	9	–	89	11	Internal - dark Inclusions
2400	86.9	10	–	100	0	
2500	72.3	10	–	100	0	

R.T. = Room Temperature

8071(03)-8A

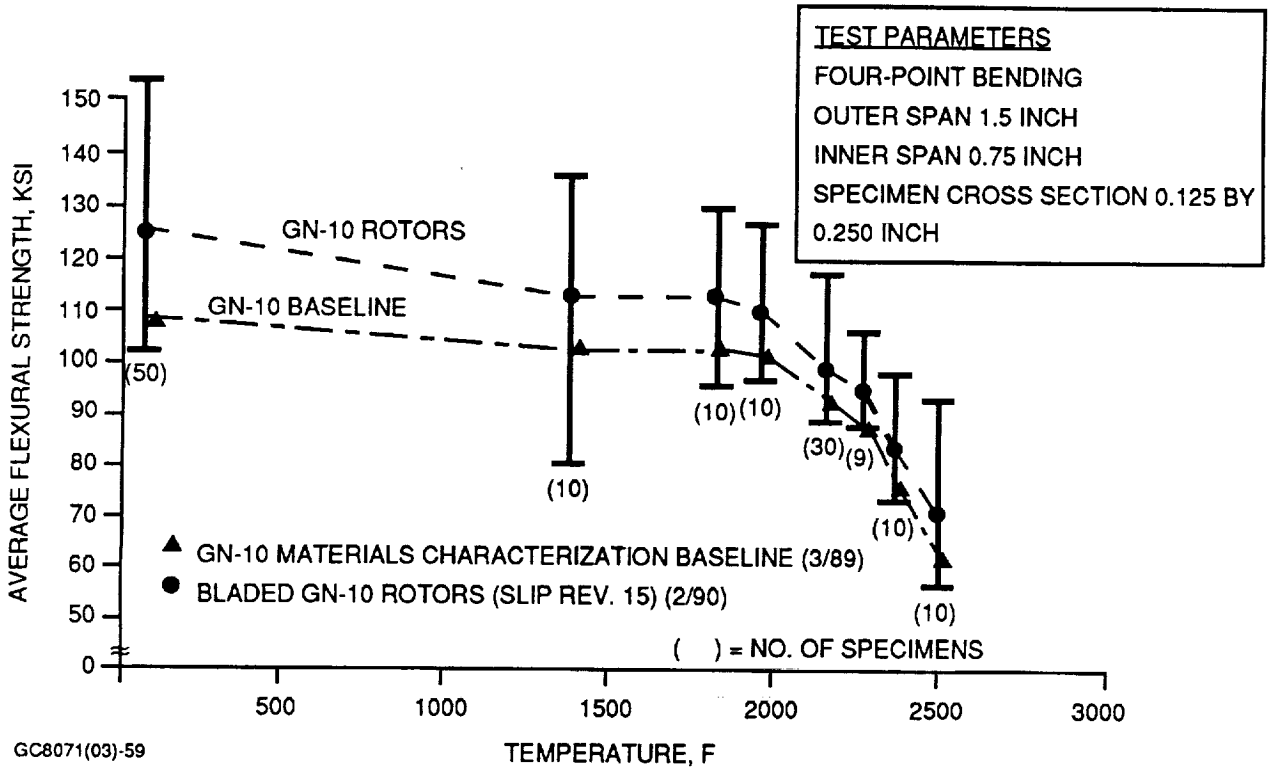

Figure 58. GN-10 Slip Revision 15 Rotor Flexural Strength Was Better Than 1989 ATTAP Material Characterization Baseline at All Temperatures.

The toughness values for bars cut from GN-10 radial rotors are shown in Table 9. The toughness values for the 1990 vintage rotor material and the 1989 GN-10 baseline material are equivalent.

TABLE 9. GN-10 ROTOR FRACTURE TOUGHNESS TEST RESULTS

Material: GN-10 (Slip Rev. 15) Rotors
Test: Chevron Notch Toughness, 3-Point Flexure
Date Received: 02/20
Test Specimens: V-Notched, 0.25 x 0.25 x 2.0 inch (See Figure 5)
Test Span: 1.5 inch

Test Temperature, F	Average K_{IC}, ksi*in $^{1/2}$	Specimen Quantity
R.T.	5.78	5
1800	5.45	3
2200	5.25	4
2500	9.55	4

R.T. = Room Temperature
8071(03)-9B

The stress rupture test results are shown in Figure 59. The Slip Revision 15 rotor flexural stress rupture life was better than the 1989 GN-10 baseline at all test temperatures.

Materials characterization specimens for GN-10 Slip Revision 15 material are due for delivery during the next reporting period. New baseline properties for GN-10 will be generated after receipt of the specimens.

5.1.1.1.2 GCC GN-10 As-Processed Surface Strength Characterization

In 1990, GAPD measured the as-processed surface strength of GN-10 silicon nitride hot isostatic pressed (HIPped) by ASEA, AB (a swedish subcontractor to GCC) using the "clean-glass" encapsulation process. This ASEA HIPped version of GN-10 was evaluated to provide a comparison for GN-10 HIPped at GCC; evaluation of GCC HIPped GN-10 is scheduled for early 1991.

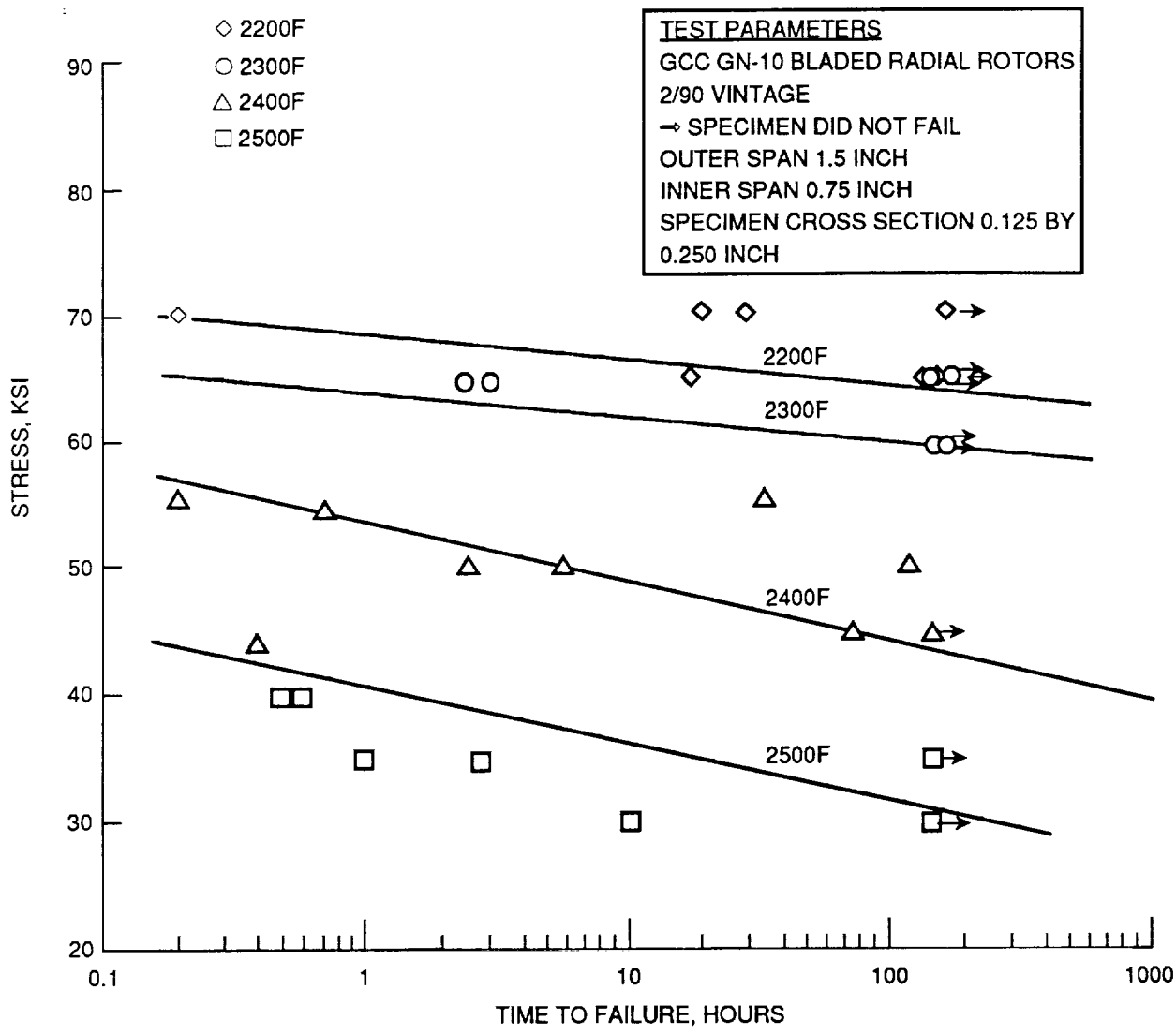

Figure 59. Flexural Stress Rupture Test Results for GCC GN-10 Slip Revision 15 Bladed Rotors (2/90 Vintage).

The as-processed surface strength of ASEA clean-glass HIPped GN-10 is plotted as a function of temperature in Figure 60. The room temperature, as-processed surface strength was approximately 55 percent of the machined strength for ASEA clean-glass HIPped GN-10. The elevated temperature, as processed surface strength ranged from 60 to 70 percent of the machined strength. The dominant fracture originating flaws were irregularities in the as-HIPped surface, as illustrated in Figure 61.

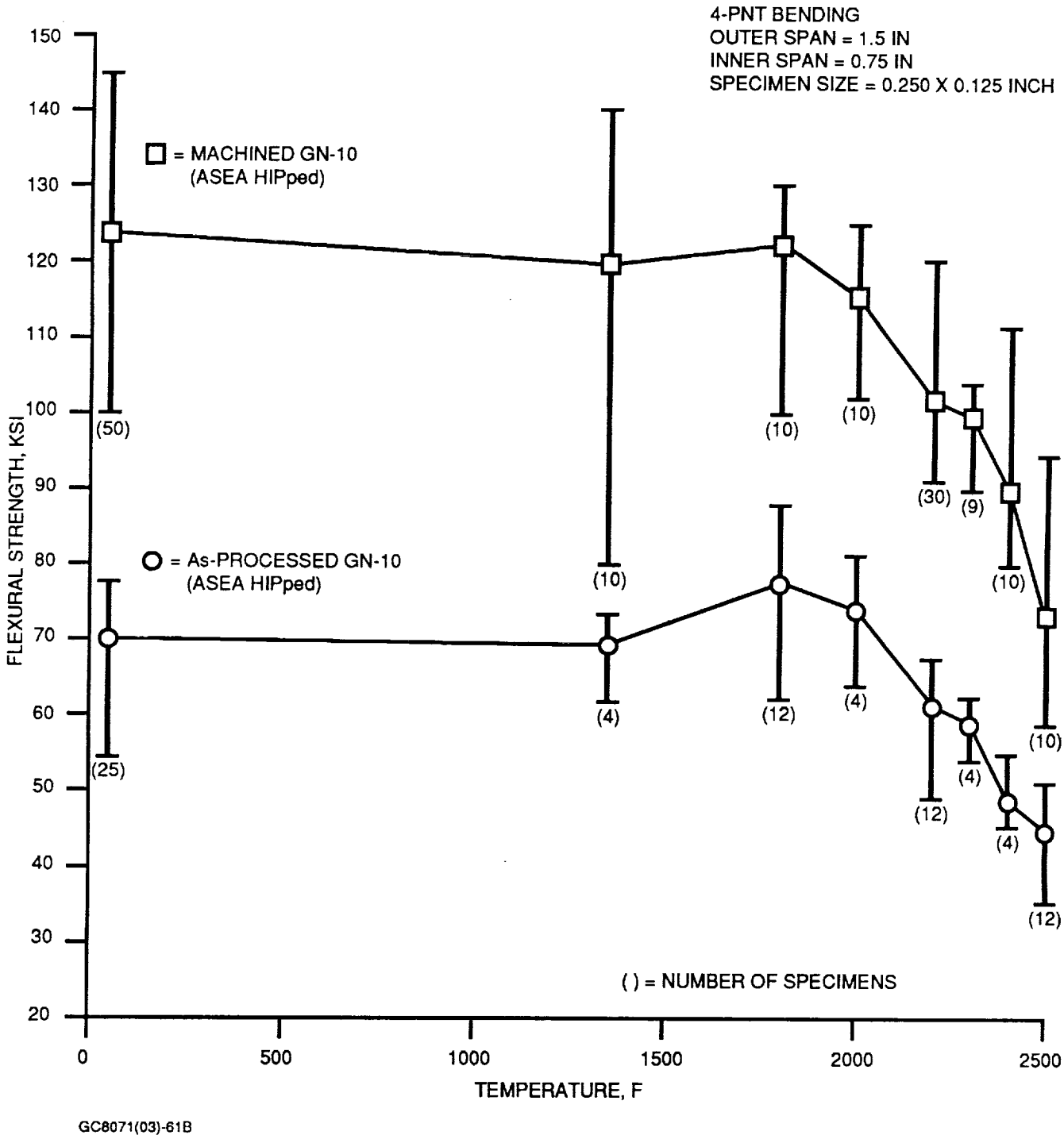

Figure 60. Flexural Strength of GCC As-Processed Surface ASEA Clean-Glass HIPped Specimens Is Substantially Less Than For Machined Specimens.

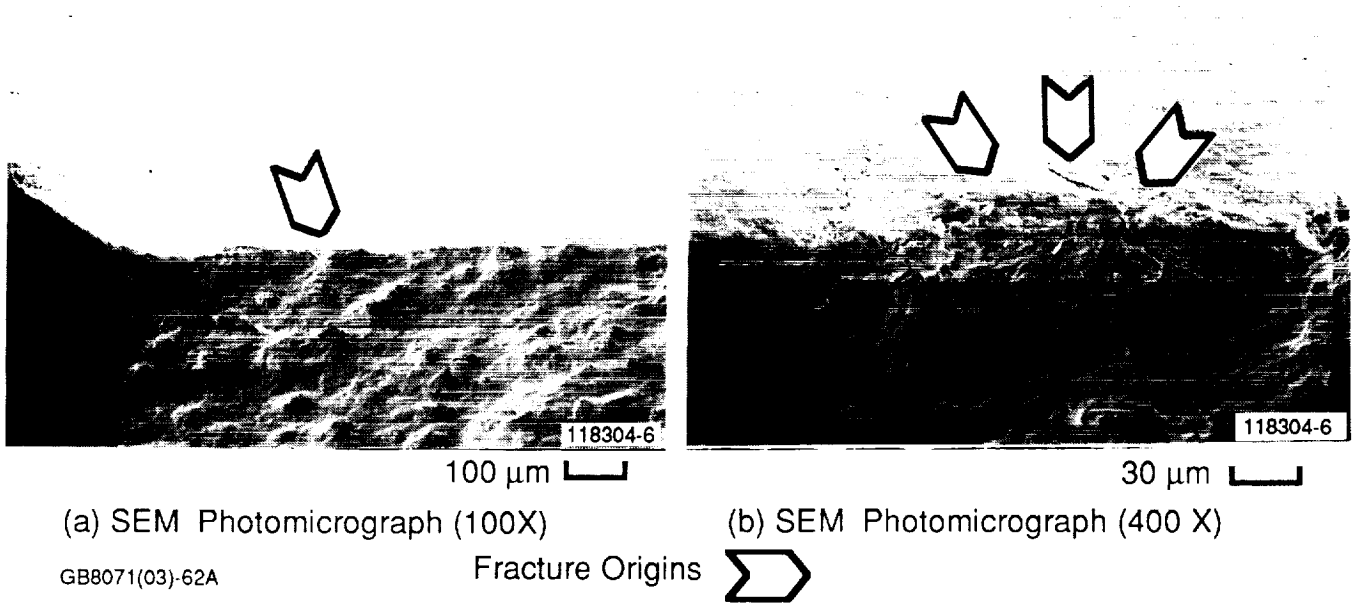

Figure 61. Dominant Fracture-Originating Flaws in ASEA HIPped GN-10 Were Irregularities in the As-HIPped Surface.

5.1.1.1.3 Norton/TRW NT154 Rotor Hub Characterization

Nine NT154 silicon nitride unbladed rotor hubs were received from Norton/TRW in June 1989. These parts were pressure slip cast using non-agglomerated powder. (Note that the current process required for bladed rotors uses agglomerated powders). Specimens were cut from the rotor hubs for characterization. Flexural strength and fracture toughness test results were reported in the 1989 ATTAP annual report and are summarized in Tables 10 and 11, respectively, for reference.

During 1990, flexural stress rupture testing was performed at temperatures between 2200F and 2500F. The results are shown in Figure 62. The stress rupture characteristics were better than the 1988 vintage NT154 characterized under ATTAP (baseline) for NT154 at all temperatures.

5.1.1.1.4 Norton/TRW NT154 Stator Characterization

Fast fracture flexural strength was performed on pressure slip cast NT154 silicon nitride test specimens co-processed with the first Norton/TRW stator delivery (3/90). The first delivery of stators were pressure slip cast using agglomerated powder, which is the process currently specified for bladed rotors.

TABLE 10. NORTON/TRW NT154 ROTOR HUB FLEXURE STRENGTH TEST RESULTS

Material: NT154 Rotor Hubs
Date Received: 06/89
Test Specimens: 0.250 x 0.125 x 2.0 inch
Test: 4-Point Flexure
Test Span: 1.5 x 0.75 inch

Test Temp., F	Average MOR, ksi	Specimen Quantity	Weibull Modulus	Percent Surface Fractures	Percent Internal Fractures	Predominant Fracture Originals
R.T.	144.2	30	11.1	97	3	Surface - Machined surface, and chamfer failures Internal - dark Inclusions
1000	149.3	10	--	90	10	
1400	135.8	9	--	67	33	
1800	120.6	9	--	78	22	
2000	112.5	9	--	67	33	
2200	107.4	30	16.2	80	20	
2300	104.8	11	--	64	36	
2400	99.7	10	--	90	10	
2500	91.5	9	--	100	0	

R.T. = Room Temperature

8071(03)-10A

TABLE 11. NORTON/TRW NT154 ROTOR HUB FRACTURE TOUGHNESS TEST RESULTS

Material: NT154 Rotor Hubs
Date Received: 06/89
Test: Chevron Notch Toughness, 3-Point Flexure
Test Specimens: V-Notched, 0.25 x 0.25 x 2.0 inch (See Figure 5)
Test Span: 1.5 inch

Test Temperature, F	Average K_{IC}, ksi*in $^{1/2}$	Specimen Quantity
R.T.	5.78	3
1800	5.22	4
2200	5.40	4
2500	10.58	4

R.T. = Room Temperature

8071(03)-11B

The flexural strength test results for the NT154 stator certification bars are shown in Table 12. The average strength was 115.5 ksi at room temperature, and decreased gradually with increasing temperature to 77.5 ksi at 2500F. The measured strengths were notably lower than for previously tested NT154 specimens at all temperatures.

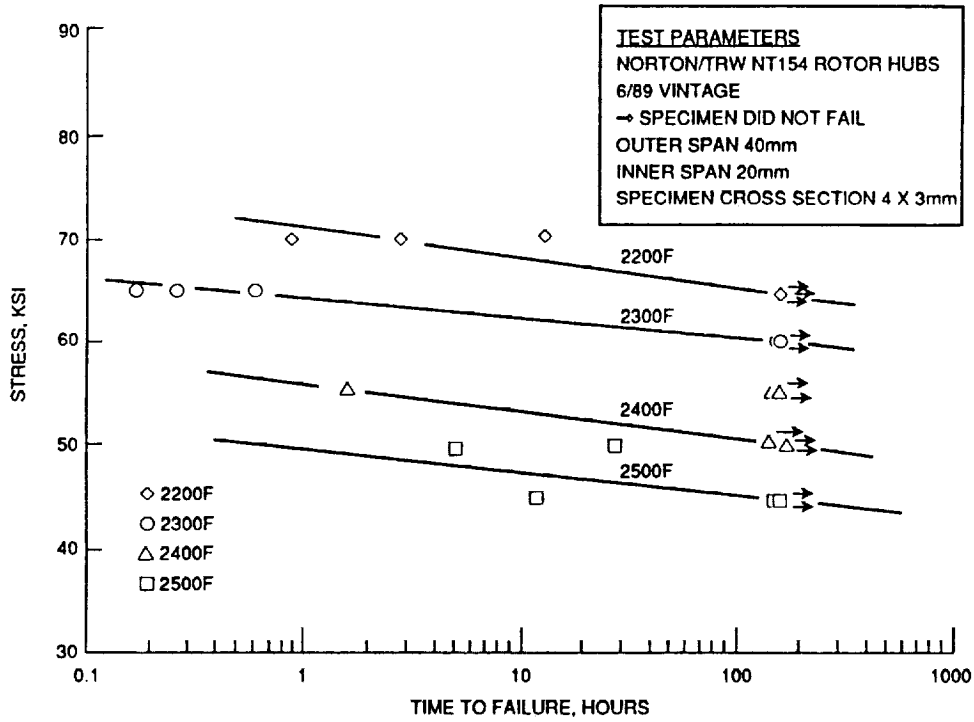

Figure 62. Flexural Stress Rupture Life Data for Norton/TRW NT154 Rotor Hub Specimens (6/89 Vintage).

TABLE 12. NORTON/TRW NT154 STATOR FLEXURAL STRENGTH TEST RESULTS

Material: NT154 Stators
Test: 4-Point Flexure

Date Received: 03/90
Test Specimens: 4 x 3 mm
Test Span: 40 x 20 mm

Test Temp., F	Average MOR, ksi	Specimen Quantity	Weibull Modulus	Percent Surface Fractures	Percent Internal Fractures	Predominant Fracture Originals
R.T.	115.5	30	8.2	87	10	Surface - Machined surface, chamfers, and dark (iron) inclusions Internal - Dark iron inclusions
2200	91.9	9	--	100	0	
2300	84.6	10	--	90	10	
2400	85.7	10	--	90	10	
2500	77.5	10	--	100	0	
NOTE: Failure origin percentages do not total 100 percent, since some origins were damaged or missing on some specimens.						

R.T. = Room Temperature

8071(03)-12A

The fracture-originating flaws were predominantly iron-based inclusions (Figure 63). Norton/TRW has also measured low strength in pressure slip cast material using agglomerated powders, and attributes the low strength to metallic inclusions introduced during the powder agglomeration. Norton/TRW has since made equipment modifications to eliminate the contaminant source, and preliminary results look encouraging (see Appendix I).

ORIGINAL PAGE
BLACK AND WHITE PHOTOGRAPH

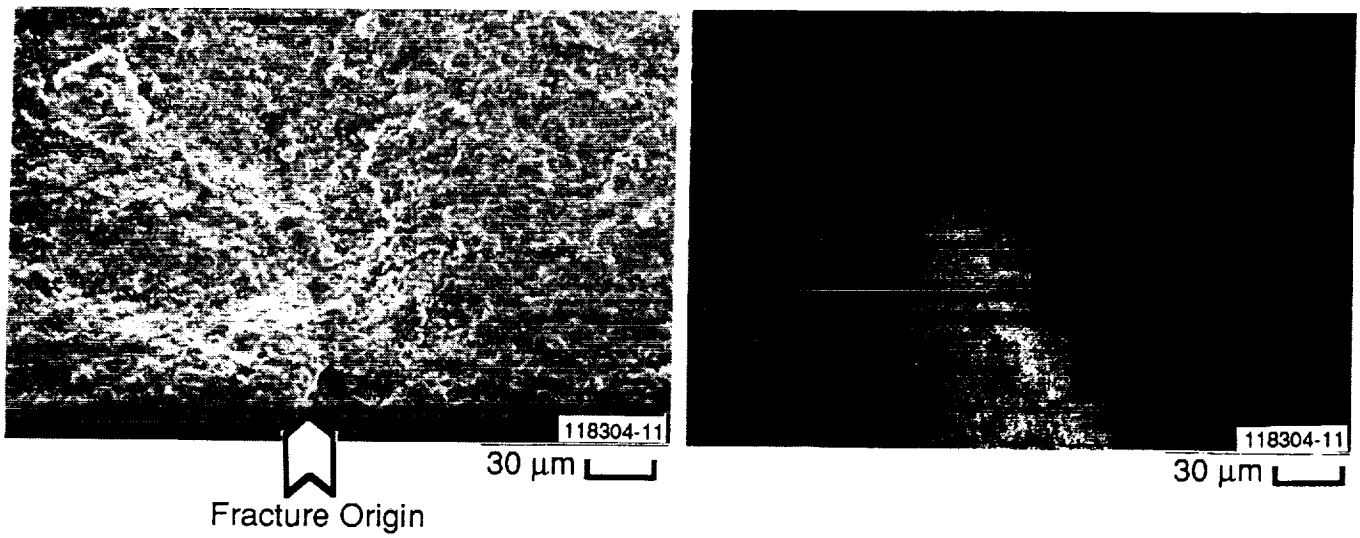

(a) SEM Photomicrograph (400X)

(b) WDX Iron (Fe) Element Map of Fracture Origin (400X)

GB8071(03)-63A

Figure 63. Fracture Origins of NT154 Stator Specimens Were Predominantly Iron-Based Inclusions.

5.1.2 Nondestructive Evaluation (NDE)

During 1990, the majority of the ATTAP NDE efforts were devoted to the inspection of test bars for the Materials Assessment and Materials Characterization Tasks, and components for the Materials Characterization Task and Rig Testing Tasks. Time was spent interfacing with component suppliers to ensure that comparable NDE results are obtained by all parties. Fluorescent penetrant inspection (FPI) and microfocus x-ray radiography continue to be the primary inspection techniques, along with visual examination at up to 40X magnification.

FPI was conducted on all test bars and components except for those made from lithium aluminum silicate (LAS). This material is porous and produces a very high background reading, making it impossible to detect any flaw indications. A procedure has been established to apply Level 4 penetrant, the highest sensitivity, to finish-machined test bars and components. The low background level obtained on machined surfaces makes the use of Level 4 penetrant possible. Level 3 penetrant is used for test bars and components with as-processed surfaces. A study has been designed to compare GAPD and vendor FPI results on a collection of defective parts.

During 1990, a specification for microfocus radiography was established which calls for all radiographs to achieve an image quality level of 2-1T. The 2-1T designation means that, in the case of a 0.250 inch thick part, the radiograph must be capable of discerning a 0.005 inch diameter hole in a 0.005 inch thick penetrameter placed on the part, or on a block having the same thickness as the part. The penetrameter, or image quality indicator (IQI), is fabricated from Si_3N_4. The "2" in the image quality designation specifies that the IQI thickness must be 2 percent of the part thickness (i.e., 0.005 inch in this case). For parts less than 0.250 inch thickness, there is a problem in fabricating IQIs as thin as 2 percent of the part thickness. As a result, for parts less than 0.200 inch thickness, the specification calls for being able to discern a 0.002 inch diameter hole in the 0.005 inch thick IQI. This specification avoids problems in applying the ASTM radiography specification (ASTM E 142, developed for metals) to ceramics. The highest image quality that can be specified by the ASTM specification is 2-2T (on sections 0.250 inch or less) and the smallest hole size in the aluminum IQI is 0.010 inch.

The 2-1T image quality is consistent with published work (See NASA Report Nos. TM-86945 and TM-87164) which indicates that a sensitivity of 1.5 percent of part thickness can be achieved with microfocus x-ray on ceramic parts.

To obtain high image quality with the 2-1T specification also requires special handling of the film. The use of "standard" cassettes can result in imaging the texture of the cassette surface onto the film. This problem has been resolved by switching to "day pack" film.

A total of 142 pieces of engine-quality hardware were inspected in 1990. Most FPI indications consisted of very small dimples and/or machining marks. The only rejectable radiographic indications were attributed to constituent segregation in an Si_3N_4 inner diffuser.

Although these indications had the appearance of a crack network along grain boundaries, no cracks were found. Considering the temperatures and stress in this part, these indications may not be relevant. However, their effect on high-temperature properties is being evaluated.

The use of acoustic emissions to monitor rig testing continued in 1990. However, no component failures occurred during thermal screening rig testing for correlation with the acoustic emission signals.

5.1.3 Miscellaneous Materials Issues

5.1.3.1 Intermediate Temperature Stability

A gradient furnace heat treatment study of candidate ATTAP component materials was performed during 1990. The purpose of the investigation was to determine if intermediate temperature stability problems (characterized by excessive oxidation weight gain) exist in ATTAP component materials. This study was initiated after discovering an 1800F oxidation stability problem in Kyocera SN-251 and SN-252 Si_3N_4. (Kyocera has since developed a "flash oxidation" heat treatment which cures the intermediate temperature effects).

Eight ceramic materials were included in the study:

- Norton/TRW Ceramics NT154 Si_3N_4
- GCC GN-10 Si_3N_4
- NGK SN-84 Si_3N_4
- Kyocera SN-250m Si_3N_4
- Kyocera SN-251 Si_3N_4 (flash oxidized)
- Kyocera SN-252 Si_3N_4 (flash oxidized)
- Carborundum Co. Hexoloy SA SiC
- Carborundum Co. Hexoloy ST TiB_2/SiC

Eighteen coupons of each material were placed in a gradient temperature furnace (static air) and exposed at 100F intervals covering the 800F to 2500F temperature range. The exposure duration was 100 hours.

The results of this study indicate no intermediate temperature stability problems exist in the materials studied. None of the materials evaluated exhibited excessive weight gains at intermediate temperatures. The Kyocera SN-250m material exhibited a slight increase in weight gain between 1700F and 2000F. The other ceramics exhibited a gradual increase in weight gain as a function of temperature.

5.1.3.2 Vacuum and Nitrogen Exposures Supporting High-Temperature Spin Testing

ATTAP and the DOE Oak Ridge National Laboratory (ORNL) Ceramic Life Prediction Program both plan to use an elevated temperature spin test to verify ceramic life prediction models. A heat-treatment study using NT154 was initiated in 1989 to identify suitable environments for operation of the high-temperature spin pit. Preliminary results, reported previously in the 1989 ATTAP Annual Report, indicated the vacuum conditions used in conventional room-temperature spin pits (2.4×10^{-4} atm) were not suitable for ceramics. Excessive weight and strength loss resulted above 2300F in short duration tests. As a result, a broader range of environments, including weaker vacuum and nitrogen environments, was evaluated in 1990.

The results of heat-treatment studies performed to date are summarized in Table 13. Weaker vacuum (0.001 and 0.01 atm air) proved unsuitable at 2400F and 2500F, since moderate weight loss and slight strength loss were observed after short-duration exposures. The results from nitrogen heat treatments were more encouraging, but spin pit operation would likely be limited to 2300F operation for long-duration tests.

TABLE 13. RESULTS OF HEAT TREATMENT STUDIES SUPPORTING HIGH-TEMPERATURE SPIN PIT TESTING

Temperature, F	Environment	Duration, hours	Weight Change, mg/cm^2	Retained Strength, ksi
2000	2.4E-4 atm air	20	-0.0227	(Not Measured)
2100	2.4E-4 atm air	20	-0.0132	126.0
	1.0 atm N2	20	-0.0179	158.7
2200	2.4E-4 atm air	20	-0.0200	(Not Measured)
	1.0 atm N2	20	-0.0377	156.0
	1.0 atm N2	100	-0.0516	141.8
2300	2.4E-4 atm air	20	-0.0003	121.3
	1.0 atm N2	20	-0.0636	149.8
2400	2.4E-4 atm air	20	-0.3345	66.6
	0.001 atm air	20	-0.0935	99.4
	0.01 atm air	20	0.0040	57.6
	1.0 atm N2	20	-0.1903	116.1
2500	2.4E-4 atm air	20	-1.6897	(Not Measured)
	0.001 atm air	20	-0.2904	21.0
	0.01 atm air	20	-0.0038	51.0
	1.0 atm N2	20	-0.2582	101.4

8071(03)-13A

The results generated indicate that 1.0 atm air capability will likely be required for spin pit tests on ceramics performed above 2300F, to avoid material degradation modes not likely to be encountered in gas turbine engine environments. ATTAP Si_3N_4 materials require partial pressures of both oxygen and nitrogen to avoid:

(1) Dissociation of Si_3N_4
(2) Dissociation of silicate grain boundary phases
(3) Active oxidation of Si_3N_4

As a result, the heat-treatment studies have been terminated, and efforts have been refocused on developing a high-temperature spin pit with 1.0 atm air capability.

5.2 Ceramic Component Fabrication

Activities of the three ATTAP ceramic component subcontractors (Norton/TRW Ceramics, Carborundum Co., and Garrett Ceramic Components) are detailed in the Appendices to this report. A brief synopsis of activities is presented in the following paragraphs.

5.2.1 Norton/TRW Ceramics (NTC)

In the course of redesigning the ATTAP flowpath, NTC assisted by carefully reviewing designs for the impact-resistant turbine rotor and stator components. NTC's inputs resulted in a change to the rotor blade shape allowing a single tool segment to be pulled from between each pair of adjacent blades, following a simple motion. Stator vane geometry was also modified to enhance the ability of material to flow toward the trailing edge during the casting process. NTC's input on dimensional inspection procedures for the new impact-tolerant turbine rotors and stators was also useful in establishing meaningful part datum structures (datum refers to the reference point from which dimensions during fabrication and final inspection are measured).

In September 1990, the first ceramic rotor and stators of the new design, formed from tooling which used stereolithographic models* as a pattern, were made available. Fabricability of the new rotor and stator geometries was thus demonstrated well prior to the actual release of component drawings.

*See Section 1.3

During the year NTC introduced the new NT-230 siliconized silicon carbide material. NTC property data shows significant improvement over the predecessor Norton NC-430 material. An order for NT-230 transition ducts was made, and delivery is scheduled for 1991.

5.2.2 The Carborundum Company (CBO)

Activity with CBO was redirected towards fabrication of structural components using isopressing and green machining of their Hexoloy SA material. This established, familiar process will be employed for fabrication of the latest design ATTAP pilot combustor supports, transition ducts, and combustor baffles for the demanding requirements of gas turbine applications. Five pieces each of the three parts are on order. Delivery is scheduled by the end of March 1991.

In May 1990, CBO personnel visited GAPD to discuss fabricability of ATTAP engine components. For the shapes considered, suggestions to ease fabrication in silicon carbide were made, and limitations of the isopress/green machining process were reviewed.

Shortly after this visit, CBO provided a sample pilot combustor support made by the isopress/green machining process. The short turnaround time was impressive for this complex part, as it includes a number of small angled holes which would be difficult and time-consuming to machine into a fully-dense part.

At mid-year 1990, a letter subcontract between GAPD and CBO was drafted, with significant incentives for CBO to meet the blueprint requirements within the timeframe necessary to support engine test activities. Discussions on the scope of work and the acceptance criteria for the deliveries were held. Batch qualification and other activities had already begun at the time of the letter subcontract draft, so that by year's end 1990 the pilot combustor supports had been processed past the sintering stage and were in final machining.

5.2.3 Garrett Ceramic Components (GCC)

In early 1990, GAPD personnel visited GCC to consult and assist in the setup of GCC's new microfocus x-ray radiography unit. A new scanning electron microscope (SEM) unit also became fully operational at GCC in 1990. During the year, HIPping activities, previously done at ASEA in Sweden, were brought in-house at GCC, allowing them to build their own

experience in this area. Improved control over the HIP process and improved HIP turnaround times were soon realized.

In August 1990, GCC delivered a calcined impact-resistant design rotor made from a stereolithographic pattern*, and shortly thereafter HIPped rotors of the new geometry were available for evaluation. Time from the receipt of the sterolithographic pattern to successful HIPping of the new rotor geometry was approximately eight weeks.

Hard metal tooling to fabricate final engine-quality rotors was received in late November 1990, and at the end of the reporting period, initial casting trials using the new tooling had begun.

5.3 Ceramic Component Preparation

Certain ceramic hardware items were machined in-house by GAPD during 1990. Combustor hardware is being produced from hardware previously used in the AGT101 program; this hardware will be used to test a new combustor configuration. Ceramic bolts were also machined from hardware already on hand. The bolt neck was reduced in diameter, to allow installation of a metallic nut of new design which will not creep at high temperatures.

New hardware was processed through an inspection loop. The loop consisted of visual, penetrant, radiographic, and dimensional inspections. The following new hardware was processed in 1990:

- Bolts
- Rockers
- Lower contract washers
- Crowned washers
- Inner diffusers
- Outer diffusers
- Diffuser spacers
- Spring plates
- Backshrouds
- Piston ring seals

Some of the hardware was also subjected to proof testing, discussed in Section 6.4.

*See Section 1.3

6.0 COMPONENT RIG TESTING

6.1 Hot Spin Pit Design and Fabrication

The objective of this effort is to use data generated from test specimens to formulate methods to analytically predict ceramic component life, and to apply these methods to successfully predict the life of ceramic disks of the same material spun under both room temperature and heated conditions.

The spin tests are necessary to generate the biaxial stress fields that can demonstrate successful life prediction under more than just a uniaxial state of stress (as would be generated in a test specimen). Such spin testing at high rotational speeds is normally accomplished in a near-complete vacuum so as to eliminate the effect of viscous drag, which can limit speed and affect the stability of the spinning member. However, spin testing silicon nitride (Si_3N_4) specimens in a near-complete vacuum for prolonged time periods (more than 1 hour) can cause dissociation of the Si_3N_4 test material; thus, spin testing under atmospheric conditions is indicated.

A titanium disk of a geometry nearly identical to that of the spin disk was used to quantify what speeds can be reached under standard atmospheric conditions. A maximum speed of 100,000 rpm was reached using this combination.

A system analysis was also conducted to determine the time required to reach the maximum operating temperature of 2500F in the hot spin pit. In an experiment, eight silicon carbide rods surrounded by insulation heated the spin pit to 2500F in less than an hour.

The arbor cooling flow was also quantified during this test, so as to cool the arbor attachment, but not cool the pit. Flows up to 0.08 lb/sec will be allowed for this test.

Some new designs and improvements were also initiated for the hot spin pit configuration during 1990. Arbor attachment, arbor cooling, insulation requirements, and safety issues have all been addressed, and these finalized designs will be completed in 1991.

6.2 Combustor Rig Testing

Combustor rig testing concentrated on evaluating the ability of the stepped pilot combustor (present design) and the constant-diameter pilot combustor (redesign) in combina-

tion with old (six-point) and new (simplex) fuel nozzle configurations to operate successfully without creating coke (configurations are described in Section 3.4.2). This series of tests represents a means of addressing the risk of foreign object damage (FOD) to the gas turbine hot section. Four combinations of hardware (Table 14) are being tested in light-off, cold inlet coking tests, and hot inlet coking tests. The hot and cold inlet coking tests are being evaluated at the AGT101 ceramic engine idle, cruise, and maximum power conditions.

TABLE 14. COMBUSTION SYSTEM TESTS WILL UTILIZE FOUR HARDWARE COMBINATIONS

Pilot Combustor Geometry	Fuel Nozzle	
	Simplex	Six-Point
Stepped	1	2
Constant Diameter	3	4

8071(03)-14A

Figure 64 shows the relative improvements that have been seen during lightoff conditions while utilizing the new ATTAP simplex nozzle design. A much more varied range of air flow and fuel flow conditions can be obtained with the new nozzle design. This lightoff envelope also seems to be indifferent with respect to the combustor section that is utilized during testing.

Presently, the cold inlet and hot inlet coking tests are still being conducted; completion is scheduled for the first quarter of 1991. Some improvements to the nozzle design are still being implemented.

In the early series of tests that utilized the stepped pilot combustor and the simplex nozzle design, coke was found to have adhered to the nozzle face, during the idle and maximum power test points. To solve this problem, an airwipe sweep has been added to the face of the second-generation fuel nozzle (Figure 65). Additionally, the spray angle has been reduced in the nozzle tip to improve the concentration of atomized fuel at the center of the combustor bore. This combination should eliminate the dripping effect which is causing coking on the nozzle face.

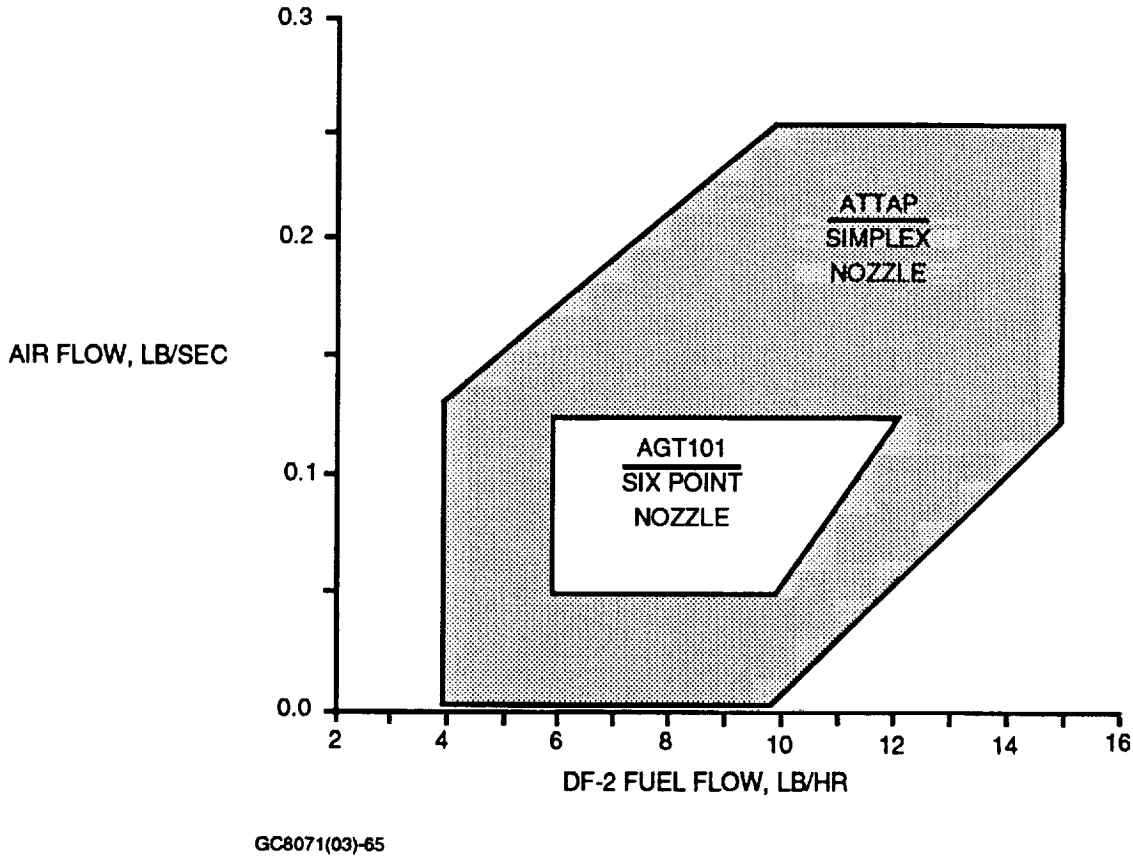

Figure 64. Improved Combustor Lightoff Range Has Been Demonstrated Using the Simplex Fuel Nozzle Design.

6.3 Regenerator Rig Testing

Regenerator rig testing concentrated on regenerator hot seal durability. The regenerator rig build configuration reflects the metallic and ceramic structures of the AGT101 ceramic engine, except for replacement of the rotating group with an adjustable ceramic valve. The regenerator hot seal tested had the baseline coating configuration, and incorporated a new mechanical design to relieve thermal stress. A Taguchi experiment was also performed to reduce regenerator torque.

Two regenerator rig tests were performed in 1990. A total of 72 hours test time were accumulated. The rig temperature range for this testing was 1200F to 1600F regenerator inlet temperature. Rig pressures ranged from 20 to 40 psig. Seal durability proved to be very promising: at the completion of testing, there was insignificant wear and no signs of coating spalling or mechanical deformation.

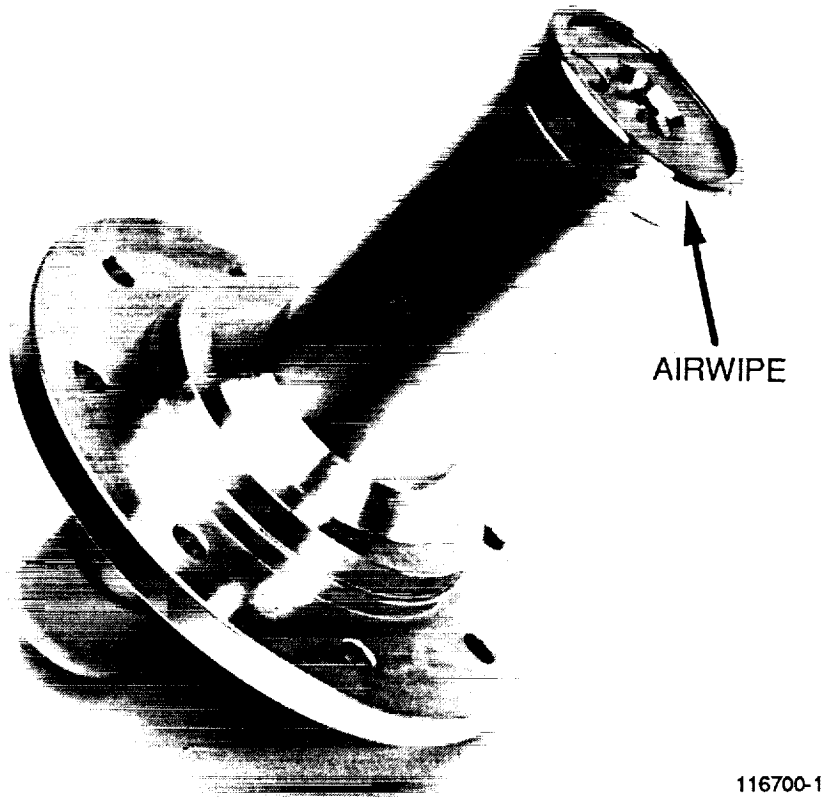

Figure 65. Second-Generation Fuel Nozzle Has Added Air Wipe.

As part of the rig tests, a Taguchi experiment was performed to reduce regenerator torque. The Taguchi test matrix consisted of three different exhaust housings, machined to give different clearance distributions in the seal area. The three configurations were: a baseline housing, machined flat along the seal area; and two concave housings, machined concave 0.020 and 0.030 inch, respectively, to give more clearance at the seal ID. The Taguchi experiment results defined an optimum build configuration for the rig. The test results showed a reduction in torque for both concave exhaust housings. The reduction in torque for either of the two concave housings was not large, so the 0.020 inch concave housing was selected, for leakage reasons.

6.4 Structural Proof Testing

The NDE techniques to assure high reliability of ceramic components have not yet been fully identified or developed and it remains necessary to perform component proof tests to

qualify ceramic hardware for use in the ATTAP test bed engine. These tests generally simulate a worst-case stress condition with a 25 percent overstress margin. Information from these proof tests, when combined with results of prior NDE testing, can be valuable in determining the critical flaw characteristics and aids in establishing specifications for ceramic components. The proof tests conducted during 1990 are summarized in the following paragraphs.

6.4.1 Transition Duct/Baffle Rig

Three baffles were successfully tested in the transition duct/baffle thermal screening rig. The hardware screened is listed below:

Item	S/N
Transition Duct	128-6
Baffles	304
	305
	306

This rig places the hardware in 25 percent overstress at worst-case conditions. Each baffle was run through two rig cycles, as illustrated in Figure 66. One transition duct was used in conjunction with all of the baffles, since no transition ducts required screening.

6.4.2 Diffuser Test Rig

A thermal shock test rig was used to screen inner and outer diffusers. A schematic of the rig is shown in Figure 67. The inner and outer diffuser thermal screening rig subjects the hardware to 25 percent overstress at worst-case conditions. Each diffuser was run through two test cycles, as illustrated in Figure 68. The following hardware was screened in early 1990:

Item	S/N
Inner Diffusers	114-1
	114-2
Outer Diffusers	113-1
	113-2

All of the hardware tested was deemed of engine quality, after passing posttest inspections.

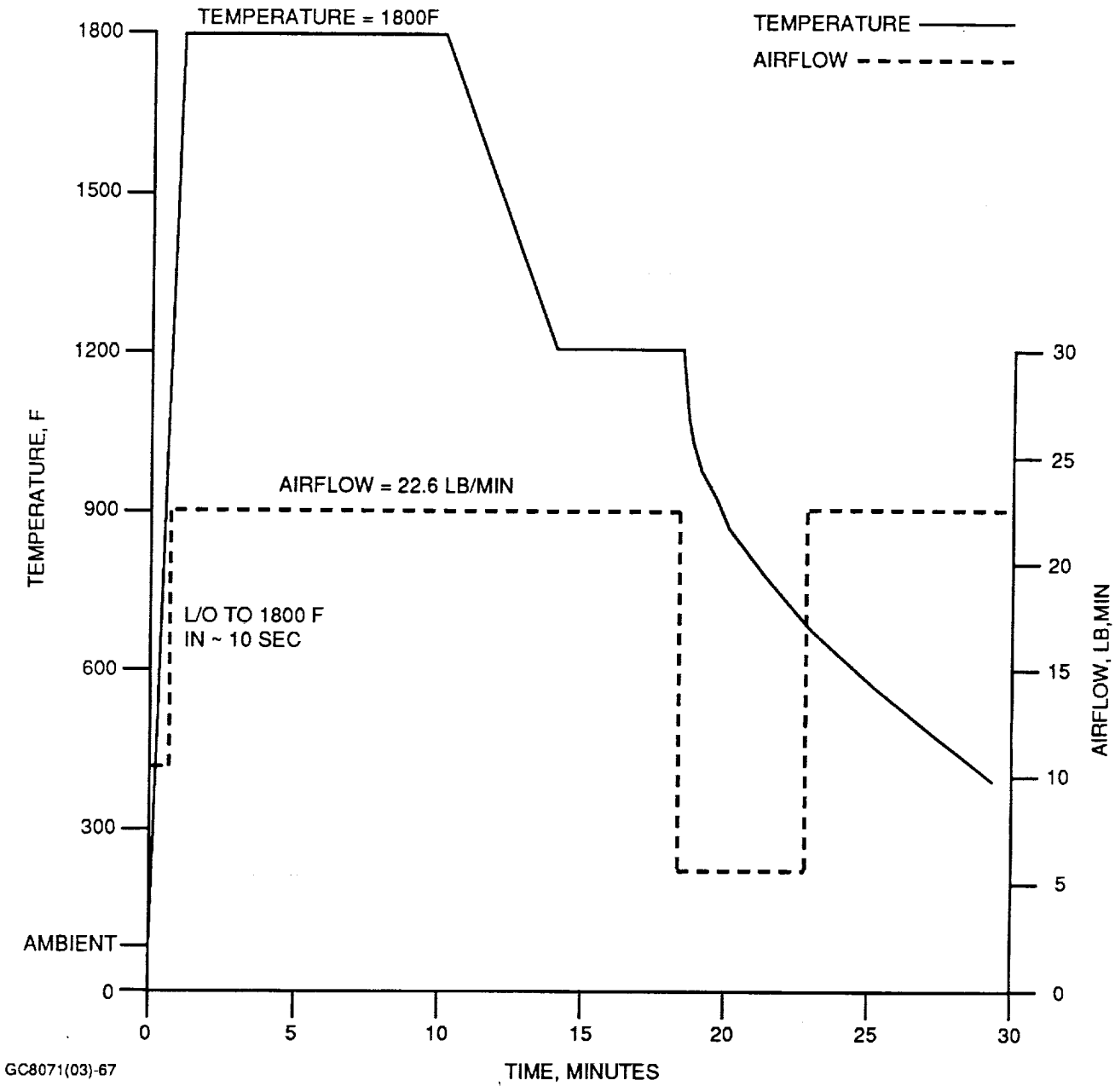

Figure 66. Typical Transition Duct/Baffle Thermal Screening Cycle.

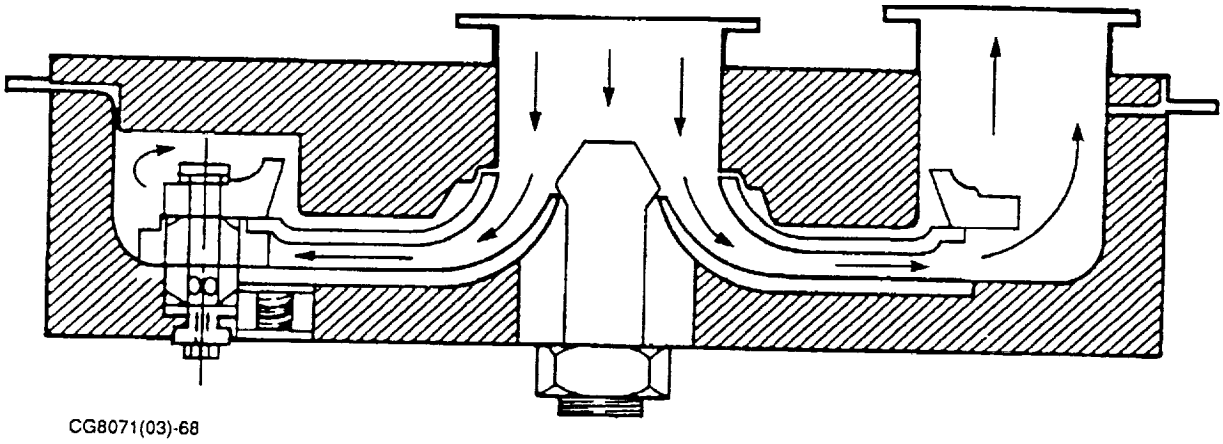

Figure 67. **Airflow in the Inner/Outer Diffuser Thermal Proof-Test Rig Closely Simulates the ATTAP Test Bed Engine Flow Path.**

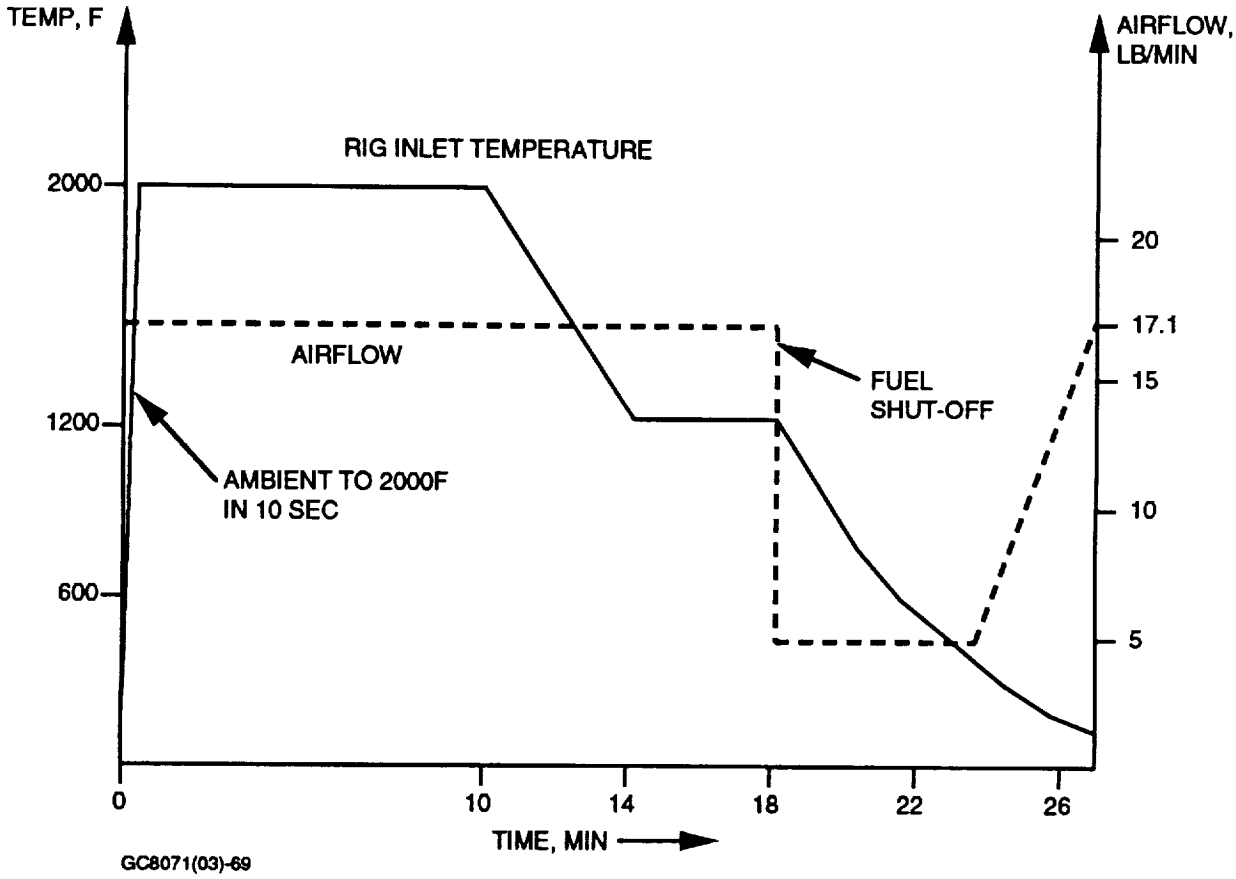

Figure 68. **Typical Inner/Outer Diffuser Housing Thermal Screening Cycle.**

Additional inner and outer diffusers were screened in late 1990:

Item	S/N	Item	S/N
Inner Diffusers	0133	Outer Diffusers	0131
	0138		0132
	0139		0134
	0140		0135
			0136

This hardware was subjected to test cycles as described earlier at the Garrett San Tan Mountains remote test site southeast of Chandler, Arizona. All of the hardware passed the required inspections following the tests.

6.5 1371C (2500F) Test Rig

The 2500 degree test rig will subject ceramic hardware to high temperatures for extended periods of time, to simulate the 100-hour engine test, and assess the durability of ceramic stators and other components. Testing is planned for early 1991. Preparations for testing continued during 1990. NT154 stators were received from Norton/TRW Ceramics and machined to fit the current rig configuration.

6.6 Turbine Inlet Particle Separator (TIPS) Testing

Testing of the center-supported TIPS design was completed in 1990. This design (Figure 69) utilized radial struts, tailored and untailored cones, and superseded the previous ramp design. From results of this study, the separation efficiency ranged from 83.4 to 98.7 percent.

From an analysis of the test data, a best configuration (Figure 70) was identified. This configuration utilized a cone angle of 30 degrees, a bleed gap of 0.08 inch, a cone-to-combustor distance of 5.5 inches, and a splitter gap of 0.80 inch. This combination provided a separation efficiency of 98.7 percent at a pressure loss of approximately 3 percent.

As reported in Section 3.4.4, 2-D thermal analysis results indicate the TIPS cone temperatures would exceed available ceramic material capabilities. Therefore, program activity on this component has been discontinued.

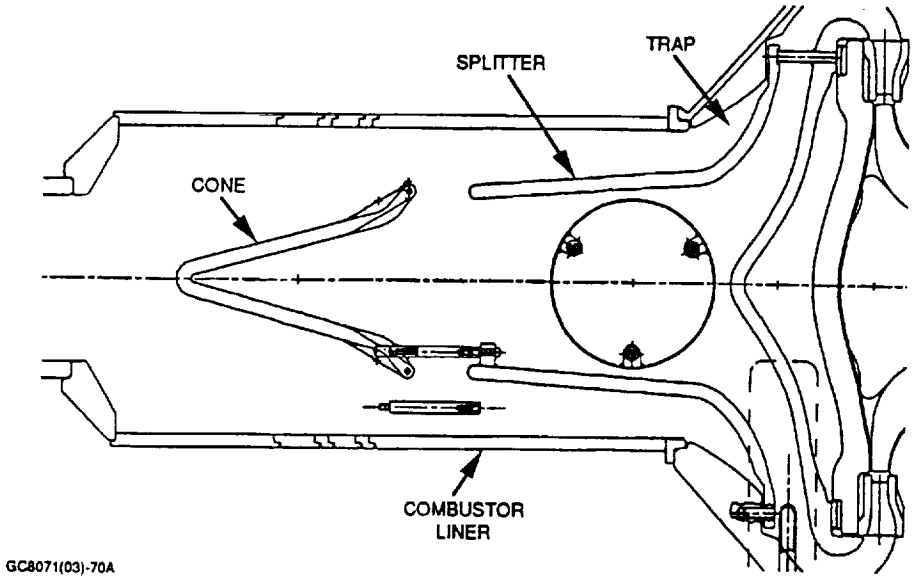

Figure 69. Testing of Center-Supported TIPS Design Was Completed in 1990.

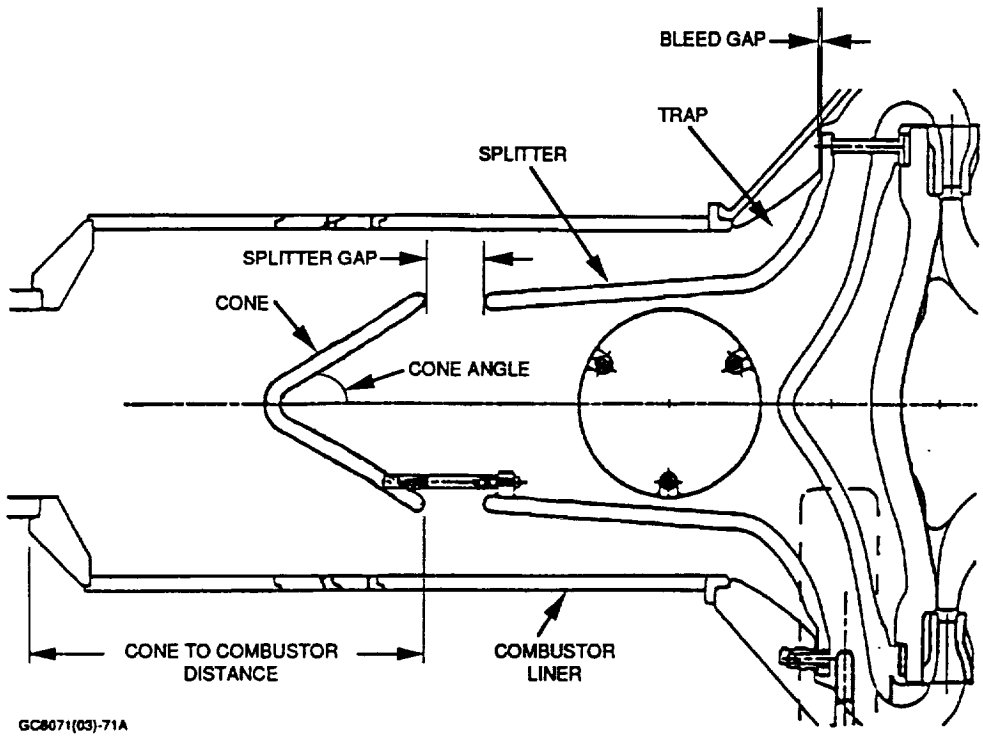

Figure 70. Best Configuration TIPS Was Determined.

6.7 Turbine Stage Aerodynamic Test Rig

The objectives of the turbine stage aerodynamic rig testing are to validate the theoretical aerodynamic design of the ATTAP turbine and obtain actual turbine aerodynamic trends that will allow accurate prediction of the turbine stage performance in the engine.

During 1990, work on the test rig consisted of completing the component rig design, detailing and releasing component blueprints, and initiating fabrication of hardware. The rig design goals are to match the engine conditions and hardware as closely as possible, while maintaining a mechanically sound system and facilitating the instrumentation requirements for retrieval of aerodynamic data Detailing of blueprints and fabrication of long-lead-time hardware started in mid-1990, with completion of all parts expected by late March 1991.

7.0 ENGINE TEST BED TRIALS

The metallic AGT101 engine test bed was assembled and tested during 1990, to evaluate an improved electronic control unit (ECU), and to acquire data for thermal analysis of the ceramic flow separator housing (FSH) and combustor geometries. These tests incorporated geometries similar to the ceramic AGT101 engine test bed.

During three tests conducted in 1990, 9 hours of run time and 27 starts were accumulated on the AGT101 metallic engine test bed. Testing was hampered by a compressor surge problem which had not been seen in previous tests. The engine was operated at between 50 to 80 percent speeds during these tests. Surge investigation and resolution took the bulk of the test time.

During the series of tests, additional instrumentation was added to the engine at a variety of engine stations to locate the cause of the surge. Presently, the engine contains the following instrumentation: inlet flow pressures and temperatures, compressor exit pressures and temperatures, turbine inlet pressures, turbine exit pressures, and exit flow and emissions sampling instrumentation. Identification of the cause of the surge has become the primary goal for the first quarter of 1991.

8.0 PROJECT MANAGEMENT AND REPORTING

The ATTAP Milestone Schedule is shown in Figure 2. Milestone 3, Component Fabrication, has slipped beyond December 1990, due to the increased efforts required by the subcontractors to develop the technology necessary to fabricate hardware that will meet RPD temperature requirements and the test bed engine specification, and the changes in turbine design for the ATTAP test bed engine. Ceramic component deliveries are scheduled to be completed by mid-1991.

GAPD issued five Bi-Monthly Technical Progress Reports during 1990 and conducted five Bi-Monthly Review Meetings with NASA/DOE.

GAPD personnel attended the "Twenty-Eighth Automotive Technology Development Contractors' Coordination Meeting" in Dearborn, MI, October 22-25, 1990. Two presentations were made reporting on ATTAP accomplishments over the past year:

- "ATTAP/AGT101 Ceramic Technology Development" (GAPD Report No. 31-9344)
- "Methods for Designing Impact-Resistant Ceramic Components" (GAPD Report No. 31-9346)

At the Dearborn meeting, two other presentations were made on the following ATTAP support programs:

- "Life Prediction Methodology for Ceramic Components of Advanced Heat Engines (GAPD Report No. 31-9350)
- "Cyclic Oxidation of Advanced Silicon Nitrides" (GAPD Report No. 31-9348)

These four presentations will be published by the Society of Automotive Engineers (SAE) in the Proceedings of the Dearborn meeting. GAPD personnel made an additional presentation on the ATTAP effort in June 1990 at the 35th International Gas Turbine and Aeroengine Congress and Exposition, Brussels, Belgium sponsored by the American Society of Mechanical Engineers (ASME).

The following peer-reviewed papers on the ATTAP effort were submitted to ASME for presentation and publication at the 36th International Gas Turbine Conference, to be held at Orlando, Florida in June 1991:

- "Impact Design Methods for Ceramic Components in Gas Turbine Engines," by J. Song, J. Cuccio, and H. Kington (GAPD Report No. 31-9528).

- "Advanced Turbine Ceramic Engine Technology for Gas Turbines," by W.D. Carruthers and J.R. Smyth (GAPD Report No. 31-9421).

APPENDIX I

ANNUAL TECHNICAL PROGRESS REPORT
NORTON/TRW CERAMICS COMPANY

ADVANCED TURBINE TECHNOLOGY APPLICATIONS PROJECT
COMPONENT DEVELOPMENT PROGRAM

ANNUAL TECHNICAL PROGRESS REPORT

for the period
January 1, 1990 to December 31, 1990

under GAPD Purchase Order Nos.
P11776307, dated February 18, 1988 and
P1772578, P1772588, P1772598,
and P1772608 dated July 7, 1988.

Submitted by:

NORTON/TRW CERAMICS
Goddard Road
Northboro, MA 01532-1545

Bryan J. McEntire
Program Manager

Report Date: August 7, 1991

Prepared for:

NASA-LEWIS RESEARCH CENTER
Cleveland, OH 44135

Submitted to:

Garrett Auxiliary Power Division
ALLIED-SIGNAL AEROSPACE COMPANY
Phoenix, AZ 85034

TABLE OF CONTENTS

8071(03)-41A

EXECUTIVE SUMMARY

Norton/TRW Ceramics (NTC) completed its third-year effort of the ATTAP. Process and component development work continued for the AGT101 rotor and stator. Work during the year shifted from an emphasis on process development to component specific fabrication operations. Using stereolithographic masters, NTC successfully incorporated the new impact-tolerant rotor and stator design changes into its process and produced demonstration hardware of each component. A summary of significant accomplishments for the year is given below.

- Characterization of NT154 continued during the year. A significant data-base of critical mechanical properties for this material now exists both at GAPD, NTC, and a number of independent laboratories. Flexural strength, fracture toughness, static and dynamic fatigue, creep, and thermal property information are available for engine design and analyses. Overall, properties for this material continue to exceed program specifications.

- A new generation siliconized silicon carbide (Si·SiC) was developed.* Designated NT230, this material has approximately double the strength of existing Si·SiC compositions. At elevated temperatures (up to 1370°C), its strength is essentially equivalent to NT154. Characterization of its properties is being accomplished by several laboratories. Preliminary data suggest that it is an excellent candidate for static structural components within advanced gas turbine engines.

- All powder beneficiation development was completed. Process specifications, acceptance criteria and SPC methods were developed and implemented for this operation.

- Casting development was emphasized during the year. Work focused on fabrication of rotor and stator hardware. Significant efforts were devoted to overcoming problems associated with green cracking of components. NTC explored several methods, the most significant of which were adopted. They include the incorporation of: (1) Calcination (to improve dispersion and rheology); (2) Agglomeration (for improved casting rates and density uniformity); and (3) Freezing/Freeze Drying (to improve wet-green strength). Laboratory pressure casting apparatus and plaster molds were developed for component casting trials. From these combined techniques, impact-tolerant AGT101 rotors and stators were successfully cast, densified, characterized, and delivered to GAPD for evaluation. Mechanical properties for these components met program requirements, and were comparable to data acquired from co-processed test-tile. Room-temperature strength and Weibull Modulus were ≈890 MPa (129 Ksi) and 8, respectively. At 1370°C, a flexural strength of ≈590 MPa (86 Ksi) was observed. Problems were encountered in maintaining high strength levels within the casting process. Although components produced from this process achieved ATTAP specifications, impurities resulted in a slight reduction in strength over prior year's values. Yet the process itself demonstrated its capability to form the complex ATTAP components to near-net-shape in a crack-free condition. As an engineering compromise, NTC elected to sacrifice ultra-high strengths in order to achieve acceptable component fabrication. Continued refinements of the process are planned for 1991.

---

* Development of this material was performed exclusive of ATTAP funding. It is reported here because of its relevance to the overall ATTAP.

- Degas development was completed. Process specifications, acceptance criteria and SPC methods were implemented.

- HIP development was conducted in six areas: (1) HIP Encapsulant Glass; (2) Barrier Coatings; (3) Decapsulation Methods; (4) Abrasive Flow Machining; (5) HIP Control; and (6) An L16 "As-Fired Surface Optimization Experiment. During the year, work on encapsulant glass development, barrier coatings and decapsulation methods was discontinued due to a lack of significant results or improvements. Efforts in abrasive flow machining, while initially promising, have been delayed until NTC completes its component forming and firing optimization plans. In lieu of this work, efforts were re-directed at investigating and optimizing conditions for as-fired surfaces. An L16 Taguchi experiment was designed and conducted in this area. The experiment served to verify selected process conditions for powders, degas, HIP densification, decapsulation, crystallization and oxidation. Preferred conditions were selected which resulted in substantial advancements in as-fired properties. Strengths of as-fired surfaces were improved from ≈345 MPa (50 Ksi) to ≈552 MPa (80 Ksi), and found to be independent of test-temperature.

- Post-HIP Component Integrity development was completed. Process specifications, acceptance criteria and SPC methods were implemented for crystallization and oxidation operations.

- NDE development utilized microfocus x-ray radiography (MFXR) and fluorescent dye-penetrant checking. Procedures for these operations were reviewed in light of the new impact-tolerant rotor and stator. They are currently being upgraded to be in compliance with GAPD specifications.

- Under Quality Assurance Development, a Quality Manual/Plan was reviewed by GAPD during the year. This document was returned to NTC, revised, approved and formally implemented. Measurement techniques and standards were upgraded for several process and inspection operations. Along with component specific operation sheets and procedures, the documentation system under ATTAP has been revised to reflect changes to the impact-tolerant hardware designs. Documentation of the process continued through the writing of standard procedures and specifications based on results from the Work Plan. SPC has been implemented for all operations except for machining. Complete implementation is slated to coincide with the culmination of the process developmental work and delivery of the final engine quality components.

Continued effort in each of the above areas is scheduled for the 1991 program year. Work will focus on component specific problems for the rotor and stator.

INTRODUCTION

Efficient gas turbine engines require the incorporation of high-reliability advanced ceramic components. To achieve this goal, the Department of Energy (DOE) is sponsoring several major ceramic development and characterization programs. The Advanced Turbine Technology Applications Project (ATTAP) is one of them. Initiated in 1987, and administered by NASA (Lewis Research Center), the ATTAP is a five-year effort devoted to the development of ceramics for advanced gas turbine engines. Its goals include: (1) The optimization and demonstration of reliable ceramic fabrication processes; (2) Production of the required ceramic components; and (3) Evaluation of these components in actual gas turbine engine tests.

Norton/TRW Ceramics (NTC) is a participant with, and subcontractor to Garrett Auxiliary Power Division (GAPD) of Allied-Signal Aerospace Company under the ATTAP. NTC has been assigned component processing development work on AGT101 rotors and stators. NTC's effort centers on the development of controlled manufacturing processes for each component. NTC has performed this work in accordance with GAPD's overall program schedule, as shown in Figure 71. This schedule represents a revision to the original ATTAP. Changes were needed to account for design modifications in the rotor and stator initiated by GAPD in 1989.

Based on GAPD's requirements, NTC has been responsive in altering its own SOW and Work Plans to coincide with GAPD's needs. During 1990, a detailed Work Plan was developed. This plan, and subsequent revisions which occurred during the year, incorporated technological developments in forming, firing and finishing of stators and rotors. The plan defined the technical approach of the program, extent of design and analysis, experiments, deliverable hardware and other activities directed at achievement of program objectives and milestones. The 1990 Work Plan Schedule is shown in Figure 72. Work performed during the year and summarized in this report include: (1) Design information on NTC's NT154 Si_3N_4 used for rotor and stator fabrication; (2) The development of a new siliconized-silicon carbide material, designated NT230, for potential future use in the ATTAP; (3) Component fabrication development using pressure slip-casting (PSC) and injection molding (IM); (4) The completion, or reported status of certain experiments in powder beneficiation, degas, HIP and post-HIP heat-treatments; (5) Compilation and documentation of standard procedures for these operations along with implementation of statistical process control (SPC); and (6) Continued implementation of a quality assurance plan.

This report presents a summary of NTC's third-year developmental endeavors. Reporting of results follows tasks identified within NTC's SOW and include: (1) Design and Cost Analysis; (2) Forming Methods; (3) Process Engineering; (4) NDE; (5) Quality Assurance; (6) Deliverables; and (7) Project Management.

DESIGN AND COST ANALYSIS

DESIGN - NTC has developed two principal materials for use in the ATTAP: (1) NT154 HIPed silicon-nitride, Si_3N_4; and (2) NT230 siliconized silicon carbide, Si-SiC. NT154 is a 4% Y_2O_3-doped composition densified by hot-isostatic pressing (HIP). HIPing is accomplished using glass encapsulation techniques. A flow-chart for component fabrication is given in Figure 73. Assessment and characterization of this material has been conducted both at NTC, GAPD, other engine builders, or independent laboratories.[1-4]

Figure 71 - ATTAP Statement of Work Schedule

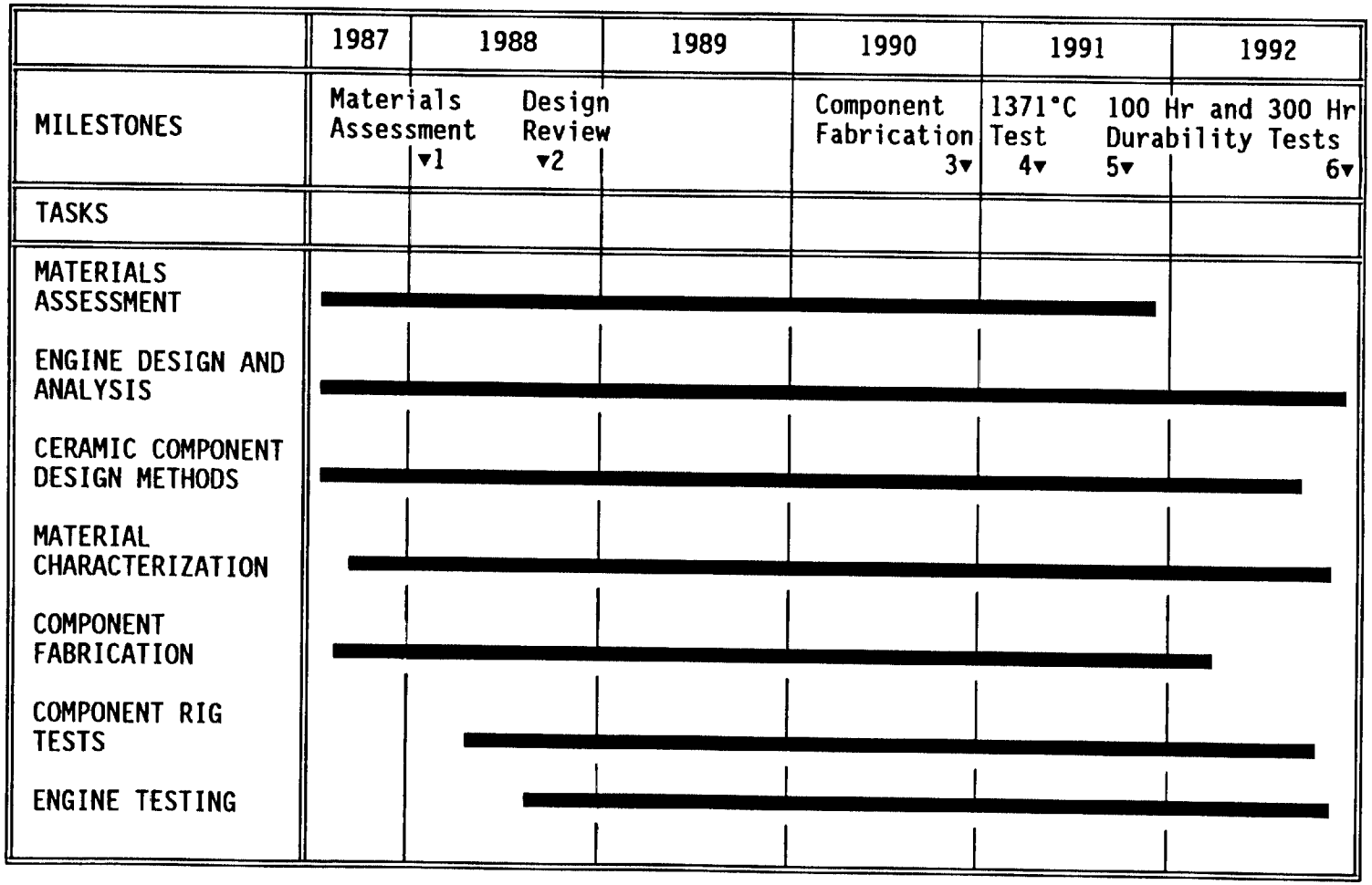

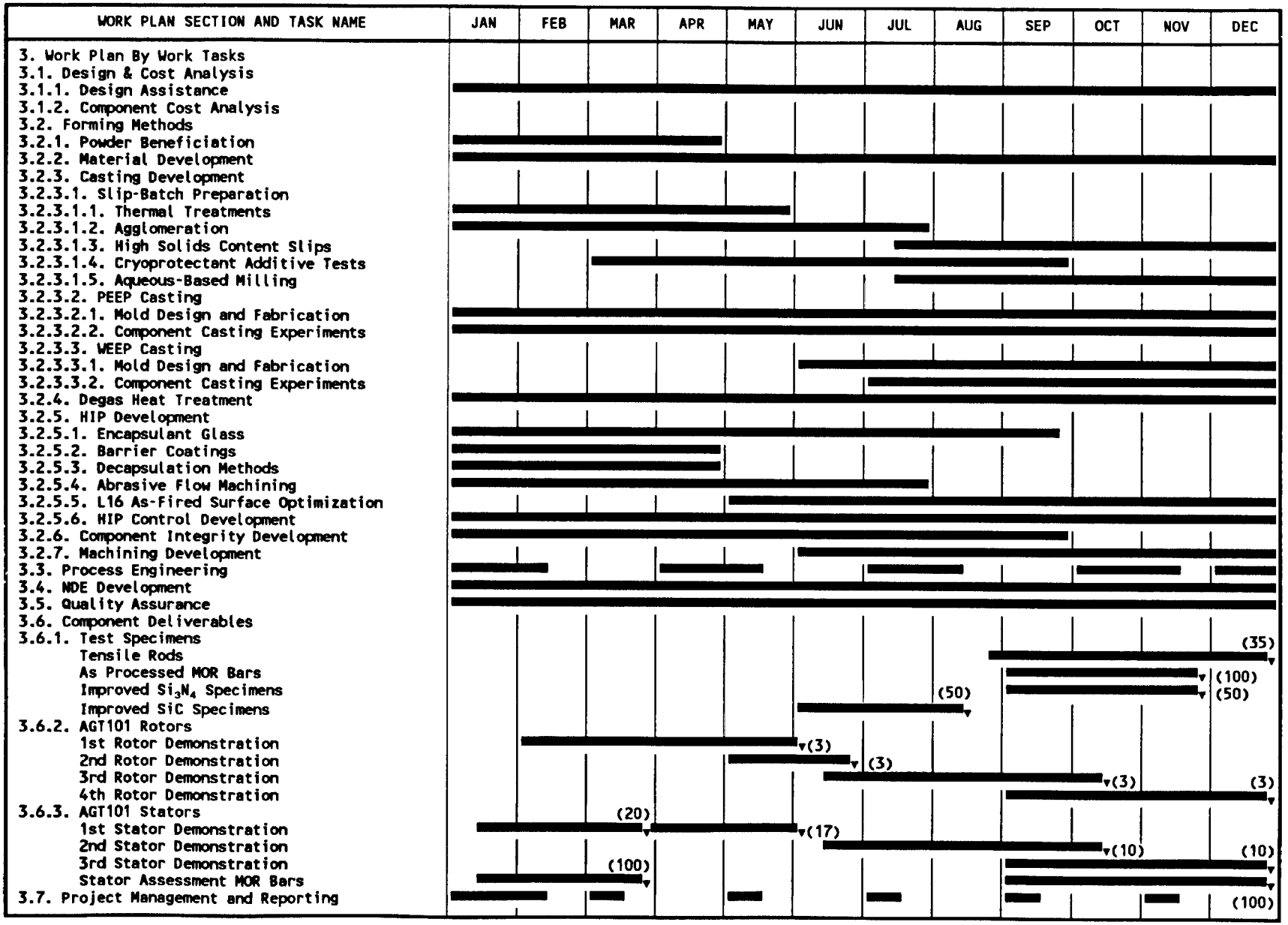
WORK PLAN SECTION AND TASK NAME
JAN
FEB
MAR
APR
MAY
JUN
JUL
AUG
SEP
OCT
NOV
DEC
3. Work Plan By Work Tasks
3.1. Design & Cost Analysis
3.1.1. Design Assistance
3.1.2. Component Cost Analysis
3.2. Forming Methods
3.2.1. Powder Beneficiation
3.2.2. Material Development
3.2.3. Casting Development
3.2.3.1. Slip-Batch Preparation
3.2.3.1.1. Thermal Treatments
3.2.3.1.2. Agglomeration
3.2.3.1.3. High Solids Content Slips
3.2.3.1.4. Cryoprotectant Additive Tests
3.2.3.1.5. Aqueous-Based Milling
3.2.3.2. PEEP Casting
3.2.3.2.1. Mold Design and Fabrication
3.2.3.2.2. Component Casting Experiments
3.2.3.3. WEEP Casting
3.2.3.3.1. Mold Design and Fabrication
3.2.3.3.2. Component Casting Experiments
3.2.4. Degas Heat Treatment
3.2.5. HIP Development
3.2.5.1. Encapsulant Glass
3.2.5.2. Barrier Coatings
3.2.5.3. Decapsulation Methods
3.2.5.4. Abrasive Flow Machining
3.2.5.5. L16 As-Fired Surface Optimization
3.2.5.6. HIP Control Development
3.2.6. Component Integrity Development
3.2.7. Machining Development
3.3. Process Engineering
3.4. NDE Development
3.5. Quality Assurance
3.6. Component Deliverables
3.6.1. Test Specimens
Tensile Rods
As Processed MOR Bars
Improved Si_3N_4 Specimens
Improved SiC Specimens
3.6.2. AGT101 Rotors
1st Rotor Demonstration
2nd Rotor Demonstration
3rd Rotor Demonstration
4th Rotor Demonstration
3.6.3. AGT101 Stators
1st Stator Demonstration
2nd Stator Demonstration
3rd Stator Demonstration
Stator Assessment MOR Bars
3.7. Project Management and Reporting
(35)
(100)
(50)
(50)
(3)
(3)
(3)
(3)
(20)
(17)
(10)
(10)
(100)
(100)

Figure 73
NT154 Process Flow-Chart

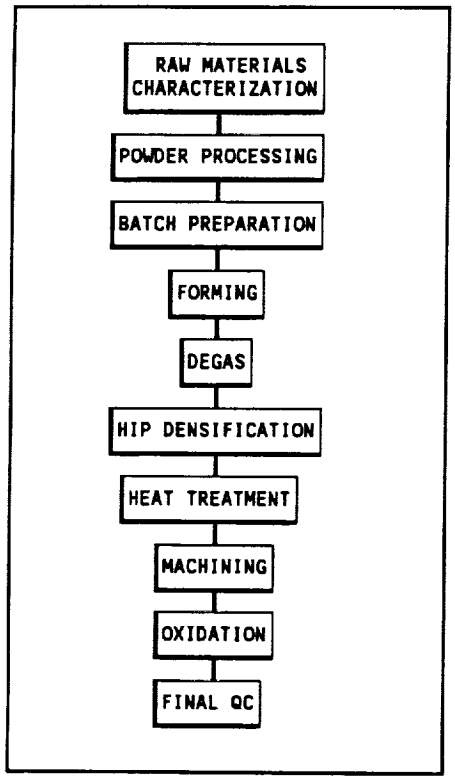

Table 15
Properties of NT154 Si_3N_4

Properties	Values
1. Density (g/cc)	3.232 ± 0.004
2. Elastic Modulus (GPa)	310 - 320
3. Shear Modulus (GPa)	126
4. Poisson's Ratio	0.273
5. Hardness (Kg/mm^2)	1620
6. Thermal Expansion Coefficient	3.93×10^{-6}/°C
7. Thermal Conductivity (W/m°K)	
(25°C)	37.6
(900°C)	20.7
(1400°C)	15.8
8. 22°C Mechanical Properties	
Average Flexural Strength (MPa)	890 - 960
Characteristic Strength (MPa)	≈980
Weibull Modulus	8 - 19
Fracture Toughness ($MPa\cdot m^{½}$)	4.7 - 7.5*
Tensile Strength (MPa)	700 - 920**
9. 1370°C Mechanical Properties	
Average Flexural Strength (MPa)	520 - 650
Characteristic Strength (MPa)	≈600
Weibull Modulus	11.4
Fracture Toughness (1200-1400°C $MPa\cdot m^{½}$)	4.1 - 13*
Tensile Strength (MPa)	240 - 520***
Steady State Tensile Creep Exponent	4 - 6
Slow-Crack Growth Exponent	8 - 13

* Chevron Notch or Controlled Flaw Methods; NT154 exhibits R-Curve Behavior. Higher values are for crack extensions of ≤ 1 mm; (NTC and UDRI Data).
** Includes CIP and Cast Samples, (UDRI and ORNL Data).
*** Loading Rate Dependent, (UDRI and ORNL Data).

It continues to be the material of choice for a number of DOE-sponsored heat-engine programs including the ORNL/GAPD Life Prediction Methodology contract.* Updated typical physical, thermal and mechanical properties are given in Table 15. NT154 possesses excellent flexural fast-fracture behavior up to 1370°C, accompanied by an acceptable Weibull Modulus. Failure origins have been associated with surface related machining flaws or internal impurities. Reported tensile strengths under fast-loading conditions parallel flexural tests. For tensile tests, principal failure origins were volume inclusions--generally identified as iron impurities. Under slow-loading conditions at elevated temperatures, creep and slow crack growth behavior have been characterized.[1-2,5]. NT154 exhibits creep through a cavity nucleation and growth mechanism. Failure occurs via cavity link-up. Despite these observations--in comparison with other advanced materials--excellent durability has been noted; and NT154 remains as one of the foremost high-temperature ceramic materials available today.

* Life Prediction Methodology For Ceramic Components Of Advanced Heat Engines, ORNL Contract No. 86X-SC674C.

During 1990, NTC began IR&D developmental work on a siliconized silicon carbide (Si·SiC) for potential use as a static-structural material within advanced gas turbine engines. Initial studies utilized an existing Si·SiC, designated NT235. This material has been previously examined for heat-engine applications [6-7], and is commonly known as NC430. In turn, NC430 is a Norton designation for a variation on a better known class of materials currently produced and marketed under the name *Crystar*™.[8-9] These products are densified, reaction-sintered silicon carbides featuring a bimodal distribution of silicon carbide grains and metallic silicon. Compositionally, they contain between 5 and 15% silicon, along with extremely low levels of trace impurities. NTC's efforts were directed at improving the mechanical behavior of these Si·SiC materials. By modification of the grain size distribution, and through selective changes to the fabrication process, NTC was able to essentially double the strength of existing Si·SiC compositions. A new material resulted from this effort--designated NT230. Typical material properties for both NT235 and NT230, along with the process utilized in producing components, are shown in Table 16 and Figure 74, respectively. The flexural strength behavior of this material at various temperatures has been evaluated by several organizations. GAPD's comparative assessment is shown in Figure 75, along with NTC's data.[10] Good agreement is noted between to the two organizations. Siliconized silicon carbides, and NT230 in particular, exhibit an interesting behavior. Strengths at elevated temperatures (up to 1370°C) are higher than room temperature values. Improvements have been attributed to increases in fracture toughness associated with localized flaw blunting.[11] Above about 1400°C, reductions in strength are noted due to the softening and melting of the silicon phase. This material

Figure 74
NT230 Process Flow Chart

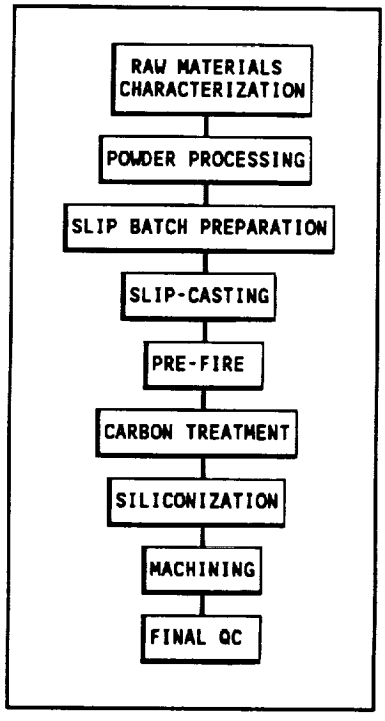

Table 16
Physical, Thermal and Mechanical Properties
of NT235 And NT230 Si·SiC

Properties	NT235 Values	NT230 Values
1. Density (g/cc)	3.10 - 3.15	3.05
2. Elastic Modulus (GPa)	383	395
3. Shear Modulus (GPa)	187	165
4. Poisson's Ratio	0.24	0.17
5. Hardness (Kg/mm²)	1620	-
6. Thermal Expansion Coefficient	4.8 x 10^{-6}/°C	4.7 x 10^{-6}/°C
7. Thermal Conductivity (W/m°K)		
(25°C)	135	-
(1000°C)	36	-
8. Flexural Strength		
(25°C)	245	410
(1260°C)	274	540
(1370°C)	251	500
Weibull Modulus	10	8
9. Fracture Toughness (MPa·m$^{\frac{1}{2}}$)		
(25°C)	3.0 - 3.5*	3.2*
(25°C)	-	3.2**
(1370°C)	4.4*	8.1*
(1370°C)	-	5.5**

* Controlled Flaw Method at 25°C and 1370°C, respectively.
** Single Edge Pre-cracked Beam Method at 25°C and 1370°C, respectively, ORNL Data.

is an ideal candidate for static structural components within the engine at temperatures below about 1400°C. Due to the fact that the material exhibits little or no shrinkage upon densification, complex large components such as shrouds and transition ducts can be readily produced to near final size. Also, because NT230 utilizes low cost raw materials and excludes HIP as the densification step, total material and processing costs remain relatively low in comparison with NT154 Si_3N_4. Within ATTAP, GAPD is currently considering use of NT230 for some of the stationary structures within the AGT101 engine.

Figure 75
Comparative Flexural Strengths Of NT235
And NT230 Siliconized Silicon Carbides

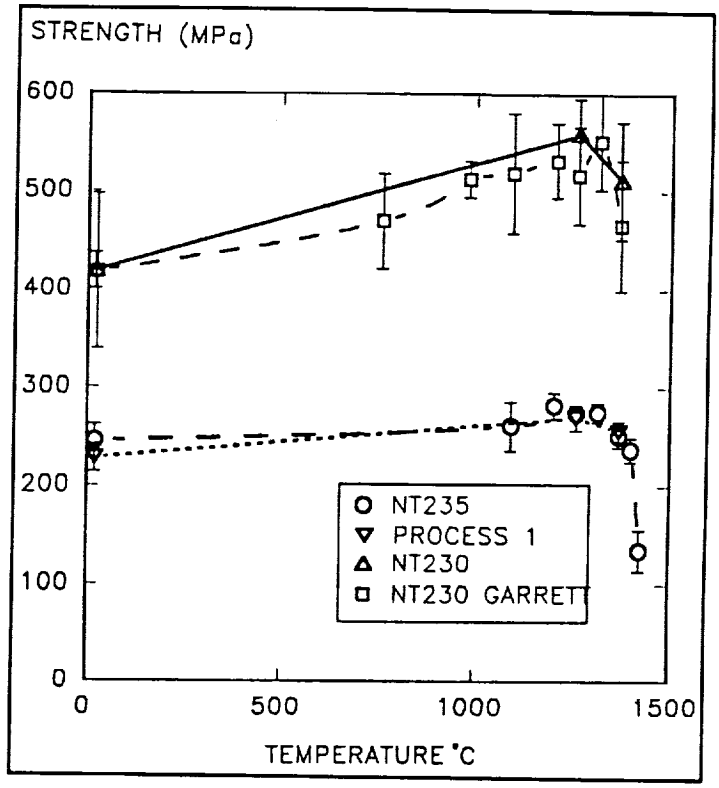

COST ANALYSIS - NTC performed no formal cost analyses work during the year. A cost analysis task for the NT154 process is scheduled as part of the ATTAP program during 1992.

FORMING METHODS

In accordance with the 1990 Work Plan, sub-tasks within the Forming Methods section include: (1) Powder Beneficiation; (2) Casting Development; (3) CIP Processing; (4) Injection Molding Development; (5) Degas Heat-Treatments; (6) HIP Development; and (7) Component Integrity Development.

POWDER BENEFICIATION - Three Taguchi experiments were completed in this area during the first two years of the ATTAP. With the exception of implementation of statistical process controls, no significant additional experimental efforts were conducted in 1990. The current status of the NT154 powder beneficiation process is as follows:

- All NT154 raw material specifications were set and standard operational procedures for qualification of powders formally implemented.
- NT154 powder processing conditions were selected and implemented. Standard operational procedures were written.
- NT154 processed powder material specifications and qualification criteria were implemented.
- SPC variables were selected and formally implemented via standard procedures.

CASTING DEVELOPMENT - During the first two program years, pressure casting activities concentrated on issues surrounding basic slip composition, dispersion and binding agents, mold design, mold coatings and casting techniques. A limited number of additives were investigated which proved partially beneficial in slip rheology and green forming. From this work, rotor hubs were successfully prepared. Mechanical properties from these hubs were found to be equivalent to flexural test-bars cut from tile. However, hub cracking during the drying operation was a

persistent problem. Screening tests and Taguchi-based experiments were therefore completed to assess the controlling parameters of this behavior. From these experiments, it was found that cracking could be significantly reduced, or eliminated by the combination of at least three techniques: (1) Modification of the powder surface by thermal treatments; (2) Adjustments of effective size distribution of the dispersed powder by agglomeration; and (3) The development of innovative mold designs and casting procedures. When combined, these treatments and designs affected dispersion, particle-packing, drying, shrinkage uniformity, and mold release. However, prior to 1990 the robust elimination of component cracking for rotors, (blade and hub regions), and stators (platform and airfoil) was not totally realized. Consequently, during the first half of 1990, NTC critically reviewed its casting technology along with an assessment of comparable alternatives. As a result of this effort, NTC tested, then incorporated an existing Norton forming technology into the standard NT154 process. Over the past 10 years, Norton has developed an innovative casting technique which involved the combination of slip-casting, freezing and freeze-drying. In connection with earlier casting developments on rotors and stators, freezing and freeze-drying resulted in adequate feature definition and crack-free production of components. A flow-chart for the fabrication of components using this method is given in Figure 76. It has been designated as PEEP Casting by NTC (Pressure-assisted Endothermic Extraction Process).

Concurrent with the demonstration of components by PEEP casting, exploratory tests were also conducted on forming of components by a freeze casting/drying step, exclusive of pressure or de-watering assistance. This forming method, also shown in Figure 76 is designated as WEEP, for Water Endothermic Extraction Process. Under this system, an aqueous-based slurry of NT154 was pumped at low pressure into a non-porous mold and frozen in-place at cryogenic temperatures. Subsequent to the freezing operation, the part was removed from the mold and placed in a vacuum chamber. Water

Figure 76
NT154 Process Flow Diagram

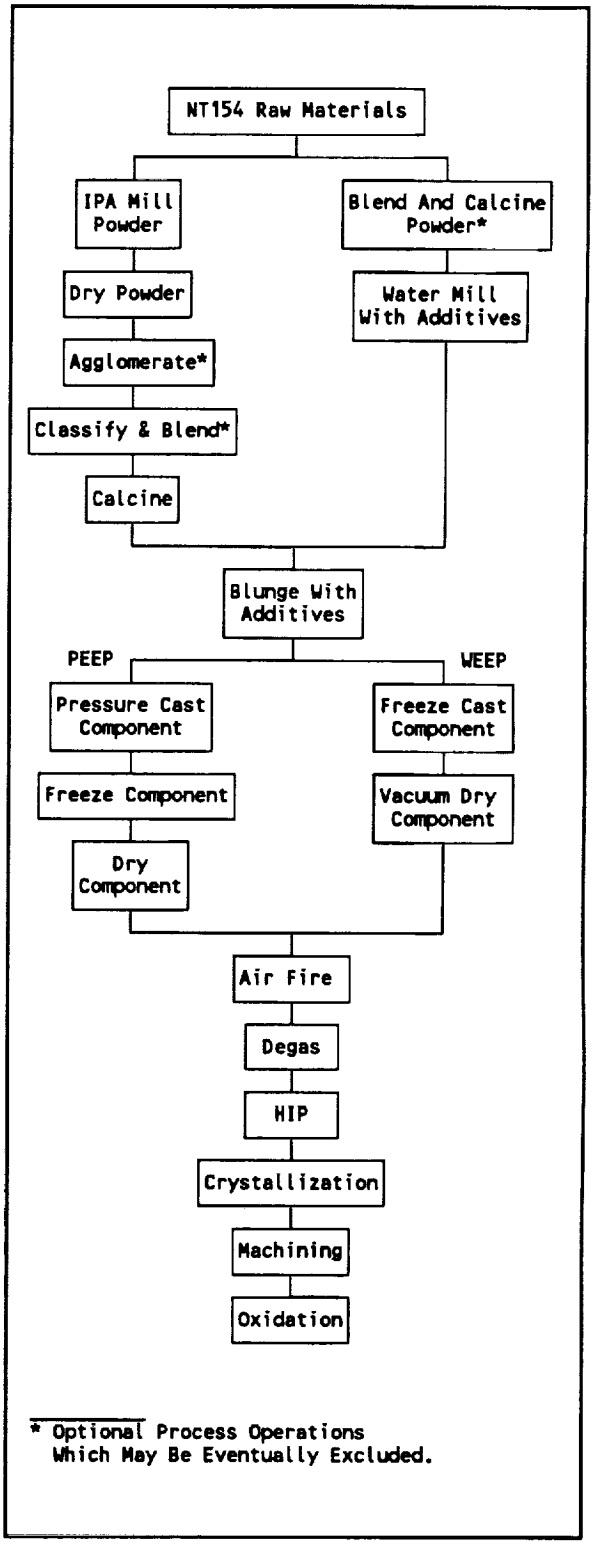

extraction occurs by sublimation.*

By the end of 1990, both processes had produced green gas turbine components possessing good feature definition and control. Under the PEEP process, dense rotors and stators were successfully prepared. As will be reported below, adequate mechanical properties were demonstrated both on components and coprocessed tile, although impurity control within the process remains an issue. However, for the WEEP process, dense component demonstration was never achieved. Cracking associated with drying or firing shrinkage precluded successful part fabrication. This was particularly true for larger cross-sectional components--such as the AGT101 rotor; but small shapes, like the stator could be adequately prepared. Consequently, because of the lack of robustness in this system, as well as successes within PEEP casting, work on the WEEP process route was discontinued.

In the discussion that follows, a review of 1990 Casting Development Work in three areas is given: (1) Slip-Batch Preparation; (2) PEEP Casting; and (3) WEEP Casting. Component fabrication activities were performed for rotors and stators.

Slip-Batch Preparation - For either the PEEP or WEEP forming methods, simplification and control of the slip-batch preparation operations was seen as a critical 1990 challenge. Improvements in impurity control, process stability and reliability were needed. The optimization of thermal treatments and agglomeration methods for powders was seen as an essential requirement. Slip-stability and increased solids loading was also important, although not as critical. With the incorporation of freezing and freezing-drying, the selection and proper use of cryoprotectants was needed; and testing of various binders and additives was performed. Developmental activities in slip-batch preparation during 1990 focused on these issues. Discussed below are results from experimental studies on thermal treatments (i.e., calcination) and size distribution modifications (i.e., agglomeration), the development of high solids content slurries, cryoprotectants, binders and additives.

Thermal Treatments - As noted in the flow diagram of Figure 76, calcination was employed as a powder treatment both with and without the agglomeration step. As described in several published reports [12-13], thermal treatment of Si_3N_4 powders under various process gases controls surface chemistry and improves the ability of the material to be dispersed. NTC's work in this area included the completion of a time-temperature screening experiment. This was a full-factorial test involving three temperatures at four time-intervals. It was designed to cover a broad range of potential heat treatment conditions and correlate changes in surface chemistry and morphology with casting, cracking behavior, and mechanical properties. This experiment was conducted using batch calcining operations. From these tests, preliminary calcination conditions were set. To improve uniformity of the powder, and simplification of the process, NTC procured a continuous rotary calcination furnace. This unit was ordered, installed and commissioned during 1990. Verification trials were performed in an effort to duplicated calcined powder characteristics previously achieved by batch processing of both agglomerated and non-agglomerated powders. As a result of these verification trials, processing conditions were set and the continuous powder calcination furnace was implemented into the standard NT154 process. NT154 powders are currently being calcined at low temperatures in flowing air using

* The forming technologies described herein are covered under an existing Norton Patent, No. 4,341,725, (July 27, 1982).

a rotating fused quartz tube. The temperature-time schedule for calcination is accurately controlled by the angle of the tube, rotation, powder feed rate and power settings. At preferred conditions, organic, ammonia, and hydroxyl surface groups are removed from the powder surface. SPC techniques have been applied to this process. Implementation of this furnace appears to provide a uniformly calcined powder and consistent slip rheology. Use of the equipment has also improved powder output to $\geq$ 20 kg/day, when compared with the batch process.

Size Distribution Modifications - Various agglomeration techniques were explored during 1990 as a method of preparing artificially large silicon nitride powder grains. By mimicking larger grained material, casting rates were enhanced significantly, and green cracking minimized. Most of NTC's work in this area was directed at conventional agglomeration methods. During the year, equipment was ordered and installed to perform mechanical agglomeration. To optimize the use this equipment, a Taguchi L4 ($2^3 \times 2^1$) design was selected and employed. Experimental trials were conducted to determine operational limits of the equipment. Variables included three inside factors for machine controls (i.e., operational speeds, temperatures and feed rates) and one outside factor (solids loading). Response variables included average particle size and particle size distribution along with rheological characteristics. ANOVA results for average particle size are shown in Table 17. Similar values for the width of the distribution (d_{90} - d_{10}) are presented in Table 18. The data indicate that this operation is principally controlled by two machine variables. From the four trials of the experiment, custom blending of selected powders from the L4 design was accomplished in a effort to further broaden the apparent size distribution of the material. Blending fractions were determined from distributions generated by a commercially available computer program developed specifically for this purpose.[14] PEEP casting trials were then conducted for each blend, followed by freezing and drying. For the custom blending work, three distributions were selected including two different bimodal blends designated as Bimodal Blend No. 1 and No 2.; and a trimodal blend. In addition, a non-agglomerated powder

Table 17
Average Particle Size
ANOVA For L4 Agglomeration Experiment

I. Low Solids Loading

Factor	% Contribution
Machine Control No. 1	23
Machine Control No. 2	0
Machine Control No. 3	76
Experimental Error	1

II. High Solids Loading

Factor	% Contribution
Machine Control No. 1	2
Machine Control No. 2	37
Machine Control No. 3	0
Experimental Error	61

Table 18
Particle Size Distribution (d_{90} - d_{10})
ANOVA For L4 Agglomeration Experiment

I. Low Solids Loading

Factor	% Contribution
Machine Control No. 1	28
Machine Control No. 2	0
Machine Control No. 3	69
Experimental Error	3

II. High Solids Loading

Factor	% Contribution
Machine Control No. 1	20
Machine Control No. 2	0
Machine Control No. 3	79
Experimental Error	1

was included for comparison. A listing of these four powders and their slip properties is presented in Table 19. All slips achieved approximately identical solids loading, with notable differences in rheological behavior. Apparent viscosities for agglomerated powders were higher than the non-agglomerated case. However, the agglomerated powders cast in two-thirds the time required for the non-agglomerated material. Using these blends, casting of both AGT101 stators and fully-bladed rotors was successfully accomplished. After several iterations on tooling and insert design, no notable cracking was observed for either component. The trimodal blend provided the best quality components. Green densities for agglomerated powders were essentially equivalent, regardless of blend and ranged between ≈ 1.95 and 2.05 g/cc. For the non-agglomerated powder, the density values were notably higher at 2.14 ± 0.03 g/cc, but severe blade and hub cracking in rotors occurred. Green density distributions were determined for sectioned rotors. Values are presented for the hub base to the top of the shaft in Table 20. Results suggests that all three agglomerated powder blends provide fairly uniform green density, with slight differences occurring axially within components. Of the three blends, the trimodal mix appeared to provide the highest degree of uniformity.

Table 19
Powder Blend Composition and Slip Properties

Batch No.	Blend Description	pH	Viscosity (cps)	Specific Gravity (g/cc)
439	Bimodal No. 1	8.28	92	2.10
448	Bimodal No. 2	8.42	74	2.09
447	Trimodal No. 1	8.30	98	2.11
458	Non-Agglomerated	8.49	42	2.11

Mechanical properties were determined for several early batches of the agglomerated

Table 20
Green Density Distribution For AGT101 Rotors

Section No.	Bimodal Blend No. 1 Density (g/cc)	n	Bimodal Blend No. 2 Density (g/cc)	n	Trimodal Blend Density (g/cc)	n
9	N/A	-	N/A	-	N/A	-
8	N/A	-	1.97	1	N/A	-
7	N/A	-	1.96	1	N/A	-
6	1.98 ± 0.01	4	1.95	1	N/A	-
5	1.98 ± 0.01	3	1.94	2	1.96	1
4	1.95 ± 0.03	4	1.94	2	1.97	1
3	1.94 ± 0.03	4	1.95	2	1.95	2
2	1.94 ± 0.03	7	1.96	2	1.91	1
1	1.94 ± 0.02	7	1.99	1	1.96 ± 0.01	4
Overall	1.95 ± 0.03	29	1.94 ± 0.03	12	1.96 ± 0.01	9

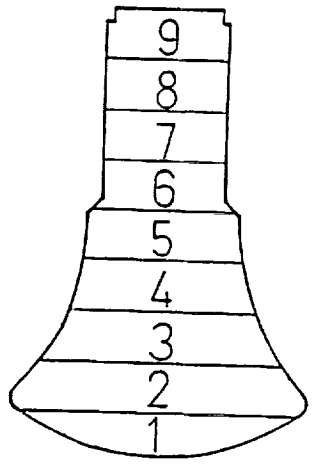

powders. Observed room temperature and 1370°C flexural strengths were found to be 805 ± 117 MPa (117 ± 17 Ksi; n = 15); and 604 ± 37 MPa (88 ± 5 Ksi; n = 7), respectively. The apparent low values observed in the room temperature fractures were traced to black inclusions. SEM and EDS evaluation indicated that these black fracture origins were iron inclusions. Their presence was initially linked to the agglomerator itself. Abrasive wear was noted on one particular rotating stainless steel component of the agglomerator. To correct this problem, NTC redesigned and fabricated this part from NT154. To insure that the part would perform in its intended application, NTC prepared and proof-spin-tested several components. The first part failed below the design spin speed. Slight modifications to the design were made and a second part fabricated and tested. This component passed the proof-test and was installed successfully in the agglomerator. To eliminate other dynamic metal-to-metal wear, the agglomerator was completely overhauled, and new higher tolerance wear resistant materials installed where appropriate. Standard operating procedures (SOPs) for the agglomeration process were also written and implemented. These included three key documents covering: (1) Powder preparation prior to agglomeration; (2) Agglomeration itself; and (3) Agglomerated powder qualification. Process response variables for the agglomeration process were selected and SPC charting implemented. After completing the equipment upgrades and procedural implementation, additional agglomeration runs were preformed from which a number of ATTAP rotor and stator components, and test-tile were cast, densified, and sectioned into flexural specimens for mechanical properties assessment. Comparative results for the three iterative processes are shown in Table 21. Presented here are combined data for: (1) NT154 batches prepared from non-agglomerated powders; (2) Agglomerated powders prior to modifications to the agglomerator; and (3) Agglomerated powders after modification of the agglomerator. From this data, it was observed that flexural strengths at room temperature decreased for the agglomerated powders despite implementation of the upgraded equipment and procedures. At room temperature, a statistically significant difference was noted between all three processes (95% confidence). Some variability was also observed at 1370°C--although without a definitive trend. Statistical testing of high temperature values also showed differences between the non-agglomerated and agglomerated powders; but no differences between the two agglomerated processes. Batch variations were also observed in flexural stress rupture behavior; but because of the limited amount of data these may not be significant. Failure origins for bars from each population occurred predominately at the surface and were mostly related to machining damage. However, for both bulk and surface failures from all three processes, fractography revealed that approximately 10 to 20% of the bars broke at metallic inclusions. Despite this fact, qualitative observations indicated that the concentration of metallic inclusions from the modified agglomeration process were comparable with the non-agglomerated material and lower than agglomerated powders produced prior to equipment modifications. Overall, these results suggest that the agglomeration process is detrimental to strength. Yet, observed mean values are well within ATTAP specifications. Given this fact, and the realization that casting of agglomerated powders enhances NTC's capability for producing crack-free components, NTC has elected to select the agglomerated powder process as the preferred method for near-term production of components. This represents an engineering compromise. Ultra-high-strength materials were sacrificed in favor of an improved ability to produce hardware. As part of its 1991 Work Plan, NTC plans to further optimize either the agglomeration process itself, or develop a suitable replacement (i.e., flocculation) in an effort to improve overall strength without forfeiting formability.

High Solids Content Slurries - Minor work on improvements in solids content was initiated during the year. Higher solids slurries can lead to both faster casting rates and intrinsically

Table 21
Comparative Flexural Properties For Various
Agglomerated and Non-Agglomerated NT154 Powders

Property	Non-Agglomerated	Agglomerated Original Process	Agglomerated Modified Process
Room Temperature Flexural Properties			
Average Strength (MPa)	958 ± 117	923 ± 138	889 ± 138
Average Strength (Ksi)	139 ± 17	134 ± 20	129 ± 20
Characteristic Strength (MPa)	1013	985	951
Characteristic Strength (Ksi)	147	143	138
Maximum Likelihood Weibull Modulus	9.5	8.1	8.1
Number of Specimens	303	296	61
1370°C Flexural Properties			
Average Strength (MPa)	607 ± 48	572 ± 41	586 ± 34
Average Strength (Ksi)	88 ± 7	83 ± 6	85 ± 5
Characteristic Strength (MPa)	627	593	600
Characteristic Strength (Ksi)	91	86	87
Maximum Likelihood Weibull Modulus	15.2	14.0	21.5
Number of Specimens	195	144	22
Flexural Stress Rupture Properties			
No. of Samples Surviving:			
1204°C, 350 MPa, ≥ 150 Hours	-	3 for 3	-
1204°C, 400 MPa, ≥ 150 Hours	-	2 for 2	-
1260°C, 350 MPa, ≥ 150 Hours	5 for 5	3 for 3	-
1260°C, 400 MPa, ≥ 150 Hours	-	0 for 2	-
1316°C, 200 MPa, ≥ 150 Hours	-	3 for 3	-
1316°C, 250 MPa, ≥ 150 Hours	-	2 for 2	-
1370°C, 200 MPa, ≥ 150 Hours	5 for 5	4 for 5	-
1370°C, 276 MPa, ≥ 10 Hours	-	65 for 82	8 for 8
1370°C, 300 MPa, ≥ 150 Hours	-	-	8 for 8

higher green densities. Exploratory efforts were conducted to determine whether solids contents of > 52 volume % could be achieved by adjusting the agglomerate size distribution, or through the selective use of additives. Minor alterations to the Si_3N_4 size distribution were performed using a computer based modeling program on solids loading. Slight improvements in solids loading were achieved (i.e., up to 55 volume %); but slip viscosity levels nearly doubled. Thixotropy and air entrapment during casting became a major concern at higher viscosities. NTC also investigated the effects of a series of novel dispersants in connection with the optimum blend. However, none of these proved beneficial in increasing solids loading. The results, therefore, suggest that NTC's current powder blend and dispersant are optimal and no further work in this area was warranted. Specifications and procedures on agglomerate powder blends and the use of dispersants have been set. SPC monitoring of slip-batch characteristics, such as pH, viscosity, and solids loading were implemented.

Cryoprotectants - To aid in prevention of ice-crystals during the freezing operation, screening tests were completed on five cryoprotectant additives. A summary of results obtained with each additive is presented in Table 22. For these tests, fully-bladed AGT101 and AGT100

rotors were PEEP cast, frozen, dried and assessed for cracking characteristics. From qualitative observations, a quantitative ranking of rotor quality was given. A rank of "10" was assigned to rotors free of cracks in both the hub and blade regions. Conversely, a "1" rank was given for severe cracking in all areas of the rotor. Of the five additives examined, two proved to be highly beneficial. Both demonstrated their ability to produce entirely crack free components. These two additives (Nos. 1 and 5) were incorporated into casting optimization experiments for rotors described later in the report. From that particular experiment, one cryoprotectant was eventually selected for use within the process. No further work in this area was planned or conducted.

Binders/Additives - Work in this area centered on: (1) An examination of various binder systems for green strength enhancement; and (2) The use novel additives to prepare in situ agglomerates by either emulsification or flocculation.

During prior program years, several binders were evaluated for their ability to improve green forming. Of these, one class of materials was eventually selected because they minimized or eliminated the problem of axial cracking in rotor hubs. From this group, two binders were subsequently chosen for trials on fully bladed rotors. A series of ten casting tests were conducted for each. For the first binder, it was observed that as the number of casts increased, the percentage of blades retained on the rotor decreased. By the sixth cast, all blades broke due to severe sticking to the mold. It was concluded from these tests that binder penetration into the mold caused sticking. The best blade yield was 4 out of 12. Four rotors were attempted with the second binder. None of the trials were successful. Blade sticking, poor castability and axial cracking were observed. Similar tests were conducted for the stator. In this case, air entrapment, large variations in viscosities, and mold sticking were also noted--resulting in poor component yields. As a result, no successful stators were prepared. From this work, it appears that binders lead to inherent problems in slip stability, casting behavior and mold release which may be fundamentally difficult to overcome. Because of these problems, further work on

Table 22
Cryoprotectant Screening Experiments - Slip Composition And Casting Results

Batch No.	Additive Type Or Amount	pH	Viscosity (cps)	Specific Gravity (g/cc)	Green Density (g/cc)	Cast Rotor Quality (1-10 best) AGT101	AGT100	Average
431	Additive No. 1 - A%	8.22	68	2.10	1.78	10	8	9
432	Additive No. 1 - B%	8.14	86	2.13	1.81	9	8	8.5
435*	Additive No. 2 - A%	8.32	104	2.10	1.86	1	5	3
436*	Additive No. 2 - A%	8.25	78	2.08	1.87	6	7	6.5
437	Additive No. 3 - A%	8.28	99	2.08	1.87	1	1	1
438	Additive No. 4 - A%	8.26	70	2.09	1.99	6	9	7.5
439	Additive No. 4 - B%	8.28	92	2.10	1.83	7	5	6
444	Additive No. 5 - A%	8.47	91	2.10	1.81	10	10	10
445	Additive No. 5 - B%	8.72	84	2.09	1.93	6	6	6

* Batches 435 and 436 were frozen at different temperatures.

conventional binders under the ATTAP has been curtailed.

However, during the course of NTC's examination of conventional binders, a series of additives were identified which provided beneficial effects in agglomeration behavior, Si_3N_4 surface modification, and cast particle packing. Studies were conducted on forming artificially agglomerated slips via emulsification and additive flocculation methods.

Water in oil emulsification tests were conducted by coating the Si_3N_4 powders with a high-purity hydrophobic compound and then emulsification of the coated powder in water. In so doing, stable suspensions were formed for fairly coarse agglomerates ($\approx$2 to 50μm). Fast casting rates were observed with these suspensions. However, only low solids content slurries were achieved which led to low green densities. Additionally, cast green components had poor green strength. Because of these features, work in this area was also stopped.

Towards the end of 1990, several effective flocculation additives were located and tested. Work compared additive concentration and slurry solids content with slip rheology and casting behavior. These tests were used to determine casting parameters for the additives. A number of conditions were found which produced crack-free components. Remarkably, casting rates for these flocced slurries were also substantially higher than fully dispersed slips; yet green density values were nearly equivalent. In connection with these tests, and with the abandonment of injection molding, NTC no longer required batching and milling of powders in IPA.* Adoption of a water milling process in connection with flocculation for NT154 was seen as a desirable refinement. Therefore, using selected flocculents, an exploratory L4 aqueous-based milling experiment was planned and conducted. Within the experiment, selected levels of dispersant, flocculent, and a special anti-oxidant were varied along with comminution time. Particle size, surface area, oxygen content, and slip-rheology were monitored. Response data showed that aqueous milling can prepare materials with equivalent powder properties to the alcohol milled material. By the appropriate selection of comminution conditions, particle size, surface area and oxygen content were reproduced to current NT154 specifications. The results of these tests suggest that NT154 raw materials can be collectively milled in water without detrimental effects. Mechanical property confirmation of these results are currently being acquired. If these values are acceptable, then significant simplification of the NT154 process can be realized. Further efforts in optimizing this system have become a part of NTC's 1991 Work Plan. If successful, the process will be adopted in lieu of the alcohol milling and mechanical agglomeration methods developed in 1990.

PEEP Casting Development - Described within this section is ongoing work in two areas: (1) Mold Development and Fabrication; and (2) Component Casting Experiments.

Mold Design and Fabrication - Iterative changes in mold designs for rotors and stators were conducted during the year. Initial work was performed using radial flow hardware designs. These components proved to be difficult to cast and separate from their respective molds. With

---

* Under the ORNL Processing For Reliability Program, Norton Company has been involved in the development of aqueous based processing of 4% Y_2O_3-doped HIPed Si_3N_4 materials. Norton's results suggested that well behaved slips, of good forming behavior, and excellent mechanical properties are achievable using water processing. (ORNL Contract No. 86X-SB182C, under DOE Prime Contract No. DE-AC05-84-OR21400.)

the incorporation of freezing operation subsequent to casting, improvements in component quality and yields were realized. However, significant alterations in mold designs were required to accommodate this process. Porous plaster portions of each mold were replaced with non-porous plastic or rubber segments. Upon completion of the casting operation, the composite nature of the molds allowed the porous plaster segments to be separated, while the non-porous portions remained for the freezing cycle. After freezing, the non-porous segments were pulled, and the part was processed through the drying operation. The freezing operation incorporated into the PEEP process significantly increased the "wet-strength" of the cast body, and allowed separation of the part from the mold without fracturing delicate blade features. During the year, GAPD prepared and forwarded oversize stereolithographic patterns of the new impact tolerant ATTAP rotor and stator. Incorporation and use of these designs proved to be easier and more amenable to the PEEP casting process as well.

For the rotor, modifications were made to the mold design to minimize flashing which was recognized as source of blade cracking. Splitting angles and procedures were altered to eliminate de-molding and handling damage. Using this design, successful impact tolerant AGT101 rotors were prepared and fully densified shortly after receipt of the stereolithographic patterns. Further alterations were conducted later in the year to improve component yields. Demonstration hardware were prepared using this pattern, densified and forwarded to GAPD. From these components, shrinkage values were assessed and appropriate mold design alterations determined. By year end, all rotor design issues were resolved with GAPD; and production of a metal casting master was initiated. Receipt of this pattern is expected during the first quarter of 1991.

For the stator, incorporation of the impact tolerant design was also readily accomplished during the year. Modifications were made to the design of the stator casting mold to ease component forming, freezing and removal. Demonstration components were also produced during the year, and delivered to GAPD. Shrinkage values were determined in preparation for the fabrication of a metal master. However, as of the close of the year, the final design for the stator had not been fully set by GAPD. Completion of the design is expected during the first quarter of 1991. Subsequent its receipt, NTC will produce a metal master and initiate production of engine quality components.

Component Casting Experiments - During the year, component specific casting experiments were conducted to determine the interaction of casting parameters with freezing conditions and mold design. This work was conducted for both rotors and stators. Early work was performed on radial designed hardware; but with the receipt of the impact tolerant patterns, most of the developmental activities centered on the new design.

For the rotors, a Casting Optimization L9 experiment was designed and conducted. Based on exploratory tests, freezing temperature, time, cryoprotectant type and amount were the four factors selected for the design. The experiment was performed by casting a minimum of three rotors at each of the nine experimental conditions. The response variable of greatest interest was blade cracking. At two conditions within the experiment, blade cracks were eliminated in all cast rotors. Figure 77 presents the ANOVA for the experiment. Taken in combination, freezing temperature, cryoprotectant amount and type proved to be influential in determining crack free components. However, individually each of these factors was not statistically significant when compared with the pooled error of the experiment. However, subsequent casting trials confirmed that for a fixed type and concentration of the cryoprotectant, freezing

temperature was critical in eliminating blade cracks. Although the ANOVA indicates that other factors not included in the L9 array dominate results, it is believed that they are predominately associated with plaster mold design, and component removal operations. Rotors which were free from cracks and other visual defects after drying were processed through the degas and densification steps. Several components cracked during the degas operation. The cause for this behavior was found to be associated with heating rate. The problem was corrected by slowing the overall schedule. With the completion of the L9 experiment, optimum slip preparation enhancements and freezing methods were adopted. Production of demonstration components was initiated under rigid procedures and SPC monitoring. Yields increased dramatically through the casting operation (i.e., ≥ 80%). All components were produced crack-free after casting, degas and densification. Assessment of the mechanical properties for these components has been, or continues to be conducted and will be discussed in the later in this report.

Figure 77
ANOVA For Rotor Casting L9 Experiment

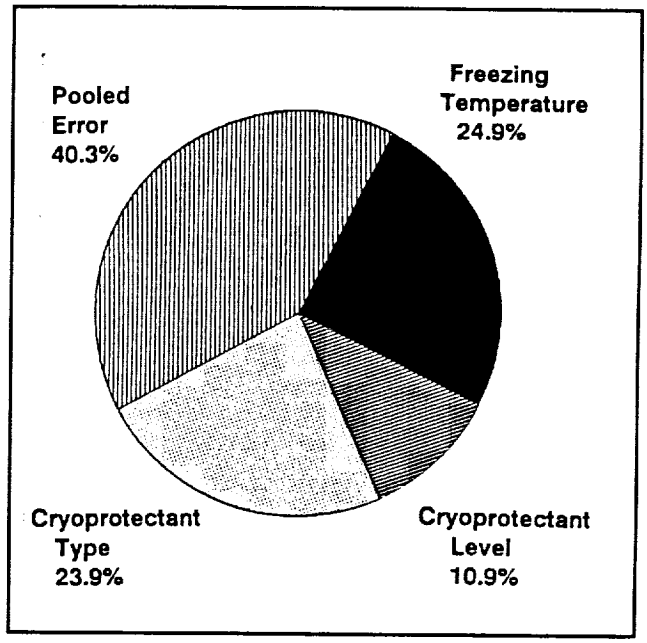

For stators, exploratory casting trials were also completed. Based on work performed for the rotor, PEEP conditions for this component were set and implemented. Using the impact-tolerant design, a "pre-production run-off" of ≥ 100 stators was performed. These demonstration components were produced to verify casting procedures, assess shrinkage and determine mechanical properties. To monitor the performance of this "pre-production" phase, a total of 34 response variables were SPC charted. These variables covered the entire fabrication process. Despite this fact, an overall process yield of only 25% was achieved. Porosity and poor surface finish were major causes for rejection. Many of the defects were traced to the poor surface quality of the stereolithographic pattern. Follow-up screening trials were conducted to assess methods for solving these problems. Each issue was corrected via modifications to the molds and the slip delivery system. These solutions will be implemented for the start-up of engine quality stator production in 1991. Based on this operation, the production process has essentially been set for delivery of first engine-quality mixed-flow stators during 1991.

WEEP Casting Development - Work was initiated during the year on the development of WEEP casting as a variation to pressure-assisted casting (PEEP). As described previously, WEEP casting consists of filling a non-porous mold cavity with an aqueous based slip, lowering the temperature of mold to below the freezing point of the slip, extraction of the frozen piece from the mold, and removal of water by sublimation. The green component is then ready for subsequent furnacing and densification operations. The WEEP technology is highly similar with, and synergistic to PEEP developments described above. Screening experiments were conducted in two areas: (1) Mold Development and Fabrication; and (2) Component Casting Experiments.

Mold Development and Fabrication - Various modifications in molds were utilized to ascertain the requirements of a mold for WEEP casting. Using existing rotor masters for a turbocharger, tensile rod, and AGT101 gas turbine rotor, non-porous rubber molds were prepared and casting trials initiated. From these tools, fully-bladed green rotors were formed without cracking. However, several mold related problems were encountered including non-uniform freezing, void formation, and air entrapment. Striping of the mold from the component was also found to be difficult. Correction of these problems required iterative changes in mold design. Alternate mold materials were also explored as a method of increasing freezing rate to prevent ice-crystal formation. The greatest progress was made in fabrication of a mold for tensile rod blanks. Using a composite design, where the thermal conductivity of the mold was modified, crack free tensile rods could be produced. Conversely, while tensile rods could be cast and densified without cracking, and with reasonably good dimensional control, larger cross-section components such as rotors could not. Inadequate freezing, ice-crystal growth and lack of dimensional uniformity prevailed for rotor components.

Component Casting Experiments - Casting tests demonstrated that green AGT101 rotors and tensile rods could be prepared, frozen, and demolded. Excellent blade definition and quality were observed on these parts. However, freezing rate, cryoprotectant type and amount were found to be important parameters in minimizing defects in large cross-sections of the hub. To improve the freeze-drying step, NTC procured the necessary equipment to perform this operation on a routine basis, both for the WEEP and PEEP processes. Using this equipment, NTC conducted an L4 Taguchi experiment to identify key factors contributing to the prevention of ice crystal formation. Three factors, (freezing rate, cryoprotectant, and sublimation temperature) were investigated within this design--each at two levels. Rotor hubs which simulated the cross-sectional thickness of the AGT101 rotor were utilized as the trial geometry. Qualitative results indicated freezing rate to be the dominant factor in preventing the formation of ice crystals. Components frozen under fast conditions showed no indication of crystal formation. Cryoprotectant level was found to have an effect on the degree of observed cracks which form either during freezing or drying.

A second L4 design was conducted to more clearly understand factors which control the incidence of cracking. Factors in this design included cryoprotectant level, binder content, and cast component geometry--each at two levels. Component geometry was found to be the only factor which correlated to a reduction in cracking. Test tile from the experiment were crack-free, while rotor hubs contained small cracks. The test tile were densified and assessed for mechanical properties. Results are presented in Table 23. Data demonstrate that the WEEP process is capable of producing components possessing excellent mechanical properties. However, despite improved properties, NTC continued to experience difficulties in preparing larger cross-sectional components. Because of these problems, as well as successes in PEEP casting, further work in this area was curtailed. For NT154, the WEEP process appears to have good applicability for complex thin-cross-section components; but seems inappropriate for large thick parts.

CIP PROCESSING - All forming activities using cold-isostatic pressing (CIP) were directed at tile components. During 1990, CIP processing was only used in characterization of processed powders, degas, HIP, and post-HIP heat-treatment operations.

INJECTION MOLDING DEVELOPMENT - During the last quarter of 1989, a final injection molding experiment was conducted in an effort to produce a number of acceptable quality

stators. However, severe internal and external cracking occurred for most of these components. Nevertheless, enough tile survived intact to fabricate a limited quantity of test bars. A truncated ATTAP test matrix was performed as a final evaluation of material produced from the process. The data are shown in Table 24. As can be seen from the data, the average strength values are high, particularly at elevated temperatures. However, the Weibull modulus was somewhat low, (<6) and a plot of the data revealed several outliers. Corner breaks and impurity inclusions were observed as fracture origins in low-strength bars. Titanium was also found at one of the origins. TiN coatings were used on the mixing unit in an attempt to improve wear resistance. Thus, although injection molding shows the potential for forming net-shape components with acceptable strength characteristics, the inclusion problem still needs further attention. Because of these problems, no further work is planned on injection molding under the ATTAP.

Table 23
Physical and Mechanical Properties Of WEEP Cast NT154

Measured Property	Value	No. of Samples
Density (g/cc)	3.230 ± 0.005	5
22°C Flexural Strength		
(MPa)	979 ± 103	8
(Ksi)	142 ± 15	8
1370°C Flexural Strength		
(MPa)	592 ± 36	5
(Ksi)	86 ± 5	5

All Test Bars Were 0.25" x 0.125" x 2.0".

DEGAS HEAT-TREATMENT DEVELOPMENT - Two Taguchi designed experiments were completed and reported on during the first two years of ATTAP. No additional work was planned in this area for 1990. The current status of the NT154 degas process is as follows:

- NT154 degas processing conditions have been finalized and implemented. Standard operating procedures for this process step were written.
- NT154 degassed material specifications were implemented; and material qualification criteria written.
- SPC methods were finalized and charting implemented.

HIP DEVELOPMENT - During the first two years of ATTAP, a HIP L4 Taguchi experiment and follow-up confirmatory tests were completed and reported. Going into the year, the status of the NT154 HIP process was as follows:

- Preliminary NT154 HIP processing conditions were determined and implemented. Standard operating procedures were written.
- NT154 HIP material specifications were set and qualification criteria implemented.
- SPC monitoring was initiated.

For 1990, five additional sub-

Table 24
ATTAP Test Matrix - Mechanical Properties of Injection Molded NT154

Temperature	No. Of Samples	Flexural Strength (MPa)	Flexural Strength (Ksi)
22°C	30	897 ± 145	130 ± 21
1093°C	5	724 ± 131	105 ± 19
1204°C	5	718 ± 28	104 ± 4
1260°C	5	718 ± 35	104 ± 5
1316°C	5	690 ± 41	100 ± 6
1370°C	5	676 ± 28	98 ± 4

tasks were planned within HIP development. They included: (1) HIP Encapsulant Glass; (2) Barrier Coatings; (3) Decapsulation Methods; (4) Abrasive Flow Machining; and (5) HIP Control. The first four sub-tasks were designed to investigate or identify materials and procedures which control the HIP reaction layer. The goal of these four sub-tasks was to maximize both bulk and as-fired mechanical properties. The fifth sub-task was aimed at understanding, then minimizing material variation (both within and between components) associated with the HIP process. During the year, work on encapsulant glass development, barrier coatings and decapsulation methods was discontinued due to either: (1) Lack of significant results or improvements; or (2) Combination of these operations into a single optimization experiment. Efforts in abrasive flow machining, while initially promising, have been delayed until NTC completes its component forming and firing optimization plans. In lieu of this work, efforts in these areas were combined into a Taguchi L16 experiment. This array was designed to fully investigate and optimize conditions for as-fired surfaces. A discussion of each of the individual sub-tasks along with the L16 experiment is provided below.

HIP Encapsulant Glass Development - This sub-task was originally planned around the development of an encapsulant glass specifically for NT154--one which was more chemically compatible to NT154 than the current glass utilized under the ASEA license. In this way, control over the reaction between the encapsulant glass and NT154 components could be realized, and mechanical properties maximized. During the year, a total of eight glass compositions were prepared and melt trials conducted. Based on phase analyses of the fused product, two compositions were then selected for HIP trials. Sufficient quantities of these compositions were prepared and a total of three HIP trials were completed using NT154 tile components. Basic ASEA procedures for HIP operations were utilized. However, full densification was not routinely achieved for any of the glass compositions for various reasons--mainly associated with hermeticity of the encapsulant. In general, density values on tile components were $\leq$ 3.19 g/cc; but ranged from 2.11 g/cc to 3.27 g/cc. In the latter case, full densification was achieved, but the part fractured during cool-down, presumably due to thermal-expansion mismatch between the glass and NT154. Because of the lack of success in locating a suitable replacement glass, all work in this area was terminated.

Barrier Coatings - This sub-task involved the development of boron nitride barrier coatings. Its objective was to eliminate the reaction between the encapsulant glass and NT154 components. Work on barrier coatings actually began in the 1989 program year. A dipping process was developed to apply a uniform coating which effectively sealed the component from the glass and eliminated the reaction layer while yielding smooth, warpage-free test tile surfaces. Work performed in 1990 was directed at assessing mechanical properties; followed by optimization of the robustness and repeatability of this operation. Early in the year, barrier coated tiles were densified. These components were determined to be free of a reaction-layer. The as-HIPed surface quality of these tiles were superior to all prior materials and represented NTC's "best effort" in preparing reaction-layer-free, warpage-free, NT154 surfaces. A number of the tiles were subjected to a post-HIP crystallization heat treatment. As-fired test bars were taken from both sets of tiles. Table 25 shows as-fired mechanical properties for both the crystallized and non-crystallized material. The results are quite interesting in that for this test, the fast fracture mechanical properties of reaction layer-free surfaces were no better than those with a reaction layer, even with superior as-HIPed surface quality.

Additional screening trials were completed to determine the effects of different coating techniques, powder characteristics and HIP conditions on mechanical properties. The powder

characteristics were altered by changing calcination parameters. Changes in powder characteristics along with HIP conditions were explored to determine the effects of different material and densification factors on the effectiveness of barrier coats. The results of these trials are presented in Table 26 and Table 27. In Table 26, data from bulk ground samples are presented. Results suggest no improvements either by using alternative HIP conditions or different powder characteristics. At best, room temperature values were only ≈80% of the uncoated baseline, whereas 1370°C strength was essentially equivalent. In Table 27, data for barrier-coated as-fired surfaces are reported. These results show that barrier-coated surface properties were inferior to those typical of NT154 possessing a reaction layer. Of particular interest is the low fracture-toughness associated with barrier-coated as-fired surfaces (3.7 MPa·m^{½}). This general trend has been observed over the past two years of development. When the reaction-layer is minimized or eliminated, toughness decreases below bulk material levels. The high toughness of reaction-layer surfaces (typically > 7 MPa·m^{½}) may not be an anomaly of the testing technique; but it may be an actual manifestation of a crack arresting mechanism. Based on these results, NTC now believes that elimination of the reaction-layer is undesirable. Conversely, improvement and control of the reaction-layer appears to be an appropriate tactic. Because of this, NTC elected to curtail further work on barrier coating technology.

Table 25
Boron Nitride Barrier Coating - Reaction Layer-Free, As-Fired Surface Mechanical Properties

	Barrier Coated Materials		
Flexural Strength	Non-Crystallized	Crystallized	Uncoated Crystallized
22°C (MPa)	352 ± 62	538 ± 76	610 ± 74
(Ksi)	51 ± 9	78 ± 11	88 ± 11
No. of Bars	15	10	71
1370°C (MPa)	441 ± 34	552 ± 28	608 ± 97
(Ksi)	64 ± 5	80 ± 4	88 ± 14
No. of Bars	9	5	42

Table 26
Bulk-Ground Mechanical Property Results From Barrier Coating Trials Using Modified HIP Conditions

Response Variable	Uncoated Baseline	Barrier Coated No.1*	Barrier Coated No. 2*
Density (g/cc)	3.226	3.236	3.235
K_{IC} (MPa·m^{½})	5.2 ± 0.1	5.1 ± 0.3	5.6 ± 0.1
22°C Flexural Strength (MPa)	1054 ± 62	814 ± 48	800 ± 110
(Ksi)	153 ± 9	118 ± 7	116 ± 16
1370°C Flexural Strength (MPa)	586 ± 7**	565 ± 27	559 ± 41
(Ksi)	85 ± 1	82 ± 4	81 ± 6

* No. 1 and No. 2 Were Densified At Non-Standard HIP Conditions.
** Post-Machining Oxidation Heat-Treatment Applied.
K_{IC} Measured By Controlled-Flaw Technique.

Decapsulation Methods - In late 1989, NTC received and installed a state-of-the-art sandblaster. This unit is capable of handling a broad range of abrasive material under variable pressure and flow-rate conditions. A self-contained classifier and recycling unit was also installed with the equipment. NTC believed that the methods used in removal of the encapsulant glass could be critical in determining as-fired strength. This work centered on developing an understanding of the potential deleterious effects of different media type, grit size, and blast velocity on the surface integrity

of components. In essence, the objective of this work was to develop effective procedures for removal of encapsulant glass and minimize impact damage to NT154 components.

Table 27
Mechanical Property Results From
Barrier Coating Trials

Response Variable	Uncoated Bulk	Barrier Coated Bulk	Uncoated As-Fired	Barrier Coated As-Fired
K_{IC} (MPa·m^{½})	5.3 ± 0.1	5.6 ± 0.3	7.2 ± 0.2	3.7 ± 01
22°C Flexural Strength (MPa)	841 ± 69	882 ± 34	610 ± 74	330 ± 34
(Ksi)	122 ± 10	128 ± 5	88 ± 11	48 ± 5
1370°C Flexural Strength (MPa)	669 ± 4	703 ± 8	608 ± 98	365 ± 34
(Ksi)	97 ± 4	102 ± 8	88 ± 14	53 ± 5

K_{IC} Measured By Controlled-Flaw Technique.

Screening trials involving selected sandblast media were initiated early in the year. These included a wide array of commercially available sandblasting materials. Hardness was used as a main selection criteria. "Softer" media were preferred because of their apparent ability to decrease impact damage. Typical ceramic sandblast media have a hardness of about 9 Mohs. Plastic and walnut shell media generally have a hardness of about 3 Mohs. From the survey, properly sized plastic and walnut shell media were selected and ordered. Testing of these media were performed using a Taguchi designed L4 experiment. Upon evaluation of the results, it was found that regardless of pressure or media flow rate, alternate sandblasting materials were ineffective in completely removing encapsulant from complex components. In comparison, the standard media was found to be very effective even at very low blasting pressures. Because the alternative media were incapable of removing the encapsulant, NTC elected to curtail further developmental work in this area as well. Rather than performing a specific sandblasting test involving different media, optimization of sandblasting procedures using standard ceramic media was incorporated as part of the L16 As-Fired Optimization Experiment described below.

Abrasive Flow Machining - This sub-task involved the investigation of industrial equipment commonly used to polish surface features on complex shapes. Known as abrasive flow machining (AFM), the process involves abrading of the surface of the component using a viscous fluid which has been highly loaded with an abrasive grain. NTC envisioned use of AFM as a post-HIP process for physically removing the reaction layer and improving surface finish. Screening trials were performed using a selected vendor of this equipment in an effort to identify generally applicable AFM process parameters for removal of the NT154 reaction layer. Abrasive flow media type, media size, number of flow passes, and flow patterns were investigated. The first trial was successful in completely removing the NT154 reaction layer. In fact, over 0.5 cm (0.2") of surface material was removed using a mixture of B_4C and SiC. The result demonstrated that the AFM process was capable of physically removing the NT154 reaction layer. However, it also demonstrated that the AFM process required more exploratory studies before any optimization experiments could be planned and conducted. Although 0.5 cm of material was removed, the resulting surface was severely scored by the media. Also, the flow pattern used resulted in a "wavy" surface. A second trial was conducted in an effort to solve these problems. Control over the formation of the rough surface was addressed by investigating a two-step process similar to typical practice for diamond grinding of Si_3N_4. The first step used coarse media to remove the reaction layer. The second step used fine media to smooth the surface. NT154 tile were prepared and run at four different process condition. All of the tiles for this test

had a heavy reaction layer. From this work, mechanical property data were acquired. Table 28 presents room temperature strength data for these conditions. The results indicate that as the severity of the AFM process conditions decrease, flexural strength increases. The majority of the data also showed that the AFM process can be detrimental to strength. Fractography revealed that the predominant flaw origins under all conditions were pits which appeared to result from "pullouts". It was speculated that the sandblasting operation may have introduced impact Hertzian cracks into the glassy reaction-layer. Then, during the AFM process, these areas were preferentially removed appearing as pits on the surface. Their frequency and size was therefore expected to increase as the severity of the AFM process increased--resulting in reduced strength. To test this postulate, an additional paired comparison screening trial was performed using both sandblasted and non-sandblasted as-fired tiles. A severe AFM treatment was applied to both tiles. However, in this case, the surfaces of the tiles had a minimal reaction layer. Surprisingly, both tile showed no sign of pitting, and possessed a good surface finish with only minimal stock removal. However, mechanical property data indicated no improvement over the previously acquired results. In summary, the AFM screening tests generally demonstrated that the process is capable of removing the reaction layer and improving surface finish. However, because it also appears that the use of the process is intricately linked to the depth and character of the reaction layer, NTC elected to delay further optimization of the AFM process until after completion of remaining optimization experiments in casting and firing.

HIP Control Development - This sub-task involved the completion of a Taguchi experiment directed at understanding the parameters which control HIP variability. HIP variability may be divided into three major categories.

- Component Cross Section (thickness).
- HIP Location (temperature profile).
- Run-to-Run Consistency (reproducibility).

As part of the Work Plan, a "HIP Variation L4 Experiment" was designed and performed. This experiment involved three inside factors at two levels each and one outside factor at two levels. The design is shown in Table 29. This experiment addressed the three categories of variation. The three inside factors were aimed at understanding variation within a single HIP run. The outside factor addressed variation between two HIP runs. Results of this experiment are given in Table 30. Shown here are complete ANOVA and level averaging summaries. As-fired density of thin and thick tiles was clearly dominated by cross sectional thickness. Thicker tile gave higher density values as expected since surface to volume ratio decreases. Test-bar (or bulk-ground) density was dominated mostly by HIP location. Material in the upper-half of the HIP unit was higher in density than those HIPed at the bottom. Toughness was controlled

Table 28
Room-Temperature Flexural Strengths Of
Abrasive-Flow Machined NT154 Tile

AFM Treatment Condition	Severity of Pitting	AFM Grit Size	AFM Pressure (Psi)	No. of AFM Cycles	Flexural Strength (MPa)	(Ksi)
None - As-Fired	None	-	-	-	620 ± 62	90 ± 9
AFM - One Step	Minimal	Fine	200	400	703 ± 97	102 ± 14
AFM - Two Step		Coarse Fine	200 200	200 150	517 ± 62	75 ± 9
AFM - One Step		Coarse	400	175	365 ± 48	53 ± 7
AFM - One Step	Severe	Coarse	400	300	331 ± 62	48 ± 9

mostly by cross sectional thickness. As thickness decreased, toughness increased. Room temperature strength was dominated by error (i.e., processing factors outside this experiment). Room temperature values were secondarily controlled by cooling rate. Strengths apparently increased under slow-controlled cooling. Toughness also apparently increased for this condition. 1370°C flexural strength was controlled mostly by HIP location. Material HIPed in the bottom of the HIP unit clearly had higher 1370°C strength. Finally, it is notable that all response variables were virtually uninfluenced by HIP repetition. In other words, run to run variation is virtually non-existent. Flexural stress-rupture testing of these various conditions is in progress. Pending acquisition of the data, optimum HIP processing conditions will be selected, verified, and implemented into the NT154 process. Beyond an analysis of this

Table 29
HIP Variation L4 Experiment

Inside Factors
A. Cooling Rate
    1. Free Fall
    2. Controlled
B. HIP Location
    1. Top
    2. Bottom
C. Component Cross Section
    1. Thin
    2. Thick

Outside Factor
D. HIP Run Repetition
    1. Run #1
    2. Run #2

Table 30
HIP L4 Experiment - ANOVA and Level Average Values

I. Analysis Of Variance (% Contribution)

Response Variables	Cooling Rate	HIP Location	Cross-Section	HIP Run	Error
"As-Fired" Density	1	0	93	1	5
"Bulk-Ground Density	4	45	0	8	43
Fracture-Toughness	17	16	54	0	13
22°C Flexural Strength	34	6	1	0	59
1370°C Flexural Strength	11	45	11	0	33

II. Level Average Values

HIP L4 Factors & Levels	"As-Fired" Density (g/cc)	"Bulk-Ground" Density (g/cc)	Fracture Toughness ($MPa \cdot m^{\frac{1}{2}}$)	22°C Flexural (MPa)	1370°C Flexural (MPa)
Cooling Rate					
Fast	3.229	3.222	4.7	965	634
Slow	3.230	3.223	4.9	1016	608
HIP Location					
Top	3.223	3.223	4.9	1002	596
Bottom	3.229	3.221	4.8	980	646
Cross-Sectional Thickness					
Thick	3.234	3.222	4.7	985	634
Thin	3.225	3.222	4.9	995	608
HIP-Run					
Run No. 1	3.223	3.223	4.8	987	616
Run No. 2	3.230	3.221	4.8	995	626

pending information, no further work in this area is planned.

As-Fired Surface Optimization L16 Experiment - As a result of the combined developments in encapsulant glass engineering, decapsulation methods, barrier coatings, and abrasive flow machining--all of which demonstrated that a "controlled reaction layer" is potentially desirable--an optimization experiment was planned and conducted. The experiment focused on known factors which influenced the reaction layer such as: Powder Characteristics, Degas Conditions, HIP, Sandblasting, Crystallization, and Oxidation. The interactive effects of these separate process steps were evaluated by this experiment. The factors and response variables for the experiment are presented in Table 31. The experiment was designed with one outside factor--test bar surface condition. Both bulk-ground and as-fired surface test bars were prepared for each of the sixteen trials of this experiment.

Table 32 shows an ANOVA summary for both as-fired and bulk surfaces. Table 33 and Table 34 present level average values of the raw data. For either as-fired or bulk-ground surfaces, two factors dominated most results: (1) Powder Type; and (2) Sandblasting Conditions. Results for as-fired surfaces showed that sandblasting conditions generally affected all response variables except for test bar density, room temperature flexural strength and fracture-toughness. Powder type, and degas conditions played a role in determining density, strength and toughness. Room temperature strength increased by using a preferred powder type, lower degas temperatures and milder sandblast conditions. Figure 78 shows as-fired surface room temperature strength as a function of powder type and sandblast conditions. Sandblast condition Nos. 1 and 2 appeared to maximize strength to $\geq$ 620 MPa (90 Ksi). The difference between these conditions and conditions 3 and 4 was in the coarseness of the sandblast grit. Fracture toughness at room temperature appeared to be controlled by powder type. At 1370°C, strength was influenced most by sandblasting conditions and powder type. Mild sandblast conditions coupled with an appropriate powder selection maximized as-fired 1370°C strength. Figure 79 presents a graphical interpretation of the effect of powder type and sandblast conditions on 1370°C strength. Strengths above 620 MPa (90 Ksi) were common for sandblast condition No. 2. Apparent changes in toughness followed this same trend. In summary, for as-fired surfaces, powder type, sandblast condition and degas temperature were dominant factors governing strength. Minimizing the coarse nature of the sandblast media was found to be the most effective method of improving as-fired strength.

Table 31
L16 "As-Fired" Surface
Optimization Experiment

Inside Factors
Powder Calcination Conditions
Degas Soak Temperature
Sandblasting Media/Pressure
Crystallization Soak Temperature
Oxidation Time/Temperature
Outside Factors
Test Bar Surface Condition:
"As-Fired"
Bulk-Ground
Response Variables
Powder and Component Chemistry
Component Density
Phase Composition
Mechanical Properties

ANOVA and level average data for bulk-ground surfaces showed that powder type was the dominant factor affecting most properties. The only two exceptions were room temperature flexural strength and fracture-toughness. Room temperature flexural strengths of bulk ground bars were influenced by the oxidation treatment. It appears that application of an oxidation treatment increased strength values as expected. Error, however, overshadowed all factors for room temperature flexural behavior. Other factors, such as diamond grinding for example, may have

Table 32
Analysis of Variance For The L16 As-Fired Surface Optimization Experiment
(% Contribution)

I. ANOVA For "As-Fired" Surfaces

Response Variable	A	B	C	D	E	Error
Test Bar Density	95	0	2	2	1	0
Room-Temperature Flexural Strength	15	31	29	2	4	19
Controlled Flaw Fracture-Toughness	41	8	27	7	0	17
1260°C Flexural Strength	8	0	29	15	22	26
1370°C Flexural Strength	14	4	63	18	0	1

II. ANOVA For "Bulk Ground" Surfaces

Response Variable	A	B	C	D	E	Error
Test Bar Density	97	0	0	0	0	3
Room-Temperature Flexural-Strength	0	1	1	5	25	68
Controlled-Flaw Fracture-Toughness	33	4	10	0	46	7
1370°C Flexural Strength	72	5	0	6	1	17
1370°C Stress Rupture, 300 MPa	52	3	3	3	3	35
1370°C Strain, 300 MPa	96	1	1	1	0	1
1370°C Stress Rupture, 325 MPa	43	14	14	14	0	15
1370°C Strain, 300 MPa	26	20	25	16	0	13

A = Powder Type. B = Degas Temperature.
C = Sandblasting Conditions. D = Crystallization Conditions.
E = Oxidation Conditions.

influenced room temperature fast fracture. Toughness appeared to be affected mostly by oxidation treatment and secondarily by powder type. Application of the oxidation treatment seemed to lower toughness while changes in powder type apparently increased it. Trends in the data show that changes in powder type lead to 100% survival under fairly severe stress rupture conditions, (1370°C/300 MPa and 1370°C/325 MPa). Flexural strain, (or creep) also increased; but appears to plateau with changes in powder type. Values at the highest stress levels are typical of NT154.

In summary, optimum processing conditions to maximize as-fired and bulk-ground surface mechanical property behavior have been determined. Optimum conditions include an intermediate powder calcination condition, high temperature degas, mild sandblasting, high temperature crystallization, followed by an oxidation heat-treatment. Implementation of these processing conditions is currently being conducted.

COMPONENT INTEGRITY DEVELOPMENT - Two Taguchi designed experiments (i.e., an L16 and L4 arrays) were completed and reported on during the first two years of ATTAP. No additional work was planned in this area for 1990. The current status of post-HIP heat treatment processes is listed as follows:

Table 33
Level Average Results For The L16 "As-Fired" Experiment

Experimental Factors and Levels	Density (g/cc)	22°C Flexural Strength (MPa)	22°C Flexural Strength (Ksi)	22°C Fracture Toughness (MPa·m$^{\frac{1}{2}}$)	1260°C Flexural Strength (MPa)	1260°C Flexural Strength (Ksi)	1370°C Flexural Strength (MPa)	1370°C Flexural Strength (Ksi)
A. Powder Type								
Level 1	3.219	576	84	5.5	567	82	530	77
Level 2	3.216	606	88	5.7	569	83	537	78
Level 3	3.202	594	86	5.9	519	75	609	88
Level 4	3.188	568	82	5.6	565	82	560	81
B. Degas Temperature								
Level 1	3.206	616	89	5.8	554	80	581	84
Level 2	3.204	595	86	5.7	567	82	560	81
Level 3	3.204	573	83	5.7	536	78	557	81
Level 4	3.203	559	81	5.6	564	82	537	78
C. Sandblast Conditions								
Level 1	3.202	574	83	5.7	583	85	565	82
Level 2	3.207	621	90	5.6	573	83	664	96
Level 3	3.204	574	83	5.6	567	82	499	72
Level 4	3.204	574	83	5.9	496	72	505	73
D. Crystallization Conditions								
Level 1	3.206	598	87	5.7	563	82	563	82
Level 2	3.206	574	83	5.7	534	78	540	78
Level 3	3.202	590	86	5.8	528	77	520	75
Level 4	3.203	582	84	5.6	595	86	614	89
E. Oxidation Conditions								
Level 1	3.205	594	86	5.7	525	76	559	81
Level 2	3.203	577	84	5.7	584	85	559	81

Table 34
Level Average Results For The L16 "As-Fired" Experiment
Bulk Ground Surface Data

Experimental Factors and Levels	Density (g/cc)	22°C Flexural Strength (MPa)	22°C Flexural Strength (Ksi)	1370°C Flexural Strength (MPa)	1370°C Flexural Strength (Ksi)	22°C Fracture Toughness ($MPa \cdot m^{\frac{1}{2}}$)	Stress Rupture Life at 1370°C 300 MPa (Hrs)	Stress Rupture Strain at 1370°C 300 MPa (cm/cm)	Stress Rupture Life at 1370°C 325 MPa (Hrs)	Stress Rupture Strain at 1370°C 325 MPa (cm/cm)
A. Powder Type										
Level 1	3.229	803	117	564	82	5.3	52	0.12	51	0.39
Level 2	3.217	810	117	601	87	5.2	>100	0.34	100	0.39
Level 3	3.206	847	123	685	99	5.5	>100	0.34	>100	0.34
Level 4	3.190	853	124	700	102	5.4	>100	0.34	>100	0.44
B. Degas Temperature										
Level 1	3.212	820	119	609	88	5.4	75	0.29	>100	0.37
Level 2	3.210	858	125	653	95	5.3	89	0.29	75	0.36
Level 3	3.211	798	116	634	92	5.3	88	0.27	76	0.44
Level 4	3.210	836	121	654	95	5.4	>100	0.28	>100	0.40
C. Sandblast Conditions										
Level 1	3.211	817	119	647	94	5.3	75	0.28	>100	0.43
Level 2	3.211	834	121	623	90	5.3	89	0.28	75	0.42
Level 3	3.212	800	116	637	92	5.4	88	0.27	76	0.36
Level 4	3.209	862	125	644	93	5.4	>100	0.30	>100	0.36
D. Crystallization Conditions										
Level 1	3.211	820	119	621	90	5.3	75	0.28	>100	0.35
Level 2	3.210	836	121	645	94	5.3	89	0.29	75	0.40
Level 3	3.212	791	115	620	90	5.4	88	0.26	76	0.40
Level 4	3.210	865	126	665	96	5.4	>100	0.30	>100	0.36
E. Oxidation Conditions										

- NT154 crystallization and oxidation processing conditions were finalized and implemented. Standard operating procedures were developed.
- NT154 crystallized and oxidized material qualification criteria have been determined.
- SPC was implemented on this process operation.

Figure 78
L16 As-Fired Optimization Experiment - Room Temperature Flexural Strength

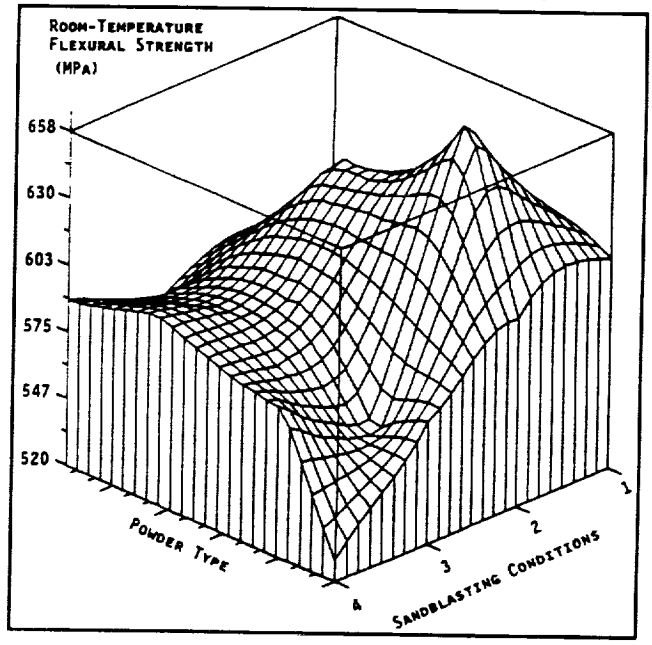

PROCESS ENGINEERING

As a result of significant breakthroughs in casting development, coupled with the need to abide by existing funding limitations, NTC revised its 1990 Work Plan twice during the year. The incorporation of freezing as part of the PEEP casting process enabled NTC to produce crack-free components. Once this discovery was made, the Work Plan was revised to optimize this particular process. Because of funding restrictions, work on automated pressure casting was dropped from the overall program.

NDE DEVELOPMENT

In the prior two years within the ATTAP, NTC completed essentially all of its assigned developmental activities in NDE. Work was directed at optimizing Microfocus X-Ray Radiography (MFXR) techniques and dye-penetrant inspection procedures for the AGT101 rotor and stator. During 1990, the MFXR inspection protocols for green and dense AGT101 rotors and stators were jointly reviewed by NTC and GAPD personnel. As a result, these documents are currently being modified to incorporate: (1) Changes associated with the impact-tolerant component designs; (2) Inspection pass/fail criteria; and (3) Modifications to exposure times, or additional exposures to improve inspection coverage. These changes are intended bring NTC's MFXR inspection procedures into compliance with GAPD's radiography specification, EMS52334, which is called out on the AGT101 impact-tolerant rotor drawing. It was also agreed that characterization of AGT101 rotors in the green state only was

Figure 79
L16 As-Fired Optimization Experiment - 1370°C Flexural Strength

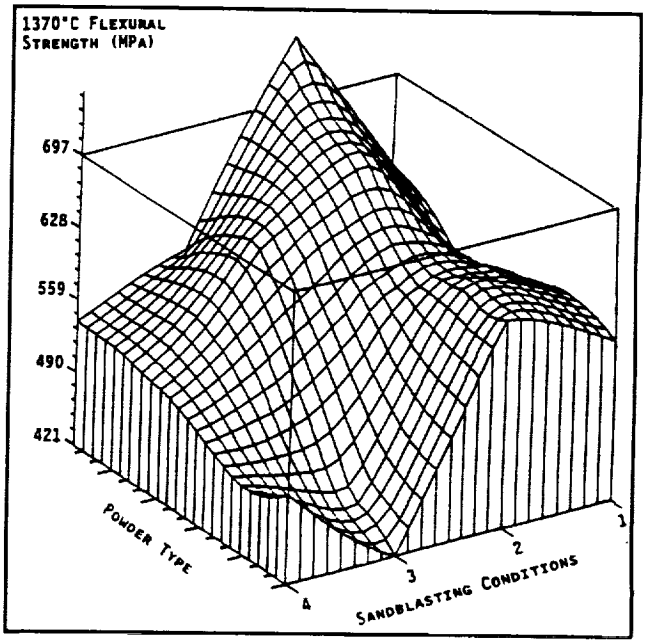

acceptable, as long as all actual films and inspection data are provided to GAPD.

Fluorescent dye penetrant inspection procedures that were previously developed, documented, and reported to GAPD were also reviewed. These documents, one specifying level 3 water washable penetrant and one specifying level 3 hydrophilic post-emulsifiable penetrant, are being modified to incorporate: (1) Penetrant dwell times; (2) Developer dwell times; and (3) Inspection pass/fail criteria as indicated on GAPD Drawing No. R45302. These changes are intended to bring NTC's fluorescent dye penetrant inspection procedures into compliance with GAPD's specification, EMS52309. A fluorescent dye penetrant system optimization experiment was proposed by NTC and reviewed by GAPD. It was decided to modify the experiment design based on GAPD commentary and to include the experiment in NTC's 1991 ATTAP technical Work Plan.

QUALITY ASSURANCE

Efforts in developing a quality assurance system under ATTAP include the following sub-tasks: (1) Documentation of the Quality System - ATTAP Quality Manual; (2) Process Documentation; (3) SPC Development and Implementation; and (4) Component Manufacturing and Inspection Plans.

DOCUMENTATION OF THE QUALITY SYSTEM - NTC prepared and forwarded a draft of a Quality Manual to GAPD for review and commentary. This document was returned to NTC with suggested modifications. These changes were made and the manual formally adopted and implemented throughout NTC's organization. No significant additional modifications are projected for this document.

PROCESS DOCUMENTATION - Work is continuing in documenting specifications, fabrication instructions, and inspection procedures under the NTC's formal documentation system. Procedures dealing with the agglomeration process, slip-preparation, degas, HIP, crystallization, oxidation, and mechanical property testing have been prepared, formally approved and added to the NTC's Gas Turbine Operations Manual.

SPC DEVELOPMENT AND IMPLEMENTATION - Statistical Process Control (SPC) monitoring has been an on-going activity at NTC since the beginning of the ATTAP. SPC techniques have been implemented in on all major process operations including raw materials, powder beneficiation, slip-batch preparation, component forming, degas, HIP, post-HIP crystallization, and oxidation. Presented in Figure 80 is an example of the value of SPC charting. Shown here are 1370°C strengths as a function of consecutive powder batch and HIP run. These data show the effects of cumulative process changes implemented as a result of the completion of Taguchi experiments and SPC monitoring. The first powder batches showed a high degree of variability in strength. This was initially thought to result from variations in the powder itself. However, after grouping and correlating the data to successive HIP runs, it became apparent that most of the scatter was due to the HIP itself. Consequently, based on this SPC chart, NTC took corrective action to tighten the HIP process parameters. At the same time, NTC implemented one process change associated with the degas operation. This is shown on the diagram as occurring at about Batch No. 31. The combined effect of tightened HIP controls and the degas process change improved overall strength and reduced variability. Later, after completion of experiments in crystallization and oxidation, NTC elected to make one additional process change. This change, shown on the diagram at ≈ Batch No. 44, was chosen because it further reduced

Figure 80
SPC Chart For 1370°C Flexural Strength As A Function Of
Powder Batch And HIP Run

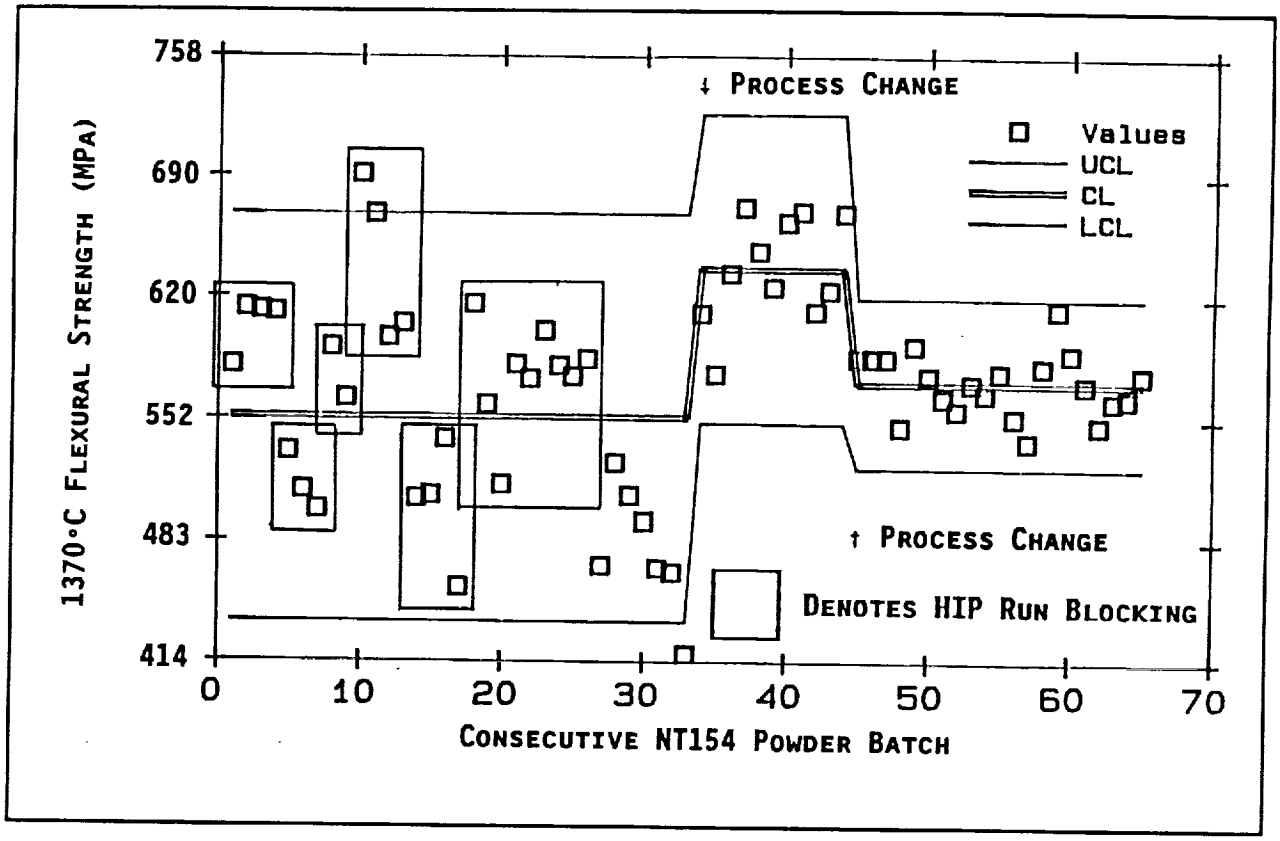

process variability. Note that NTC preferred lower process noise to higher strength. This represented an engineering compromise which should improve component reliability. In comparison with the beginning batches, SPC data at Batch Nos. 50+ show improved strength and a tight distribution.

In addition to process SPC, job-specific SPC was also performed as necessary. These include component mechanical properties, yields and dimensions. Parameters monitored for each job by SPC are reviewed on an ongoing basis, and are dropped if they are found to be ineffective in correlating to product or process performance. The only remaining area to be brought under full SPC control is machining. With the fabrication of engine quality components during 1991, it is expected that SPC techniques will be implemented in this area as well.

COMPONENT MANUFACTURING AND INSPECTION PLANS - With the selection of PEEP casting for initial fabrication of the AGT101 rotor and stator, component-specific manufacturing procedures have been written and implemented. Process flow charts, inspection plans, and operations sheets (i.e., a detailed set of proprietary work instructions) were developed for the two components. Fabrication of demonstration hardware using stereolithographic masters was accomplished per these instructions.

DELIVERABLES

Delivery of quarterly demonstration hardware was made a part of the Work Plan as a method of evaluating current process capability and tracking progress in forming development. During 1991, a total of 8 rotors and 57 stators were prepared for delivery to GAPD. Of this number 1 rotor and 15 stators represented the new impact tolerant designs. The balance of these components were prepared using either the radial designed AGT101 components; or in the case of rotors, mock AGT101 parts were also fabricated. Problems in adopting and optimizing the PEEP process delayed some of the component deliverables. Instead of direct deliveries to GAPD, demonstration rotors were assessed for mechanical properties at NTC with the results being reported to GAPD. Given below is a chronological discussion of the challenges and progress in fabricating these components during 1990.

ROTORS - NTC selected PEEP casting as the preferred method for forming these components. Because the final design for the impact-tolerant rotor had not been set, a radial rotor master was modified to mimic the impact-tolerant design. Two fully dense mock AGT101, and two AGT101 were prepared as part of the first rotor demonstration. Fabrication of these components utilized the best PEEP casting techniques available at the time of their production. Cast rotors were approximately three-fourths fully-bladed. Blade loss occurred during extraction of the components from the molds and was attributed to inappropriate mold design. The rotors were successfully processed through degas and HIP operations without inducing further cracks. NTC machined flexural bars from these rotors and assessed mechanical properties. Observed values are presented in Table 35. Fracture toughness values for these components were slightly lower than normal for NT154, but within SPC tolerance. Strengths were notably lower than prior rotor-hub data, and somewhat dissimilar from co-processed tile. Strengths of co-processed tile were 882 ± 124 MPa (128 ± 18 Ksi) and 579 ± 5 MPa (84 ± 5 Ksi) for room temperature and 1370°C, respectively. Fractography revealed that many of the low strength breaks resulted from impurity inclusions which were traced to the agglomeration equipment used within the PEEP process.

A second series of demonstration rotors was subsequently prepared. Four AGT101 rotors were cast and densified. Using an improved mold design, two of the rotors possessed no cracks in either the hub or blade regions. These rotors were also fabricated from PEEP powders where measures were taken to control the impurities. Two of the rotors were cut into test bars and assessed for mechanical properties. Results are presented in Table 36. The data are essentially equivalent to the first rotor demonstration. Fractography suggested some improvement in impurity related failures. However, impurity inclusions were still found at some of the origins.

Table 35
Mechanical Properties Of Rotors
First Component Demonstration

Temperature °C	Flexural Strength (MPa)	Flexural Strength (Ksi)	Fracture Toughness MPa·m$^{\frac{1}{2}}$	No. of Samples
21	881 ± 103	128 ± 15	5.0 ± 0.3	23
1093	586 ± 101	85 ± 10	-	5
1204	580 ± 62	84 ± 9	5.1 ± 0.6	5
1260	592 ± 66	86 ± 10	-	5
1316	572 ± 19	83 ± 19	-	5
1370	486 ± 48	70 ± 7	-	5

All Test Bars Were 0.25" x 0.125" x 2.0"
Fracture Toughness By Chevron Notch Method.

Impact-tolerant demonstration

rotors were subsequently prepared from a stereolithographic pattern supplied by GAPD. Using PEEP casting techniques and optimized mold designs for these components, cast or green component cracking was eliminated. A number of these components were fully densified, of which 1 part was provided to GAPD towards the end of the year. A photograph of this component is shown in Figure 81. A number of additional impact-tolerant design rotors were prepared and are currently being assessed for mechanical properties. These components will be delivered to GAPD in early 1991.

Table 36
Mechanical Properties Of Rotors
Second Component Demonstration

Temperature °C	Flexural Strength (MPa)	Flexural Strength (Ksi)	No. of Samples
21	864 ± 128	125 ± 19	23
1093	640 ± 61	93 ± 9	5
1204	553 ± 91	80 ± 13	5
1260	551 ± 39	80 ± 6	5
1316	538 ± 50	78 ± 7	5
1370	498 ± 50	72 ± 7	5

All Test Bars Were 0.25" x 0.125" x 2.0"

STATORS - NTC delivered 57 stators to GAPD during the year. Like rotors, quarterly demonstration hardware was produced. The first demonstration components consisted of 20 stators from the old radial design. These components were prepared using PEEP casting. Also, similar to the rotors, initial mechanical properties for co-processed tile were lower than anticipated, but still acceptable per the ATTAP specification. Later in the year, a "pre-production" run of ≈ 100 stators was initiated for the new impact-tolerant design. In an effort to correlate the mechanical behavior of PEEP prepared components, statistical process controls were initiated on agglomeration runs and slip-batches. A summary of fast-fracture data from co-processed tile for stator casting batches is given in Table 37. Comparative analyses of the means and low breaks (i.e., extreme value statistics) suggested an "out-of-control" condition for agglomeration batch Nos. 21 through 23. The majority of these low fracture breaks were discovered to be impurity inclusions. For stator and tile components, no defects associated with remnants from agglomerates were noted in these, or the other batches. Overall, the data portray again the importance of impurity control within the process operation. Stress rupture testing has also been completed for these components. Results are shown in Table 38. These data show that the material exhibits acceptable behavior at moderate stresses, although some variability was noted at high temperatures and rapid failure occurs at stresses exceeding ATTAP specifications.

Figure 81
Impact-Tolerant AGT101 Rotor

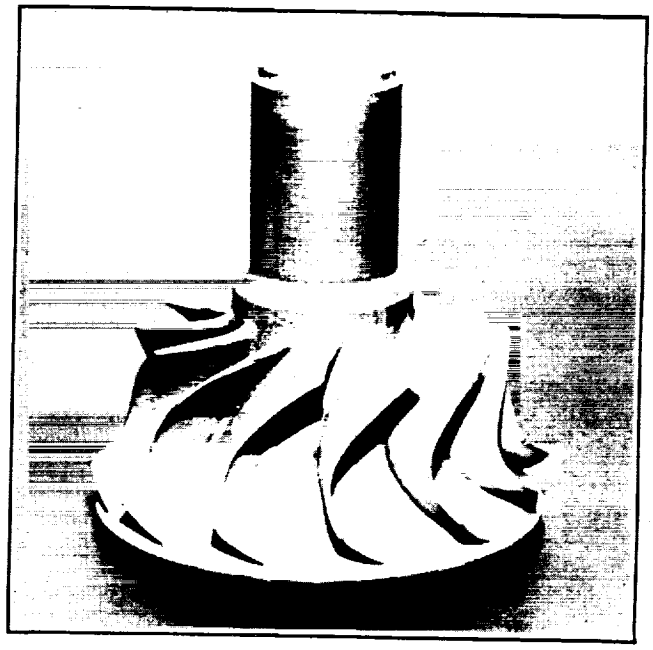

Demonstration stators of the new impact tolerant design were prepared by year end and forwarded to GAPD. Mechanical property assessment of these components is still in progress. A photograph of these components is given in Figure 82.

Table 37
Flexural Strength Data From AGT101 Stator Batches

Agglom-eration Batch	Slip Batch	Room-Temperature Flexural Strength Average (MPa)	Average (Ksi)	Low Break (MPa)	Low Break (Ksi)	1370°C Flexural Strength Average (MPa)	Average (Ksi)	Low Break (MPa)	Low Break (Ksi)
8	H	1055 ± 69	153 ± 10	924	134	614 ± 28	89 ± 4	579	84
10	J	979 ± 152	142 ± 22	944	137	600 ± 14	87 ± 2	579	84
10	K	1089 ± 62	158 ± 9	710	103	579 ± 55	84 ± 8	531	77
10	L	986 ± 117	143 ± 17	751	109	558 ± 7	81 ± 1	552	80
10	M	944 ± 159	137 ± 23	724	105	593 ± 14	86 ± 2	586	85
11	N	951 ± 90	138 ± 13	807	117	565 ± 28	82 ± 4	531	77
21	411	848 ± 62	123 ± 9	614	89	572 ± 28	83 ± 4	538	78
21	413	869 ± 145	126 ± 21	586	85	579 ± 5	84 ± 5	517	75
23	421	807 ± 214	117 ± 31	331	48	531 ± 76	77 ± 11	393	57
22/23	422	841 ± 145	122 ± 21	448	65	572 ± 34	83 ± 5	531	77
23	424	910 ± 117	132 ± 17	731	106	600 ± 21	87 ± 3	572	83
23	425	855 ± 131	124 ± 19	489	71	558 ± 48	81 ± 7	510	74
23/25	428	841 ± 165	122 ± 24	634	92	586 ± 28	85 ± 4	552	80
25	429	944 ± 145	137 ± 21	683	99	586 ± 28	85 ± 4	545	79

Table 38
Stress Rupture Results - ATTAP Demonstration Stators

Bar ID No.	1204°C 350 MPa	1204°C 400 MPa	1260°C 350 MPa	1260°C 400 MPa	1316°C 200 MPa	1316°C 250 MPa	1370°C 200 MPa
JT-1-1	150+						
KT-1-2	150+						
KT-1-3	160+						
LT-4-4		161+					
LT-5-5		161+					
JT-1-6			160+				
JT-1-7			161+				
KT-1-8			161+				
LT-4-9				2.5			
LT-4-10				2.1			
JT-1-11					163+		
KT-1-12					161+		
KT-1-13					161+		
LT-4-14						161+	
LT-4-15						165+	
JT-1-16							159+
KT-1-17							23.0
KT-1-18							159+
LT-4-19							209+
LT-4-20							186+

From the combined results for both stators and rotors, NTC has developed a 1991 Work Plan which addresses the issues of impurity control within the PEEP casting process. As described earlier in the report, a critical metal component in the agglomerator was replaced with a modified NT154 component. Qualitative data indicated that improvements in impurity control were achieved with this change. However, overall strength improvements were not realized. Because of this, an overall audit of the NT154 process and forming methods is currently being conducted. Additional corrective action is being applied. This includes both simplification and standardization of the process through: (1) Elimination of excessive or unnecessary handling operations; and/or (2) upgrading of equipment. In addition, experiments within the 1991 Work Plan are directed at replacing the agglomeration operation with flocculation techniques should they prove to be beneficial. It is believed that either upgrading or replacement of the existing agglomeration operation will yield improved mechanical integrity of the ATTAP hardware.

PROJECT MANAGEMENT

NTC submitted a detailed 1990 Work Plan during the year; then subsequently revised this plan twice to account for technical changes and cost limitations. Cost-support detail was provided with these plans. Monthly technical and cost reports, or other technical information was supplied in accordance with the schedule, or at GAPD's request. Several design and program review meetings occurred periodically throughout the year, both at GAPD's Phoenix location and at NTC's facility in Northboro. NTC also participated in the 28th DOE Contractor's Coordination Meeting in Dearborn, MI, on October 22-25, 1990. B. J. McEntire presented a review of this program during the meeting entitled, "ATTAP Ceramic Component Development".

Figure 82
Impact Tolerant AGT101 Stators

SUMMARY AND CONCLUSIONS

Norton/TRW Ceramics has completed its third-year effort of the ATTAP. Process and component development work continued for the AGT101 rotor and stator. Significant accomplishments for the year are summarized below.

- Characterization of NT154 was performed during the year--both by NTC and outside laboratories. A significant data-base of critical mechanical properties for this material now exists. Flexural strength, fracture toughness, static and dynamic fatigue, creep, and thermal property data are available for engine design and analyses. Overall, properties for this material continue to exceed program specifications.

- A new generation siliconized silicon carbide (Si·SiC) has been developed. Designated NT230, this material has approximately double the strength of existing Si·SiC compositions. At elevated temperatures (up to 1370°C), its strength is essentially equivalent to NT154.

Characterization of this material by several laboratories has been accomplished. Its behavior indicates that it is an excellent choice for static structural components within advanced gas turbine engines.

- All powder beneficiation development has been completed. Process specifications, acceptance criteria and SPC methods were developed and implemented.

- Casting development continued for both the rotor and stator. NTC developed and explored several techniques to overcome component cracking problems. Predominate among them were the incorporation of: (1) Calcination (to improve dispersion and rheology); (2) Agglomeration (for improved casting rates and density uniformity); and (3) Freezing/Freeze Drying (to improve wet-green strength). These particular techniques were optimized and standardized during the year. Laboratory pressure casting apparatus and plaster molds were developed and utilized. From these techniques, impact tolerant AGT101 rotors and stators were successfully cast, densified, characterized, and delivered to GAPD for evaluation. Mechanical properties for these components met program requirements, and were comparable with properties from co-processed test-tile. Room temperature strength and Weibull Modulus were ≈ 890 MPa (129 Ksi) and 8, respectively. At 1370°C, a flexural strength of ≈ 590 MPa (86 Ksi) was observed. Problems were encountered in maintaining high strength levels within the casting process. Although components produced from this process still achieved ATTAP specifications, impurities resulted in a slight reduction in strength over prior year's values. Yet the process itself demonstrated its capability to form the complex ATTAP components to near-net-shape in a crack-free condition. As an engineering compromise, NTC elected to sacrifice ultra-high strengths in order to achieve acceptable component fabrication. Continued refinements of the process are planned for 1991.

- Degas development work has been completed. Process specifications, acceptance criteria and SPC methods were developed and implemented.

- HIP development work in six areas was performed: (1) HIP Encapsulant Glass; (2) Barrier Coatings; (3) Decapsulation Methods; (4) Abrasive Flow Machining; (5) HIP Control; and (6) An L16 "As-Fired Surface Optimization Experiment. During the year, work on encapsulant glass development, barrier coatings and decapsulation methods was discontinued due to a lack of significant results or improvements. Efforts in abrasive flow machining, while initially promising, have been delayed until NTC completes its component forming and firing optimization plans. In lieu of this work, efforts in many of these areas were combined into a Taguchi L16 experiment directed at investigating and optimizing conditions for as-fired surfaces. This experiment was completed and appropriate conditions selected. Preferred conditions include an intermediate powder type, high temperature degas, mild sandblasting conditions, high temperature crystallization followed by oxidation. Using these techniques, strengths of as-fired surfaces were improved from ≈ 345 MPa (50 Ksi) to ≈ 586 MPa (85 Ksi), and found to be independent of test-temperature. No further work in HIP development is planned under the ATTAP.

- Post-HIP Component Integrity development has been completed. Process specifications, acceptance criteria and SPC methods were developed and implemented.

- NDE development utilized microfocus x-ray radiography (MFXR) and florescent dye-penetrant checking. Procedures for these operations have been reviewed in light of the new impact-

tolerant rotor and stator. They are currently being upgraded to be in compliance with GAPD specifications.

- Quality Assurance Development continues within the ATTAP. During the year, a Quality Manual/Plan was reviewed by GAPD. This document has been revised, approved and formally implemented as NTC's governing quality document. Measurement techniques and standards were implemented or upgraded for several inspection operations, including density, strength, dimensions and MFXR. Along with component specific operation sheets and procedures, the documentation system under ATTAP has been revised to reflect changes to the impact-tolerant hardware designs. Documentation of the process continued through the writing of standard procedures and specifications based on results from the Work Plan. SPC has been implemented for all operations except for machining. Complete implementation is slated to coincide with the culmination of the process developmental work and delivery of the final engine quality components.

Continued effort in each of the above areas is scheduled for the 1991 program year. Work will focus on component specific problems for the rotor and stator.

ACKNOWLEDGEMENT

Work accomplished during the 1990 program year represents the combined efforts of a number of individuals. The following principal engineers are gratefully recognized for their key contributions: R. L. Yeckley--Materials Development, A. P. Taglialavore--Powder Beneficiation Degas and HIP Development, D. N. Heichel--Casting Development, J. E. Holowczak--Casting and Injection Molding Development; R. R. Hengst--Casting Development; M. G. Bingham--Machining Development; L. D. Lynch--Design and Drafting; and E. Bright--NDE and Quality Assurance. Additionally, G. Janulewicz, D. Moylan, J. Gulcius, G. Manoogian, B. McGeary, W. Hackett, D. Karsberg, S. FitzGerald, K. Mitchell, P. Reed, L. Russell, E. Mastrovito, and G. Watson are acknowledged and appreciated for detailed performance of the technical plan. Appreciation is expressed to G. A. Fryburg, T. G. Kalamasz, and P. K. Caneen for their technical support and consultation. The Characterization and Analysis Groups of Norton Company are acknowledged for their work in chemical analysis, x-ray diffraction, microfocus x-ray characterization, mechanical property testing, and electron microscopy. A. M. Schiavitti-Smith, E. M. MacKinnon, G. D. Roberts, R. T. Foy, and D. L. Sterner, are appreciated for cost analysis, accounting and secretarial services. Special thanks go to Drs. C. L. Quackenbush and R. R. Wills who constructively reviewed program objectives, plans, and reports; and to J. M. Garwood for government contract administration review and support. T. J. Woods is gratefully acknowledged for contributions in technical, financial and program management. J. Smyth, D. Carruthers, L. Lindberg, J. Schienle, J. Minter, and B. Morey of GAPD are acknowledged and thanked for technical guidance, analyses, program direction and support. Finally, appreciation is expressed to Norton Company, TRW, GAPD, NASA and DOE for financial support.

REFERENCES

1. K. C. Liu and C. R. Brinkman, "Cyclic Fatigue of Toughened Ceramics," Ceramic Technology for Advanced Heat Engines Project - Semiannual Progress Report for October 1989 Through March 1990, (Oak Ridge, TN: ORNL Publication No. ORNL/TM-11239), 359-372.

2. K. C. Liu, H. Pih, C. O. Stevens, and C. R. Brinkman, "Tensile Creep Behavior And Cyclic Fatigue/Creep Interaction Of Hot-Isostatically Pressed Si_3N_4," Proceedings Of The 28th Annual Automotive Technology Development Contractors' Coordination Meeting, Dearborn, MI, October 22-25, 1990, (Warrendale, PA: SAE Press), in press.

3. D. W. Richerson, "Fractography of Advanced Silicon Nitride Materials For Turbine Applications," Final Report, Submitted to Naval Sea Systems Command, Contract No. N00024-88-C-5112, Washington, D. C., (Salt Lake City, UT: Ceramatec Report No. 8963201, April 1989).

4. N. L. Hecht, S. M. Goodrich, L. Chuck, and D. E. McCullum, "Effects Of The Environment On The Mechanical Behavior Of Ceramics," Proceedings of the 28th Annual Automotive Technology Development Contractors' Coordination Meeting, October 22-25, 1990, Dearborn, MI, (Warrendale, PA: SAE Press), in press.

5. K. C. Liu, H. Pih, C. O. Stevens, and C. R. Brinkman, "Tensile Creep Behavior And Cyclic Fatigue/Creep Interaction Of Hot-Isostatically-Pressed Si_3N_4," Proceedings Of The Annual Automotive Technology Development Contractors' Coordination Meeting, (Dearborn, MI: October 22-25, 1990).

6. M. L. Torti, J. W. Lucek and G. Q. Weaver, "Densified Silicon Carbide--An Interesting Material For Diesel Applications," SAE Paper No. 780071, Proceedings of the SAE Congress and Exposition, Feb. 27-Mar. 3, 1978, (Detroit, MI); (Warrendale, PA: Society Of Automotive Engineers, Inc., 1978).

7. "Advanced Gas Turbine (AGT) Technology Project," Final Report, Allison Gas Turbine Division, General Motors Corporation, Report No. DOE/NASA 0168-11, NASA CR-182127, EDR 13295, Prepared For National Aeronautics and Space Administration, Lewis Research Center, for the U.S. Department of Energy, Conservation and Renewable Energy, Office of Transportation Systems, (August 1988).

8. G. Q. Weaver, "Process For Forming High Density Silicon Carbide," U.S. Patent No. 3,998,646, (Dec. 21, 1976).

9. G. Q. Weaver and B. A. Olson, "Process For Fabricating Silicon Carbide Articles," U.S. Patent No. 4,019,913, (April 26, 1977).

10. R. E. Morey, G. A. Lucas, W. D. Carruthers and J. R. Smyth, "Eighteenth Bi-Monthly Technical Progress Report, Advanced Turbine Technology Applications Project, Contract DEN3-335, July Through August 1990, Garrett Auxiliary Power Division, Allied Signal Aerospace Company, Prepared for NASA Lewis Research Center, No. 31-6990(18), Sept. 28, 1990.

11. D. F. Carroll, R. E. Tressler, Y. Tasai, and C. Near, "High Temperature Mechanical Properties Of Siliconized Silicon Carbide Composites," Tailoring Multiphase and Composite Ceramics, Materials Science Research, 20, (New York: Plenum Press, 1987) 775-778.

12. M. H. Rahaman, Y. Boiteux and L. C. DeJonghe, "Surface Characterization of Silicon Nitride and Silicon Carbide Powders," Bull. Amer. Ceram. Soc., 65, [8], (1986), pp. 1171-76.

13. P. K. Whitman and D. L. Feke, "Colloidal Characterization Of Ultrafine Silicon Carbide and Silicon Nitride Powders," Adv. Cer. Matls., 1, [4], (1986) pp. 366-70.

14. D. R. Dinger and J. E. Funk, "Particle Size Analysis Routines Available on CERABULL: Overview and MXENTRY Program," Bull. Amer. Ceram. Soc., 69, [1], 1990, pp. 58-60.

GLOSSARY

AFM	Abrasive Flow Machining
AGT	Advanced Gas Turbine
ANOVA	Analysis of Variance
ASEA	(HIP Encapsulation Process)
ATTAP	Advanced Turbine Technology Applications Project
B_4C	Boron Carbide
C	Celsius
cc	Cubic Centimeter
CIP	Cold Isostatic Pressing
CL	Control Limit
cm	Centimeter
DOE	Department of Energy
F	Fahrenheit
FPI	Fluorescent Penetrant Inspection
g	Gram
GAPD	Garrett Auxiliary Power Division
GPa	Giga Pascals
HIP	Hot Isostatic Pressing
hr	Hour
IM	Injection Molding
in	Inch
IQI	Image Quality Indicator
K	Kelvin
Kg	Kilogram
K_{IC}	Critical Stress Intensity Factor
Ksi	Thousands of Pounds Per Square Inch
lbs	Pounds
LCL	Lower Control Limit
m	Meter
MFXR	Microfocus X-Ray Radiography
mg	Milligram
mm	Millimeter
MOR	Modulus of Rupture
MPa	Mega Pascals
N/A	Not Applicable
NASA	National Aeronautics and Space Administration
NDE	Nondestructive Evaluation
NTC	Norton/TRW Ceramics
ORNL	Oak Ridge National Laboratory
PEEP	Pressure-Assisted Endothermic Extraction Process
PSC	Pressure Slip Casting
psi	Pounds per Square Inch
QC	Quality Control
R.T.	Room Temperature
SAE	Society of Automotive Engineers
SEM	Scanning Electron Microscope
SiC	Silicon Carbide
Si-SiC	Siliconized Silicon Carbide
Si_3N_4	Silicon Nitride
SOP	Standard Operating Procedure
SOW	Statement of Work
SPC	Statistical Process Control
UCL	Upper Control Limit
UDRI	University of Dayton Research Institute
W	Watt
WEEP	Water Endothermic Extraction Process
µin	Microinch
µm	Micrometer
Y_2O_3	Yittrium Oxide

8071(03)-42B

APPENDIX II

ANNUAL TECHNICAL PROGRESS REPORT
CARBORUNDUM COMPANY

ADVANCED TURBINE TECHNOLOGY APPLICATIONS PROJECT (ATTAP)

Contract DEN3-335
Subcontract K71-2331780

ENGINE COMPONENT FABRICATION

ANNUAL TECHNICAL PROGRESS REPORT
NO. 1

September /December 1990

Submitted By:
THE CARBORUNDUM COMPANY
TECHNOLOGY DIVISION
P.O. BOX 832
NIAGARA FALLS, NY 14032

Prepared By: Dean Owens Date: 2/7/91
Dean Owens

Date:

Approved By: Harry A. Lawler Date: 2/7/91
Harry A. Lawler

Prepared For:
Garrett Auxiliary Power Division
Allied-Signal Aerospace Company
Phoenix, Arizona

NOTICE

Introduction

This report, prepared by The Carborundum Company, represents the first annual progress report submitted under the ceramic component fabrication contract. This subcontract is part of the U.S. Department of Energy sponsored and NASA administered 5-year contract DEN3-335. The prime contractor is Garrett Auxiliary Power Division--Advanced Turbine Technology Applications Project (ATTAP) with Dr. Jay Smyth as Project Manager. Work reported herein covers the period of September through December 1990.

The objective of this program is to fabricate and deliver by 31 Mar. 1991 five engine quality sets of three different Hexoloy SA Silicon Carbide components. In accomplishing this, Carborundum is to establish dimensional tolerance capabilities of the isopressing/green machining process to provide the basis for meeting the anticipated GAPD requirement for nine additional sets to be delivered through 1992.

Technical Progress Summary

The three Hexoloy SA SiC components required are:

Dwg. No. PA361290-1	Pilot Combustor Support
Dwg. No. R45315	Combustor Baffle
Dwg. No. R45319	Transition Duct

The processing parameters and capabilities have been well established for non-engine components. However, the stringent dimensional and NDE specifications along with the very limited time frame available makes it imperative that very close control be exercised at every processing step. These specifications are:

Specification for Sets 1 - 5

Material:

- o MOR > 50 ksi
- o m > 7.5 (maximum likelihood method)

Dimensional Tolerances:

- o Machined to drawing tolerances specified, with the exception of as-sintered flow path surfaces.
- o Carborundum shall exert its best efforts to achieve the objectives +/-0.5% dimensional tolerances on as-sintered flow path surfaces (except where designated as a critical surface). Please note the +/-0.5% objective is on a best efforts basis, and the formal dimensional tolerances capability will not exceed +/-1.0%. The machining vendor selected by Carborundum cannot machine the following surfaces:

  Baffle - exterior surfaces between the fins
  Transition Duct - exterior surface of the air diverter

  At the present time, we are not aware of any other machining vendor with this capability, therefore, the first five sets will not be machined on these surfaces.

  Carborundum will continue to survey other machining vendors to determine the feasibility of machining these surfaces in subsequent sets of component deliverables.

NDE:

- o X-Ray — Maximum allowable indication 1% of thickness or 0.010", whichever is larger in high stress regions (to be identified by GAPD). In high stress regions, no indications by the procedure described below.

o	FPI	No defects >.005" on as-fired surfaces in high stress regions (to be identified by GAPD). Maximum allowable defect on machined surfaces 1% of thickness, or 0.010", whichever is larger. Subsequent finishing to remove surface defects which do not meet this criteria will be performed subject to approval by Garrett.

Procedures:

X-ray inspection will be performed using a Magnaflux M-100 Unit located in Niagara Falls. Procedures shall be mutually agreed to by Carborundum and Garrett, and shall include both part orientations and the number of views. The zero degree point will be identified by Carborundum and shall be used to determine the part orientation during inspections at both locations. Radiograph quality shall be measured in accordance with MIL-STD-453 to a 1-1T quality level, and duplicate films will be processed at Carborundum. Fluorescent Penetrant Inspection shall be accomplished using a high sensitivity post-emulsifiable penetrant and lipophyllic emulsifer. Parts are to be evaluated prior to and after application of non-aqueous wet developer.

Specifications on subsequent sets of deliverables shall be developed iteratively during the course of fabricating the first five (5) sets.

Carborundum developed a work plan which requires material qualification at each process step in order to minimize risk and ensure that material or processing problems are identified as soon as possible and corrected.

The following tasks were established:

Task I:	Qualify Premix
Task II:	Qualify Isopressed Billets
Task III:	Green Machine and Sinter Components
Task IV:	Finish Machine and Anneal Components
Task V:	Program Management

The progress made during this reporting period is summarized below:

Task I: Qualify Premix

Qualification of powder lot D90040 allocated for the fabrication of all three components was completed. Plates 2-1/2" x 2-1/2" x 3/8 were green machined from 4" x 4" isopressed billets. These were sintered, inspected, machined into size B test bars, and annealed.

Average room temperature strength and Weibull Modulus for a group of 20 specimens were 65.7 ksi and m=15.7, respectively. These values exceed the requirements of >50 ksi and >7.5. Fracture analysis results are reported in Figure 83.

Task II. Qualify Isopressed Billets

Billets in three different sizes were isopressed for the different sized components from powder lot D90040. Plates were sliced from these billets adjacent to the blanks for the components.

The plates for the transition duct and combustor baffle billet qualifications were sintered. Two groups of test bars were subsequently machined. After NDE and annealing, the test specimens were broken. The results shown below exceed the MOR and Weibull Modulus requirements of >50 ksi and >7.5, respectively.

Billet Qualifiers	No. of Samples	MOR (Ksi)	m
Baffle	19	66.4	14.2
Transition Duct	17	64.3	8.5

The above data are also compared with previous qualification results in the Qualification Test Summary (Table 39).

Because the combustor support drawing was available and green machining could be initiated immediately (see Task III), the combustor support billet qualification was waived. Instead, the test specimen plates were sintered with the green machined components for both the sintered and machined/annealed qualification specimens.

GAPD #2331780

ATTAP SPECIMEN INSPECTION RECORD

Premix Qualification
MATERIAL/SUPPLIER SiC/Carborundum
DATE RECEIVED
FABRICATED TEST BAR YES ✓ NO __ CHECK ONE
CUT FROM COMPONENT YES __ NO ✓

NDE METHODS USED: PT, RT
NDE INSPECTOR: Anthony Travis
INSPECTION DATE: 8-24-90
COMPONENT DESCRIPTION, S/N

SPECIMEN SERIAL NUMBER	DEFECT LOCATION	COMMENTS	FLEXURE STRENGTH (KSI)	FRACTURE ORIGIN	
				SURFACE	INTERNAL
90C40-100-1	None Detected (ND)	possible void	70.391		✓
2	ND	enlarged grain	71.168		✓
3	ND	possible void	72.272		✓
4	ND	enlarged grain	71.806		✓
5	ND	missing	68.841		
6	ND	enlarged grain	58.302		✓
7	ND	possible void	57.268		✓
8	ND	missing	60.382		
9	ND	missing	66.254		
10	ND	missing	66.856		
11	ND	possible void	69.151		✓
12	ND	enlarged grain	57.514		✓
13	ND	possible void	59.532	✓	
14	ND	missing	69.663		
15	ND	missing	63.721		
16	ND	possible void	64.586		✓
17	ND	enlarged grain	53.775		✓
18	ND	possible void	73.077		✓
19	ND	agglomerates	67.977		✓
20	ND	possible void	65.852		✓

FIGURE 83. FRACTURE ANALYSIS RESULTS

TABLE 39. GAPD MATERIAL QUALIFICATION SUMMARY
LETTER SUBCONTRACT K71-231780
DENS 3-335

Qualification Sample	No. of Specimens	Ave. R.T. Strength (Ksi)	Std. Dev.	Weibull Modulus - Linear Regression	Weibull Modulus - Maximum Likelihood
SA SiC Powder Lot D90040	20	65.7	5.3	12.7	15.7
Billet Qualifiers					
- Combustor Support	(Replaced by Sintered Component Qualifiers)				
- Baffle	19	66.4	6.0	11.0	14.2
- Transition Duct	19	64.3	7.5	8.8	8.5
Sintered Component Qualifiers					
- Combustor Support	20	69.2	5.9	12.1	12.4
- Baffle					
- Transition Duct					
Machined/Annealed Component Qualifers					
- Combustor Support					
- Baffle					
- Transition Duct					

Task III. Green Machine and Sinter Components

Green machining, sintering and NDE of the combustor supports was completed. Test specimens were prepared from the plates sintered in the same furnace runs as the components. Averaged room temperature strength and Weibull Modulus for a group of 20 specimens were 69.2 ksi and m=12.4, respectively.

The green machined dimensions on the combustor support were established from the powder lot shrink factor plus an additional .035" on the diameters and heights for finish machining stock where necessary.

Twelve combustor supports were delivered to Therm, Inc., for finish machining.

Ten of twelve combustor supports returned to Carborundum were excessively chipped as discussed in Task IV. Six replacement blanks and qualification specimens were machined from replacement billets and sintered. Four NDE-acceptable blanks were delivered to Therm, Inc. and the plates were delivered for preparation of qualification test specimens. The attached Milestone Schedule (Figure 84) defines the anticipated schedule for completing these components.

Contour coordinate numbers for the transition duct and baffle flow paths were received on October 3, at which time green machining templates were initiated. These were completed October 10.

Green machining of a prototype baffle and transition duct component commenced immediately and tooling verification samples were produced. These were processed through sintering and forwarded to Therm, Inc. for coordinate measurement plots of the flow path surfaces. These surfaces are particularly important in view of the fact that some of these are critical and must be machined after sintering. These were defined on marked up drawings received October 24, 1990, two weeks after the templates were completed.

The 10X mylars of the contours were reviewed and forwarded to GAPD on December 19, 1990. Based upon these and the physical dimensions measured by our inspection department, minor revisions were made to the green machine dimensions on the subsequent group of deliverables.

A group of ten baffles and qualification specimens were completed and sintered along with the six combustors described above. Dimensional inspection of the baffles indicated that the reference 6.307" diameter was undersize in all instances. This was attributed to the hand finishing and feathering of this surface with the milled surfaces in between the three fins. In addition, the wall thickness varied from the 0.200±.007 specification with five oversize and one undersize.

Fabrication of ten replacement baffles and qualification specimens was initiated immediately and anticipated completion is shown in Milestone Schedule (Figure 85). A group of ten transition ducts and qualification specimens were initiated and are scheduled for completion of green machining by January 4, 1991. The anticipated completion date is shown in Milestone Schedule (Figure 85).

Task IV. Finish Machine and Anneal Components

Therm, Inc. submitted a revised machining/fixture quotation based upon the final drawings received November 12, 1990. At the same time, they advised that they do not have the capabilities to finish machine the critical surfaces on the transition duct air divertor or on the baffle in between the fins. Furthermore, they know of no other ceramic machining vendor equipped to do so.

Carborundum subsequently provided GAPD with a revised cost estimate incorporating the increased machining charges and fixture costs in a letter dated December 19, 1990.

As stated previously, twelve combustor supports were delivered to Therm, Inc., eleven of which were returned completely machined.

In general, the overall quality and appearance was very good with the exception of one type of flaw. Nine of the eleven exhibited severe chipping at the intersection of the combustor support ID and four of the eight large side holes at 90° intervals. The chips were traced to the four-pin fixture used in one of the last machining operations. Nine combustors were effected before the problem was discovered. The last two combustors do not exhibit these chips and both passed visual, FPI and X-ray inspection.

Four sintered replacement components were subsequently provided to Therm, Inc. for machining.

No annealing or final component qualification activity has been conducted.

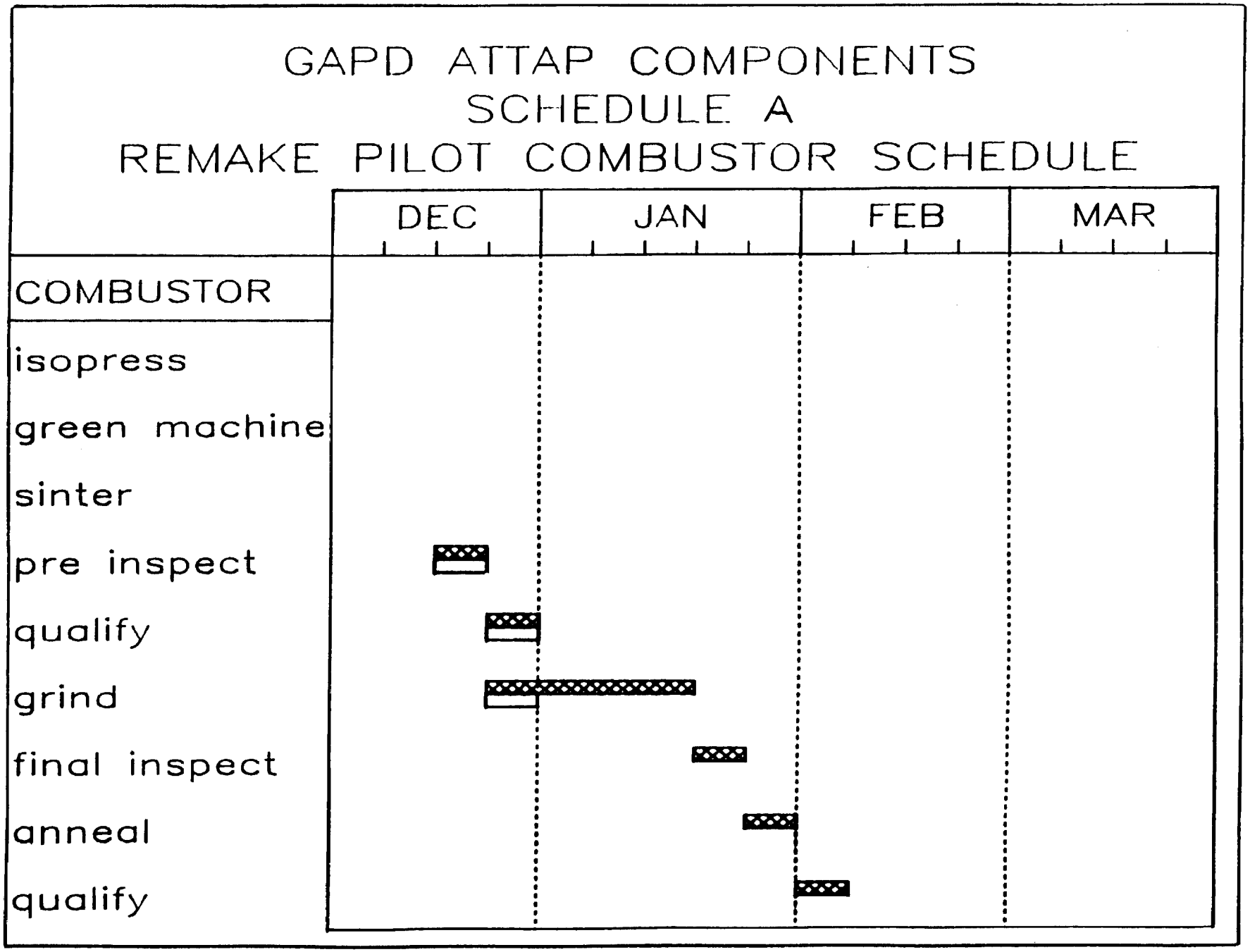

FIGURE 84. MILESTONE SCHEDULE FOR PILOT COMBUSTORS

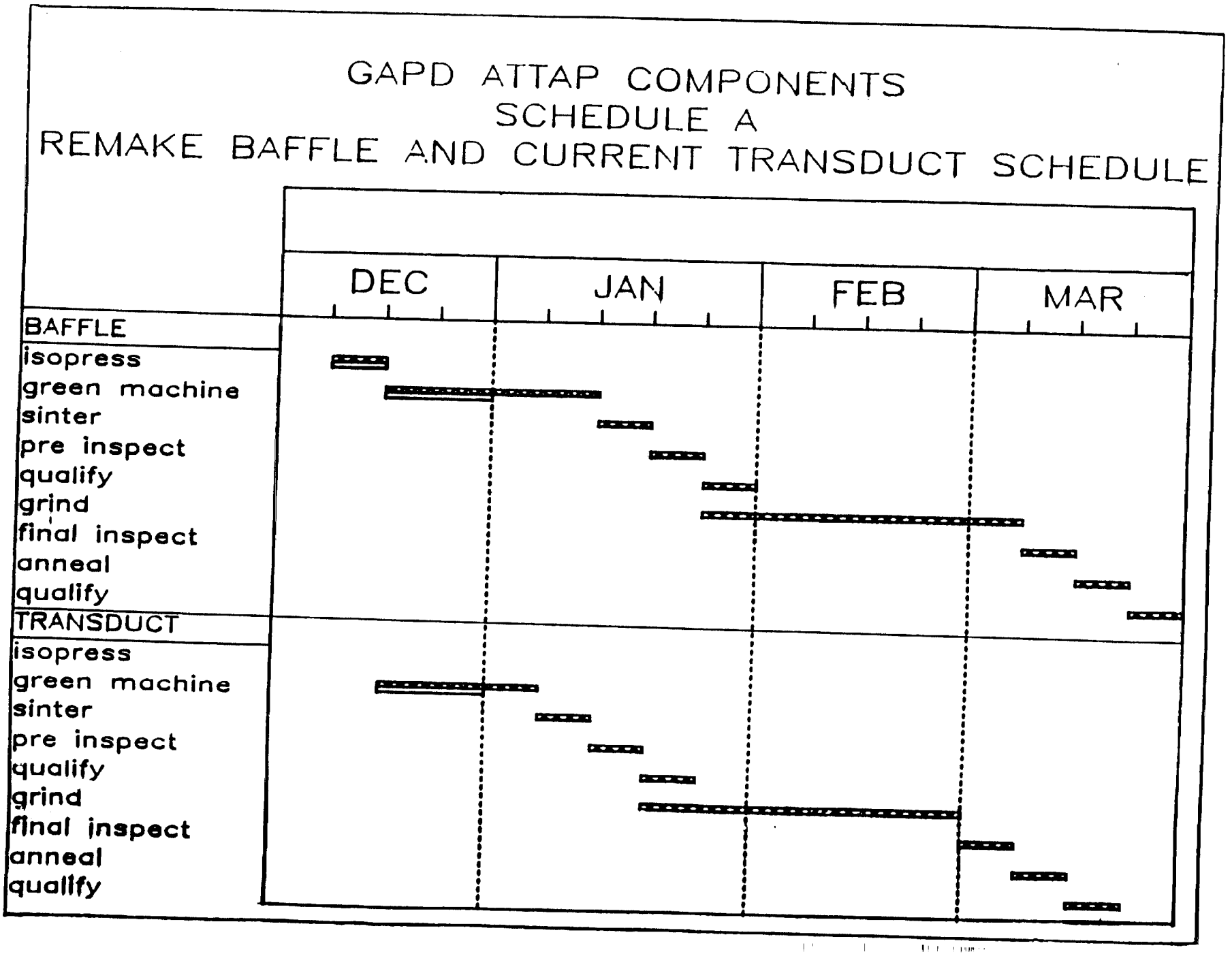
GAPD ATTAP COMPONENTS
SCHEDULE A
REMAKE BAFFLE AND CURRENT TRANSDUCT SCHEDULE
DEC
JAN
FEB
MAR
BAFFLE
isopress
green machine
sinter
pre inspect
qualify
grind
final inspect
anneal
qualify
TRANSDUCT
isopress
green machine
sinter
pre inspect
qualify
grind
final inspect
anneal
qualify

Miscellaneous

GAPD requested that we provide the finished component qualification specimens to them for MOR testing instead of testing at Carborundum. This has been agreed to; however, we requested that a prior preliminary test be conducted to verify that there is no significant difference in data due to testing facilities.

Carborundum has supplied GAPD with ten bars remaining from the baffle billet qualification for which we have already reported strength/Weibull data. GAPD will determine average MOR for this group of bars.

APPENDIX III

ANNUAL TECHNICAL PROGRESS REPORT
GARRETT CERAMIC COMPONENTS DIVISION

ADVANCED TURBINE TECHNOLOGY APPLICATIONS PROJECT

GARRETT CERAMIC COMPONENTS
1990 ANNUAL TECHNICAL PROGRESS REPORT
FOR GARRETT AUXILIARY POWER DIVISION

I. INTRODUCTION

The objective of this 37 month technical effort is to develop a fabrication process with the potential for low-cost, mass production of AGT101 turbine rotors using GCCD GN-10 silicon nitride. Pressure slip casting will be the primary fabrication approach. Materials and components will be extensively characterized and NDE methods developed and evaluated for improved process control and material/component qualification. In Task A, fabrication of the AGT-101 rotor using GN-10 silicon nitride and pressure slip casting will be developed. In Task C, GN-10 test specimens and NDE seeded defect standards will be fabricated by pressure slip casting.

II. 1990 ACHIEVEMENTS

Garrett Ceramic Components accomplished a number of important accomplishments on the Garrett Auxiliary Power Division ATTAP program in 1990:

1) Established a reproducible slipcasting process (with nearly a 100% yield through the drying step) for the fabrication of defect-free GN-10 Si_3N_4 AGT101 rotors.

2) Generated AGT101 rotors with reproducible mechanical properties that met Garrett Auxiliary Power Division ATTAP Si_3N_4 material mechanical property requirements.

3) Delivered two unmachined radial turbine AGT101 rotors to Garrett Auxiliary Power Division in September 1990 for spin testing.

4) Transferred the ASEA glass-encapsulation HIP process in-house and developed the process to generate reproducible GN-10 Si_3N_4 AGT101 rotor densification, and mechanical properties meeting the Garrett Auxiliary Power Division ATTAP requirements.

5) Demonstrated the ability to take a AGT101 impact-resistant design rotor plastic pattern (generated by stereolithography) and generate HIPed GN-10 slipcast rotors in only 8 weeks after receipt of the pattern.

6) Demonstrated fabrication of high quality impact-resistant design AGT101 rotors using engine-quality tooling received in November 1990.

III. TECHNICAL PROGRESS SUMMARY

TASK A. FABRICATION OF AGT101 ROTORS BY PRESSURE SLIPCASTING

SUBTASK A.A FABRICATION OF ROTORS AND PLATES USING BASELINE SLIP AND FORMING PROCESS

The goal of Subtask A.A was to evaluate the capability of the GN-10 slip preparation, rotor and plate forming, and densification processes on resultant component shape forming capability and mechanical properties. Subtask A.A was begun at the beginning of the program (July 1988) and completed in 1989. The summary of results are reported in the 1989 annual technical report.

SUBTASK A.B SLIPCAST ROTOR PROCESS DEVELOPMENT 1

The goal of Subtask A.B was to take the problems identified in Subtask A.A in the fabrication of AGT101 radial-design rotors using the baseline slip, forming, and densification processes and investigate their elimination using iterative process development, and designed experiments, where appropriate. Subtask A.B was begun in early 1989.

As described in the 1989 annual technical report, the primary focus of Subtask A.B was to improve GN-10 slip properties so that defect-free rotors could be pressure slipcast. The baseline slip process generated plates with acceptable mechanical properties (see Table 40) but the slip became unstable within a few hours of casting initiation. Fabrication of plates was not affected because typical casting times were less than one hour. The baseline slip became unstable after two to three hours, resulting in slip gellation and subsequent agglomerated and porous cast microstructure. The slip instability also resulted in extensive part stress during drying leading to extensive rotor blade cracking. Resulting rotor mechanical properties were poor (data is presented in Table 40).

Slip process revision #3 was developed to improve slip stability and resulting cast rotor properties. Improvements were made to slip mixing procedure and dispersion/stabilization additives. The slip stability was increased to approximately 10 to 12 hours after casting initiation. This was a large improvement compared to the baseline slip, but the rotor typically takes 14 to 16 hours to cast and the shaft section had a porous and agglomerated microstructure due to slip gellation. Rotor mechanical properties (of the hub section) were greatly improved (shown in Table 40). Some minor blade cracks also were observed, caused by the slip instability.

TABLE 40. Fast Fracture Mechanical Property Data Summary.

SOURCE	TESTED AT	MACHINE SHOP	AVG	MIN	MAX	STD. DEV.	NO.	WEIBULL
BASELINE SLIP PROCESS			**BASELINE HIP PROCESS**					
ROOM TEMPERATURE								
BILLET	GCCD	1	113.2	80.0	130.8	12.0	35	12.0
BILLET	GAPD	1	109.5	80.8	138.0	13.3	30	9.0
BILLET	GCCD	2	131.7	114.9	143.7	8.4	14	19.0
ROTOR	GCCD	2	92.3	57.5	122.7	18.9	23	5.7
2200°F								
BILLET	GAPD	1	95.4	65.6	108.0	13.2	30	17.1
BILLET	GCCD	2	90.4	85.2	101.1	5.8	5	----
ROTOR	GCCD	2	70.8	58.7	83.6	10.5	5	----
2500°F								
BILLET	GAPD	1	64.6	56.2	76.7	7.4	10	----
BILLET	GAPD	1	59.1	55.0	67.5	4.4	10	----
BILLET	GAPD	2	59.3	53.0	67.4	4.7	10	----
ROTOR	GCCD	2	39.2	36.4	41.9	2.2	5	----
BASELINE SLIP PROCESS			**REVISED HIP PROCESS #1**					
ROOM TEMPERATURE								
BILLET	GAPD	2	133.2	118.7	151.2	12.0	11	----
BILLET	GCCD	2	130.2	93.4	153.9	13.7	35	11.7
2200°F								
BILLET	GAPD	2	108.7	101.7	113.2	3.9	12	----
BILLET	GCCD	2	98.0	84.3	112.1	8.6	9	----
2500°F								
BILLET	GAPD	2	70.8	60.2	81.2	7.0	10	----
REVISION #3 SLIP PROCESS			**REVISED HIP PROCESS #1**					
ROOM TEMPERATURE								
BILLET	GCCD	2	128.2	97.7	145.8	11.7	28	12.9
ROTOR	GCCD	2	128.3	98.7	145.1	11.9	29	12.6
2200°F								
BILLET	GCCD	2	92.7	86.4	99.4	4.1	9	----
ROTOR	GCCD	2	95.8	80.5	106.4	8.7	6	----
2500°F								
BILLET	GCCD	2	56.8	51.3	62.5	3.4	10	----
ROTOR	GCCD	2	65.9	60.6	70.1	3.2	6	----

TABLE 40 CONTINUED.

REVISION #15 SLIP PROCESS REVISED HIP PROCESS #1

SOURCE	TESTED AT	MACHINE SHOP	AVG	MIN	MAX	STD. DEV.	NO.	WEIBULL
ROOM TEMPERATURE								
BILLET	GCCD	2	130.0	103.6	146.1	13.0	25	11.7
BILLET	GCCD	AS-PROCESS	72.1	65.6	81.7	5.0	15	----
ROTOR	GCCD	2	126.1	101.0	145.7	12.0	28	12.3
2200°F								
BILLET	GCCD	2	95.0	82.8	105.0	7.3	10	----
BILLET	GCCD	AS-PROCESS	45.9	41.7	53.3	5.1	10	----
ROTOR	GCCD	2	89.5	77.8	96.2	5.4	10	----
2500°F								
BILLET	GAPD	2	65.9	60.2	69.7	2.6	10	----
BILLET	GCCD	2	55.6	49.4	62.1	4.8	10	----
BILLET	GAPD	AS-PROCESS	50.5	40.6	59.3	6.4	5	----
BILLET	GCCD	AS-PROCESS	47.1	35.0	60.0	9.8	5	----
ROTOR	GCCD	2	53.9	49.9	57.8	2.4	10	----

REVISION #15 SLIP PROCESS REVISED HIP PROCESS #3

SOURCE	TESTED AT	MACHINE SHOP	AVG	MIN	MAX	STD. DEV.	NO.	WEIBULL
ROOM TEMPERATURE								
BILLET	GCCD	2	120.5	81.9	144.7	15.7	27	8.9
BILLET	GCCD	OXIDIZED	141.2	123.0	154.6	11.7	10	----
BILLET	GCCD	AS-PROCESS	68.3	57.1	79.7	5.6	30	14.6
BILLET	GCC	AS-PROC/OXI	79.5	72.1	84.3	3.3	10	----
2200°F								
BILLET	GCCD	2	92.1	71.5	102.6	9.9	10	----
BILLET	GCCD	OXIDIZED	86.0	72.2	98.7	10.7	5	----
BILLET	GCCD	AS-PROCESS	55.6	38.4	64.1	7.6	10	----
2500°F								
BILLET	GCCD	2	62.8	57.4	70.9	4.0	10	----
BILLET	GCCD	OXIDIZED	61.9	57.7	66.8	2.9	5	----
BILLET	GCCD	AS-PROCESS	40.7	35.2	46.5	4.3	10	----

TABLE 40 CONTINUED.

REVISION #15 SLIP PROCESS REVISED HIP PROCESS #5

ROOM TEMPERATURE SOURCE	TESTED AT	MACHINE SHOP	AVG	MIN	MAX	STD. DEV.	NO.	WEIBULL
BILLET	GCCD	2	107.5	62.6	141.6	17.4	30	7.0
BILLET	GCCD	AS-PROCESS	59.7	54.8	67.7	4.4	15	----
2200°F								
BILLET	GCCD	2	84.3	76.2	92.3	5.1	10	----
BILLET	GCCD	AS-PROCESS	37.4	24.5	52.2	9.8	5	----
2500°F								
BILLET	GCCD	2	52.4	48.3	55.7	2.0	10	----
BILLET	GCCD	AS-PROCESS	32.5	20.6	42.8	9.5	5	----

REVISION #15 SLIP PROCESS REVISED HIP PROCESS #8

ROOM TEMPERATURE SOURCE	TESTED AT	MACHINE SHOP	AVG	MIN	MAX	STD. DEV.	NO.	WEIBULL
BILLET	GCCD	2	119.5	81.7	149.5	19.4	30	7.2
2200°F								
BILLET	GCCD	2	92.9	75.5	101.6	7.2	10	----
2500°F								
BILLET	GCCD	2	62.8	56.0	68.7	4.0	9	----

Further slip process development was performed into early 1990 and slip process revision #15 was developed. Changes included substituting a more stable (in aqueous suspension) sintering aid powder, dispersant modification, and mixing procedure modifications. The slip was very stable and allowed the slipcasting of defect-free AGT101 radial-design rotors. Rotor mechanical properties were equivalent to slip revision #3 properties. Revision #15 has subsequently been standardized as the GN-10 pressure slipcasting slip preparation process.

Figure 86 compares plate mechanical properties for the baseline and two slip process revisions as a function of temperature. Properties are equivalent. This is due to the fact that all three slips are stable for short casting times, as is utilized in plate fabrication, even the baseline slip. The cast plate microstructure is consistent between parts. Figure 87 compares mechanical properties of rotors fabricated from each of the slip process revisions. The baseline slip's stability problems definitely result in poorer room and high temperature properties, while slip process revision #3 and #15 rotor hub properties are much better and are equivalent.

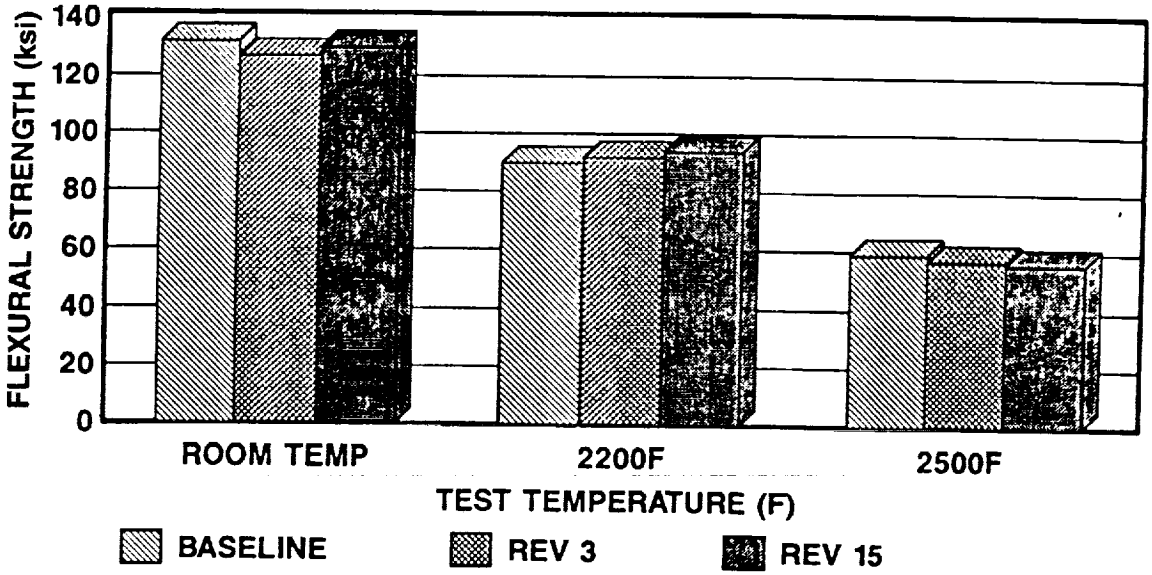

Figure 86. Comparison of GN-10 Plate Mechanical Properties as a Function of Slip Process Revision.

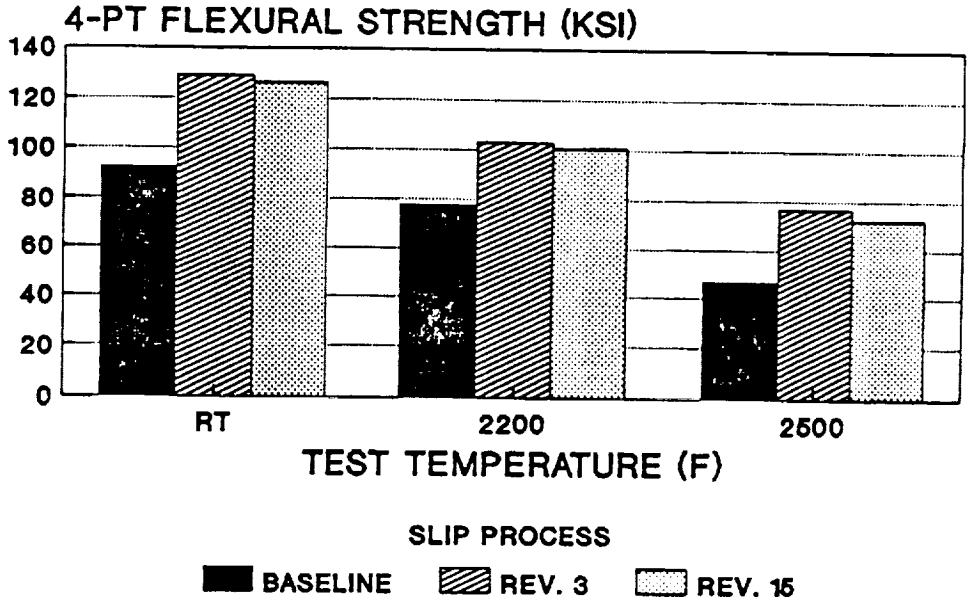

Figure 87. Comparison of Radial-Design AGT101 GN-10 Rotor Mechanical Properties as a Function of Slip Process Revision.

Figure 88 compares slip process revision #15 plate and rotor mechanical properties. The properties are equivalent, which is to be expected if the slip remains stable and high green density uniform microstructures are cast. Figure 89 compares the reliability of GN-10 Si_3N_4 AGT101 rotors prepared from each of the slip process revisions. The improvement in slip quality and stability results in a concomittant improvement in room temperature Weibull value and improvement in overall room temperature strength.

Once the slip process revision was standardized, evaluation of the vertical green density gradient of pressure slipcast AGT101 rotors was evaluated. Garrett Ceramic Components dewaters (casts) AGT101 rotors unidirectionally from the hub bottom up and this approach does induce a small vertical green density gradient. The density decreases slightly as the part is cast vertically. There is no detectable green density gradient across the part horizontally, confirmed by numerous destructive characterizations of cast rotors. In 1990 Garrett Ceramic Components examined the ability to reduce this green density gradient and improve subsequent HIPed rotor dimensional control. Increases in both solids content and casting pressure decrease the density gradient. The two factors are interactive, as shown in Figure 90. The vertical green density gradient was able to be reduced from approximately 6% for the baseline casting pressure solids content conditions down to less than 1%. The importance of being able to manipulate this density gradient will be discussed in Subtask A.D.

Subtask A.B ended in early 1990 with the delivery of four as-HIPed AGT101 radial-design rotors to Garrett Auxiliary Power Division. The rotors were fabricated using revision #15 slip and the revision #1 HIP process. They evaluated the current process capability for fabricating rotors and tested mechanical properties of the rotors. The mechanical property results are shown in Figure 91. The results correlate well with Garrett Ceramic Components results (Table 40).

SUBTASK A.C SLIP CAST ROTOR DEVELOPMENT 2

With the decision by Garrett Auxiliary Power Division to modify the AGT101 hot section turbine rotor from a radial to an impact-resistant design, the purpose of Subtask A.C was modified. Subtask A.D will address development of the impact-resistant design AGT101 turbine rotor. Subtask A.C addresses further reproducibility and improvement of the fabrication of the radial AGT101 rotor focusing on both net-shape development and material property improvements.

Subtask A.C was initiated at the beginning of 1990. Pre-HIP radial-design AGT101 rotor processing development focussed on improving rotor drying and calcining yields. Initial yields had been approximately 75 to 80%. Through iterative process development, the yield was improved to essentially 100%. The improved drying and

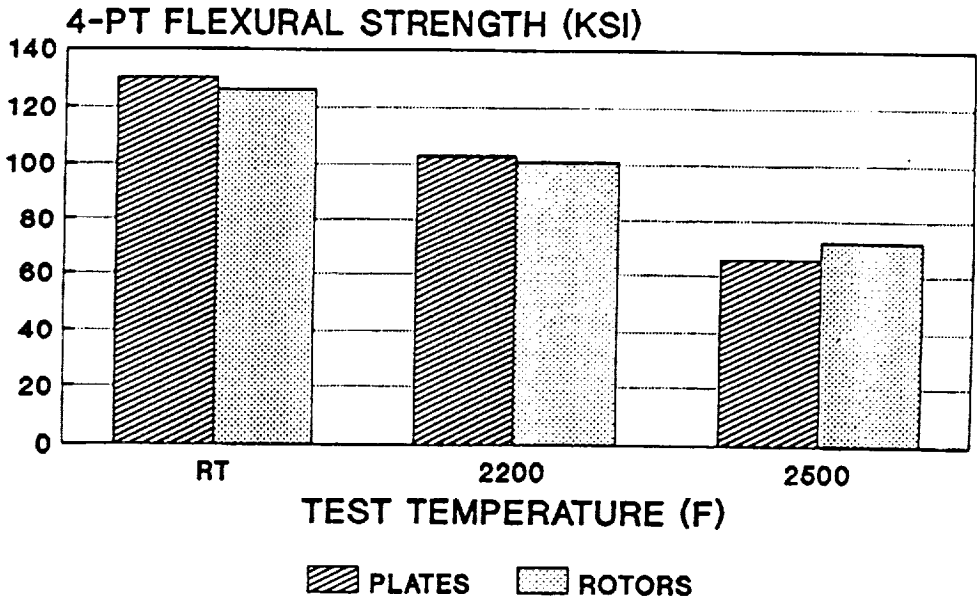

Figure 88. Comparison of GN-10 Slip Process Revision #15 Plate and Rotor Mechanical Properties.

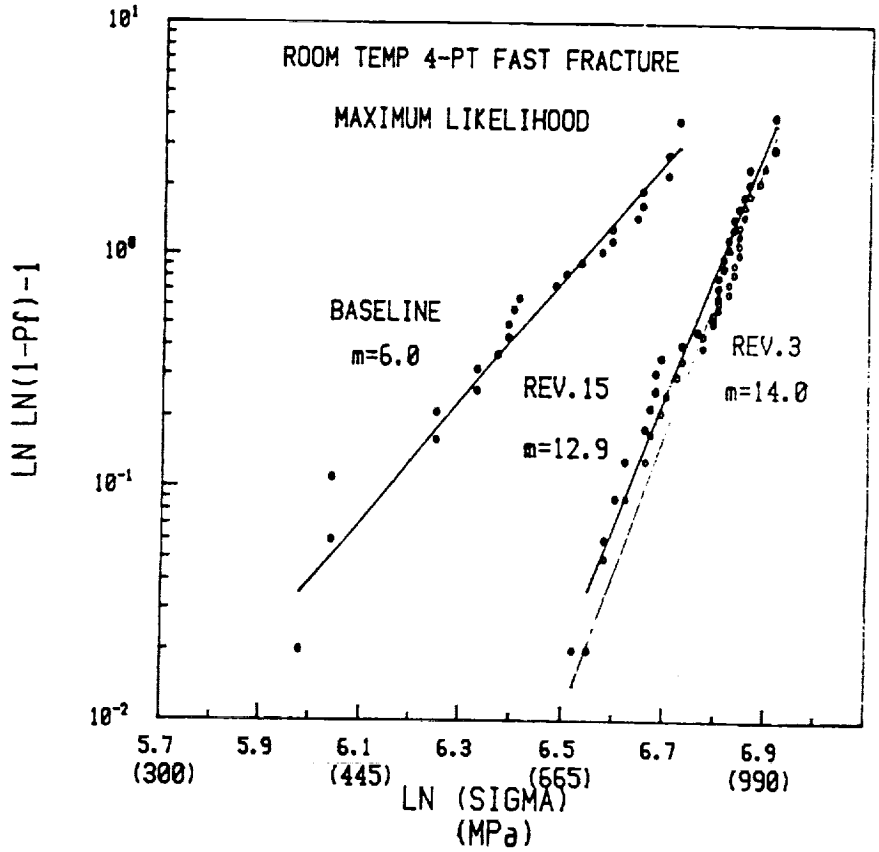

Figure 89. Reliability Improvement in AGT101 Rotor Mechanical Properties with Improvements in Slip Process.

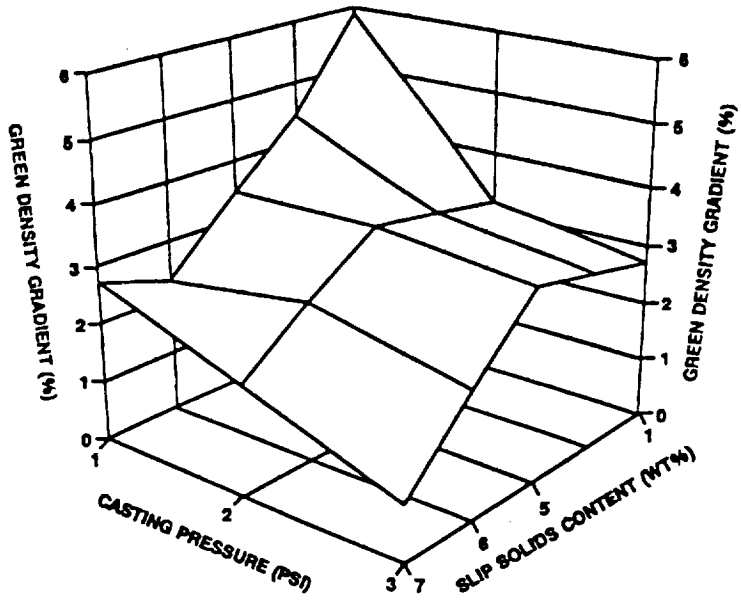

Figure 90. Reduction of AGT101 Rotor Vertical Green Density Gradient Through Interactive Manipulation of Slip Solids Content and Casting Pressure.

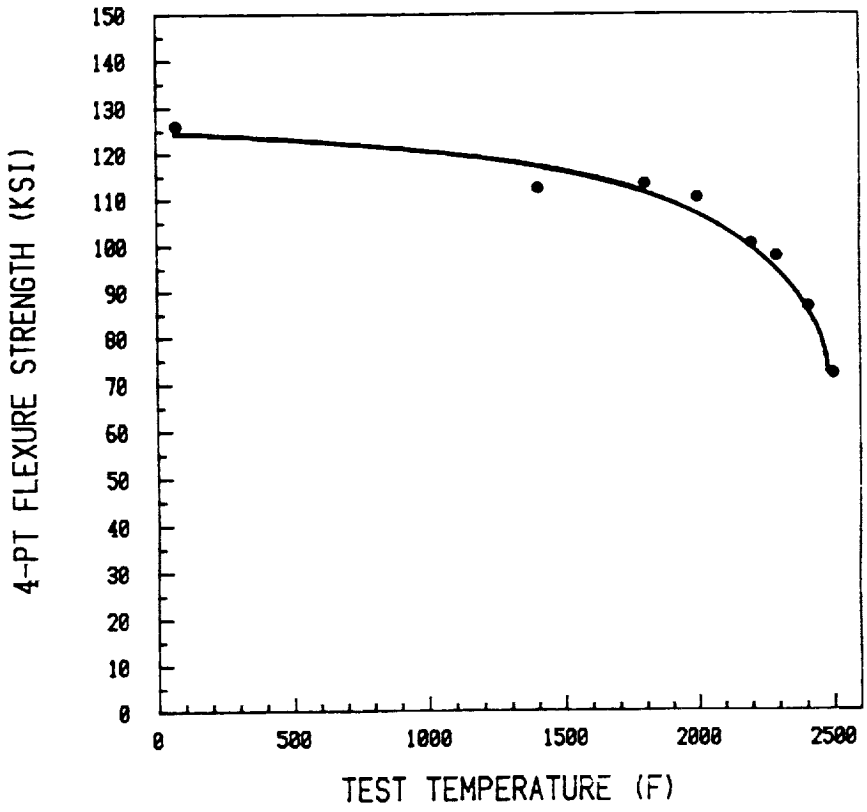

Figure 91. Radial-Design AGT101 Rotor Mechanical Properties (Rev.#15 Slip, Rev.#1 HIP) As Evaluated by Garrett Auxiliary Power Division.

calcining procedures were then implemented as standardized procedures for subsequent rotor fabrication.

Densification development continued in 1990 under Subtask A.C. The as-processed surface (as-HIPed) roughness of revision #1 HIPed GN-10 was 120-130 μin. An examination into modifications of encapsulation-HIP coating resulted in an improvement in surface roughness to approximately 90 μin. This HIP process revision was designated HIP revision #3. There was no change in bulk mechanical properties (as shown in Table 40).

In April 1990, densification of GN-10 Si_3N_4 material using the ASEA glass-encapsulation HIP process was initiated in-house. Previous to that point, all glass-encapsulation HIPed material had been processed in Sweden. The initial in-house HIP cycle (HIP revision #5) was determined to produce GN-10 material with incomplete microstructural development and resulting slightly poorer mechanical properties than previous ASEA HIPed GN-10 material (see Table 40). The revision #5 cycle was similar to the revision #3 cycle run at ASEA (revision #3 strength data was consistent with past GN-10 results) but it was determined that the different furnace and small cycle changes resulted in the different degree of microstructure development. Investigations into the HIP cycle refinement resulted in HIP process revision #8. Slip process revision #15 material HIPed using HIP revision #8 resulted in material mechanical properties equivalent or better than any previous slipcast GN-10 material HIPed at ASEA. A mechanical property comparison of slip revision #15 origin GN-10 HIPed using HIP process revisions #1, #5, and #8 is shown in Figure 92.

As-processed (as-HIPed) mechanical properties are of critical importance for the AGT101 radial and impact-resistant design rotors as many parts of the rotors will have as-processed surfaces. These surfaces will be a potential controlling factor in rotor performace/survivability. Garrett Ceramic Components undertook extensive evaluation of as-processed surface properties in 1990 and initiated exploration of ways to improve strengths.

As-processed surface test bars machined from slip process revision #15 plates and HIPed using three different HIP process revisions have been tested and compared. Mechanical property results of test bars HIPed using HIP revision #1 (HIPed at ASEA, encapsulant type #1), HIP revision #3 (at ASEA, encapsulant type #2) and #5 (HIPed at GCC, encapsulant #3) are presented in Table 40. The as-processed surfaces of revision #1 HIPed bars exhibited 120-130 μin R_a surface roughnesses, the revision #3 HIPed bars 90-100 μin, and the in-house HIPed bars (HIP revision #5) smoother surfaces (50-60 μin R_a).

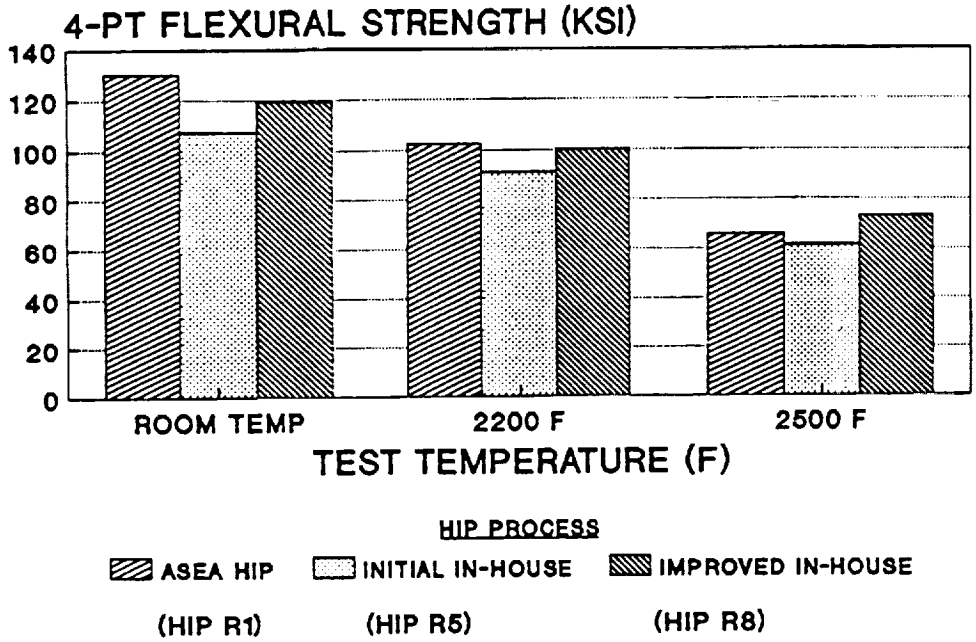

Figure 92. Mechanical Property Comparison of GN-10 Si_3N_4 as a Function of HIP Process Revision.

Comparing HIP revisions #1 and #3, the as-processed surface strengths are similar. The HIP process revision #5 as-processed surface strengths are much lower due to the incomplete microstructure development, so the effect of surface roughness on as-processed surface strengths was not able to be determined. It is important to note that a preliminary examination of post-machining oxidation of HIP revision #3 as-processed surface test bars reveals that the room temperature strength increases 16%, to 80 ksi.

The surface reaction layers due to encapsulation-HIPing are being evaluated both chemically and structurally for the various HIP process revisions and the results will be correlated with mechanical property results. Plates made from revision #15 slip have been HIPed using HIP revision #8 and at the end of 1990 were being machined into as-processed surface test bars for evaluation of HIP revision #8 effects on surface properties and for further oxidation experiments.

Oxidative post-HIP treatments were initiated on GN-10 test bars machined from plates to evaluate oxidation resistance, and oxidation layer protection mechanisms as related to mechanical properties. It was determined that GN-10 exhibited parabolic rate decreasing kinetics by measuring oxidation weight gains at temperatures ranging between 1100 and 2500°F. This is indicative of a passivating oxide layer and is the desired oxidation mechanism. A set of optimized oxidation conditions resulting in improved room temperature strengths has been determined. HIP process revision #3 processed

test bars exhibit an average room temperature strength increase upto 141 ksi, compared to unoxidized average strength of 121 ksi, a 16.5% increase. As presented in Table 40 and shown graphically in Figure 93, high temperature strengths are not affected by oxidation, as expected. Oxidation also improves as-processed room temperature surface strengths, as described in the previous section. Further oxidation experiments of both machined and as-processed surfaces of HIP revision #8 material will be performed in 1991 when the test bars are prepared.

Subtask A.C was completed in October 1990 with the delivery to Garrett Auxiliary Power Division of two radial-design AGT101 rotors fabricated using slip process revision #15 and HIP revision #1. The rotors were utilized for spin balancing and spin-to-burst evaluation. Due to a small shaft-hub misalignment in the original mold fabrication tool, the radial-design rotors required extensive stock removal for spin balancing. The first rotor burst at approximately 80,000 rpm, suspected to be due to the size of the balancing groove that needed to be machined into the part. The second rotor burst at 114,000 rpm, within 1% of the required proof

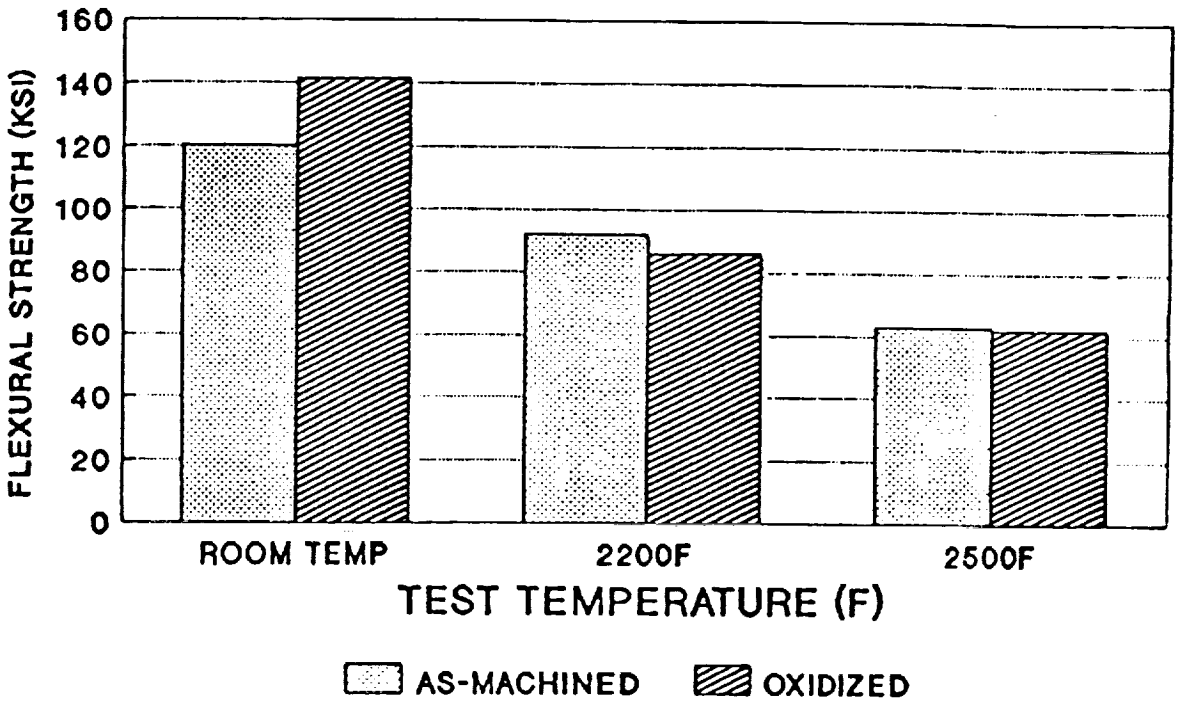

Figure 93. Comparison of Unoxidized and Oxidized Rev. #15 Slip, Rev. #3 HIP Process GN-10 Si_3N_4 Mechanical Properties.

test spin speed for deliverable rotors. This is an excellent result based on the fact that this is an unmachined rotor (all as-processed surfaces) and the extensive material removal needed for spin balancing. The engine quality rotors that will be delivered in 1991 will have extensive amounts of surface machined including much of the high stress surface areas.

SUBTASK A.D IMPACT-RESISTANT DESIGN ROTOR DEVELOPMENT 1

This subtask was initiated in January 1990 to develop the fabrication of the impact-resistant design AGT101 rotor, building on the GN-10 silicon nitride pressure slip casting process developed for the radial-design radial shaped AGT101 rotor. Initial work centered on design and procurement of a hard (steel) tool for fabrication of impact-resistant design rotor slip casting molds. A mold hard tooling vendor was selected in April 1990 and tooling fabrication was initiated. Due to rotor and mold design changes, the impact-resistant design rotor mold hard tool delivery was delayed until late November 1990.

In order to evaluate the castability of the impact-resistant design rotor shape before the hard tool was delivered in November, a stereolithographically generated plastic pattern of an appropriately oversized (to account for densification shrinkage) impact-resistant design rotor was provided to Garrett Ceramic Components by Garrett Auxiliary Power Division to fabricate slipcasting molds for rotor casting evaluations. The only significant difference between the mold developed from the stereolithographic pattern and the hard tool being built was that the stereo pattern has approximately 0.003" ridges on its surface due to the limited surface detail resolution of the stereolithographic process.

The prototype plastic rotor pattern was received in mid-July and mold making and casting experiments initiated. Casting of the prototype impact-resistant design rotors was very successful, with high quality rotors able to be cast within 3 weeks of initiation of casting experiments. Besides the surface ridges due to the plastic mold pattern, two minor as-cast defects were observed. Some blade leading edges had small cracks near the blade root and the hub saddle region circumference was rough. Both defects were traced to the quality of the prototype rotor mold pattern and susequent mold quality. Subsequent processing (drying, calcining, and HIPing) was also successful with minimal problems encountered using the process cycles developed for the radial design AGT101. The only defect observed to occur was some small radial cracks along the hub saddle region observed after HIPing. These were thought to be due to pre-HIP conditioning and modification of the pre-HIP procedure resulted in substantial reduction of these defects. Two prototype impact-resistant-design AGT101 rotors were provided to Garrett Auxiliary Power Division for evaluation in January 1991.

The hard tooling for the impact-resistant design rotors was received in late November 1990. Pressure slipcasting of hardtool derived rotors was begun in mid-December 1990 and is continuing. The goal of Subtask is to deliver engine quality rotors (spin balanced and proof spun-test) to Garrett Auxiliary Power Division in 1991.

Also initiated under Subtask A.D was an investigation into further improvements in GN-10 silicon nitride raw materials. Specifically, silicon nitride powders with improved reactivity and purity are being evaluated to potentially improve GN-10 properties and provide alternate raw material sources. Initial work focussed on slip development of two different silicon nitride alternate powders. Determination of surface chemistry and subsequent compatability/slip property optimization was completed and slips were developed of each of the two powders having adequate rheological properties and solids contents. Plates were cast and HIPed to full density and at the end of 1990 were being machined into test bars so that mechanical properties and microstructure can be evaluated.

In addition, improvements to slip process revision #15 are being explored to see if potential improvements in mechanical properties through modification of slip preparation process procedures and slip composition such as slip mixing time and dispersant composition can be achieved. An alternative dispersant composition has been developed that eliminates the questionable constituent of the dispersant used in slip process revision #15. A slip process incorporating the new dispersant and the standard GN-10 Si_3N_4 raw materials has been developed in 1990. This new slip process revision will be referred to as revision #16. The revision #16 slip exhibits excellent rheological properties and has been cast into plates. These plates have been HIPed and were being machined into test bars for property evaluation at the end of 1990. The effect of mixing time of the revision #15 slip is also being evaluated to see how it affects resulting microstructural uniformity and mechanical properties. Plates have been cast using revision #15 slip milled for longer times. The plates have been HIPed using HIP revision #8 and were being cut into test bars for mechanical property evaluation.

SUBTASK A.F SLIPCAST ROTOR COMPONENT QUALIFICATION/NDE DEVELOPMENT - The focus of this subtask is to develop techniques and apparatus for nondestructive characterization and quality assurance of ATTAP test material and components. In 1990, work focussed on development of GN-10 part thickness exposure charts for X-ray film applications for calcined and HIPed GN-10 using step blocks to generate optimum film exposure conditions. As part of this effort, work was initiated on fabrication and evaluation of GN-10 silicon nitride hole penetrameters and step blocks for X-ray inspection applications.

GN-10 image quality indicators (IQI's) with holes ranging down to 0.003" diameter and thicknesses down to 0.005" were fabricated and used to evaluate contrast and spatial resolution. Contrast resolution achieved so far has been 1.3% for a 0.5" thick part with a corresponding spatial resolution of 0.008" using 1X magnification on film. IQI's with a wider range of thicknesses and hole sizes will be designed and fabricated based on initial film thickness exposure/IQI results now being generated. This will allow more quantitative evaluation of both film and realtime contrast and spatial resolution.

TASK C FABRICATION OF TEST SPECIMENS AND NDE STANDARDS

SUBTASK C.A MATERIAL EVALUATION SPECIMEN FABRICATION

Garrett Ceramic Components fabricated 100 as-processed surface flexure specimens utilizing revision #15 slip and revision #1 HIP. The test bars were delivered to Garrett Auxiliary Power Division in September 1990 per a 1990 program deliverable requirement. Garrett Auxiliary Power Division subsequently tested the specimens at room and high temperatures for fast fracture properties. Results are presented in Figure 94.

A scheduled 1991 delivery is 250 material evaluation test specimens (various size, machined, fast fracture and fracture toughness test bars) and 100 as-processed surface test bars representative of the fabrication process being used to make 1991 engine quality rotor deliveries. Fabrication of plates from which these test bars will be machined was initiated in December 1990. The planned delivery date is February-March 1991.

SUBTASK C.C FABRICATION OF SLIPCAST DEFECT SEEDED BILLETS FOR NDE DEVELOPMENT

Garrett Ceramic Components has fabricated GN-10 seeded defect specimens (containing both controlled size iron inclusions and voids) for evaluation of X-Ray radiographic and ultrasonic NDE detection capabilities. Seeded defect sizes ranged from 25 μm to 500 μm in diameter. The specimens were to be inspected at each intermediate processing step nondestructively and then the results quantified using destructive cut-up and characterization. The three processing steps being evaluated are green (dried after slip casting, calcined (presintered), and HIPed (fully densified). In 1989, green inspection was completed at both Garrett Ceramic Components and Garrett Auxiliary Power Division.

In February 1990, Garrett Ceramic Components completed nondestructive characterization of the calcined specimens. The specimens were then delivered to Garrett Auxiliary Power Division for nondestructive evaluation. Garrett Auxiliary Power Division

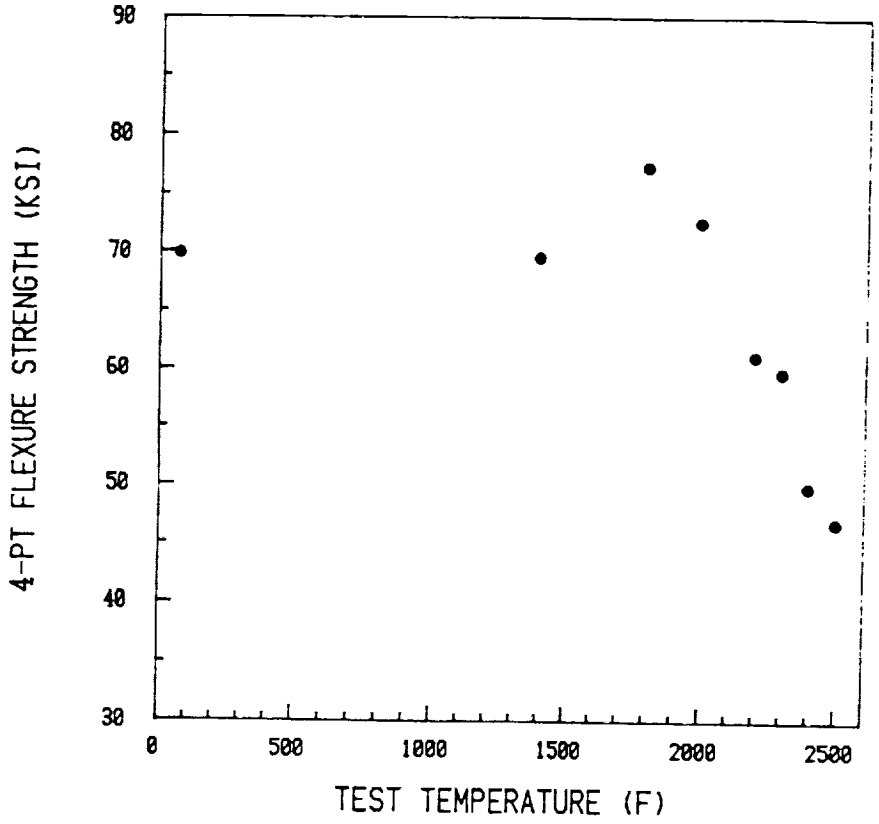

Figure 94. As-Processed (As-HIPed) Surface Strengths of Slip Rev.#15, HIP Rev.#1 GN-10 Si_3N_4 as Evaluated by Garrett Auxiliary Power Division.

returned the samples and in July 1990 Garrett Ceramic Components completed destructive characterization of one of the three calcined specimens. Destructive characterization revealed smallest detectable voids as 0.002" diameter and 0.002" diameter for iron inclusions. Using nondestructive techniques, the smallest detectable voids 0.003" diameter using realtime fluoroscopy at 10X magnification and 0.002" diameter using film radiography at 1X magnification. The smallest detectable iron inclusion using either realtime or film radiographic techniques was 0.002".

The remaining calcined specimens were then HIPed at Garrett Ceramic Components and characterized by realtime and film microfocus X-ray. The specimens were delivered to Garrett Auxiliary Power Division in early November 1990 for evaluation. Garrett Auxiliary Power Division will then return the HIPed specimens and Garrett Ceramic Components will destructively characterize them. The complete set of nondestructive and destructive characterization data for green, calcined, and HIPed seeded defect specimens will then be correlated and utilized as a guideline for NDE analysis of GN-10 components.

1. Report No. NASA CR-187146	2. Government Accession No.	3. Recipient's Catalog No.
4. Title and Subtitle Advanced Turbine Technology Applications Project (ATTAP) - 1990 Annual Report		5. Report Date March 1991 6. Performing Organization Code 99193
7. Author(s) Engineering Staff of Garrett Auxiliary Power Division, A Unit of Allied-Signal Aerospace Company		8. Performing Organization Report No. 31-8071(03) 10. Work Unit No
9. Performing Organization Name and Address Garrett Auxiliary Power Division 2739 East Washington Street P.O. Box 5227 Phoenix, Arizona 85010-5227		11. Contract or Grant No. DEN3-335
12. Sponsoring Agency Name and Address U.S. Department of Energy Office of Transportation Technologies, Heat Engine Propulsion Division, Washington, D.C. 20585		13. Type of Report and Period Covered Annual Report 1990 14. Sponsoring Agency Code DOE/NASA/0335-3

15. Supplementary Notes
Annual Report Under Interagency Agreement
Project Manager: T.N. Strom, Propulsion Systems Division
NASA-Lewis Research Center, Cleveland, Ohio 44135

16. Abstract

This report is the third in a series of Annual Technical Summary Reports for the Advanced Turbine Technology Applications Project (ATTAP), authorized under NASA Contract DEN3-335 and sponsored by the U.S. Department of Energy. The report was prepared by Garrett Auxiliary Power Division (GAPD), a unit of Allied-Signal Aerospace Company. The report includes information provided by Garrett Ceramic Components (GCC), the Norton/TRW Ceramics Company (NTC), and the Carborundum Company, all subcontractors to GAPD on the ATTAP. The project is administered by Mr. Thomas Strom, Project Manager, NASA-Lewis Research Center, Cleveland, OH. This report covers plans and progress on ceramics development for commercial automotive applications over the period January 1 through December 31, 1990.

Project effort conducted under this contract is part of the DOE Gas Turbine Highway Vehicle System program. This program is directed to provide the U.S. automotive industry the high-risk, long-range technology necessary to produce gas turbine engines for automobiles with reduced fuel consumption, reduced environmental impact, and a decreased reliance on scarce materials and resources. The program is oriented toward developing the high-risk technology of ceramic structural component design and fabrication, such that industry can carry this technology forward to production in the 1990s. The ATTAP test bed engine, carried over from the previous AGT101 project, is being used for verification testing of the durability of next-generation ceramic components, and their suitability for service at Reference Powertrain Design conditions.

This document reports the technical effort conducted by GAPD and the ATTAP subcontractors during the third year of the project. Topics covered include ceramic processing definition and refinement, design improvements to the ATTAP test bed engine and test rigs and the methodology development of ceramic impact and fracture mechanisms. Appendices include reports by ATTAP subcontractors in the development of silicon nitride and silicon carbide families of materials and processes.

17. Key Words (Suggested by Author(s)) Ceramic-Engine Ceramic-Technology	18. Distribution Statement Unclassified-Unlimited Subject Category 85 DOE Category UC-96		
19. Security Classif. (of this report) Unclassified	20. Security Classif. (of this page) Unclassified	21. No. of Pages 185	22. Price* A09

*For sale by the National Technical Information Service, Springfield, Virginia 22161

SUBTASK C.D FABRICATE TENSILE TEST SPECIMENS

Work continued in 1990 on development of fabrication of large plates (5" by 9" by 1") from which Oak Ridge designed buttonhead tensile test bars could be machined. One plate yields 5 tensile test bars. In December 1990 a glass-encapsulation HIP technique was developed, using HIP process revision #8, to densify the large tensile test bar plates. Successful densification of large plates was demonstrated in December. At the end of 1990, Garrett Auxiliary Power Division requested a delivery of 35 Oak Ridge tensile test bars in March 1991, fabricated using the same slip (revision #15) and HIP (revision #8) processes being used to fabricate the first set of engine quality impact-resistant design rotors to be delivered in March 1991. The tensile test bars will be used to evaluate tensile rupture properties of the current process GN-10 Si_3N_4.